

**RWE Renewables UK Dogger Bank  
South (West) Limited**

**RWE Renewables UK Dogger Bank  
South (East) Limited**

**Dogger Bank South Offshore  
Wind Farms**

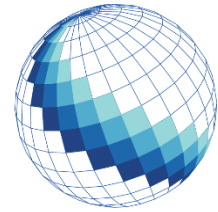
**Bed Mobility & Thermal Environment**

<b>Document Date:</b>	<b>March 2025</b>
<b>Document Reference:</b>	<b>13.7</b>
<b>Revision Number:</b>	<b>01</b>
<b>Classification:</b>	<b>Unrestricted</b>

Company:	RWE Renewables UK Dogger Bank South (West) Limited and RWE Renewables UK Dogger Bank South (East) Limited	Asset:	Development		
Project:	Dogger Bank South Offshore Wind Farms	Sub Project/Package	Consents		
Document Title or Description:	Bed Mobility & Thermal Environment				
Document Number:	004688005-02	Contractor Reference Number:	J/7/55/22		
<p><i>COPYRIGHT © RWE Renewables UK Dogger Bank South (West) Limited and RWE Renewables UK Dogger Bank South (East) Limited, 2024. All rights reserved.</i></p> <p><i>This document is supplied on and subject to the terms and conditions of the Contractual Agreement relating to this work, under which this document has been supplied, in particular:</i></p> <p><b>LIABILITY</b></p> <p><i>In preparation of this document RWE Renewables UK Dogger Bank South (West) Limited and RWE Renewables UK Dogger Bank South (East) Limited has made reasonable efforts to ensure that the content is accurate, up to date and complete for the purpose for which it was contracted. RWE Renewables UK Dogger Bank South (West) Limited and RWE Renewables UK Dogger Bank South (East) Limited makes no warranty as to the accuracy or completeness of material supplied by the client or their agent.</i></p> <p><i>Other than any liability on RWE Renewables UK Dogger Bank South (West) Limited and RWE Renewables UK Dogger Bank South (East) Limited detailed in the contracts between the parties for this work RWE Renewables UK Dogger Bank South (West) Limited and RWE Renewables UK Dogger Bank South (East) Limited shall have no liability for any loss, damage, injury, claim, expense, cost or other consequence arising as a result of use or reliance upon any information contained in or omitted from this document.</i></p> <p><i>Any persons intending to use this document should satisfy themselves as to its applicability for their intended purpose.</i></p> <p><i>The user of this document has the obligation to employ safe working practices for any activities referred to and to adopt specific practices appropriate to local conditions.</i></p>					
Rev No.	Date	Status/Reason for Issue	Author	Checked by	Approved by
01	March 2025	Submission for Deadline 3	RHDHV	RWE	RWE

# MarineSpace

Making Sense of the Marine Environment <sup>TM</sup>



## **Dogger Bank South Background Review: Bed mobility & Thermal Environment**

Document Ref: J/7/55/22	Originator: H Lane and J Dix
Date: 31/05/2023	Circulation: Restricted - Commercial-in-confidence

# **Dogger Bank South Background Review: Bed mobility & Thermal Environment**

Prepared by:

**MarineSpace Ltd**

**MarineSpace**  
Making Sense of the Marine Environment™




**MarineSpace Ltd  
Ocean Village Innovation Centre  
Ocean Way  
Southampton  
SO14 3JZ**

Prepared for:



**RWE Renewables GmbH  
Unit Offshore Wind  
Site Characterisation and Ground  
Modelling  
Windmill Hill Business Park,  
Whitehill Way, Swindon,  
Wiltshire SN5 6PB**



Date	Originator	Version	Action	Signature
20/01/2023	Helena Lane and Justin Dix	1.0	Internal DraftInternal Draft	
31/05/2023	Helena Lane and Justin Dix	2.0	Director Sign-off / External Document	

Any reproduction must include acknowledgement of the source of the material. This report should be cited as:

**MarineSpace Ltd, 2023. *Dogger Bank South Background Review: Bed mobility & Thermal Environment*.**

All advice or information presented in this report from MarineSpace Ltd is intended only for use in the UK by those who will evaluate the significance and limitations of its contents and take responsibility for its use and application. No liability (including that for negligence) for any loss resulting from such advice or information is accepted by MarineSpace Ltd, subcontractors, suppliers or advisors.

## **Data Licenses**

EMODnet Bathymetry Consortium (2020): EMODnet Digital Bathymetry (DTM). Charts NOT TO BE USED FOR NAVIGATION. <https://doi.org/10.12770/bb6a87dd-e579-4036-abe1-e649cea9881a>.

Contains British Geological Survey materials © UKRI 2022

Contains OS data © Crown copyright and database right 2022

Contains public sector information licensed under the Open Government Licence v3.0.

Contains data with Copyright of New Forest District Council

Acknowledgement: National Network of Regional Coastal Monitoring Programmes

Acknowledgement: Coastal retreat monitoring data was provided by East Riding of Yorkshire Council (Neil McLachlan – Senior Coastal Engineer – Flood Coastal Erosion Risk Management Team). EYRC are not responsible for any inaccuracies within these data.

## Glossary

Abbreviation	Definition
BGS	British Geological Survey
BH	Borehole
BLC	Bed Level Change
CD	Chart Datum
CPT	Cone Penetration Test
ECC	Export Cable Corridor
KP	Kilometre Post
LAT	Lowest Astronomical Tide
m	meters
MBES	Multi-Beam Echo Sounder
mbsf	Meters below seafloor
MSBL	Mean Seabed Level
M/V	Motor Vessel
LAT	Lowest Astronomical Tide
OWF	Offshore Windfarm
pCPT	Piezo Cone Penetration Test
SBP	Sub-bottom Profiler
SSS	Sidescan Sonar
VC	Vibrocore

## Contents

1.	Introduction .....	1-1
1.1.	Project Summary .....	1-1
1.2.	Scope and Objectives of Document .....	1-5
2.	Data Source Summary .....	2-1
2.1.	Geophysical Survey .....	2-1
2.1.1.	Bathymetry .....	2-1
2.1.2.	Seismic Data .....	2-5
2.2.	Geological Data .....	2-7
3.	Geological Context .....	3-1
3.1.	Offshore Bedrock Geology .....	3-1
3.1.1.	Jurassic: Lias Group, West Sole Group Oxford Clay, Corallian Group and the Kimmeridge Clay Formation .....	3-1
3.1.2.	Cretaceous Cromer Knoll Group and Chalk Group .....	3-2
3.1.3.	Undifferentiated Palaeocene and Eocene .....	3-3
3.2.	Late Quaternary Geology .....	3-6
3.3.	Hydrodynamics and Sediment Transport Pathways .....	3-10
4.	Route Specific Morphology and Mobility .....	4-1
4.1.1.	Landfall Site .....	4-1
4.1.2.	Export Cable Corridor .....	4-17
4.1.3.	Offshore Windfarm .....	4-58
4.2.	Gross Scale Morphology and Mobility .....	4-69
5.	Thermal Analysis of Export Cable Route, Offshore Windfarm and Landfall Site .....	5-1
5.1.	Ambient Ocean Temperature Analysis .....	5-2
5.2.	Thermal Conductivity and Thermal Resistivity Overview .....	5-14
5.2.1.	Thermal Data preparation .....	5-15
5.3.	Post-Installation Depth of Cover Changes .....	5-24
6.	References .....	6-1
	Appendix A. Data Sources .....	6-7
6.1.	Client Provided Reports .....	6-7
6.2.	Client Provided Data .....	6-7
6.3.	Additional Information Sources .....	6-8
	Appendix B. ....	6-10

## List of Figures

Figure 1-1: Dogger Bank South general site location, overlain on EMODnet bathymetry data.....	1-2
Figure 1-2: Dogger Bank South export cable route landfall sites. Left-hand panel South Wilsthorpe to Auburn Farm land-fall site, right-hand panel Skipsea to north Skirlington landfall site.....	1-3
Figure 1-3: Zone 1 cable route options, as named by MarineSpace .....	1-4
Figure 1-4: Zone 2 cable corridor options, as named by MarineSpace .....	1-4
Figure 1-5: Dogger Bank South site location and landfall (inset), overlain on Admiralty charts 2182A-0 and 1190-0 .....	1-5
Figure 2-1: Overview of bathymetric survey footprints for Dogger Bank South export cables and offshore wind farm .....	2-4
Figure 3-1: Offshore Bedrock, faults and hard substrate from British Geological Survey (2022). Offshore boreholes reviewed as part of this study are also marked.....	3-4
Figure 3-2: Offshore seabed sediment and sediment (Folk Classification) from British Geological Survey (2022) .....	3-5
Figure 3-3: Location overview of the DBS OWF array locations and ECR. The North Sea mapped ice limits for the LGM, with the Dogger Bank are shown, overlain with BRITICE v2 data (Sources: Roberts et al., 2018; Clark et al., 2017).....	3-7
Figure 3-4: Relative sea level curve and rate of Relative Sea Level Rise for the Dogger Bank area as determined by Emery et al (2019a) based on Shennan et al., 2006; Bradley et al., 2011 and Kuchar et al., 2012). Note the absolute dates do not correspond directly with those quoted from the literature but re-calibration is beyond the scope of this report.....	3-10
Figure 3-5: Modelled depth-averaged current speeds at Pts 1, 2 and 3 within Dogger Bank Tranche A Zone. Based on the model of Mathiesen and Nygaard (2010) and presented in Godwin and Brew (2014).....	3-11
Figure 3-6: Modelled significant wave heights (m) at Pts 1, 2 and 3 within Dogger Bank Tranche A Zone. Based on the model of Mathiesen et al (2011) and presented in Godwin and Brew (2014). .....	3-12
Figure 3-7: Wave rose for the Hornsea waverider buoy and inferred sediment transport directions after Pye and Blott (2015). .....	3-13
Figure 3-8: Southern North Sea Sediment Transport Model outputs for the Holderness coast representing tidally driven sediment transport for fine sand (100 microns - Panel A); medium sand (400 microns - Panel B) and very fine gravels 2000 microns – Panel C).....	3-14

Figure 4-1: BGS borehole record of depth below surface of the upper boundary of the Chalk bedrock, as well as the northern limit of the Skipsea Till, determined using borehole records (Source: Evans and Thomson, 2010). .....	4-3
Figure 4-2: Panel A the stratigraphic sequence at Skipsea showing extensive interbedded cross-laminated ripple sands within the Skipsea Till. Panel B vertical profile log of the Skipsea Till sequence at Skipsea (OS Grid reference TA176573) both after Evans and Thomson (2010). For full legend see Table 1 in Evans and Thomson, 2010. From: Evans and Thomson (2010) .4-4	4
Figure 4-3: Landfall locations and associated beach profile locations cited in the text and sourced from the East Riding of Yorkshire Council (2022) .....	4-6
Figure 4-4: Erosion rates for the Holderness coastline, including the landfall sites marked with red bracket or box and a N or S for the northern and southern landfall sites respectively. Figure shows the variation in recession rate for different time periods between 1852 and 2015 in a cumulative way (Source: Figure 8c, Pye and Blott, 2015). On the right the change in relative coastline position from mid-1990 to 2010 is shown, with the zero-line representing an initial 1994/96/97 survey (Source: Montreuil and Bullard, 2012) .....	4-9
Figure 4-5: Profile 12 at the northern landfall site cross-sectional profile showing cliff position and therefore retreat between 2003 and 2021 (From: East Riding of Yorkshire Council, 2022 .4-11	4-11
Figure 4-6: Profile 28 at the southern landfall site cross-sectional profile showing cliff position and therefore retreat between 2003 and 2021 (From: East Riding of Yorkshire Council, 2022) 4-12	4-12
Figure 4-7: Northern landfall site cliff loss per year along beach profiles 9 -13, between 2003 and 2022. Source: East Riding of Yorkshire Council, 2022 .....	4-14
Figure 4-8: Southern landfall site cliff loss per year along beach profiles 25 -30, between 2003 and 2022. Source: East Riding of Yorkshire Council, 2022 .....	4-14
Figure 4-9: Landfall site military defences (anti-tank blocks) visible in 2011 aerial photographs from the National Coastal Monitoring Programme, with label information from the Defence of Britain Archive (Source: Council for British Archaeology, 2006)z. ....	4-15
Figure 4-10: Zone 1 cable routes (named by MarineSpace) overlain on British Geological Survey offshore bedrock geology and EMODnet hillshade (Source: British Geological Survey, 2022) 4-20	4-20
Figure 4-11: Linear erosion features on the eastern margin of the southerly extension of the Smithic Bank Complex in the vicinity of Zone 1 CB Route 7 ~KP 8. Further west are a series of discontinuous north-south retreat moraines that are common along all Zone 1 CB Routes 2, 5 and 7 (with updated 2023 Route A Centreline and KPs visible).....	4-22
Figure 4-12: Recessional moraine ridges and associated bed level change between 2020 and 2022 along Zone 1 CB Route 7 .....	4-23

Figure 4-13: Scour patterns around the wrecks of the Villa de Valenciennes and Feltre along Zone 1 CB Route 7 .....	4-24
Figure 4-14: Zone 1 CB Route 5 and 7 (and 1 and 2) seabed topography .....	4-26
Figure 4-15: Outcropping West Sole Group, Oxford Clay and Corallian Group (with updated 2023 Route A Centreline and KPs visible) .....	4-27
Figure 4-16: Exposure of Langede Gas Pipeline with total lack of sedimentary infill (with updated 2023 Route A Centreline and KPs visible) .....	4-29
Figure 4-17: Cross-sections along Zone 1 CB Route 7, showing the horizons encountered by a cable at 1m or 2m depth below seabed .....	4-30
Figure 4-18: MBES anomaly and North-South oriented linear depressions along Zone 1 CB Route 5 at ~ KP 15.5 (with updated 2023 Route A Centreline and KPs visible) .....	4-32
Figure 4-19: Cross-section along Zone 1 CB Route 5, showing the horizons encountered by a cable at 1m or 2m depth below seabed .....	4-34
Figure 4-20: Cross-section along Zone 1 CB Route 2, showing the Horizons encountered by a cable at 1m or 2m depth below seabed. ....	4-36
Figure 4-21: Seabed morphology along Zone 1 CB Route 1 nearshore of Dogger Bank South export cable corridor .....	4-38
Figure 4-22: Seabed morphology of subaqueous dunes along Zone 1 CB Route 1 nearshore of Dogger Bank South export cable corridor, between KP 8 and 9, including bed level change.....	4-39
Figure 4-23: Cross-section along Zone 1 CB Route 1, showing the Horizons encountered by a cable at 1m or 2m depth below seabed .....	4-40
Figure 4-24: Zone 2 cable corridors (named by MarineSpace) overlain on British Geological Survey offshore bedrock geology and EMODnet hillshade .....	4-42
Figure 4-25: Cross-section along Zone 2 Corridor 1, showing the horizons encountered by a cable at 1m or 2m depth below seabed .....	4-45
Figure 4-26: Cross-section along Zone 2 Corridor 2, showing the horizons encountered by a cable at 1m or 2m depth below seabed .....	4-47
Figure 4-27: Cross-section along Zone 2 Corridor 3, showing the horizons encountered by a cable at 1m or 2m depth below seabed .....	4-49
Figure 4-28: Ridge and Runnel features on the southern margin of the Dogger Bank .....	4-51
Figure 4-29: Rippled Scour Depressions along Zone 2 Corridor 4, subparallel to the Doggerbank southwest margin (with updated 2023 Route A1 Centreline and KPs visible) .....	4-53
Figure 4-30: Rippled scour depressions crossing Zone 2 Corridor 4, between KP 154 and KP 155, and associated bed level change between 2021 and 2022 .....	4-54

Figure 4-31: Cross-section along Zone 2 Corridor 4, showing the horizons encountered by a cable at 1m or 2m depth below seabed .....	4-55
Figure 4-32: Cross-section along Zone 2 Corridor 5, showing the horizons encountered by a cable at 1m or 2m depth below seabed .....	4-57
Figure 4-33: Irregular depression features along the northern margin of the Dogger Bank South offshore wind farm area, and bed level change between 2011, 2021 and 2022 .....	4-60
Figure 4-34: Ridge and runnel features along the Dogger Bank South offshore wind farm margin, showing bed level change between 2019 and 2022 .....	4-62
Figure 4-35: A field of Rippled Scour Depressions along the northwestern margin of the Dogger Bank South offshore wind farm, with bed level change between 2019 and 2022 .....	4-64
Figure 4-36: Cable and pipeline infrastructure present within the DBS East offshore wind farm area	4-67
Figure 4-37: Rippled Scour Depressions interacting with the Cygnus A to Cygnus B gas pipeline ....	4-68
Figure 4-38: Digitised Twenty Fathom Contours from the 1812, 1854, 1916 and 1942 Admiralty Charts. EMODNET -36.5 and -36 mLAT (equivalents of Twenty Fathom Contour) contours have been added for comparison against an extensive “modern” dataset .....	4-70
Figure 4-39: Digitised -20 and -30 mLAT contours from the 1973 Admiralty Charts. EMODNET contours are also plotted .....	4-70
Figure 5-1: Simple model of controls on conductor temperature and hence cable rating. Boxes shaded in blue are non-environmental input parameters.....	5-1
Figure 5-2: The spatial and temporal (March [Upper Panel] vs September [Lower Panel]) variation in ocean bottom temperature from the AMM15v2 model for the Dogger Bank South cable routes and OWF – please note the different legend scales.....	5-4
Figure 5-3: Monthly ocean bottom temperature variation, from the AMM15v2 model at 20 km intervals along the Dogger Bank South northernmost cable route to DBS West centre. Smaller 1km intervals are shown between 110 and 120 to better demonstrate the variation along the Dogger Bank margin.....	5-6
Figure 5-4: Monthly ocean bottom temperature variation, from the AMM15v2 model at 20 km intervals along the Dogger Bank South northernmost cable route to DBS East centre .....	5-6
Figure 5-5: Monthly ocean bottom temperature variation, from the AMM15v2 model at 20 km intervals along the Dogger Bank South southernmost cable route to DBS East centre .....	5-7
Figure 5-6: Monthly ocean bottom temperature variation, from the AMM7v5 model at 20 km intervals along the Dogger Bank South southernmost cable route to DBS East centre .....	5-7
Figure 5-7: Daily mean ocean bottom temperature time series from the AMM15v2 model and the ODYSSEA satellite derived SST at each Dogger Bank South array centre .....	5-8

Figure 5-8: Location of the minimum and Maximum in August mean monthly ocean bottom temperature from the AMM15v2 model across the Dogger Bank South OWF areas .....	5-9
Figure 5-9: Location of the minimum and Maximum in August mean monthly ocean bottom temperature from the AMM7v5 model across the Dogger Bank South OWF areas .....	5-9
Figure 5-10: The spatial and temporal variation in difference between sea surface temperature and ocean bottom temperature from the AMM15v2 model for the Dogger Bank South cable routes and OWF, with values < 0.2 °C blanked out, showing onset of thermal stratification..	5-11
Figure 5-11: Difference between monthly mean sea surface temperature and sea surface temperature from the AMM15v2 model, at key intervals along the northernmost Dogger Bank South cable route (equivalent to Route A) .....	5-12
Figure 5-12: Difference between monthly mean sea surface temperature and sea surface temperature from the AMM15v2 model, at key intervals along Route C .....	5-12
Figure 5-13: CTD profiles taken across the general Dogger Bank South site in August (when stratification is strongest). The locations of the CTD profiles are marked in Figure 5-10 ....	5-13
Figure 5-14: 1015 thermal resistivity and porosity measurements taken on marine sediments from across the globe .....	5-14
Figure 5-15: Generic combined box, whisker & beeswarm scatter plot to define statistical parameters. In cases where the Maximum or Minimum values are within the IQR*1.5 or 3 limits the whiskers automatically snap to those real values. In this representation the whiskers represent.....	5-17
Figure 5-16: Combined box, whisker & beeswarm scatter plot of a thermal conductivity geodatabase. <i>Whiskers are based on <math>UQ+1.5*IQR</math> and <math>LQ-1.5*IQR</math> and snapped to highest/lowest values within these.</i> .....	5-18
Figure 5-17: Combined box, whisker & beeswarm scatter plot of the SOFIA thermal conductivity. <i>Whiskers are based on <math>UQ+1.5*IQR</math> and <math>LQ-1.5*IQR</math> and snapped to highest/lowest values within these.</i> .....	5-19

## List of Tables

Table 2-1: Fugro interpretation of seismic data for the Dogger Bank export cable centrelines, giving velocities used by Fugro for time to depth conversion .....	2-5
Table 4-1: Annual cliff erosion rates for the landfall sites, from Profiles 9-13 for the northern landfall and Profiles 25-30 for the southern landfall .....	4-7



Table 4-2: Predicted rates of erosion at the southern landfall, based on 3 methods. (From: Table 4, Castedo et al., 2015) .....	4-16
Table 5-1: Estimated daily accuracy for AMM7 V5 (Renshaw et al., 2021).....	5-2
Table 5-2: Normal Distribution Statistical Parameters used in WP2 .....	5-16
Table 5-3: Thermal Conductivity (W/mK) Geodatabase values and equivalents from the SOFIA site investigation campaign of potential sediments encountered in the Dogger Bank South area	5-20
Table 5-4: Standard statistical parameters calculated for each soil classification .....	5-24
Table 7-1: Extant reports for the Dogger Bank South, Landfall Site, Export Cable Corridor and Offshore Windfarm .....	6-7
Table 7-2: Extant data for the Dogger Bank South, Landfall Site, Export cable Corridor and Offshore Windfarm .....	6-7
Table 7-3: Extant data from external sources for the Dogger Bank South, Landfall Site, Export cable Corridor and Offshore Windfarm.....	6-8

# 1. Introduction

## 1.1. Project Summary

The Dogger Bank South (DBS) Offshore Wind Farm (OWF) is located approximately 135 km off the Holderness coast, East Riding, Yorkshire. The site has the potential to have an installed capacity of up to 3000 MW. The OWF covers an area of 989 km<sup>2</sup> and is split into DBS West (495 km<sup>2</sup>) and DBS East (494 km<sup>2</sup>) (Figure 1-1). At present there are 4 proposed export cable corridors (ECCs), with 2 landfall sites: one in the north, ~1 km south of Wilsthorpe near Auburn Farm, and the other in the south between Skipsea and Skirlington (Figure 1-2). All 4 ECCs meet approximately 43 km offshore. From 58-60 km offshore the routes split again, with 8 cable route combinations being considered to connect to the OWFs. These can be placed within an area ~1900 km<sup>2</sup>. The proposed scheme of work for this project will review the: general geology; the ambient temperature; thermal properties; and seabed mobility of both the OWF and the proposed ECCs.

The ECCs have been split for analysis purposes. Centrelines and kilometer points (KPs) have been generated for each route, and these have been referred to throughout. The routes were named based on the attributes in the shapefile provided to MarineSpace by RWE. “Zone 1” is from the landfall to the divergence of the CB Route Options at ~ KP60 offshore. Zone 1 consists of CB Routes 1, 2, 5 and 7 (Figure 1-3). Zone 2 consists of CB Routes Options DBS-CB-1(A) through to DBS-CB-1(H) from ~ KP60 offshore to the OWF areas. The CB Route Options in Zone 2 have been split into 3 main corridors, which are oriented approximately SW-NE, with a northernmost, central and southernmost corridor, named Zone 2 Corridors 1, 2 and 3 respectively. Two additional corridors, Corridors 4 and 5, are oriented approximately WNW-ESE from Corridor 2. Finally, Corridor 6 extends from Corridor 5. Each route and name for Zone 2 are shown in Figure 1-4.

The KPs for Zone 2 Corridors 1, 2 and 3 extend from the final point of Zone 1 Corridor 7: ~ KP 60. The KPs for Zone 2 Corridor 4 extend from the end of Zone 2 Corridor 1, at KP 124.9. The KPs for Zone 2 Corridor 5 extend from Zone 2 Corridor 2 KP 95. Due to the lack of any viable data in Corridor 6 it has not been necessary to assign KPs at this stage.

The above nomenclature has since been updated, as below:

**Table 1-1: The updated route nomenclature, as provided by RWE in February 2023**

MS Nomenclature	Updated RWE Nomenclature
Zone 1 CB Route 5	OF_RPL_Route_A_Centreline_20230216 (to KP 58)
Zone 1 CB Route 7	Deselected
Zone 1 CB Route 2	Deselected
Zone 1 CB Route 1	Deselected
Zone 2 - Corridor 1	OF_RPL_Route_A_Centreline_20230216 (from KP 58)

Zone 2 - Corridor 2	OF_RPL_Route_B_Centreline_20230216 (from KP 58)
Zone 2 - Corridor 3	Deselected
Zone 2 - Corridor 4	OF_RPL_Route_A1_Centreline_20230216 (from KP 123.94)
Zone 2 - Corridor 5	OF_RPL_Route_C_Centreline_20230216 (from KP 93.3)
Zone 2 - Corridor 6	Deselected

Key locations, including the major sandbanks: “South Smithic”, “The Hills”, “Bolders Bank”, “Inner” and “Outer Bank”, and “North West Riff”; have been identified in Figure 1-5: Dogger Bank South site location and landfall (inset), overlain on Admiralty charts 2182A-0 and 1190-0

**Figure 1-1: Dogger Bank South general site location, overlain on EMODnet bathymetry data**

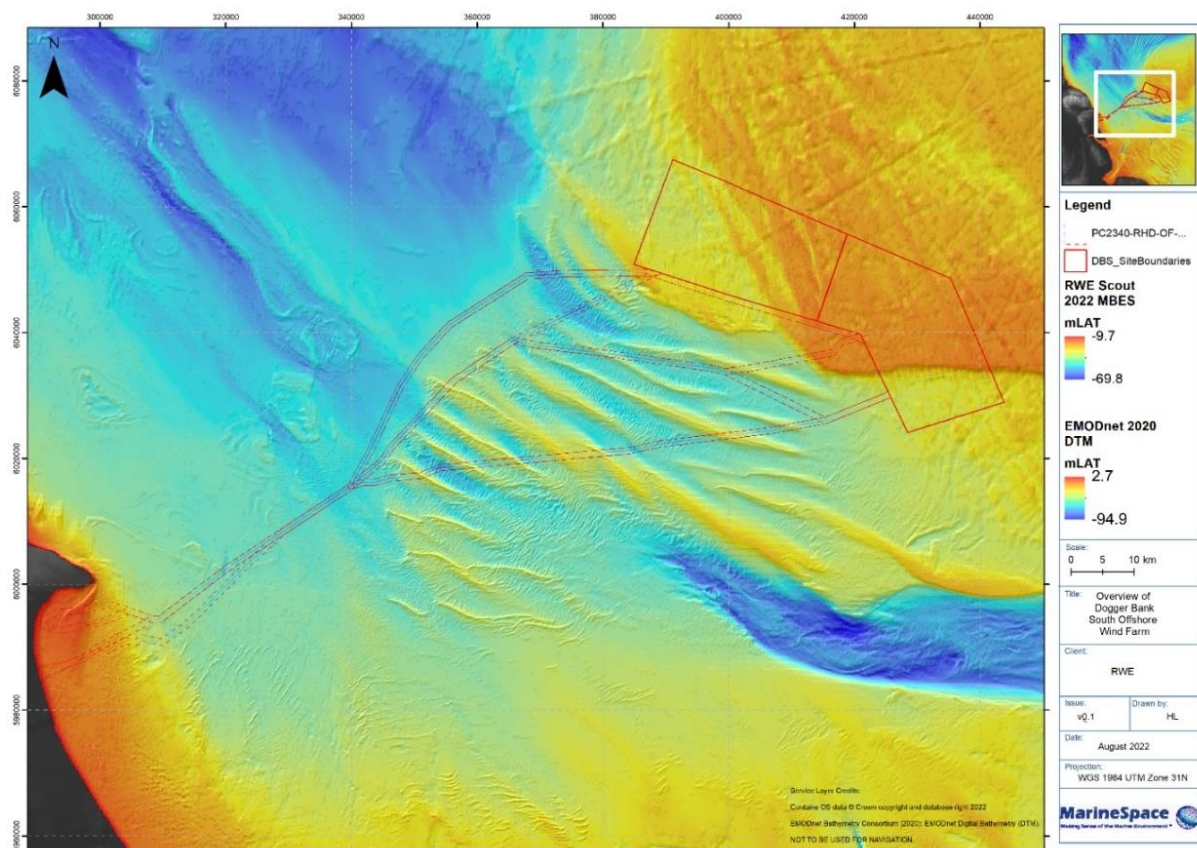


**Figure 1-2: Dogger Bank South export cable route landfall sites. Left-hand panel South Wilsthorpe to Auburn Farm land-fall site, right-hand panel Skipsea to north Skirlington landfall site**

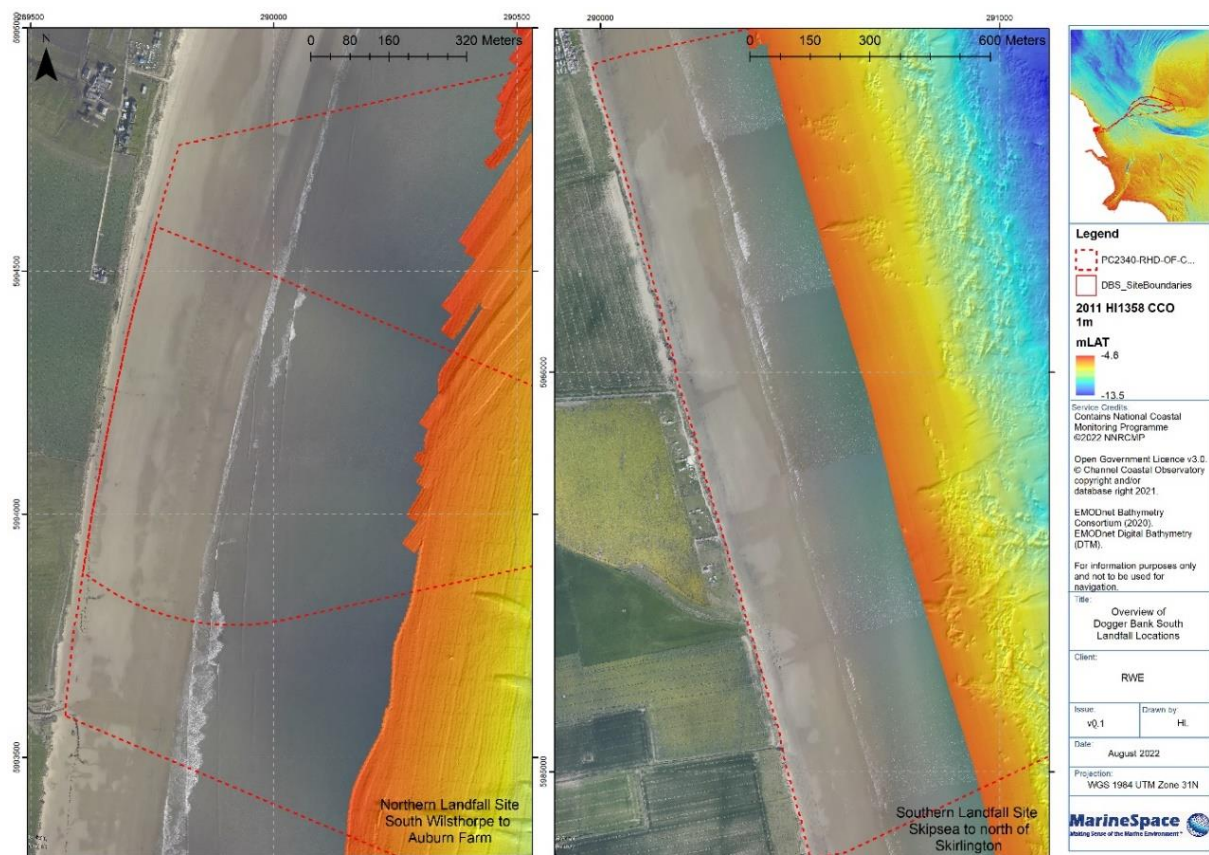




Figure 1-3: Zone 1 cable route options, as named by MarineSpace

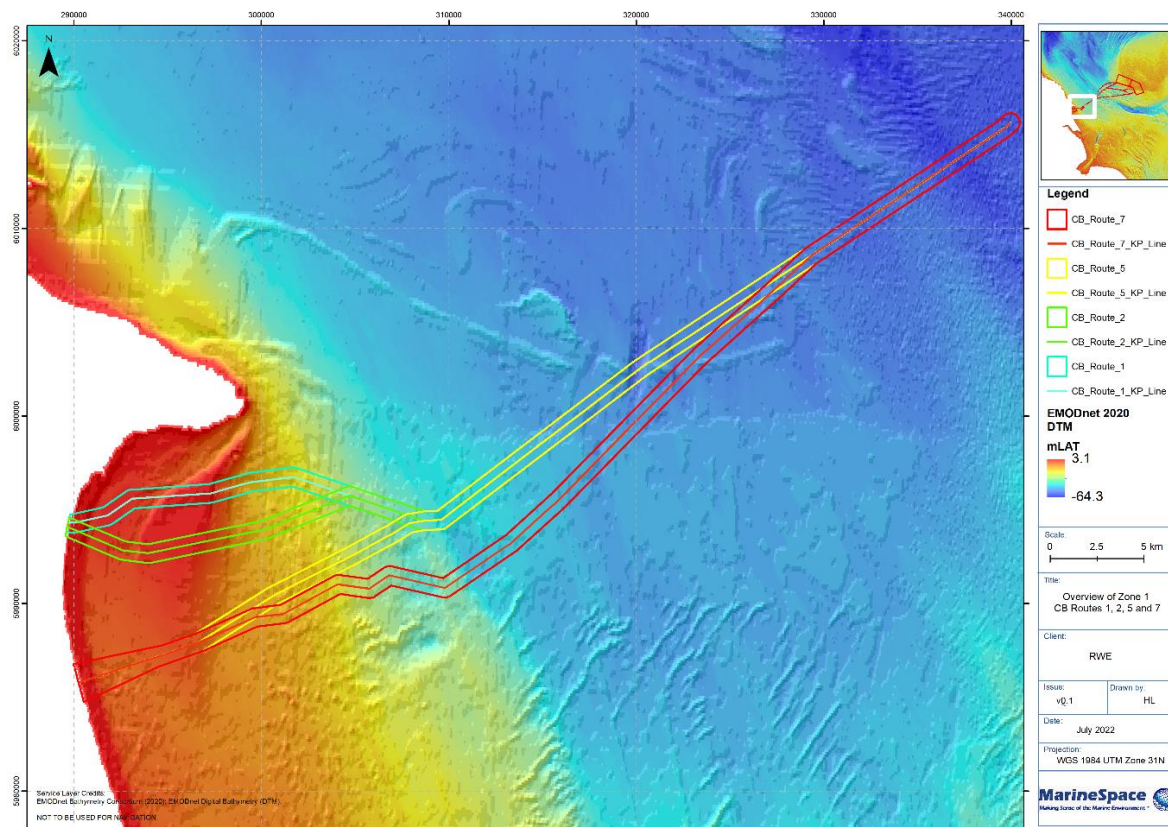
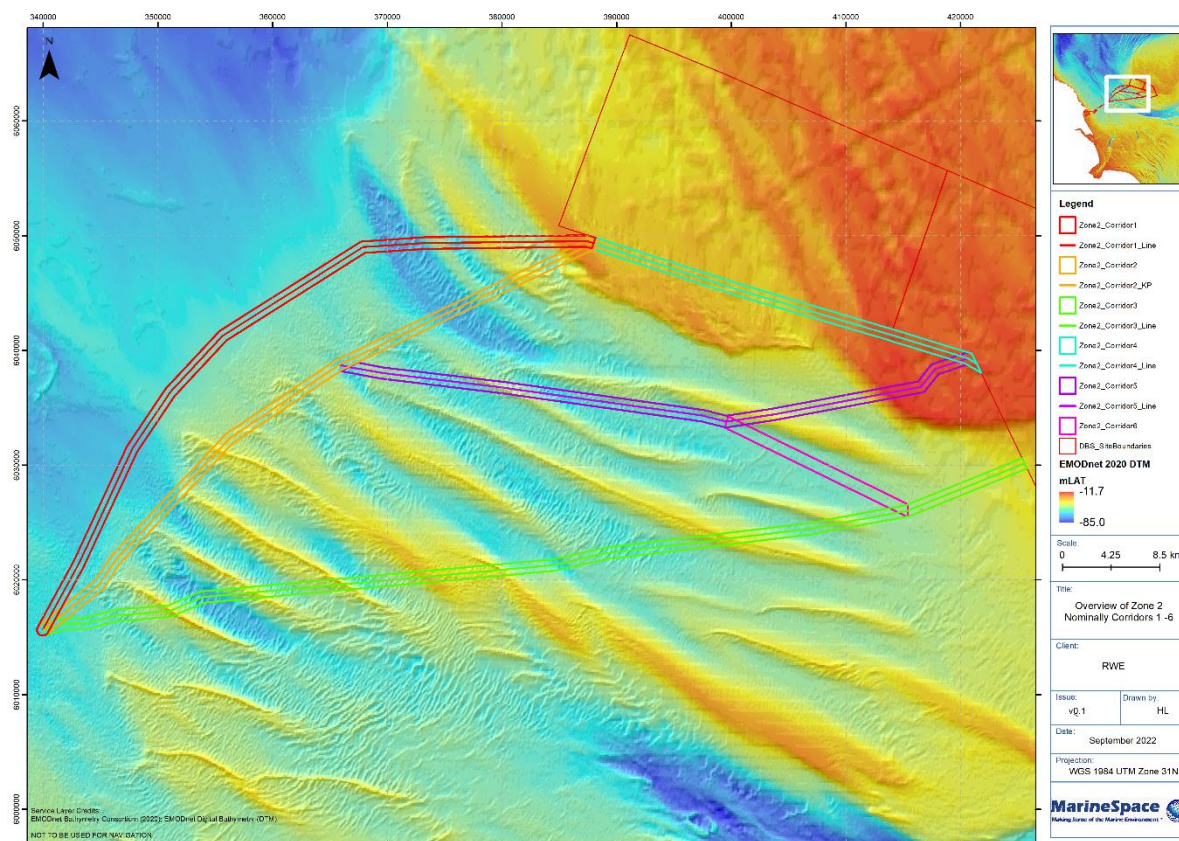
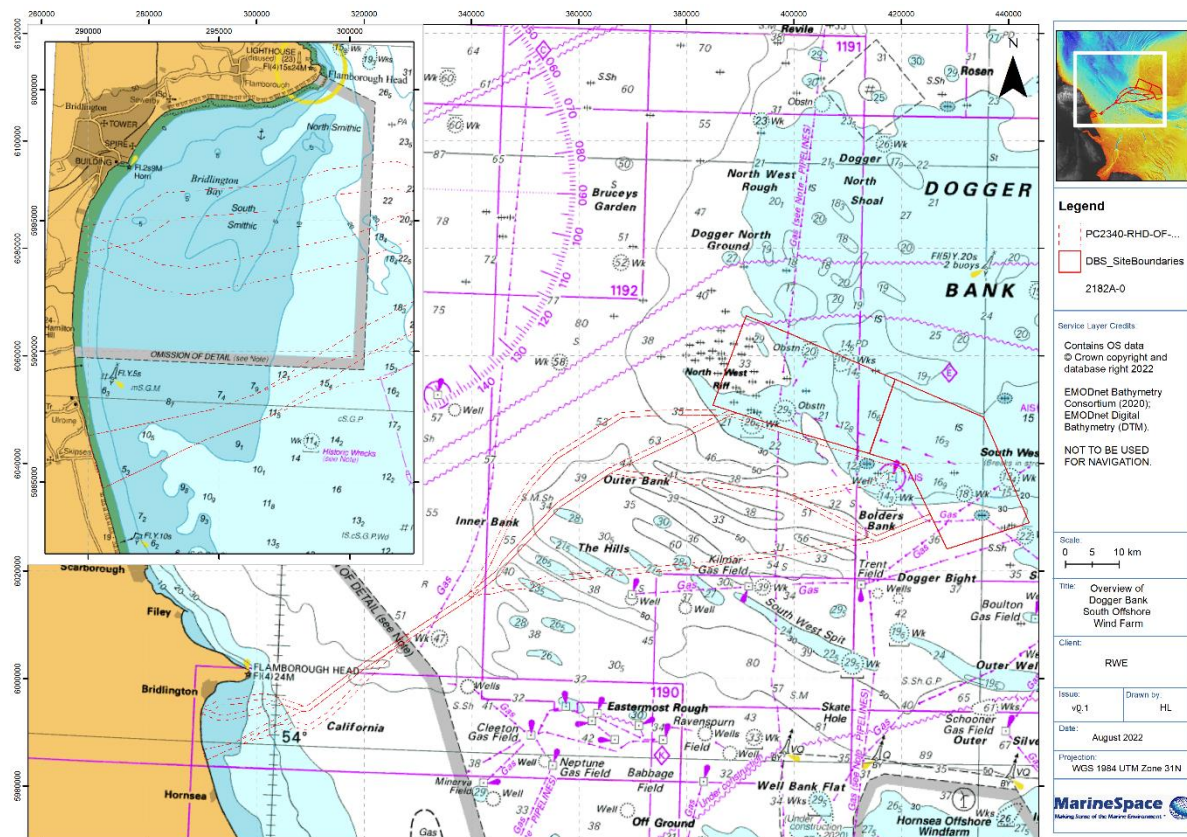


Figure 1-4: Zone 2 cable corridor options, as named by MarineSpace





**Figure 1-5: Dogger Bank South site location and landfall (inset), overlain on Admiralty charts 2182A-0 and 1190-0**



## 1.2. Scope and Objectives of Document

This document aims to:

- Provide a review of the geological history of the area covered by the proposed Dogger Bank South landfall sites, export cable corridors and offshore windfarm footprint;
- Describe the seabed morphology of the proposed Dogger Bank South landfall sites, export cable corridors and offshore windfarm footprint, with particular focus on seabed mobility and where possible place this in the context of the known hydrodynamic regime;
- Describe the spatial and temporal ocean bottom temperature environment for the ECC and the OWF and provide estimates for groundwater temperature at the landfall site;
- Based on generic measurements of similar sediment/bedrock types provide an overview of the potential thermal conductivity/resistivity values that maybe encountered across both the offshore and landfall locations and provide recommendations for a thermal sampling strategy to ensure all key geological units are captured and the best possible thermal measurements are obtained;
- Recommend locations and order of geophysical survey to best capture seabed movement within the survey timeframe, with particular emphasis on RSD's.

The report conclusions will summarise potential bed mobility across the ECCs and OWF and the thermal environment likely to be encountered in relation to ambient temperature variation; thermal conductivity/resistivity of seabed and post-installation depth of cover changes.

## 2. Data Source Summary

A small number of site-specific datasets were provided by RWE Ltd. but the majority of the data used in this assessment was acquired from a wide range of publicly available sources. The details and references for each dataset/report are provided in Appendix A. The following sections provide an overview of the data that has been used in this review.

### 2.1. Geophysical Survey

#### 2.1.1. Bathymetry

A total of 7 swath bathymetric surveys are available for the study area (Figure 2-1), 2 acquired specifically for the DBS project and 5 from publicly available sources:

- **2011 - Gardline Geosurvey, Zone 3, Tranche B, Recon ECR geophysical survey of Dogger Bank** (Sourced from the Marine Data Exchange (MDE): Table 6-3: Extant data from external sources for the Dogger Bank South, Landfall Site, Export cable Corridor and Offshore Windfarm - Item 10. A multibeam echosounder survey (MBES) was undertaken, between June and September 2011, over the southwestern margin of the Dogger Bank for Forewind Ltd. The survey was conducted over a total area measuring approximately 150 km by 35 km, split into two areas. In the west mainlines are orientated 068°, 248°, spaced at 4 km and crosslines are perpendicular, spaced at 20 km; in the east mainlines are orientated 075°, 255°, spaced at 4 km and crosslines are perpendicular, spaced at 20 km. Data was collected on the MV Tridens1 and MV L'Espoir. The survey utilised single beam and multi-beam echo sounders.

Data was provided in ASCII format, binned to a 5m resolution in WGS 1984 UTM Zone 30°N, with vertical datum equivalent to mLAT. No further information, such as a survey or interpretive report, was available. It provides limited coverage of north and west of the OWF, particularly DBS West. The data is of good quality although there is significant spacing between survey lines.

- **2011 - HI1358 Spurn Point to Flamborough Head Blk2:** An MBES survey of the coastal strip along the Holderness Coastline, from Spurn Point to Flamborough Head, extending from the 2m contour to ~ 2 – 7 km offshore, and was conducted by NetSurvey Ltd (MMT Group) between 07 January to 05 May 2011 on the vessels MV Xplorer and MV AV-IT (Sourced from the Channel Coastal Observatory (CCO): Table 6-3 - Item 11).

Positioning was provided by a POSMV using RTCM corrections from the IALA dGPS system. A Post Processed Kinematic (PPK) solution was applied to derive a full 3D navigation solution using Applanix POSMMS. A dual head Reson 7125 SV was used to acquire bathymetric data at a frequency of 400kHz, and the data processed using CARIS HIPS and IVS Fledermaus Professional. A PPK vertical height and VORF datum transitional model was used to reduce soundings to chart datum (equivalent to mLAT). The data originally processed into ETRF89 horizontal datum but was downloaded from the CCO in British National Grid as an XYZ file. It

was corrected to WGS 1984 UTM Zone 31°N in ArcGIS using transformation OSGB\_1936\_To\_WGS\_1984\_7.

It provides good coverage at a 1m resolution of the nearshore ECR landfall areas to approximately 2.2 km offshore, although more extensive coverage is provided for the northernmost route – Zone 1 CB Route 1 – to approximately 7.2 km offshore from the northern landfall site. Data quality is very good.

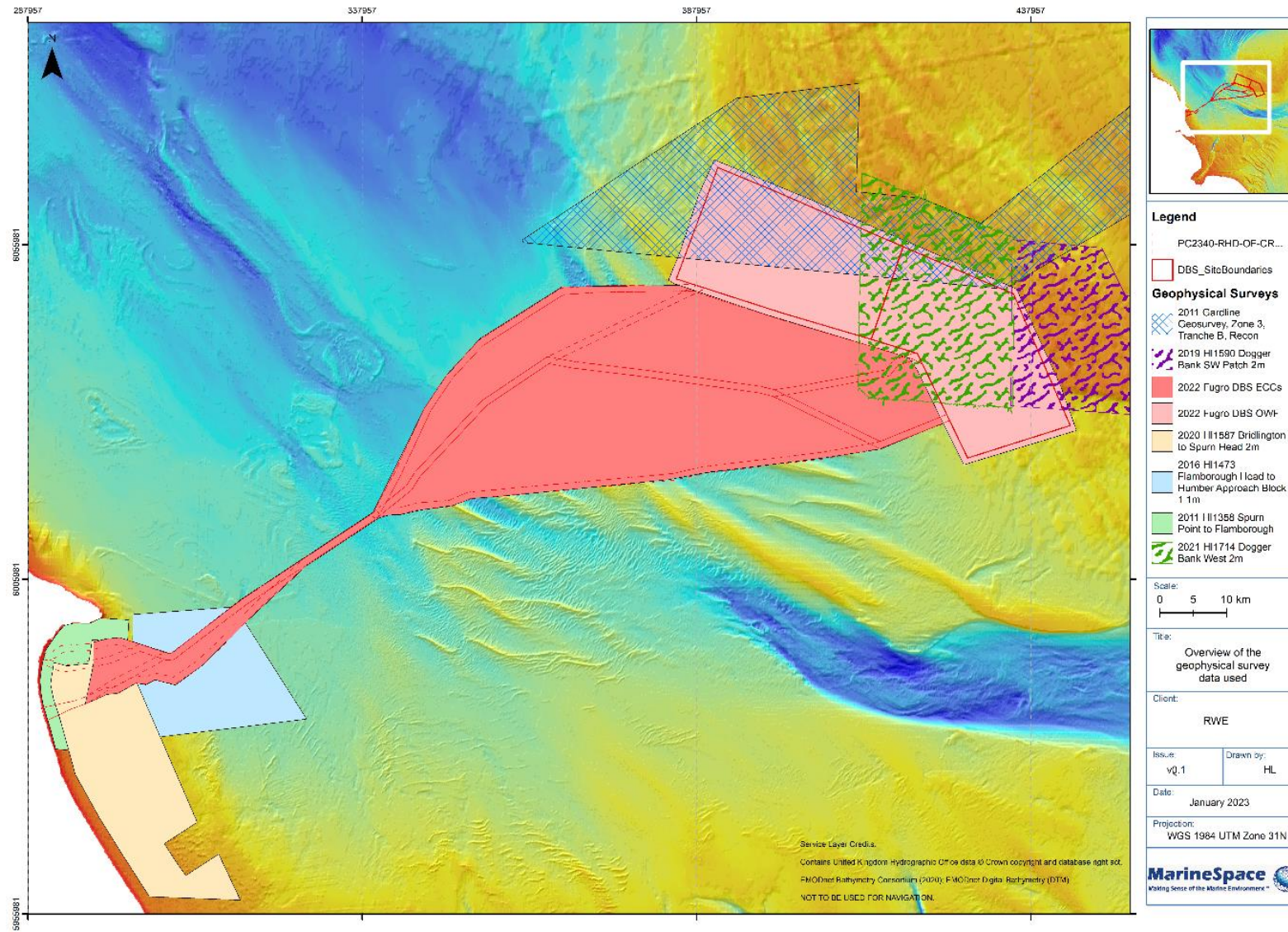
**2016 - HI1473 Flamborough Head to Humber Approach Block 1:** An MBES survey was undertaken by MMT, between 15 January and the 12 April 2016. The data was downloaded from the UKHO Admiralty Marine Data Portal (AMDP - Table 6-3; Item 12) in WGS 1984 UTM Zone 31°N and vertical datum was Chart Datum (equivalent to mLAT). No further information was available regarding data processing or instrumentation, nor was a survey or interpretive report available. The data is at a 1m resolution, complete, and of good quality. It provides coverage of the whole width of the ECR corridor area past Flamborough Head to approximately 12.7 – 14.8 km offshore from the landfall sites.

- **2019 - HI1590 Dogger Bank SW:** An MBES survey of the Dogger Bank Southwest Patch, was undertaken between 28 March and 02 June 2019. The data was downloaded from the UKHO AMDP (Table 6-3; Item 13). Horizontal datum was in WGS 1984 UTM Zone 31°N, whilst vertical was in Chart Datum (equivalent to mLAT). Navigation used RTK DGPS, but no further information or reports were available. The data is binned at a 2m resolution. The dataset covers the eastern edge of the DBS East OWF area, and further along the southern margin of the Dogger Bank. Whilst direct coverage is limited it is beneficial for considering larger scale features and the spatial extent of features where the OWF coverage is otherwise limited.
- **2020 - HI1587 Bridlington to Spurn Head:** An MBES survey of the alongshore strip from Bridlington to Spurn Head, was undertaken between 01 August and 21 September 2019. Data was downloaded from the UKHO ADMP (Table 6-3; Item 14). Horizontal datum was in WGS 1984 UTM Zone 30°N, whilst vertical was in Chart Datum. Navigation used a DGPS system, but no further information or reports were available. The data is binned at a 2m resolution. The dataset covers the complete width of the cable corridors between from 2 km offshore to approximately 12 – 14.5 km offshore. The data is of good quality, and complete.
- **2021 HI1714 Dogger Bank West:** An MBES survey of the Dogger Bank West Patch was undertaken between 30 May and 09 October 2021 by A-2-Sea Solutions Limited. Data was downloaded from the UKHO ADMP (Table 6-3; Item 14). The horizontal datum was originally in ETRS89\_UTM\_zone\_31N, transformed to WGS\_1984\_UTM\_Zone\_31N in ArcGIS. Vertical elevation was not defined but appears to align with Chart Datum or mLAT (equivalent). The data is binned at a 2m resolution. The dataset covers an area of 67.4 km<sup>2</sup> on the eastern margin of DBS West and an area of 337.7 km<sup>2</sup> across the west of DBS East. It also covers parts of 2 of the Zone 2 ECR options: Corridor 4 (KP 150.4 to end of route) and Corridor 5 (KP 141.9 to end of route). The data is of good quality and coverage.



- **2022 - Fugro:** The most recent MBES surveys were undertaken on the Fugro Scout (and Frontier for the Recon survey), between 30 May and 14 June 2022. The data was processed by Fugro, with vertical datum in mLAT and horizontal in WGS 1984 UTM Zone 31°N. It was provided to MarineSpace Ltd as a raster surface gridded at 1m bin size (RWE, 2022: Table 6-3 - Items 4, 5 and 6). The data covers a strip between 500 m and 1 km wide along the cable corridor centrelines, and a grid with approximately 1km x 2km spacing across the OWF. The data is of good quality and is complete.

Figure 2-1: Overview of bathymetric survey footprints for Dogger Bank South export cables and offshore wind farm



### 2.1.2. Seismic Data

Fugro acquired sub-bottom profile data offshore with an Innomar system on the Fugro Scout from approximately 6.5 – 8 km offshore, along the cable routes. MarineSpace Ltd. were provided with preliminary .dat files of two-way travel time to interpreted horizons (RWE, 2021: Table 6-2 – Item 8). All seismic data is acquired in two-way travel time (TWT) which can then be converted to depth in metres using the following equation:

$$D = 0.5V_{sed}t$$

Where,  $D$  is depth in metres,  $V_{sed}$  is sediment velocity ( $\text{ms}^{-1}$ ) and  $t$  is two-way travel time (seconds). The files were also provided in depth (both meters below LAT and meters below seafloor).

No reports, rasters, or ground model were provided. The velocity values used for time to depth conversion of the surfaces was  $1600 \text{ m s}^{-1}$  for all horizons.

The interpreted data identified 10 preliminary horizons: H05b, H10b, H15i, H20b, H25b, H26i, H28i, H30b, H34i, and H35b (Table 2-1). As well as the seabed surface (MBES), a further 5 horizons were identified including: “bedrock at seafloor”, “amplitude anomalies”, “acoustic blanking”, “gravel accumulation”, and “pipeline infrastructure”.

**Table 2-1: Fugro interpretation of seismic data for the Dogger Bank export cable centrelines, giving velocities used by Fugro for time to depth conversion**

Horizons	Interval Velocity Used ( $\text{ms}^{-1}$ )	Zones	Depth below seabed (m)	Initial Interpretation	Geological Correlation
H05_b	1600	All	Rarely > 2m depth below seabed	Upper Sand Unit Occurs at the near-surface, at the nearshore off the South Smithic Bank and also where large to very large subaqueous dunes or other seabed features are present	Holocene post-transgressive sand
H10_b	1600	All	Mean <5 m but up to 10 m	Lower Laminated Sand Unit Occurs often below H05_b, at the nearshore off the South Smithic Bank and also where large to very large subaqueous dunes or sandbanks are present.  Is not identified but likely is present under The Hills. Not identified on the Dogger Bank.	Holocene post-transgressive sand

Horizons	Interval Velocity Used (ms <sup>-1</sup> )	Zones	Depth below seabed (m)	Initial Interpretation	Geological Correlation
H15_i	1600	Zone 2 Corridor 4 and 5	Identified to 5m	Lower Crossbedded Sand Unit Identified only in Zone 2 Corridors 4 and 5, following the seabed morphology. Only present on the Dogger Bank margin.	Holocene post-transgressive sand
H20_b	1600	Zone 2	Generally < 5m, up to ~ 8m	Lower Crossbedded Sand Unit Only identified in the valleys between The Hills sandbanks, and over the Dogger Bank margin.	Holocene post-transgressive sand
H25_b	1600	Zone 2 Corridor 4	Highly variable, identified up to over 10m	Buried Channel Sequence Only identified along Zone 2 Corridor 4 in the runnels off the Dogger Bank southwest margin. Distinctly channel shaped deposits.	
H26_i	1600	Zone 1	< 5m	Bolders Bank Till 1 Only identified infrequently in Zone 1. Occurs around areas of rocky outcrop at the seabed, and around bathymetric depressions.	Bolders Bank Till
H28_i	1600	Zone 1	< 5m	Channel Bolders Bank Till 1 Occurs only in Zone 1, at the base and margins of the bathymetric depressions related to ridge features associated with changes in underlying bedrock.	Bolders Bank Till
H30_b	1600	Zone 1 and Zone 2 Corridor 1	Generally < 5m but up to 10m	Bolders Bank Till 1 Identified extensively in Zone 1, but only the initial 10 km of Zone 2 Corridor 1, where subaqueous dunes are present. H30_b is at or near the surface where bathymetry indicates a rocky seabed surface. It deepens where bedforms are present.	Bolders Bank Till

Horizons	Interval Velocity Used (ms <sup>-1</sup> )	Zones	Depth below seabed (m)	Initial Interpretation	Geological Correlation
				Tends to hold a high frequency of amplitude anomalies above.	
H34_i	1600	Zone 1	In channels up to 6.5m below the seabed surface	Bolders Bank Till 2 Occurs below H30_b along Zone 1 CB Route 7, where it appears to define the base of a channel feature. Along CB Route 1 it appears to define a channel feature just below the seabed surface.	Bolders Bank Till
H35_b	1600	Zone 1	Up to ~6m, likely extend further	Bolders Bank Till 2 Identified at depth, occasionally coming to the seabed surface where it is rocky.	Bolders Bank Till
Bedrock_at_Seafloor	n/a	Zone 1 and Zone 2 Corridor 2		Bedrock outcrop at seabed surface, in two-way travel time	Bedrock
Acoustic Blanking	1600	All		Acoustic Blanking	
Amplitude Anomaly	1600	All	1-4 m	Amplitude anomaly	
Gravel coarse material accumulation	1600			Gravel/coarse material accumulation	
Pipeline Infrastructure	1600	All	Surface	Pipeline infrastructure	

## 2.2. Geological Data

MarineSpace have made use of the British Geological Survey (BGS) WMS products and BGS Geoindex portals for both the onshore and offshore areas.

Onshore, these included: the bedrock geology (1:50000 scale); superficial deposits (1:50000 scale); hydrogeology (1:625000 scale); borehole records and aquifer properties. MarineSpace have also

used the BGS: offshore bedrock data, seabed and surface sediment data (all 1:250000 scale); seismic reflection data; drill sample data; core sample data; and seabed sediment data (Folk Classification). We have also referred to their Quaternary deposits summary lithologies, Quaternary deposits thickness, and bedrock summary lithologies. The offshore cores referred to were all taken from a 1981 BGS cruise: 1981/8. The drill core sample used was collected by BGS in a 1983 cruise: 1983/1. For more information on individual samples used, see Appendix B.



### 3. Geological Context

#### 3.1. Offshore Bedrock Geology

The bedrock along the export cable route and within the windfarm is composed of: the Jurassic Lias Group (LG), West Sole Group (WSG), Oxford Clay Formation (OXC), Corallian Group (CRG) and Kimmeridge Clay Formation (KCF); the Cretaceous Cromer Knoll Group (CKG) and Chalk Group (CG) and, in the OWF, undifferentiated Palaeocene and Eocene deposits (Figure 3-1, British Geological Survey, 2022a, b and c). Within the following Sections locations relate to the KP values for each Route section as outlined in Section 1.1. Further, more route specific descriptions of the at or near surface occurrence of bedrock will be described in Section 4.1.2 and 4.1.3.

##### 3.1.1. Jurassic: Lias Group, West Sole Group Oxford Clay, Corallian Group and the Kimmeridge Clay Formation

Offshore, between KP 36 of Zone 1 CB Route 7 and KP 65 or 66 of Zone 2 (all 3 corridors) are sub-crops and potential outcrops of a suite of Jurassic rocks that range from the Lias Group (Lower Jurassic – 201.4-174.1 Ma) to the Kimmeridge Clay Formation (Upper Jurassic – 157.3-152.1 Ma). From the available data and literature these can be broadly sub-divided into the following Groups and Formations (note where no specific reference rock descriptions are taken from the BGS Lexicon of Named Rock Units):

**Lias Group (LG):** offshore, this group comprises dominantly mudstones and argillaceous limestones in 4 formations: Cerdic Formation, Ida Formation, Offa Formation and Penda Formation. In DBS ECC it is probably the Cerdic Formation a dominantly dark grey marine mudstones with sporadic, thin argillaceous limestones, that is present. Correlation of the spatial distribution of the LG with the proposed cable routes suggests it may only be encountered between KP 40 and KP 45 in Zone 1 of the ECC, between KP 43 and KP 45 on Zone 1 CB Route 7 and KP 40 and KP 42 on the remaining Zone 1 routes. However, the thickness of overlying Quaternary deposits suggests it is unlikely to be encountered at trench depth ( $\leq 3$  m) other than between KP 103 and KP 106 on the Zone 2 Corridor 3 where there is a seabed depression on the southwestern margin of one of the banks.

**West Sole Group (WSG):** offshore the group comprises marine sandstones, siltstones and mudstone which can be sub-divided into 4 formations: Wroot, Strangways, Hudleston and Leckenby (Barron et al., 2012). Correlation of the recent bathymetry, and preliminary seismic interpretation (which does not directly image top bedrock but has been inferred from locations where no Quaternary horizons are present) suggest the WESG outcrops or may subcrop within potential trench depths ( $\leq 3$  m), between KP 42 and KP 45 of Zone 1 CB Route 7 and KP 42 to 43 of the other Zone 1 routes. Based on the BGS mapping the WSG crosses the ECC between KP 87.5 and KP 88.5 of Zone 2 Corridor 1; and between KP 88.5 and KP 92 of Zone 2 Corridor 2. Between these sections the bedrock does not appear or is unlikely to be at or near the seabed surface, or within potential trench depths, based on the current interpretation of the SBP data.

**Oxford Clay (OXC):** is identified in the BGS 1:250000 Offshore Bedrock map but is more typically described offshore as being part of the Humber Group (HMBG) which also includes offshore correlatives of the Corallian Group and Kimmeridge Clay Formation (Barron et al., 2012). The OXC

are dominantly silicate mudstones with sporadic beds of argillaceous limestone nodules. Bedrock clearly outcrops along the route between KP 34.5 and KP 36, and KP 43 and KP 43.5 of Zone 1 CB Route 5, and KP 38 and KP 39.5, and KP 43.7 and KP 45.5 of Zone 1 CB Route 7, at a location that correlates with the purported OXC distribution. These horizons may represent more competent sandstone or limestone beds of either the underlying WSG or the overlying CRG. OXC may also potentially occur within trench depth between KP 81.8 and KP 82.7 as well as KP 87.2 and KP 87.5 of Zone 2 Corridor 1, and KP 88.4 and KP 88.6 of Zone 2 Corridor 2 but elsewhere the occurrences of OXC appears to be at depth.

**Corallian Group (CRG):** onshore this is described as a complex succession of interdigitating limestones, marls, sandstones, siltstones and mudstones, whilst the BGS 1:250000 Offshore Bedrock map suggests the CG is a limestone dominated unit. The route may cut through this unit between KP 35 and KP 36, and KP 43 and KP 43.5 of Zone 1 CB Route 5, and KP 38.5 and KP 39.5, and KP 45.2 and KP 45.6 of Zone 1 CB Route 7, where it may outcrop or at least be very close to the surface. It may also potentially occur within trench depth between KP 81 and KP 83 as well as KP 87 and KP 87.2 of Zone 2 Corridor 1; as well as KP 88 and KP 88.4 of Zone 2 Corridor 2. As with the OXC it may well be beyond trench depth at other localities, such as between Zone 1 CB Route 7 KP 50.5 and KP 51.5. Borehole records (sample names: +54+000/316/CS/1, +54+000/372/CS/1 and +54+000/315/CR/1) across the area of bands of changing bedrock, north of KPs 47 to 52 of CB Route 7, indicate sandstones and limestones at the seabed surface (Corallian Group and Kimmeridge Clay).

**Kimmeridge Clay Formation (KCF):** in the Central North Sea the KCF comprises dominantly of non-calcareous to weakly calcareous, partly fissile, moderately to highly organic-rich mudstone. Thin sandstone and conglomerate interbeds do occur at various levels and locally have been given member status where they thicken. The KCF potentially crosses the route at a number of locations. In Zone 1, all routes may potentially be affected at locations between KP 32 and KP 35 of Zone 1 Route 5, or KP 36 and KP 39 of CB Route 7, with visible ridges in the bathymetry at these locations, and outcropping of bedrock at the surface identified in SBP interpretation. Between KP 45.5 of CB Route 7 (which all routes follow) to ~ KP 66 of all Zone 2 routes, KCF may be close to the surface and within trench depth. In Zone 2 Corridor 2, 2 boreholes from 1981 located 470m apart fall within the route corridor between KPs 62 and 63 (sample names +54+000/150/CS/1 and +54+000/320/CS/1). One borehole (+54+000/320/CS/1), in a present-day field of small to large subaqueous dunes, sampled mudstone (Kimmeridge Clay) at the surface. The other sampled sand and siltstone to its terminal depth of 0.4m.

### **3.1.2. Cretaceous Cromer Knoll Group and Chalk Group**

The Cromer Knoll Group (CKG) is a Lower Cretaceous (145-100.5 Ma) argillaceous unit consisting of calcareous claystones, siltstones and marlstones with subordinate layers of limestones and sandstones (Gradstein et al., 2016). It crosses all route options, in Zone 1, between KP 29 and 32 of CB Route 5 or KP 33.5 and KP 36 of CB Route 7. The CKG occurs as an outlier which traverses all 3 corridors (Zone 2 Corridor 1, 2 and 3) just after they split between Zone 2 KP 65 and KP 71, 72.4 and 78.6 respectively. Stratigraphically, the CKG is overlain by the Upper Cretaceous Chalk Group.

A borehole record (+54+000/338/CS/1) between KPs 30 and 31 of Zone 1 CB Routes 1 and 2 indicates a 0.1m covering of gravelly muddy sand over probable chalk (likely Cromer Knoll bedrock).



Onshore the Chalk Group has been mapped in to the lower Flamborough Formation (86.3-72.1 Ma) and the overlying Rowe Chalk Formation (72.1-66 Ma) which is the youngest of the Cretaceous Chalks in the whole Yorkshire region. The Rowe Chalk Formation is a white flint-bearing chalk with sporadic marl bands, whilst the underlying Flamborough Formation is essentially flint free. The boundary between these two Formations is just south of the northern landfall site. The whole Chalk group has an easterly dip resulting in a general expansion of the sequence offshore reaching a thickness of over 800 m ~40 km offshore in a Late Cretaceous basin adjoining the Sole Pit trough (Sumbler, 1999). The offshore geological data does not differentiate down to the Formation Level but the Chalk Group outcrops at or near the seabed until ~ KP 29 -32.

Further offshore the Chalk Group again outcrops between KP 71 and KP 73.5 of Zone 2 Corridor 1; between KP 83 and KP 88 of Zone 2 Corridor 2; and between KP 73 and 76 of Zone 2 Corridor 3. Also, between KP 90 and KP 112 of Zone 2 Corridors 1 and 2, and KPs 92 – 118 and KPs 128 – 137 of Zone 2 Corridor 3, as well as in areas between KP 95 and 132 of Zone 3 Corridor 5 and likely also along Corridor 6. In terms of Stratigraphic nomenclature, the Flamborough Formation correlates with the Jukes Formation offshore, whilst the Rowe Formation maintains the same nomenclature (Gradstein et al., 2016).

### **3.1.3. Undifferentiated Palaeocene and Eocene**

Underlying the western margin of the Dogger Bank and south toward the Outer Well Bank and Outer Silver Pit the bedrock has only been described by the BGS as consisting of undifferentiated Palaeocene and Eocene material consisting of mudstones, sandstones, tuffs and lignites. However, these earlier deposits are almost exclusively overlain by thick sequences of Quaternary deposits and so bedrock from this sequence is unlikely to be encountered at trench depth.

Figure 3-1: Offshore Bedrock, faults and hard substrate from British Geological Survey (2022). Offshore boreholes reviewed as part of this study are also marked.

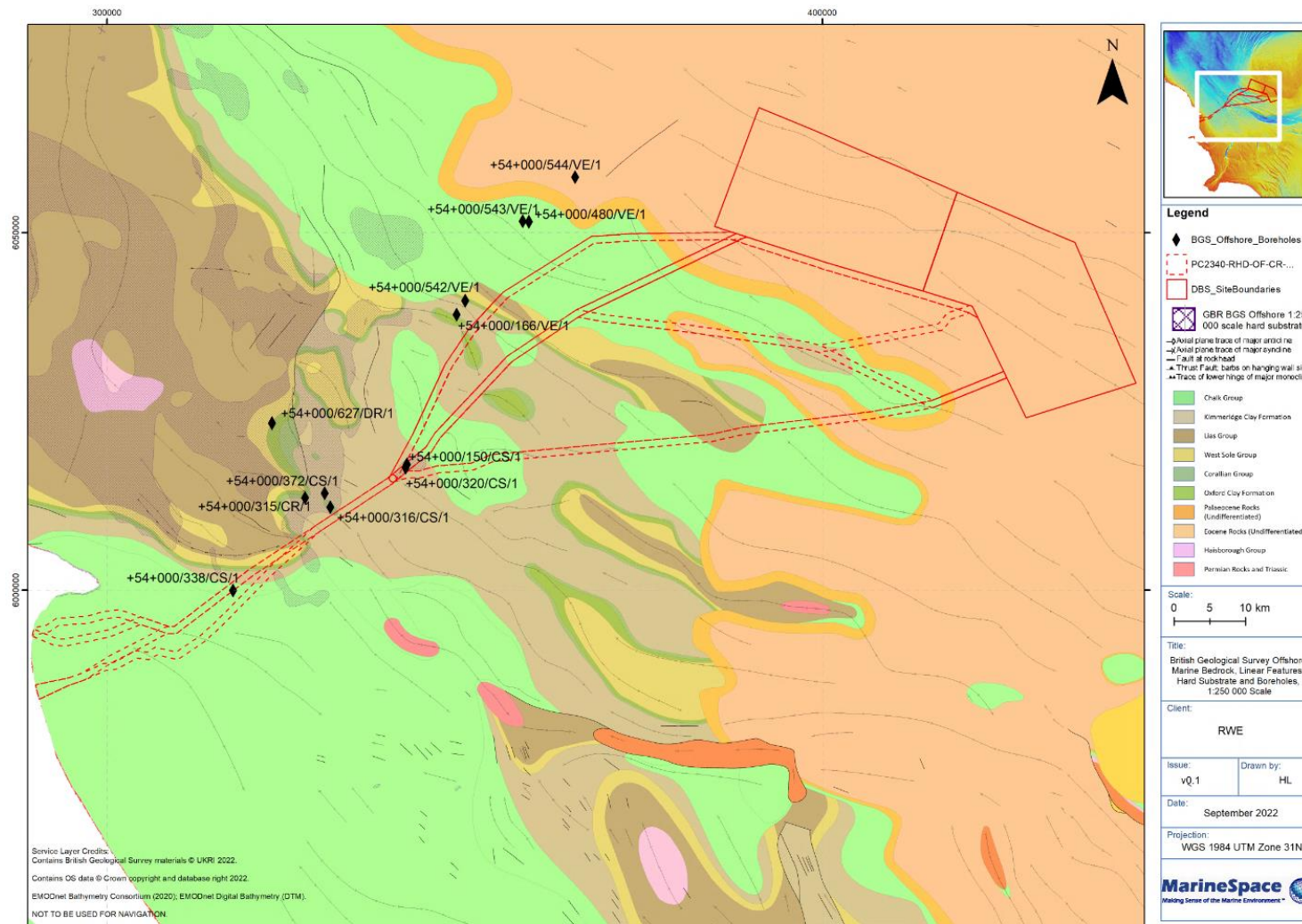
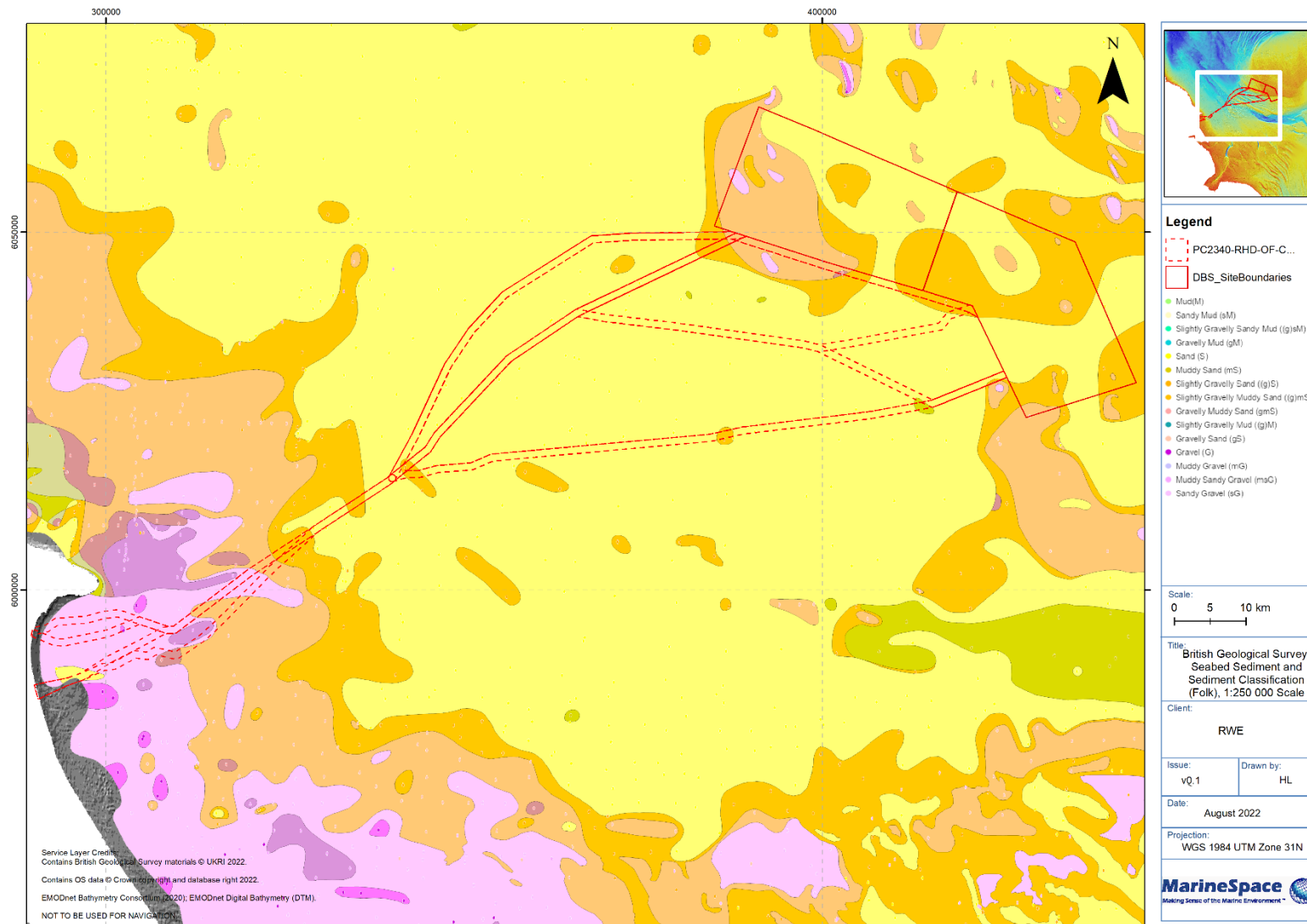


Figure 3-2: Offshore seabed sediment and sediment (Folk Classification) from British Geological Survey (2022)



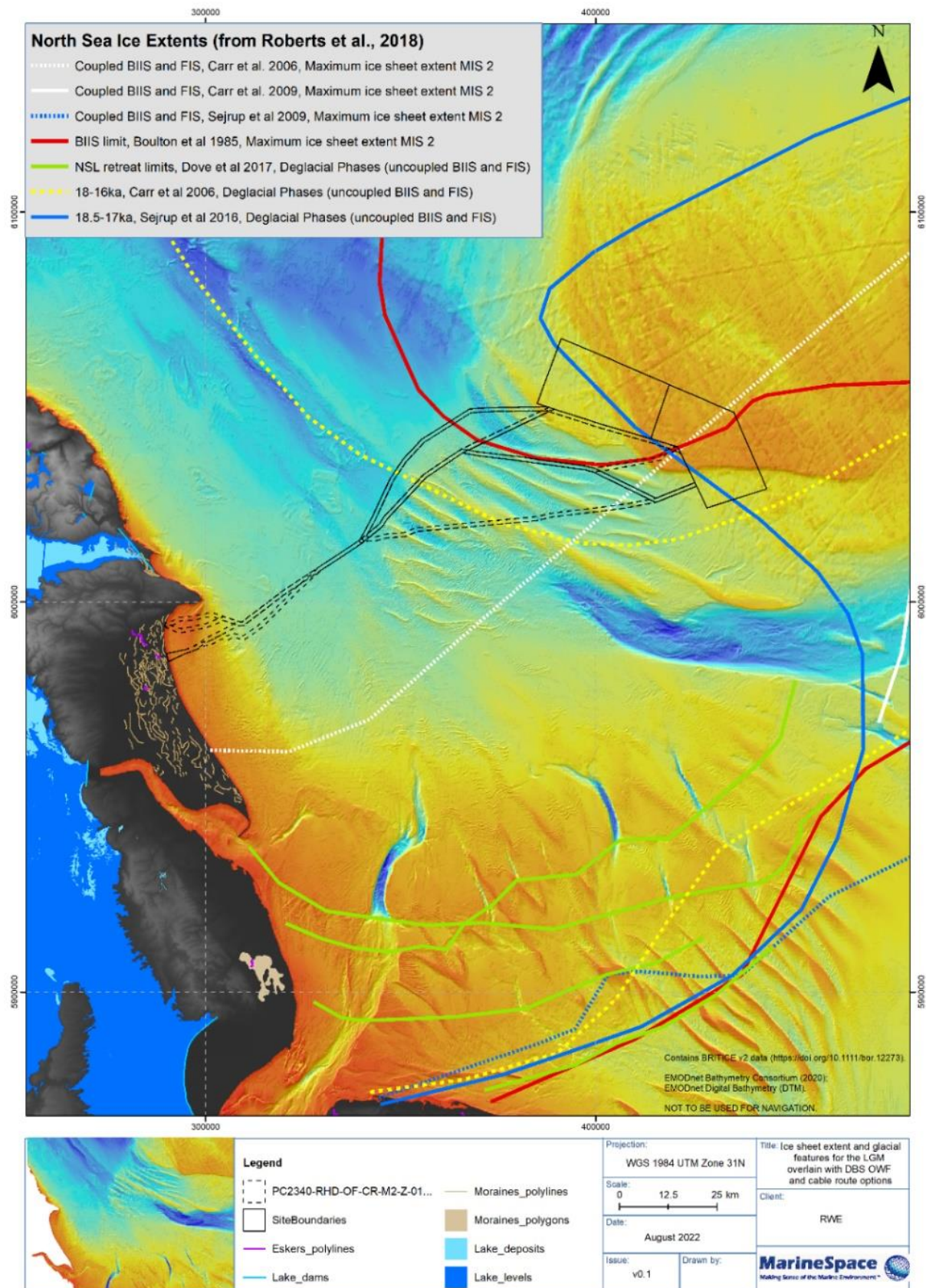
### **3.2. Late Quaternary Geology**

The North Sea is the product of its Late Quaternary glacial history and subsequent reworking since the Last Glacial Maximum (LGM). The area has been subject to 3 major glaciations during the Middle to Late Pleistocene, the Anglian (MIS 12, ~420 kaBP), Wolstonian (MIS 6, ~130 kaBP) and Devensian (MIS2 – build-up from ~35-32 kaBP, maximum LGM extent 27-21 kaBP and retreat/readvance phases between 19-17 kaBP) glaciations respectively. The geology of this area of the southern North Sea is therefore the product of the environmental change driven by the growth and decay of these ice sheets. The exact location of the maximum extent of all of these ice sheets is still the subject of debate (Clark et al., 2022), this being most clearly illustrated by the multiple interpreted maximum extents and retreat positions of the LGM ice sheet (Figure 3-3).

The Anglian ice sheet extent reached as far south as Essex, whilst the subsequent Wolstonian glaciation ice sheet extent would also have covered the Holderness coastline, reaching East Anglia and the north Norfolk coastline (Toucanne et al., 2009; Lee et al., 2012). Consequently, the Dogger Bank South Offshore Wind Farm area was affected by all 3 glaciations, although deposits from the Anglian or Wolstonian glaciations are likely to have been overridden by the Devensian glaciation, and thus no remnants of these glaciations are likely to remain in the near surface.



Figure 3-3: Location overview of the DBS OWF array locations and ECR. The North Sea mapped ice limits for the LGM, with the Dogger Bank are shown, overlain with BRITICE v2 data (Sources: Roberts et al., 2018; Clark et al., 2017)



The Dogger Bank is currently interpreted as a strongly glaciotectionised composite terminal moraine belt (Cotterill et al., 2017a; Phillips et al., 2018; Emery et al., 2019a and b; Phillips et al., 2022). The western section of the Bank is made up of 4 main formations of Late Pleistocene to Holocene age. These are the:

- **Dogger Bank Formation** (DBF— Late Pleistocene) is a predominantly clay-rich glacial till with laterally discontinuous sand lenses which overlie nearshore marine sands of the mid-Pleistocene (MIS11: ~ 400 kaBP to 120 kaBP) Egmond Ground, Cleaver Bank and Eem Formations (Cotterill et al., 2017a). Cotterill et al (2017a) informally subdivided the DBF into “Basal”, “Older/Lower” and “Younger/Upper” Dogger Bank units based on geotechnical and seismo-stratigraphic differences (Lower and Upper nomenclature was a subsequent refinement made by Phillips et al., 2018 and this will be preferentially used for the rest of this report). The Lower Dogger Bank is thickest towards the west of the area forming a series of complex ridges, with the overlying Upper Dogger Bank deposits filling the depressions between the ridges. The Lower and Upper sub-units both show indications that they have been subject to glaciotectionic deformation (Cotterill et al., 2017a and b; Phillips et al., 2018) with ice advancing from the north / northwest to create a series of ice-push moraines (Phillips et al., 2018). The Upper unit is predominantly of a greenish grey clay, with more sand laminae, particularly towards the base (Phillips et al., 2022) containing organics and detrital micas compared to the Lower Dogger Banks clays. These units represent a transition from periglacial / aeolian conditions (Basal) to glacial conditions (Lower and Upper);
- **Bolders Bank Formation** (BBF - Late Pleistocene) typically occurs west of Dogger Bank where it rests directly on the Lower Dogger Bank Formation and interdigitates with the Upper Dogger Bank Formation suggesting it is a contemporaneous unit with the latter. Boreholes from this area suggest it is a stiff to very-stiff, reddish to greyish, massive, slightly sandy and calcareous clay rich till. The presence of lithic clasts distinguish them from the clast poor olive grey clays of the DBF. The spatial restriction of these deposits to the west of the Bank suggest it was deposited by the North Sea lobe which flowed both southwards between Dogger Bank and the Yorkshire coast towards Norfolk, and westwards, entering Yorkshire. The maximum offshore extent is dated to 31.4-25.3 kaBP (Roberts et al., 2018) whilst the maximum readvance reached the north Norfolk coast by (21.5-20.7 kaBP: Evans et al., 2021). There is strong evidence of ice advance and retreat throughout this period, ~28 to 22 kaBP, both onshore and offshore (Dove et al., 2017; Roberts et al., 2018, Evans et al., 2021: Figure 3-3). Ice finally retreated from the East Yorkshire coast by ~17.3 kaBP (Evans et al., 2021). The East Yorkshire coastline and seabed eastward to the margins of the Dogger Bank is therefore made up of the subglacial deposits of the BBF and its terrestrial correlatives, which in this area are the Skipsea and Basement Till.
- **Botney Cut Formation** (BCF - Late Pleistocene) tends to exist in scaphiform valleys, up to 100 m deep and < ~8 km wide, which radiate out from the western and northwestern limits of the Dogger Bank. The Botney Cut Formation is represented by thinly laminated grey clays with laminae of silt and fine sand, interbedded with sands and occasional gravel horizons, which infill this drainage system. Traditionally, these channels have been interpreted as being of subglacial meltwater origin forming under high pressure as ice sheets decayed (Cameron et al., 1992). However, the radial pattern elucidated by more recent work suggest they may represent a proglacial drainage system (Cotterill et al., 2017a). Associated deposits

interpreted as of lacustrine origin, and which contain significant organic matter would support this latter interpretation (Cotterill et al., 2017a).

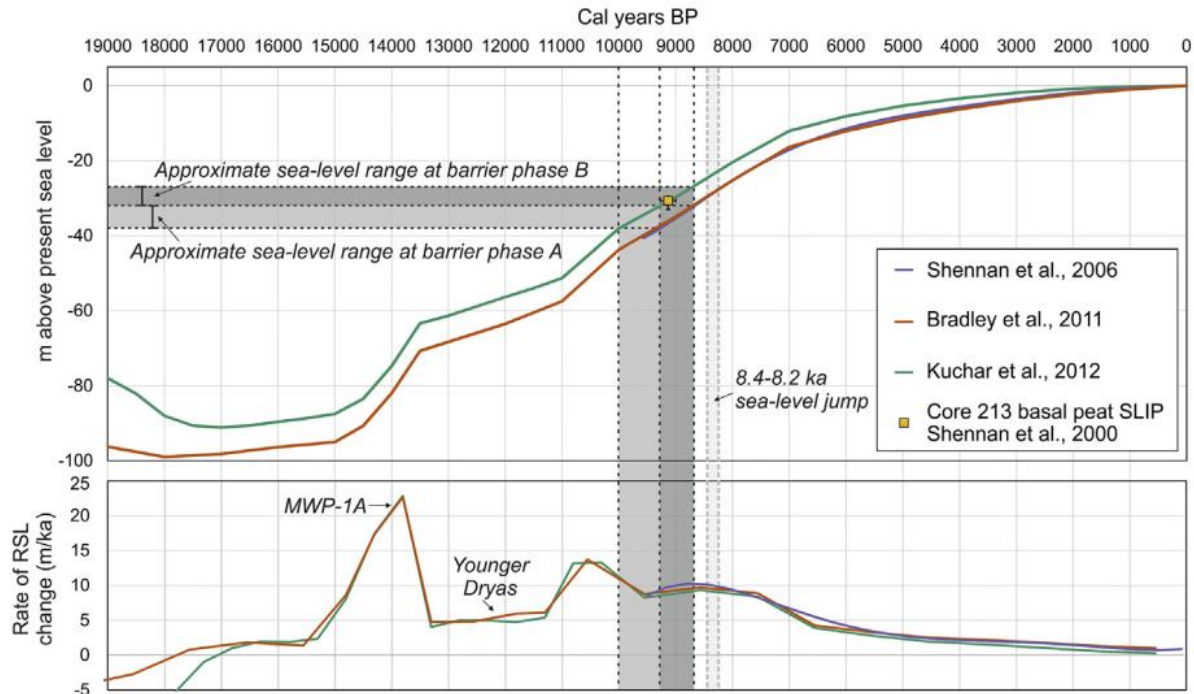
- **Holocene Deposits:** the Holocene across the western part of Dogger Bank is composed of dark olive-grey to very dark grey, fine-to medium-grained sands containing shells and a few rounded to angular, coarse gravel-sized clasts. The degree of consolidation of these sands increases downwards with an upper layer, a few centimetres thick, comprising loose silty sand overlying a much thicker (>10 m thick) sequence of dense to very dense sand. Locally this dense sand rests upon a mica-rich, fine silty sand unit, which in turn overlies a fine to coarse sandy gravel. Thicknesses of these deposits vary from being > 25 m where these deposits infill depressions and relic channels, to < 1 m thick very thin drapes (Cotterill et al., 2017a).

In summary, the Devensian ice sheet advanced over the Dogger Bank began ~30 kaBP, with maximum extent ~27 kaBP, and full retreat having occurred by ~23 kaBP (Cotterill et al., 2017a; Phillips et al., 2018; Emery et al., 2019a and b). The western side of Dogger Bank shows evidence of multiple readvances (active oscillation) of the Devensian ice sheet margin during deglaciation, indicated by the moraine complexes and deformation of the Dogger Bank Formation sediments (Phillips et al., 2018, Emery et al., 2019b; Phillips et al., 2022). To the west and southwest of Dogger Bank, the North Sea Lobe of the British Irish Ice Sheet underwent a series of advance and retreat phases, with the East Yorkshire coast area not becoming fully ice-free until 17.3 kaBP. The subglacial landscape was subsequently overlain by glaciolacustrine, glaciofluvial outwash and eventually Holocene marine sediments (Evans et al., 2021).

In response to deglaciation sea levels rose from a lowstand of ~ -120 m, at ~20 kaBP, to modern day levels along the East Yorkshire coast at ~5 kaBP (Figure 3-4: Emery et al., 2019a) in response to a combination of eustatic (increasing seawater volume) and isostatic (land subsidence) processes. During this time, the rate of relative sea level (RSL) rise has also been influenced by periodic, “instantaneous” events including Global Meltwater Pulse 1a (MWP-1A ~14.6 kaBP: Deschamps et al., 2012) and the 8.2 kaBP event (Tornqvist & Hijma, 2012). During the initial phases of deglaciation rates of relative sea level rise increased relatively slowly reaching a background level of ~ 5 mm/yr (Figure 3-4). During MWP-1A rates temporarily exceeded 20 mm/yr, before returning to rates of ~ 5 mm/yr during the Younger Dryas (Figure 3-4). At the start of the Holocene rates reached a background maximum of ~ 15 mm/yr before reducing through to modern rates of < 2.5 mm/yr (Hogarth et al., 2020). Although the exact process and timing of complete submergence of the Dogger Bank is still debated the most recent, site specific work, suggest Dogger Bank was completely inundated during the 8.2 kaBP event (Emery et al., 2019a) and the adjacent coastline reached close to modern levels in the last ~2ka.



**Figure 3-4: Relative sea level curve and rate of Relative Sea Level Rise for the Dogger Bank area as determined by Emery et al (2019a) based on Shennan et al., 2006; Bradley et al., 2011 and Kuchar et al., 2012). Note the absolute dates do not correspond directly with those quoted from the literature but re-calibration is beyond the scope of this report.**



### 3.3. Hydrodynamics and Sediment Transport Pathways

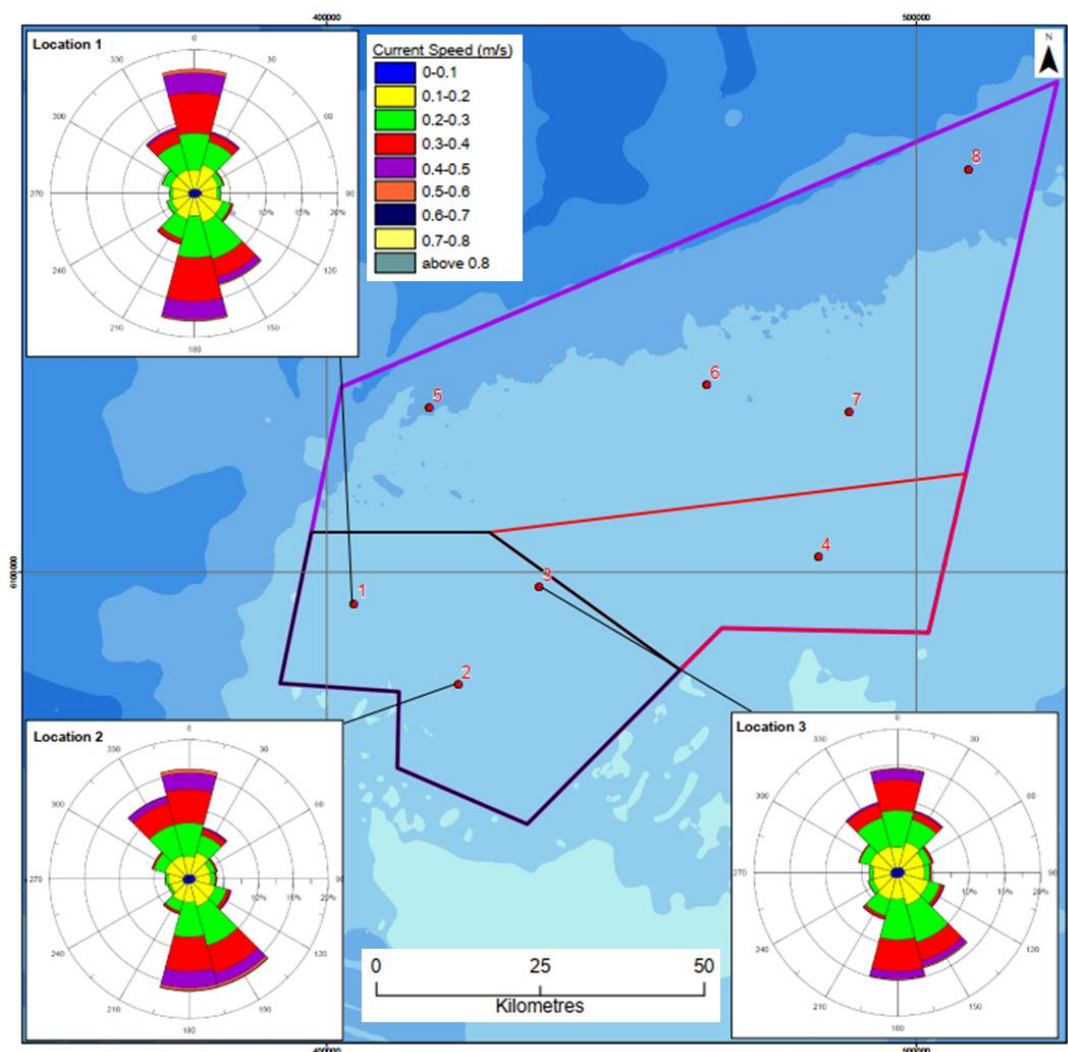
Once full marine conditions were established the developing local hydrodynamics re-worked the glacial and para-glacial deposits into a series of large (including sandbanks: Figure 1-5) and small scale bedforms. The primary source of information of the potential hydrodynamic conditions at the DBS OWF are based on the modelled and measured data from “Tranche A” of the Crown Estate Zone 3 of Round 3 of their offshore windfarm programme, an area of 2000 km<sup>2</sup> of seabed across the southwestern part of the bank (Godwin and Brew, 2014). Within Tranche A wave and current conditions were measured at two locations, 300 m apart [~GR435510, 6079820] in water depths of ~24 m LAT (Godwin and Brew, 2014). This location is ~35 km north-northwest of the centre of the DBS OWF. In addition, Statoil (Mathieson and Nygaard, 2010; and Mathiesen et al., 2011) provided modelled ocean data for 3 locations within Tranche A (Pt. 1: 404500, 6094600, depth -28.5 m LAT; Pt. 2: 422150, 6081100, depth -21.6 m LAT; and Pt 3. 435700, 6097300, depth -25.5 m LAT). Of these Pt. 2 is the closest, being 32 km north of the centre of DBS OWF with Pt. 1 at 47 km and Pt. 3 at 52 km north-northwest and north-northeast respectively.

Tidal ranges across the western margin of the Dogger Bank are estimated to be 3 m (Tranche A Pt 2.) decreasing in an easterly direction over the bank (2.65 m Tranche A Pt. 3). For Pts 1, 2 and 3, modelled depth-averaged currents had mean annual current velocities of 0.14 -0.3 m/s with maximum annual velocities of 0.39 – 0.91 m/s with the predominant flow direction being north to south, with subordinate currents flowing south-southeast and north-northwest (Mathiesen and Nygaard, 2010: and Figure 3-5). For a 10-year return period the extreme tidal current velocities



increased to 0.44 – 0.98 m/s and for a 100-year period to 0.49 – 1.08 m/s. For comparison the publicly available, ABPmer (2008), mid-depth modelled peak flows, for mean spring tides were 0.3 - 0.36 m/s and neap tides 0.14 - 0.16 m/s, so broadly comparable to the more detailed DHI model. Within the DBS footprint the ABPmer data suggests mid-depth modelled peak flows, were larger for both mean spring tides were 0.3 - 0.62 m/s and mean neap tides 0.17 - 0.3 m/s. In summary, other than under extreme conditions tidal currents are relatively low in the western part of the Dogger Bank and although the ABPmer data suggests they may increase in the DBS OWF, they would not be large enough to generate rapidly migrating bedform fields. This needs to be tested, however, through the generation of a site specific, high resolution, sediment transport model.

**Figure 3-5: Modelled depth-averaged current speeds at Pts 1, 2 and 3 within Dogger Bank Tranche A Zone. Based on the model of Mathiesen and Nygaard (2010) and presented in Godwin and Brew (2014).**

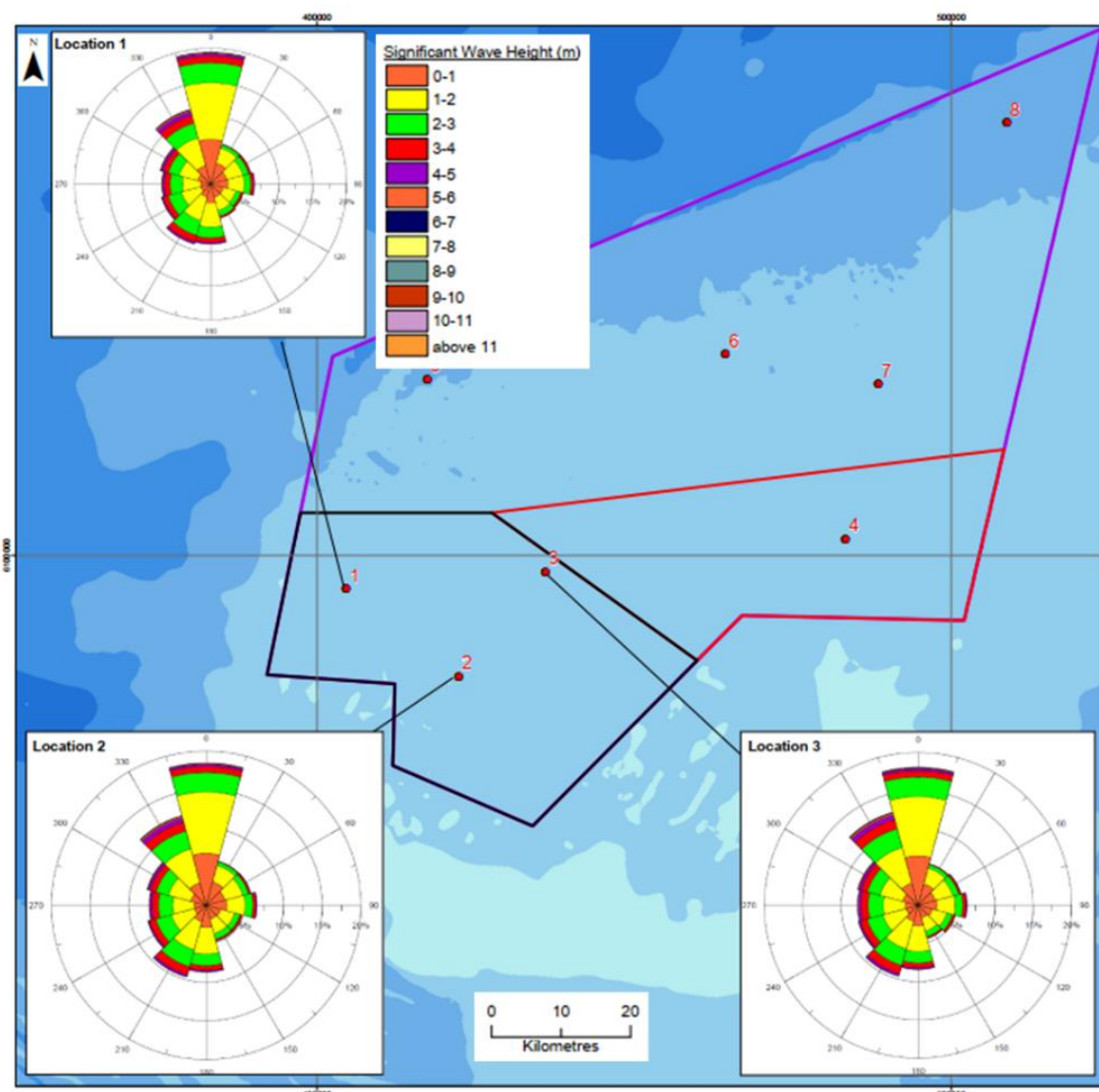


For the export cable corridor and the coastal strip, the ABPmer model predicts tidal flows will increase, giving mid-depth modelled peak flows, for mean spring tides of 0.31 – 1.2 m/s and neap tides of 0.16 - 0.61 m/s. The highest flows (> 0.9 m/s), however, are restricted to the area to the south of Flamborough head where a prominent tidal eddy is present, which is strong enough and has a spatial footprint large enough to affect all 4 cable corridor routes. The Holderness coast

experiences a much larger, macro-tidal range, with a mean tidal range of 5 m at Bridlington. Dominant, flood, tidal current directions run north to south, sub-parallel to the coast, reinforcing southerly flowing wave generated longshore currents, which are enhanced even further during storm surges (HR Wallingford, 2002; Pye and Blott, 2015).

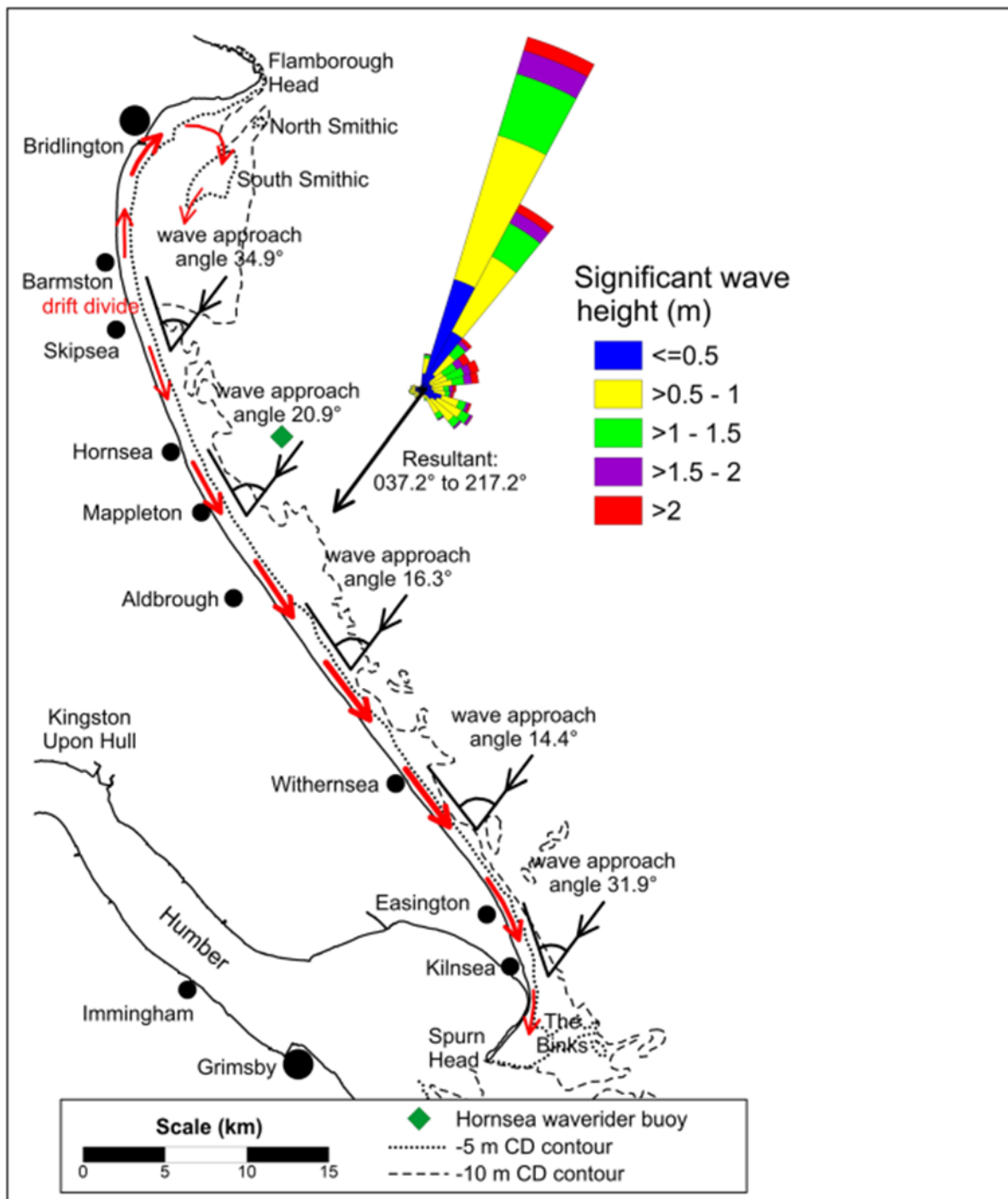
The Statoil modelled wave climate data for the western part of Dogger Bank (Mathiesen et al, 2011) predict a mean significant wave height for Pts 1-3 of between 1.2 and 2 m, with maximum significant wave heights of between 5.7 and 10.6 m. Although waves come from all directions, the largest waves are from the north and north-northwest. Due to refraction and shoaling the extreme values will have an uncertainty of at least 10-15% with the greatest uncertainty in the western part of Dogger Bank. This northerly dominant wave regime is supported by the results from waverider buoy deployment in Tranche A, visually represented in Godwin and Brew (2014). The ABPmer (2008) equivalents described annual mean significant wave heights of 1.75-2.0m, which varied seasonally from 1.25-1.5m in summer to 2.25-2.75m in winter.

**Figure 3-6: Modelled significant wave heights (m) at Pts 1, 2 and 3 within Dogger Bank Tranche A Zone. Based on the model of Mathiesen et al (2011) and presented in Godwin and Brew (2014).**



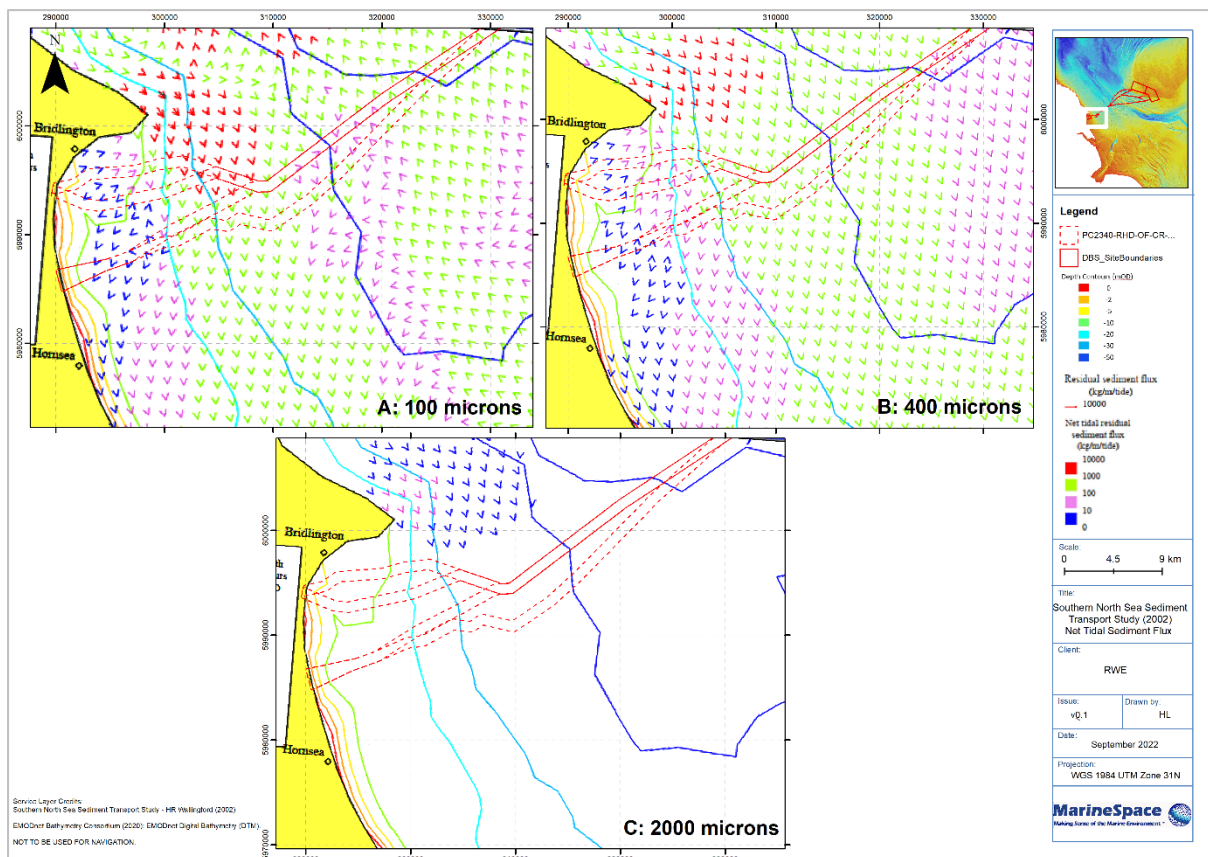
Analysis of wave data from the Hornsea waverider buoy by Pye and Blott (2015 and Figure 3-7) demonstrates the dominant wave direction is from the northeast with the largest waves approaching the shore near Skipsea resulting in net southerly longshore drift. Wave heights and wave periods are seasonal, with maximum values of both occurring between October and March. Refraction of these northeasterly waves around Flamborough Head, combined with greater exposure from southeasterly waves creates a drift divide between Skipsea and Barmston, with net northerly longshore drift occurring from here, north to Bridlington (Pye and Blott, 2015).

**Figure 3-7: Wave rose for the Hornsea waverider buoy and inferred sediment transport directions after Pye and Blott (2015).**



The export cable corridor routes will similarly be affected by these northerly to northeasterly wave regimes combined with the north to south tidal flows described previously, resulting in primarily southerly net movement. The HR Wallingford (2002) Southern North Sea Sediment transport model supports this general hypothesis of dominantly southerly sediment transport across the first 45 km of the cable corridor (Figure 3-8). This model generated calibrated depth-averaged tidal flows for 3 different grain sizes: 100 microns (Fine sands), 400 microns (medium sands) and 2000 microns (very fine gravels). For the 100 micron and 2000 micron scenarios these flows were also modelled with a range of wave conditions (1, 3 and 5 m mean significant wave height and 5, 6 and 10 second wave periods respectively) to look at the impacts of combined flows. For the fine and medium sands, under tidal flows, sediment transport is clearly to the south / south-southeast for the majority of the ECC, although nearshore the model does capture rotational flows around the Smithic bank and the initiation of the northerly flows beyond the drift divide north of Skipsea. The 2000 micron model runs show that movement of coarser sediment is only likely to occur associated with the accelerated flows around Flamborough head and again in a dominantly southeasterly direction. Movement adjacent to the coastal strip between Bridlington and Hornsea tends only to be invoked in the presence of waves, with the model once more capturing the drift divide north of Skipsea.

**Figure 3-8: Southern North Sea Sediment Transport Model outputs for the Holderness coast representing tidally driven sediment transport for fine sand (100 microns - Panel A); medium sand (400 microns - Panel B) and very fine gravels 2000 microns – Panel C).**



## 4. Route Specific Morphology and Mobility

The following sections combine the geological overview provided in Section 4, with analysis of swath bathymetry provided by both the client and from publicly available resources, the initial ground model interpretation of Fugro (Section 1.1.1 - Table 2-1) and other discrete public datasets to describe the spatial and temporal variation in landscape morphology of the landfall site (Section 4.1.1), the export cable corridor (Section 4.1.2) and the Offshore Windfarm (Section 4.1.3). Bedform descriptions are based on definitions by Ashley, 1990 (Table 4-1). Analysis of seabed level changes (bed level change – BLC) and mobility has been undertaken by subtracting the older surveys from the newer surveys, where there is crossover of bathymetric datasets.

**Table 4-1: Bedform descriptions based on Ashley (1990)**

Bedform Description	Bedform Wavelength	Bedform Height
Small subaqueous dune	0.6 - 5 m	0.075 - 0.4 m
Medium subaqueous dune	5 - 10 m	0.4 - 0.75 m
Large subaqueous dune	10 - 100 m	0.75 - 5 m
Very large subaqueous dune	Over 100 m	Over 5 m

### 4.1.1. Landfall Site

#### 4.1.1.1. Geology

The Holderness coastline (Flamborough Head to the Humber Estuary), including the landfall area of the DBS export cable options, is one of the fastest receding coastlines in Europe (Quinn et al., 2009). The coastline is, like the offshore region, a product of glacial activity in the area, particularly during and since the LGM. The coastline hosts a range of glacial features including moraine ridges both on and offshore (Bateman et al., 2015; Busfield et al., 2015; Dove et al., 2017) and understanding the geological context and stratigraphy of the onshore area is key to understanding the nature of the coastline, and its rapid erosion.

The offshore Cretaceous Chalk bedrock continues laterally onshore, where it has been more accurately identified as the White Chalk Group (British Geological Survey, 2022a). From Flamborough to Auburn Farm, bedrock is identified as the Flamborough Chalk Formation. The succeeding Rowe Formation is more flint-rich and makes up the bedrock southwards along the coastline to Withernsea (British Geological Survey, 2022a). Onshore it is generally at a depth of at over -20 mODN and is overlain by thick Quaternary deposits (Castedo et al., 2015; Pye and Blott,



2015). When considering historic borehole and core samples along the coastal strip, these also show chalk at over 15m depth below the surface (Figure 4-1: British Geological Survey, 2022b).

During the LGM, the North Sea Lobe of the British Irish Ice Sheet flowed southwards, in the topographic low of Jurassic deposits, between the outcrop of Cretaceous Chalk in the western margin of the North Sea, and the topographic high of the Dogger Bank (Busfield et al., 2015; Bateman et al., 2015; Bateman et al., 2018 and Section 3.2).

These Quaternary deposits are made up of glacial till, glaciofluvial deposits and alluvial material. They were deposited when the North Sea Ice Lobe migrated south-westward across the modern-day Holderness coastline. Moraine ridges aligned parallel to the coastline extend along the whole length of the section, indicating the perpendicular easterly retreat of ice across the region (Busfield et al., 2015). The Basement Till [also known as the Bridlington Member], is a Wolstonian or early Devensian diamicton (pre-MIS4), which directly overlies the Chalk bedrock (Bateman et al., 2015). Dimlington Silts often separate this Basement Till and the overlying Skipsea Tills (Figure 4-2 Panel I: Boston et al., 2010). The Skipsea Till Member is complex and contains several facies (Boston et al 2010, Busfield et al., 2015), overlain and incised with some sand and gravel infill of subglacial meltwater channels and gravel outwash deposits (Figure 4-2 Panel G: Pye and Blott, 2015; Bateman et al., 2015; Bateman et al., 2018). The Skipsea Till is therefore exposed in the coastal cliffs at the shoreline of all of the proposed landfall areas (Figure 4-1: Boston et al., 2010; Castedo et al., 2015).

Evans and Thomson (2010) have logged a 10.5 m sequence of the Skipsea Cliff (Figure 4-2). Here the cliff is dominated by the Skipsea Till diamicton with intrabeds of cross-stratified coarse sands and gravels. The Chalk bedrock was not reached at this locality.

It has not been possible to identify any direct sampling of the beach deposits between Skipsea and Bridlington. Simple inference from aerial photography and publicly available descriptions suggest there is a surface veneer of marine sands.

Figure 4-1: BGS borehole record of depth below surface of the upper boundary of the Chalk bedrock, as well as the northern limit of the Skipsea Till, determined using borehole records (Source: Evans and Thomson, 2010).

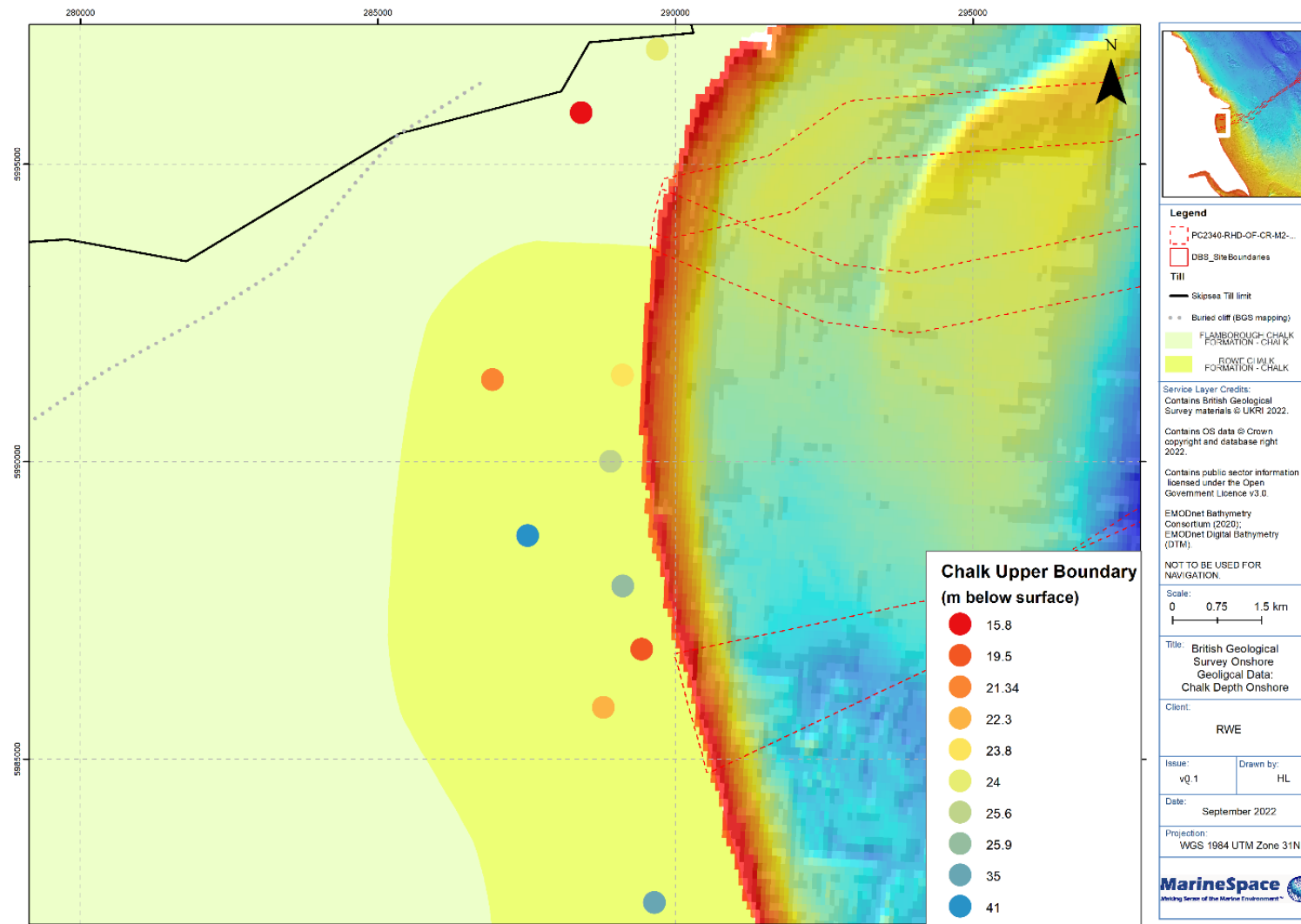


Figure 4-2: Panel A the stratigraphic sequence at Skipsea showing extensive interbedded cross-laminated ripple sands within the Skipsea Till. Panel B vertical profile log of the Skipsea Till sequence at Skipsea (OS Grid reference TA176573) both after Evans and Thomson (2010). For full legend see Table 1 in Evans and Thomson, 2010. From: Evans and Thomson (2010)





#### 4.1.1.2. Landfall Aquifer Properties

Landfall sites are commonly the most thermally limiting for any export cable or interconnector route due to:

1. the varying thermal properties encountered in the vadose zone (the zone between the land surface and the top of regional groundwater table), as this zone can have very variable water contents which can be further dried out through cable heating;
2. the typically greater burial depths encountered as landfall routes have to avoid extensive human activity within the coastal strip.

Work by the University of Southampton suggests that localised higher groundwater flows can be utilised to facilitate natural cooling around the cable through advection. Consequently, deeper installations may not generate such high conductor temperatures as commonly anticipated. Consequently, the hydraulic properties of the principal stratigraphic units (Skipsea Till and Chalk bedrock) at the landfall locations has been reviewed.

The Skipsea Till typically have low permeabilities and hence groundwater hydraulic conductivities [the maximum potential rate of flow]  $\sim 10^{-2}$  m/d (Elliot et al., 2001). Between the buried cliff line/Skipsea Till margin (Figure 4-1) and the Humber Estuary in the south, artesian flow in the near surface deposits has typically discharged through thinly buried, semi-confining layers via springs and localised sand cones which generate “blow-wells” (Elliot et al., 2001 and Younger & McHugh, 1995).

By contrast the Cretaceous Chalk is regarded as a highly transmissive aquifer (MacDonald and Allen, 2001). In reality, the transmissivity (the actual rate of groundwater flow through an aquifer, measured in  $\text{m}^2$  per day, or  $\text{m}^2 \text{d}^{-1}$ ) of the Cretaceous Chalk aquifer of Yorkshire can be highly variable laterally and vertically, affected by the topography, the density of fractures and joints, the thickness of the Quaternary sedimentary cover, and seasonal effects on groundwater. Across Yorkshire values range from  $1 \text{ m}^2 \text{d}^{-1}$  to  $10000 \text{ m}^2 \text{d}^{-1}$ , with a mean of  $1258 \text{ m}^2 \text{d}^{-1}$ . The range of transmissivity in the near coast area is  $100 - 1000 \text{ m}^2 \text{d}^{-1}$  (Gale and Rutter, 2006). MacDonald and Allen (2001) echo this with a quoted median value of  $1250 \text{ m}^2 \text{d}^{-1}$ . It must be noted, however, that most of the data was collected from sites which tend to have higher transmissivities, with few datasets being collected near or on the coastline on the Holderness Plain.

One borehole from Haisthorpe (Carnaby Moor, Grid Reference: TA 1505 6486), 3 km southwest of Bridlington and 2.3 km from the northern landfall site, showed jointing in the Chalk down to 100 m below ground level. Transmissivity values in the area were over  $6000 \text{ m}^2 \text{d}^{-1}$ . Significant flow horizons were identified at 42, 50, 56, 72 and 80m depth in the fractured Chalk, below the Quaternary cover (Gale and Rutter, 2006).

Low transmissivities do occur on the edge of the Quaternary cover and are higher moving west of the buried cliff line where the aquifer is unconfined and there is reduced Quaternary cover (Gale and Rutter, 2006). In East Anglia, overlying glacial tills do act to restrict transmissivity by limiting groundwater flow (Chadha, n.d.). Along this cliff line, fractures and springs potentially increase transmissivity. Values were highest at areas of Flamborough Chalk outcrop and in valleys. Water-

bearing sands and gravels overlying the Chalk may increase transmissivity, acting as a storage reservoir (Gale and Rutter, 2006).

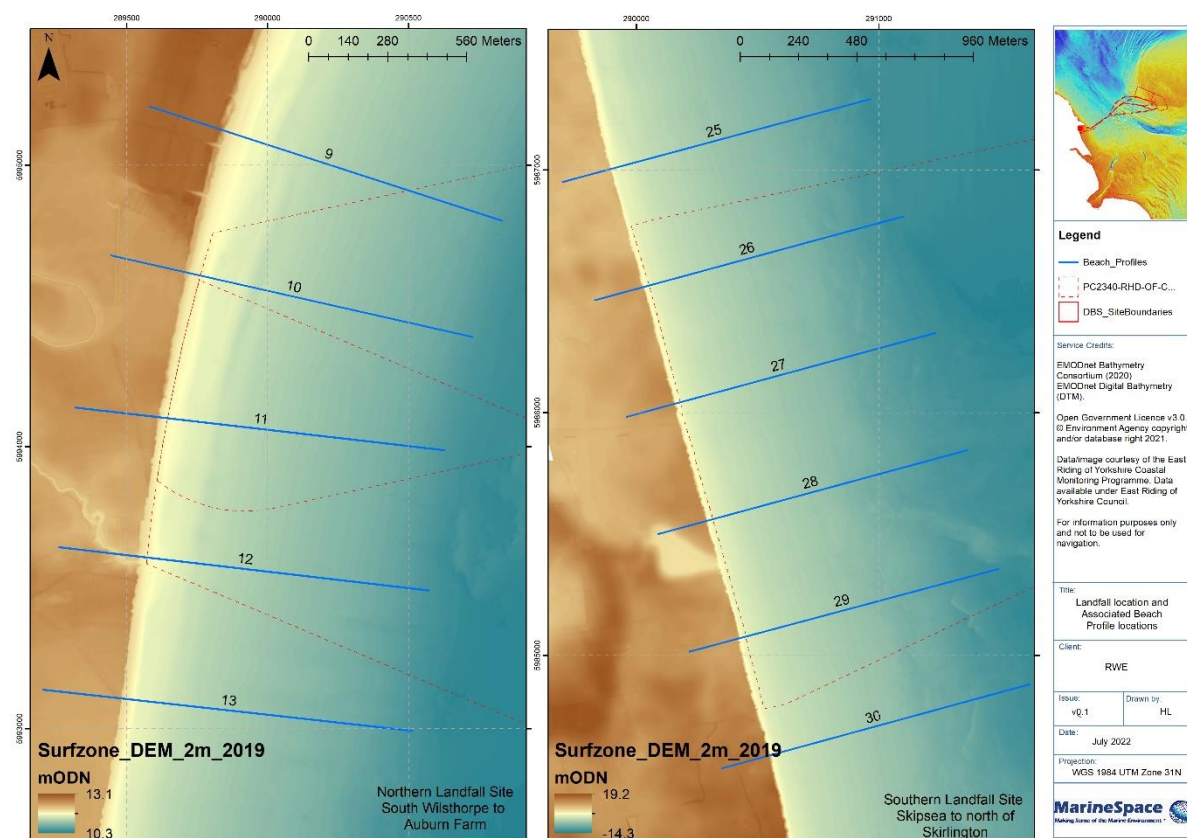
Beneath Holderness, where glacial till cover is greater, transmissivity is thought to be limited to  $< 50 \text{ m}^2 \text{ d}^{-1}$  (Gale and Rutter, 2006). This may be because of a low hydraulic gradient, as well as limited groundwater circulation and so less enlargement of fractures by solution (MacDonald and Allen, 2001). Seasonal changes occur in groundwater flow, so affecting transmissivity. A model study showed almost a doubling in Chalk transmissivities between summer and winter (Chadha, n.d.).

Although the Skipsea Till deposits are unlikely to support significant groundwater flow, the variability of the thickness of this deposit and the equal variability of the fracture density, which is a strong control on the hydraulic conductivities the depth to chalk bedrock and the groundwater flow within it is worthy of further investigation.

#### 4.1.1.3. Coastal Erosion

The cliffs tops along this section of the coastline vary from  $\sim 3.7 - 9.1 \text{ mODN}$  along the northern landfall site, and  $\sim 3.7 - 13.1 \text{ mODN}$  along the southern landfall site (Ordnance Survey, 2022), with 500m spaced beach profiles giving cliff heights between 5-11m OD in the north, and 11.2 – 14.6 mOD in the south (Figure 4-3: Pye and Blott, 2015; East Riding of Yorkshire Council, 2022). The highest cliffs in both areas occur in profiles  $< 400\text{m}$  outside of the landfall extent boundaries. These profiles have been included in the analysis to show the lateral variation along these coastal sections.

**Figure 4-3: Landfall locations and associated beach profile locations cited in the text and sourced from the East Riding of Yorkshire Council (2022)**



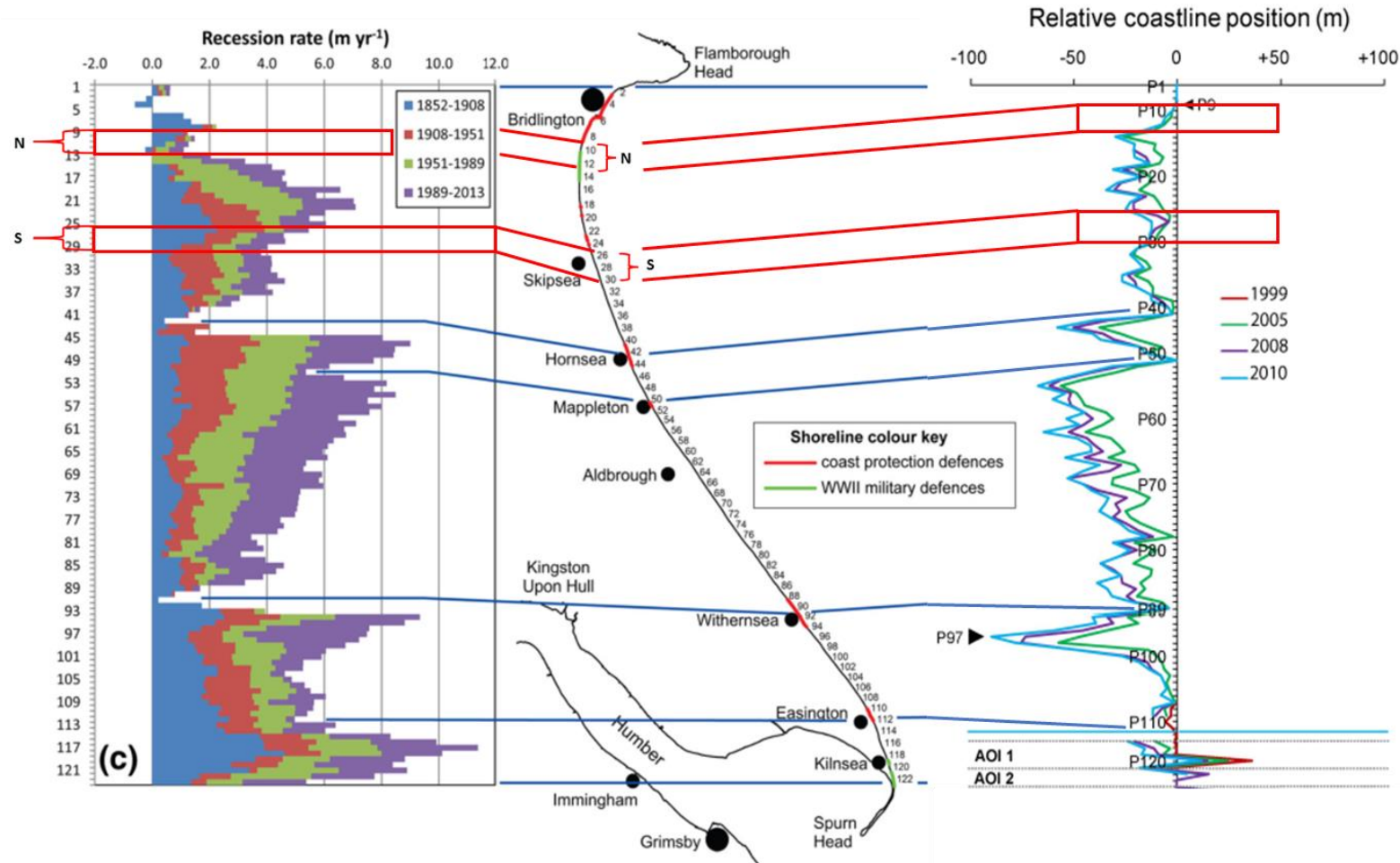
In terms of cliff recession, the Holderness coastline is one of the most extensively researched sections of coastline in Europe, being the focus of study for over 2 decades. Consequently, it has been possible to aggregate the retreat rates for both the northern landfall site (Profiles 9-13: south of Wilsthorpe – Auburn Farm - Figure 4-3) and the southern landfall site (Profiles 25-30: Skipsea - Figure 4-3). A summary of 5 major sources of cliff erosion rates are given in Table 4-2 and Figure 4-4.

**Table 4-2: Annual cliff erosion rates for the landfall sites, from Profiles 9-13 for the northern landfall and Profiles 25-30 for the southern landfall**

Source	Years of data used	Min erosion rate m/yr (N Landfall)	Max erosion rate m/yr (N Landfall)	Min erosion rate m/yr (S Landfall)	Max erosion rate m/yr (S Landfall)
East Riding Yorkshire Council (2022) Extreme Values	2003 – 2022	0	8.03	0	6.31
East Riding Yorkshire Council (2022) 10-Year Average Values	2012 - 2022	0	0.80	1.01	3.02
East Riding Yorkshire Council (2022) Long-Term Averaged Values	1989 - 2022	0.02	0.89	0.92	1.41
Pye and Blott (2015): (Historical Analysis) Table 2	1852-2013	0.14	0.44	0.96	1.58
Castedo et al. (2015): Table 3	1852-2011	-	-	1.05	1.51
Castedo et al. (2015): Table 3 (Digital Shoreline Analysis System)	1852-2011	-	-	1.08	1.43
Lee (2011): Estimated from Figure 2b	1952 - 2004	<0.2	<1.1	0.5	1.5
Quinn, Philip and Murphy (2009) After Valentin (1971) Comparison of Historic Map & Field Data Estimated from Figure 5	1852 - 1952	~ 0 - 0.1	~ 0.5	~ 1.15	~ 1.75
Quinn, Philip and Murphy (2009) Erosion Post Data Estimated from Figure 5	1953 - 2007	~ 0 - 0.1	~ 0.75	~ 0.5	~ 1.45

Source	Years of data used	Min erosion rate m/yr (N Landfall)	Max erosion rate m/yr (N Landfall)	Min erosion rate m/yr (S Landfall)	Max erosion rate m/yr (S Landfall)
Quinn, Philip and Murphy (2009) East Riding Council GPS Estimated from Figure 5	2003 - 2007	~ 0.5	~ 3.0	~ 0.5	~ 2.0

Figure 4-4: Erosion rates for the Holderness coastline, including the landfall sites marked with red bracket or box and a N or S for the northern and southern landfall sites respectively. Figure shows the variation in recession rate for different time periods between 1852 and 2015 in a cumulative way (Source: Figure 8c, Pye and Blott, 2015). On the right the change in relative coastline position from mid-1990 to 2010 is shown, with the zero-line representing an initial 1994/96/97 survey (Source: Montreuil and Bullard, 2012)



As can be seen from Table 4-2 and Figure 4-4 the northern landfall site has a maximum annual erosion rate for the 5 profiles ranges from 0.02 – 0.89 m/yr, based on a 33 year average (1989-2022) calculated from combined GPS surveys and aerial derived profile data taken by East Riding of Yorkshire Council (EYRC). For the southern landfall site, the maximum annual erosion rate based on this same 33 year period ranges from 0.92-1.41 m/yr. These medium term averages compare well with other similar analyses such as Pye & Blott (1989 – 2013: 0.03 – 0.99 northern landfall, 0.7 – 1.6 m/yr southern landfall). When the time series is extended the overall rates slightly compress in range but are of similar magnitude e.g. EYCR (1852-2022: 0.25 – 0.61 m/yr northern landfall, 1.04-1.54 m/yr southern landfall), Pye & Blott (1852 – 2013: 0.14 – 0.44 northern landfall, 0.96 – 1.58 m/yr southern landfall) and Castenado et al (1852-2011: 1.05 – 1.51 m/yr southern landfall, no data for northern landfall). The average erosion rate across the whole Holderness coastline is determined by Castedo et al. (2015) to be ~2m/year. So arguably the long term rates at the proposed landfall sites are lower than the whole coast average.

Since March 2003 the EYRC have been collecting data twice a year (March/April and September/October) which provides data on cliff retreat rates per profile at a much higher temporal resolution (Figure 4-5 and Figure 4-6). Calculating year on year averages for each profile from these data provides higher values with the maximum individual year determined erosion rates of between 0 and 8.03 m/yr, although the highest rate represented the impact of 1 storm on 1 profile, for the northern profiles. The corresponding range for the southern profiles was from 0 to 11.05 m/year, albeit rates of > 5 m/yr only occurred 6 times over the 19 years, spread across 4 years and 4 profiles. All of these data suggest that the northern landfall site has lower erosion rates than the southern site. This can be clearly illustrated by comparing the 2003-2021 beach cross-sections for Profile 12 at the northern site (Figure 4-5) and Profile 28 from the southern site (Figure 4-6).

Figure 4-5: Profile 12 at the northern landfall site cross-sectional profile showing cliff position and therefore retreat between 2003 and 2021 (From: East Riding of Yorkshire Council, 2022)

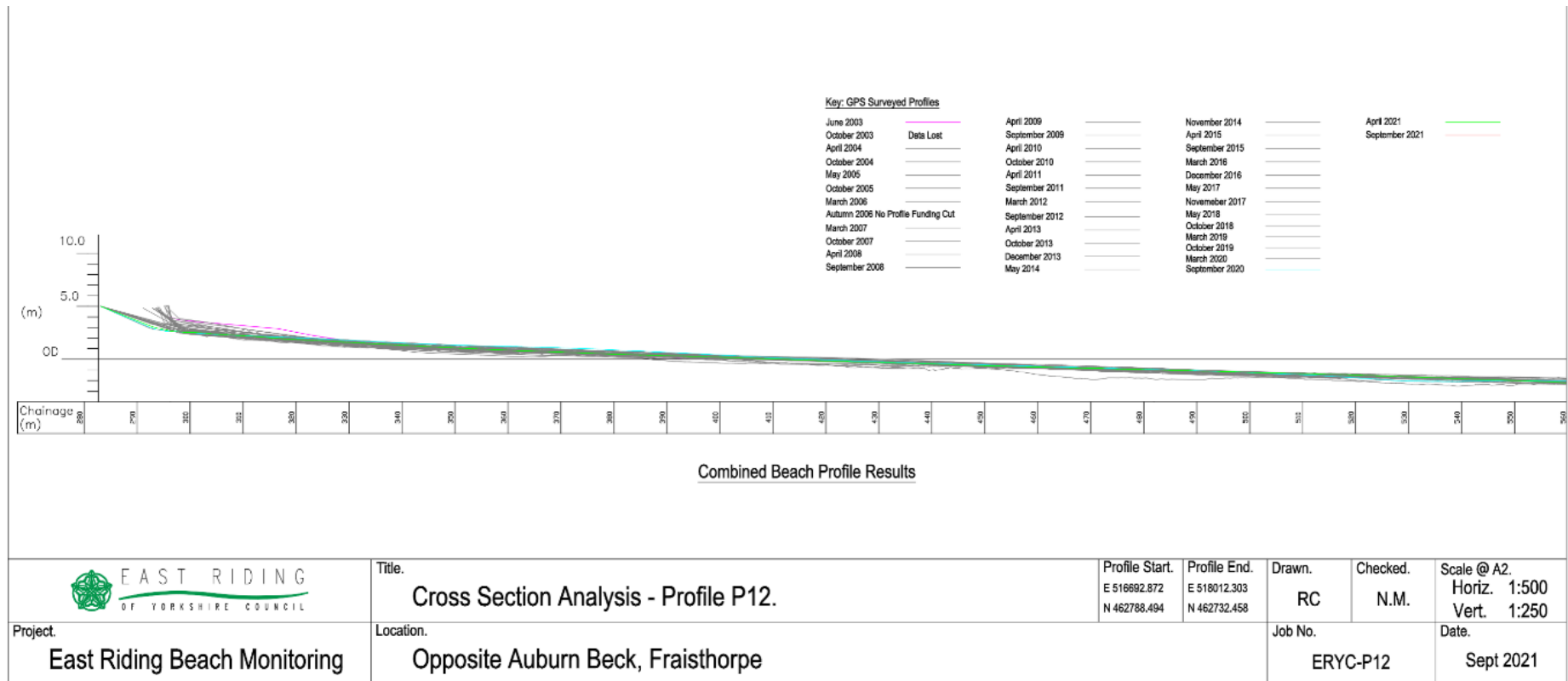
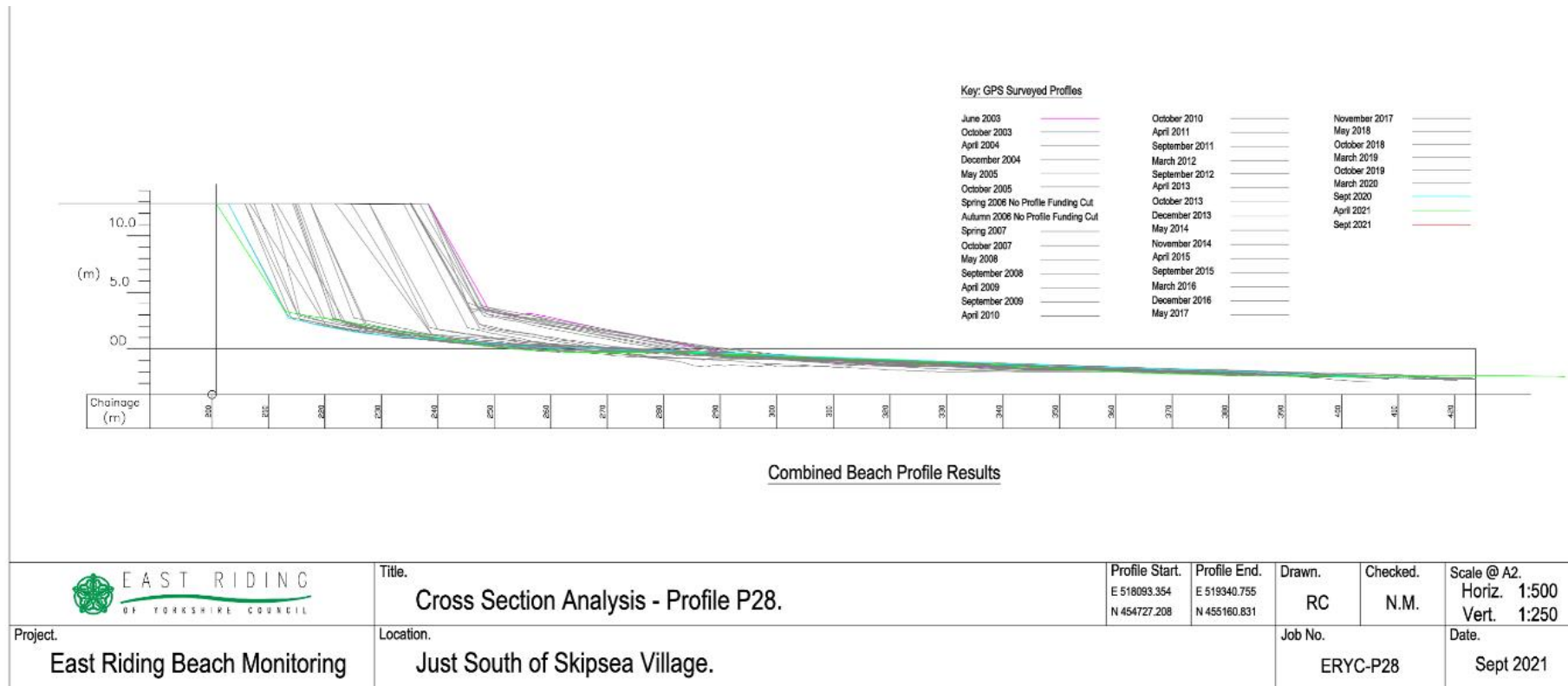




Figure 4-6: Profile 28 at the southern landfall site cross-sectional profile showing cliff position and therefore retreat between 2003 and 2021 (From: East Riding of Yorkshire Council, 2022)





All of these quoted rates assume linear retreat on an annual timescale, however it is more likely loss is associated with shorter period activity and probably individual events. This can be assessed by examining the individual surveys taken, every ~6 months, by the ERYC between 2003 and 2021 (Figure 4-7 and Figure 4-8). At the northern landfall site the overall pattern is one of limited cliff loss between surveys for Profiles 9 and 10 (the most northerly ones) showing < 0.7 m retreat over the whole 19 year period (Figure 4-7). By contrast Profiles 11-13 show between 10.44 m and 14.64 m of retreat over the whole period (note for P12 ~75% of the loss was from one winter season). The majority of the movement is associated with winter storms, with only 5 occurrences of coastal retreat between the spring and autumn surveys (2003 (P11), 2004 (P12), 2005 (P13), 2007 (P12 and P13) and 2019 (P13). The storm of winter 2013 is responsible for 8.03 m of retreat for P12 but P9-P11 show no corresponding movement and P14 only 0.85 m of retreat during the same winter season. Simple cross-correlation against the National Coastal Monitoring Storm Catalogue (NCMSC, 2018; Dhoop & Mason, 2018) for the period 2003 – 2018 identified 7 seasons (2009-2010, 2010-2011, 2012-2013, 2013-2014, 2015-2016, 2016-2017 and 2017-2018) where extreme wave events (defined by the 1 year return period of significant wave height at the Hornsea waverider buoy) affected the Holderness coast. Of these, 5 showed corresponding coastal retreat but two years (2009-2010 and 2015-2016) showed no coastal change at all. Further, another 6 years showed significant retreat but with no identified storms.

At the southern landfall site there is significantly greater annual variability (Figure 4-8). All 6 profiles show a cumulative loss of between 24.38 and 39.04 m over the 19-year period. The maximum amount of cliff loss between surveys is 6.31 m during the winter of 2009-2010. At least one profile showed retreat in every survey year with the largest retreat between surveys (5.07 to 6.31 m) occurring after the winters of 2007, 2010, 2011 and 2013. The latter storm season showed the most cumulative retreat across the 6 profiles, albeit the majority of recession related to P27 and P28. Only 6 survey periods record no cliff retreat, simultaneously across all 6 profiles, at all and there was cliff retreat along at least 1 profile in every year irrespective of the storm conditions. This would suggest that this section of the coastline is much more susceptible to erosion than the northern site.

As well as natural changes, coastal erosion has shown spatial and temporal variation as a result of human activity. Both landfall sites of the DBS ECR, on the northern section of the Holderness coastline, have not been the subject of man-made coastal erosion defence, but there are some remains of military defence such as concrete blocks which may provide some protection. It is evident that after military defences were installed in the northern landfall area that it served some protection from marine erosion as seen in a reduction in recession rate compared to the 1852 – 1908 period (Figure 4-4: Pye and Blott, 2015). Pye and Blott (2015) note that a series of shallow bays (deepest to the south of defended coastal areas) are developing – this might impact the potential landfall site of the DBS ECR, south of Bridlington (which is defended by sea walls and groynes, as well as old military defences) and also the southern site, north of which there is also coastal defences in place (Figure 4-9).

**Figure 4-7: Northern landfall site cliff loss per year along beach profiles 9 -13, between 2003 and 2022. Source: East Riding of Yorkshire Council, 2022**

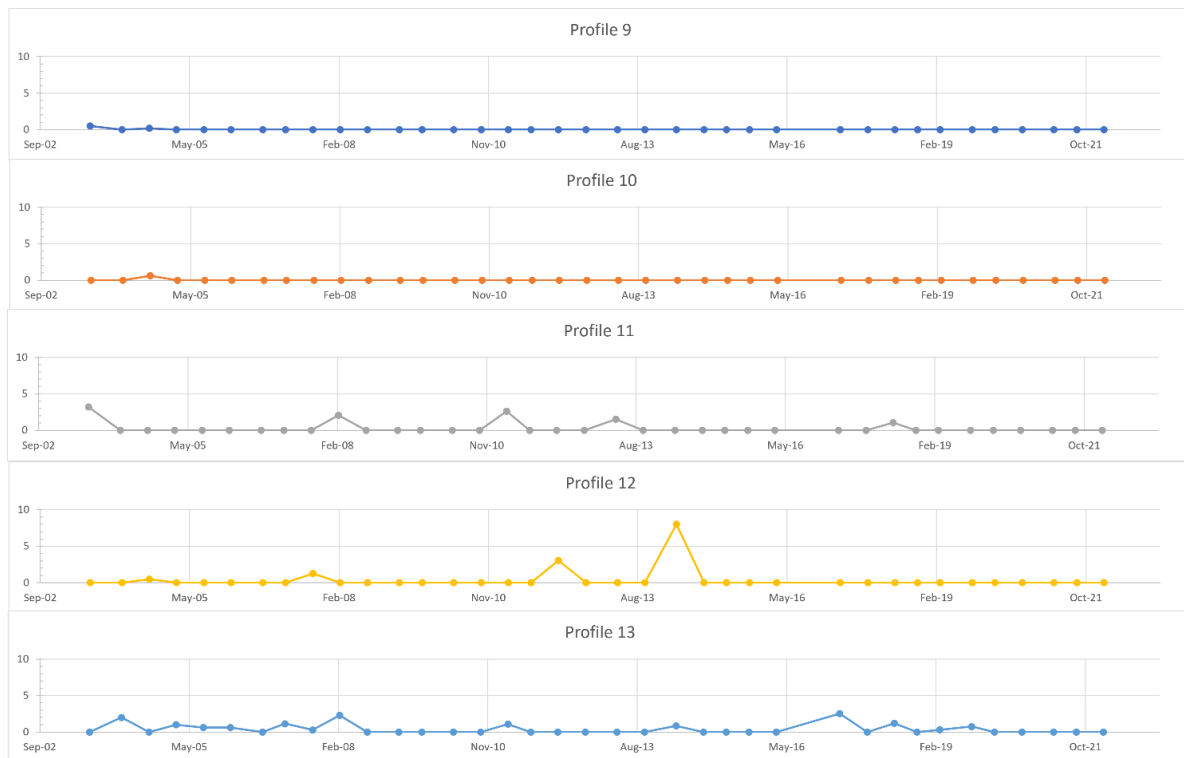


**Figure 4-8: Southern landfall site cliff loss per year along beach profiles 25 -30, between 2003 and 2022. Source: East Riding of Yorkshire Council, 2022**

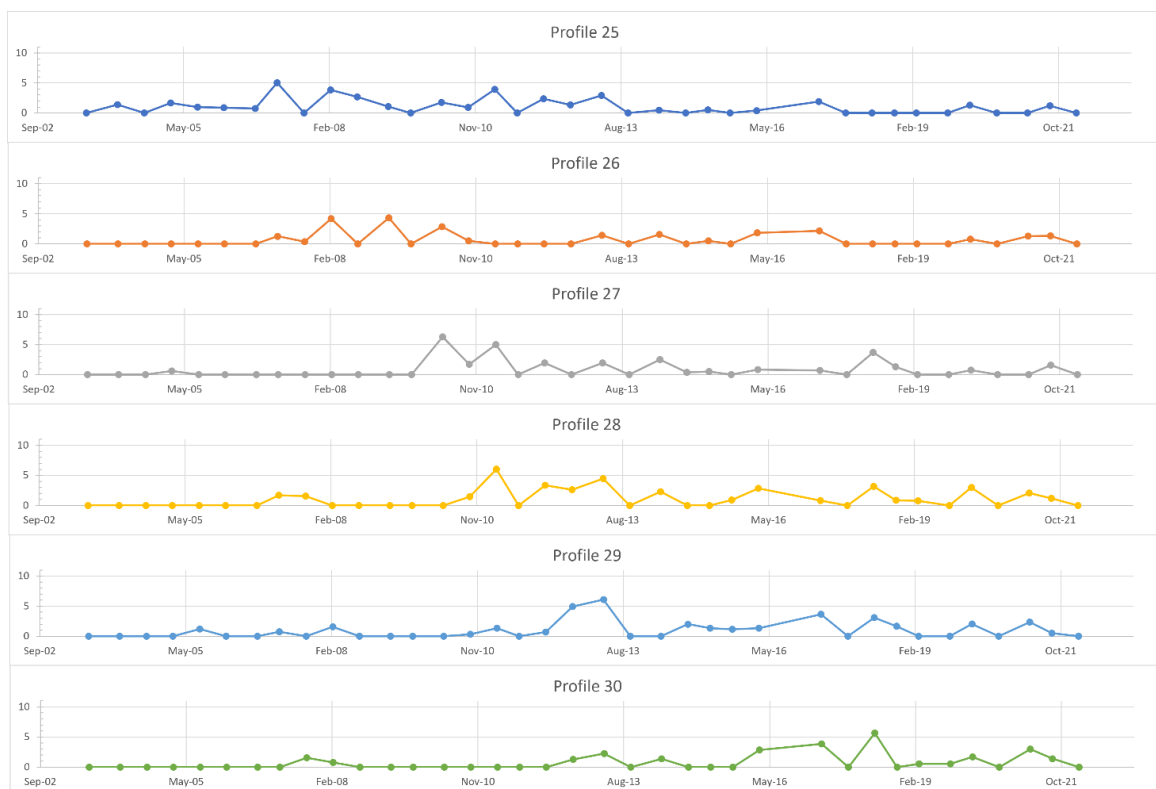
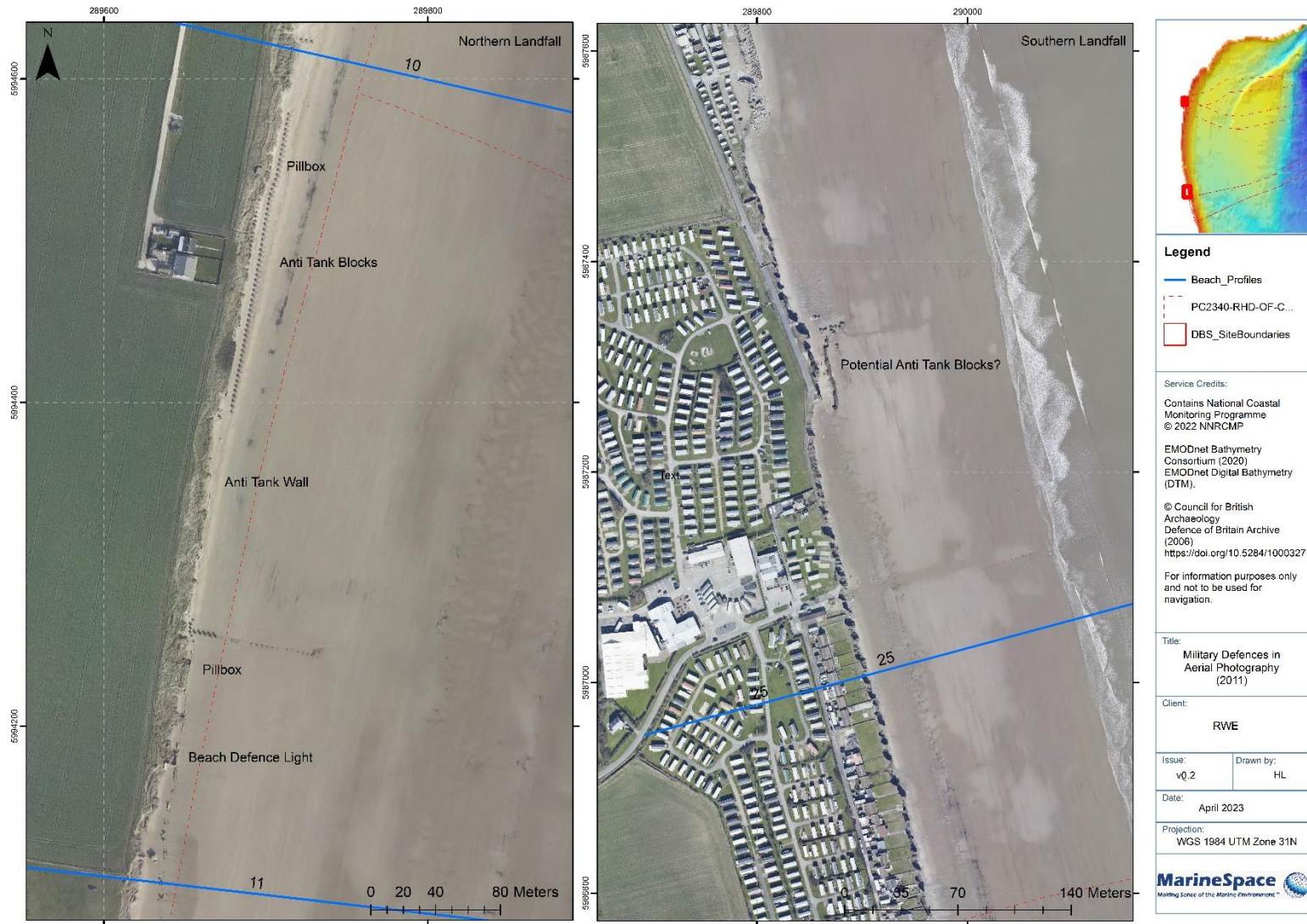


Figure 4-9: Landfall site military defences (anti-tank blocks) visible in 2011 aerial photographs from the National Coastal Monitoring Programme, with label information from the Defence of Britain Archive (Source: Council for British Archaeology, 2006)



Z.

Cliff recession rates are anticipated to increase in response to both increasing rates of sea level rise and storminess (Pye and Blott, 2015). Castedo et al. (2015) undertook predictions of the future rates of erosion based on 3 different models (Lee-Clark Model based on the extrapolation of historical data; Leatherman Model based on Historical Trend Analysis and their own process response model) for an area that included the southern landfall site. The lower and upper bounding erosion rates for each model are presented in Table 4-3, with these limits being defined by the standard deviation of the historical data for the Lee-Clark model and bounding sea level rate rises of 2 mm/yr and 6 mm/yr for the other 2 models. The Lee-Clark model (Lee & Clark, 2002) takes an historical linear erosion rate and multiplies them by the modelled time period; the Leatherman (1990) model is based on the “Bruun Rule” and combines the measured shoreline recession rate, the measured rate of sea level rise during the same period and the predicted future rate of sea-level rise to predict a future shoreline recession rate. Finally, the Castedo-Parades model is a structure response model which considers both the morphology and geotechnical properties of the coast and the coastal hydrodynamic regime to predict the future position of the cliff line and from these a new recession rate is linearly calculated. The model has been calibrated against EYRC profiles from the Skipsea area but only a semi-qualitative analysis has been undertaken “....the PRM reproduced the measured profiles well and it is able to reproduce the change in the position (horizontal and vertical) of the cliff toe from the oldest to the newest profile, which implies a good representation of the erosion processes and gives confidence to subsequent predictions” (Castedo et al., 2015). Table 4-2 generates simple linear minimum and maximum retreat distances for a 30 year period (2022 to 2052) representing the potential lifetime of the site. As has been discussed at length such linear extrapolations should be treated with extreme scepticism, the local calibration would suggest that the Castedo-Parades model may give the most realistic value of retreat.

**Table 4-3: Predicted rates of erosion at the southern landfall, based on 3 methods. (From: Table 4, Castedo et al., 2015)**

Source	Model Run	Min erosion rate m/yr (S Landfall)	Max erosion rate m/yr (S Landfall)	Min Linear Retreat	Max Linear Retreat
Lee-Clark Model (2002) – Extrapolation from Historical Data	2011 – 2051	0.31	2.21	9.3	66.3
Leatherman Model (1990) – Historical Trend Analysis	2011 – 2051	1.05	4.29	31.5	128.7
Castedo-Parades Model (2012) – Process Response Model	2011 – 2051	1.37	2.25	41.1	67.5

#### **4.1.2. Export Cable Corridor**

As described in Section 1.1 the cable route has been nominally split by MarineSpace into Zones 1 and 2 for seabed morphology and sediment transport analysis. “Zone 1” is from the landfall to the divergence of the CB Route Options at ~ KP 60 offshore. Zone 1 consists of CB Routes 1, 2, 5 and 7 (Figure 1-3). Zone 2 consists of CB Routes Options DBS-CB-1(A) through to DBS-CB-1(H) from ~ KP 60 offshore to the OWF areas. The CB Route Options in Zone 2 have been split into 3 main corridors, which are oriented approximately SW-NE, with a northernmost, central and southernmost corridor, named Zone 2 Corridors 1, 2 and 3 respectively. Two additional corridors, Corridors 4 and 5, are oriented approximately WNW-ESE from Corridor 2. Finally, Corridor 6 extends from Corridor 5. Each route and name for Zone 2 are shown in Figure 1-4.

As of February 2023, some route options have been deselected, and the nomenclature has been updated (Table 1-1). Where appropriate, new route KPs have been added to figures in order to make a direct comparison to the old KPs.

The water depth of the cable corridor area reaches a maximum of c. -70 mLAT. Along the route, slope angles generally remain below 5° (96 % of the 2022 cable route survey area), rarely exceeding 32° (0.00008% of the 2022 cable route survey area), which is the typical angle of repose of in marine sands (Soulsby, 1997). The export cable route surface in Zone 1 is dominated by featureless Holocene sands, which present as a smooth seabed surface on MBES data. Marked changes in bathymetry do exist relating to outcropping/subcropping of either glacial deposits associated with the Bolders Bank Formation (Section 3.2) or bedrock strata. The highest slope angles are related to bedrock outcrops, isolated bathymetric anomalies, as well as the steep faces of localised subaqueous dune or ridge margins.

The latter area of the export cable routes - Zone 2 - are characterised by morphological features including subaqueous dunes of varying heights and wavelengths, as defined by Ashley et al. (1990), which are defined by changes in slope angle. These slope angles are generally  $\leq 20^\circ$ , reaching a maximum of  $21.7^\circ$  on a dune features. The slope asymmetry, where determinable, can indicate dominant flow and sediment transport direction.

The SBP data provided to MarineSpace was preliminary, with horizons being assigned to different geological or lithological bounding surfaces. The preliminary interpreted horizons identified eleven surface horizons (Table 2-1). A further few horizons were identified, including amplitude anomalies, acoustic blanking, gravel accumulation, and pipeline infrastructure. These preliminary interpretations combined with the bathymetry and the review of the geological background have been combined so a preliminary description of the likely deposits that would be encountered by a cable installed at a depth of lowering of between 0 and 2 m.

##### **4.1.2.1. Export Cable Corridor Zone 1 Introduction**

Zone 1 consists of CB Routes 1, 2, 5 and 7 and is from the landfall to the divergence of the CB Route Options at ~KP 60 offshore (Figure 1-3: Zone 1 cable route options, as named by MarineSpace). The routes were attributed these names in the shapefile provided to MarineSpace by RWE, and so have been retained for analysis.



Across the Zone 1 cable routes, the bathymetry deepens from the shallowest point of  $\sim +2.4$  mLAT at the coastal strip to a deepest point of  $\sim -62.4$  mLAT along the centreline as one of a series of incised valley is crossed (Figure 1-1 and Figure 4-14). The seabed immediately offshore ( $\sim$  first 15 km) for all 4 routes is dominated by a series of shore parallel ridges, which are indicative of the retreat moraines of the Late Devensian ice sheet formed in the Skipsea and/or Basement Till seen in the coastal cliff sections (Sections 3.2, Figure 4-2 and Section 4.1.1.1, Figure 4-11 and Figure 4-12). Individual ridges are up to  $\sim 2.5$  m in relief and have asymmetric forms with steeper dipping ( $\sim 10$ – $15^\circ$ ) western facing margins, typical of recessional moraines retreating to the east. Dove et al (2017) have suggested that these ridges are not a priori glacial deposits due to their “fresh” geomorphic character, high slope angles (they recorded up to  $25^\circ$  elsewhere along the coast) and their presence close to the coast (within  $\sim 200$  m). There alternative mode of formation is ascribed to “...modern, or perhaps relict coastal processes...”. This report argues that these are glacial retreat features as: the north-south orientation is not supported by the sediment transport pathways present along this coast (Section 3.3, Figure 3-7); the asymmetric form is not atypical of recessional moraines and the angles in this area at least rarely exceed  $15^\circ$ ; and as it is difficult to support extensive development of these features very close to the shore, with the majority of the features being at water depths between  $-10$  and  $-20$  mLAT would suggest they would have been overtopped rapidly during the early part of the Holocene and hence the preservation of such topographic features is likely; and finally, as is discussed in Sections 1.1.1.1 and 4.1.2.3 the preliminary ground model suggests an area of Bolders Bank Till at the surface throughout (Figure 4-17 and Figure 4-19).

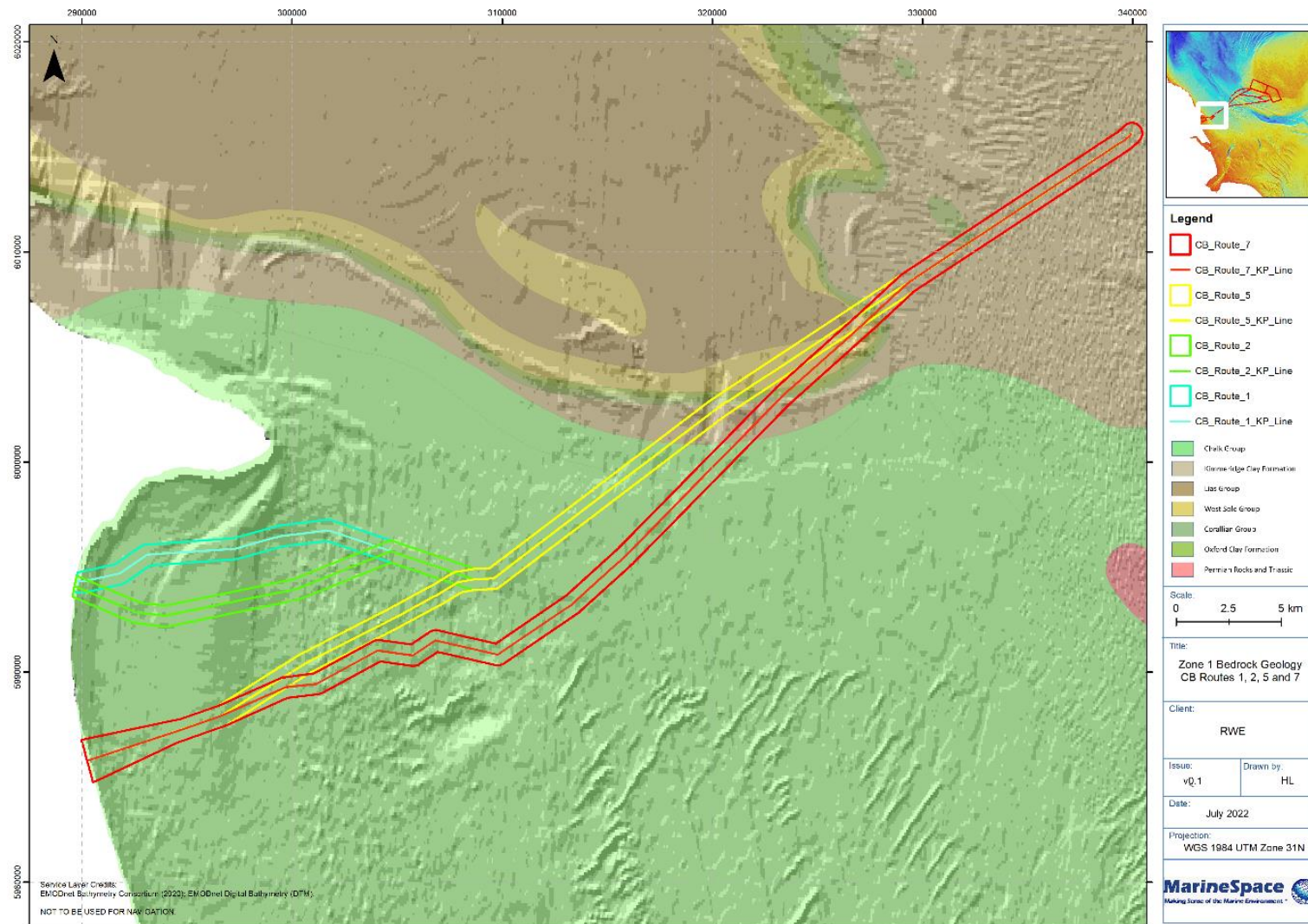
To the east of the Smithic Bank, these north to south trending ridges are interspersed by north-northwest to south-southeast (i.e. very oblique to the ridges) trending very shallow ( $< 0.5$  m relief) linear depressions that either terminate against or navigate around the ridge structures (Figure 4-18). It is unclear if these relate to post-transgressive sedimentary processes or potentially deglacial drainage processes. Irrespective of their origin time-lapse bathymetric analysis suggests there is no associated bed level change over a period of up to 8 years.

This glacial landscape is overlain in part by the southerly extension of the South Smithic Bank. The overall Smithic Bank complex is up to 4.4 km wide, approximately parallel to the coastline extending south-southwest from the tip of Flamborough Head to Skipsea (Figure 1-3, Figure 1-5 and Figure 4-21). The formal Admiralty description of the Smithic bank system only extends to the “SW Smithic Buoy”  $\sim 4.5$  km south of Bridlington and opposite Fraisthorpe Beach, and so only encompasses CB Routes 1 and 2. However, the sand body can actually be described by the  $-10$  mLAT contour and this feature extends a further  $\sim 6.5$  km south and encompasses CR B routes 5 and 7, this extended feature will be referred to as the Smithic Bank complex. Further offshore, the seabed morphology is marked by a thin veneer of Holocene marine sands, overlying intermittent Bolders Bank Tills, which are occasionally channelised and infilled with Botney Cut Formation material (Section 3.2), and variations in the underlying bedrock geology (Section 3.1).

There are no multiple, overlapping, high-resolution, swath bathymetry datasets available for multi time-step bed level change analysis, in the nearshore zone, with the Fugro ECC specific surveys terminating on the eastern margin of the Smithic Bank complex (Figure 2-1). From the single datasets that are available nearshore analysis of the limited bedforms that are present suggest sediment transport is as inferred from the hydrodynamic models (Section 3.3, Figure 3-7) with a clockwise circulation pattern around the bank. However, the dominance of till at the bed and the

relative dearth of sedimentary bedforms, and the absence of significant scour around a series of wrecks, suggest bed movement is limited in these very nearshore sections of the route west of the Smithic Bank Complex.

Figure 4-10: Zone 1 cable routes (named by MarineSpace) overlain on British Geological Survey offshore bedrock geology and EMODnet hillshade (Source: British Geological Survey, 2022)



#### **4.1.2.2. Zone 1 - CB Route 7 (Route A KP0-8.5 and KP 45-60)**

The first 650 m from the landfall (which has a 0 KP at the actual back-beach till cliff – Section 4.1.1.1) offshore represents the “sandy” beach deposits which pinch out on the underlying till surface at ~ KP 0.65 (there is an ~ 250 m strip between the offshore end of the terrestrial datasets [Aerial Photography and LiDAR] and the start of the first swath dataset). From ~ KP 0.65 to ~KP 3 the seabed is characterised by exposed glacial tills with an irregular surface morphology reworked into a series of shore parallel ridges. This section of the route is on the very northern margin of the retreat moraine topography and encounters 5 of these ridges between ~KP 2 and KP 3 as they become buried by the western margin of the sandbank. Between ~ KP3 and ~ KP 7.5 this surface is overlain by the southern margin of the South Smithic Sandbank. The eastern margin of this bank shows a series of linear erosion features (400 – 600 m in length and less than a 1 m deep: Figure 4-11), oriented perpendicular to the bank margin, which over a 2-year period, showed deepening of up to 0.6 m, with bed level increase on their southern side of up to half that magnitude.

Continuing offshore the low relief, north to south oriented, ridges cross the ECC to ~ KP 15 where the final clearly delimited ridge occurs. Although these features are static, there does appear to be a pattern of bed level change over a two-year period on the western, nearshore, side of some of these ridges, but which is limited to < 0.3m (an increase of ~0.15 m/yr) although such a magnitude of change is at the limit of the uncertainty of the datasets, especially the coarser resolution HI1587 (2020) CHP dataset (Figure 4-12). The shallow relief, north-northwest to south-southeast trending linear depressions that terminate against or navigate around the ridge structures, continue to be present beyond the easterly extent of the ridges to ~ KP 21.5. Comparison of the Fugro 2022 dataset and the HI1473 (2016) data suggests there has been no demonstrable bed level change associated with these features over this period.

South of KP 18 on the southern corridor margin lies the wreck of the VILLE DE VALENCIENNES (UKHO ID: 6469), which is oriented on the seabed in a west-northwest to east-southeast direction, has developed small localised, symmetrical scour pits, 0.7 m and 1.4 m deep respectively, indicating minor sediment transport with no dominant direction. The wreck of the FELTRE (UKHO ID: 6470), oriented north to south, lies 1.2 km NNW of KP 17, and has similarly limited evidence of active transport (Figure 4-13).



Figure 4-11: Linear erosion features on the eastern margin of the southerly extension of the Smithic Bank Complex in the vicinity of Zone 1 CB Route 7 ~KP 8. Further west are a series of discontinuous north-south retreat moraines that are common along all Zone 1 CB Routes 2, 5 and 7 (with updated 2023 Route A Centreline and KPs visible)

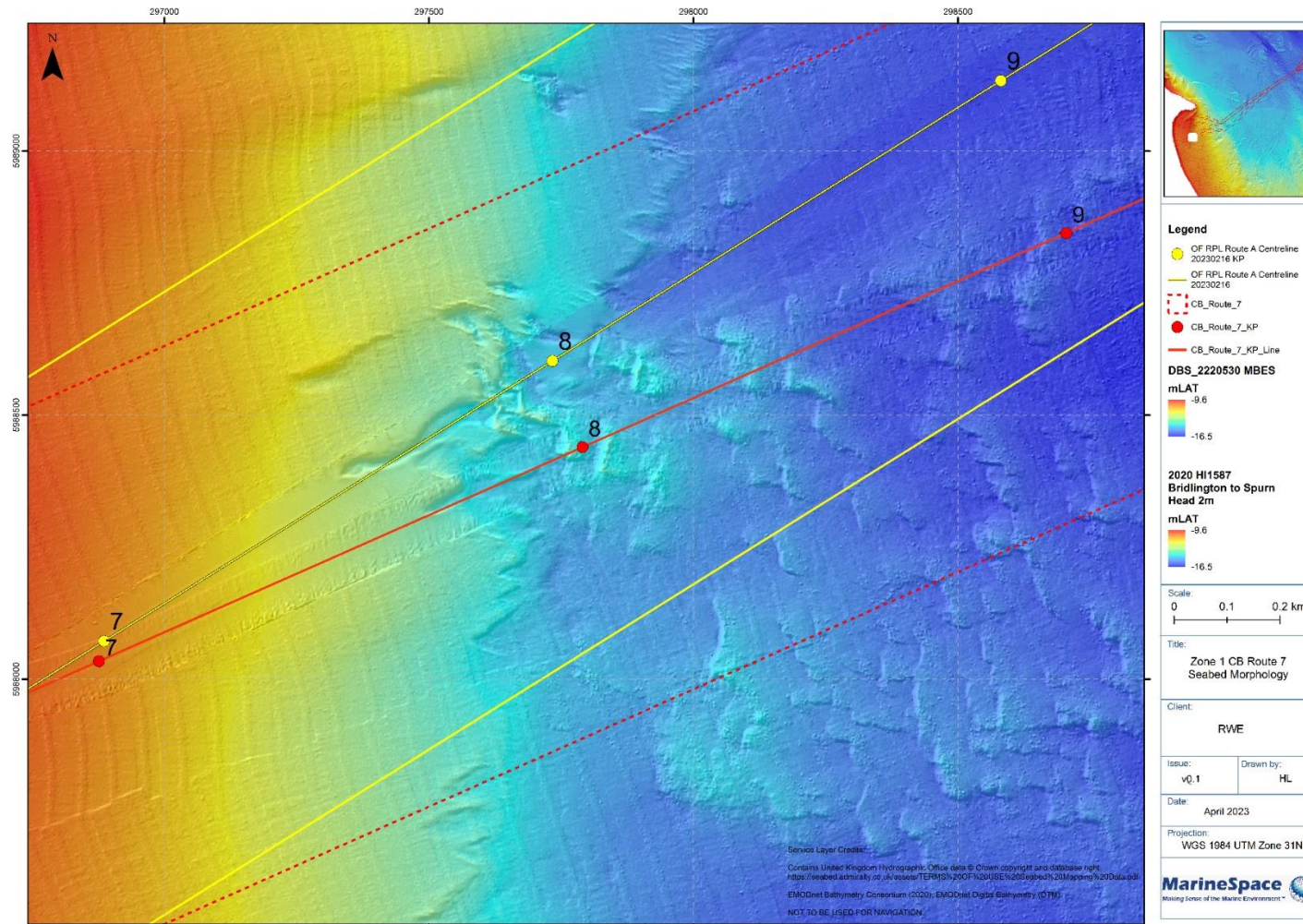




Figure 4-12: Recessional moraine ridges and associated bed level change between 2020 and 2022 along Zone 1 CB Route 7

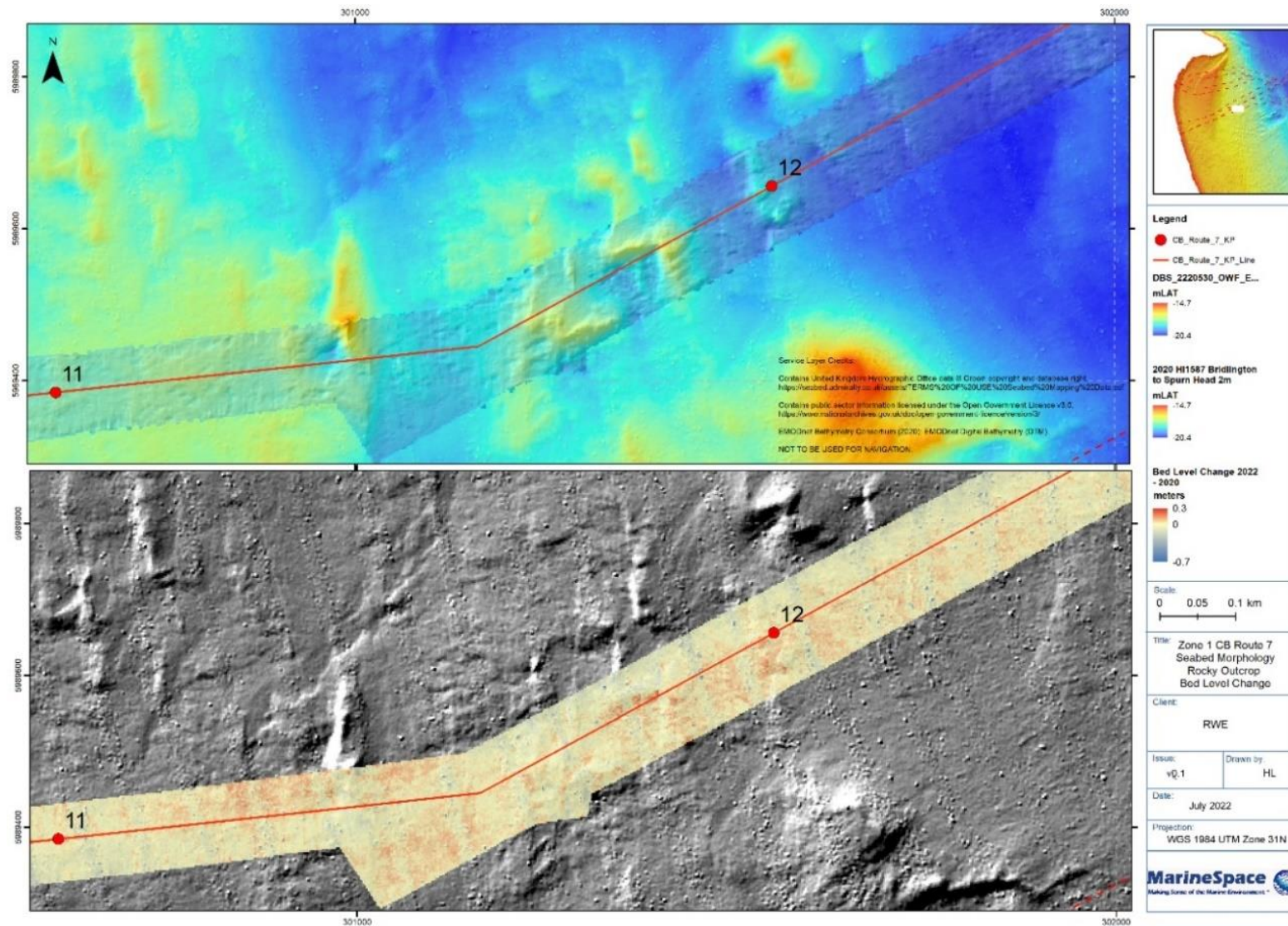
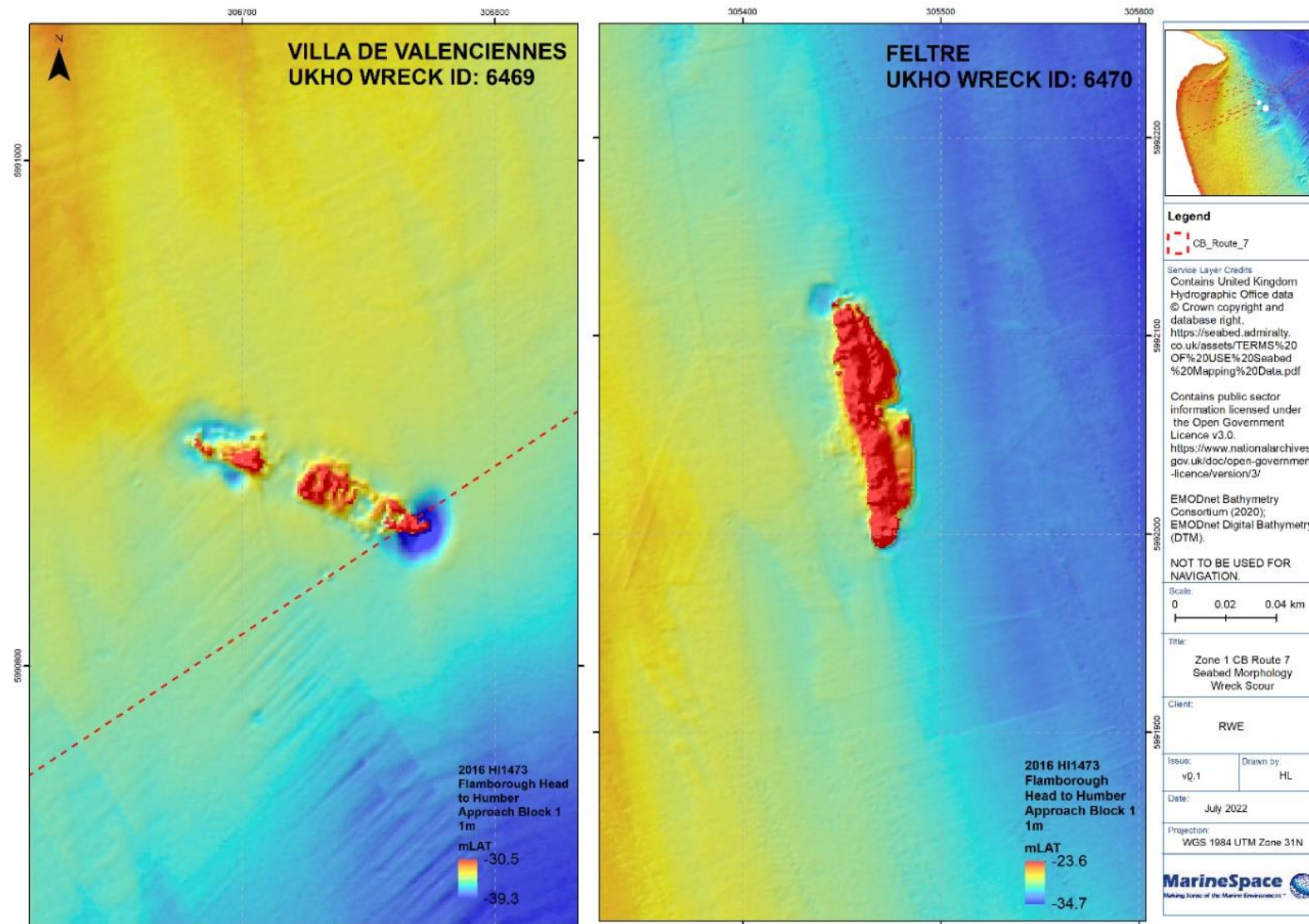


Figure 4-13: Scour patterns around the wrecks of the Villa de Valenciennes and Feltre along Zone 1 CB Route 7





From ~KP 15 to ~KP 20.5 the seabed deepens from -25 mLAT to -42 mLAT, an elongate topographic high, ~ 1 km across and with a relief of ~3.5 m crosses the route between KP 20.5 and KP 21.5 with the bathymetry flattening out to ~ -47.5 mLAT and then gently shelving offshore until a depth of -60 mLAT is reached at KP 60. It is worth noting that ~ 2.7 km to the southwest of the route is a field of large, asymmetric, subaqueous dunes, oriented southwest to northeast, with bedform heights of over 7 m and wavelengths of typically 1.2 km. These features have steep lee slopes suggesting migration to the southeast and time-lapse bathymetry suggests they are in fact moribund (i.e. not active) with no discernible bed level change over a 7-year period. Consequently, these do not represent a lifetime threat to the cable corridor.

There are localised topographic feature along this section of the route including between KP 31.5 and KP 32 where a north to south oriented linear depression, ~2.5 m deep and ~800 m wide (Figure 4-14: Transect A – A') crosses the route. This depression contains isolated topographic highs a few 10's metres in XY dimensions along its base and margins. This appears to be the southerly extension of a potential subglacial tunnel valley system, formed during the Late Devensian glaciation (Dove et al., 2017) and which are more prominently seen further south opposite the Humber Estuary.

CHP survey HI1473 (2016) covers the Zone 1 - CB Route 7 ECC between KP 15 to KP 34.75, so bed level change across this area can be calculated for this six-year period, and is shown to be effectively zero being within a survey uncertainty of  $\pm 0.2$  m. Additionally, 2 further wrecks of a steam ship (UKHO ID: 6473, 1 km SE of KP 23) and the TEES (UKHO ID: 6474, 1.8 km SE of KP 25) have really restricted scour patterns with no indication of a dominant sediment transport direction.

Beyond KP34.75 the only available bathymetric data is the Fugro corridor specific survey and the EMODNET bathymetry (note 2D echosounder data from the 1980's is publicly available but as this is what underpins the EMODNET data has not been studied separately. Between KP 37.3 and 38 a v-shaped channel, ~700m wide and with a relief of ~4m, is crossed by the route and this again appears to be a southerly extension of another sub-glacial tunnel valley (Figure 4-14: Transect B – B').

Between ~ KP 33.5 and 34 the seabed drops by 1.5 m over a distance of ~ 400 m. This gentle break in slope extends from Flamborough Head due east and broadly corresponds to the boundary between Chalk Group and underlying Cromer Knoll Group (Section 3.1). The seabed between KP 38.5 and 39.5 encounters a bathymetric high of ~ -51 mLAT with irregular relief which corresponds to the outcropping of the boundary between the Kimmeridge Clay and Corallian Group limestones (Section 3.1.1). Beds of the Corallian Group also outcrop at ~KP 45.4 of Zone 1 - CB Route 7 ECC with these outcrops describing either side of a plunging anticline (Figure 4-15). On the northeastern margin of this anticline sandstones and mudstones associated with the underlying Oxford Clay (~KP 44.8 – 45) and West Sole Group (~ KP 43.8 – 44.5) also appear to be outcropping (Figure 4-15).

Figure 4-14: Zone 1 CB Route 5 and 7 (and 1 and 2) seabed topography

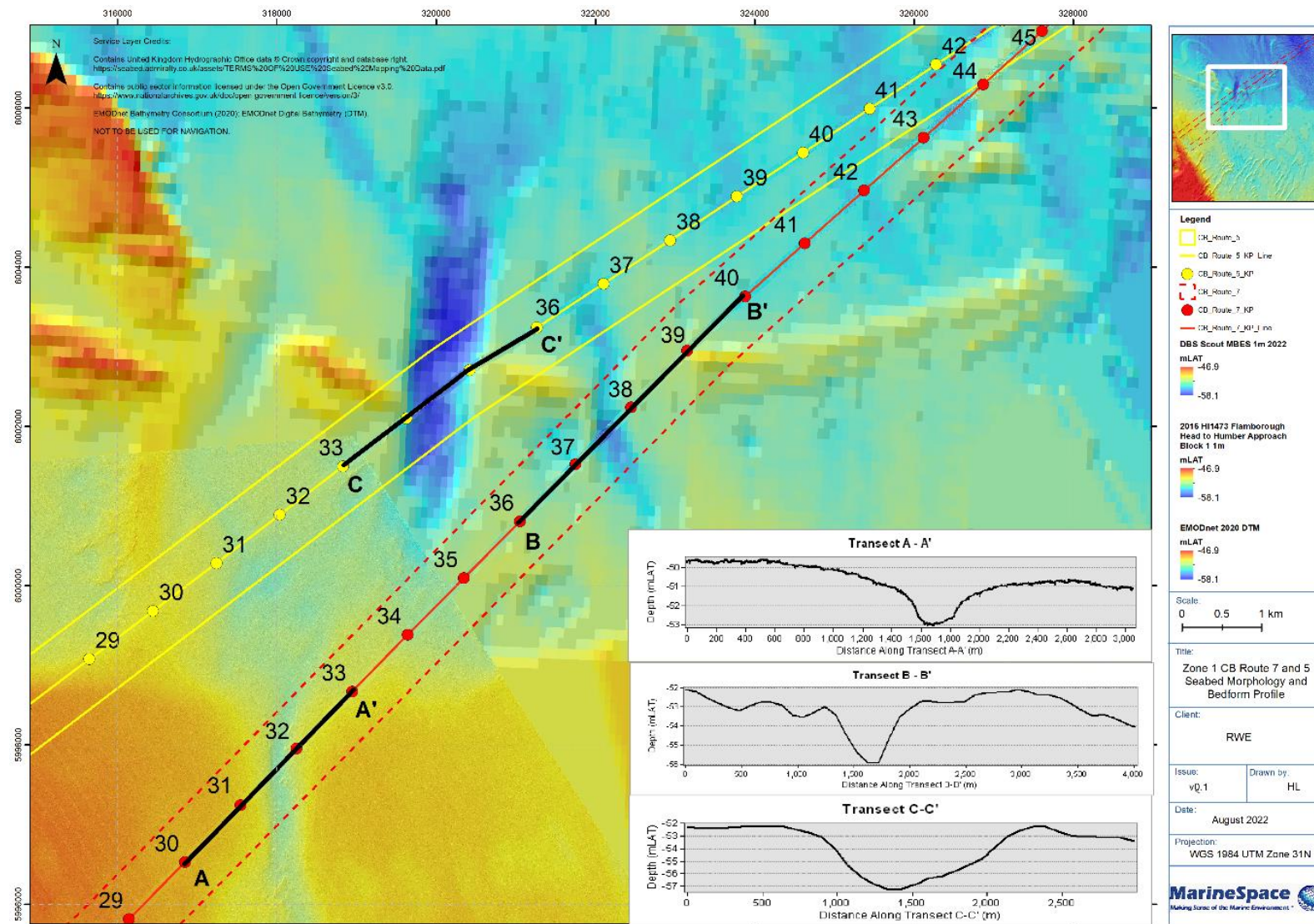
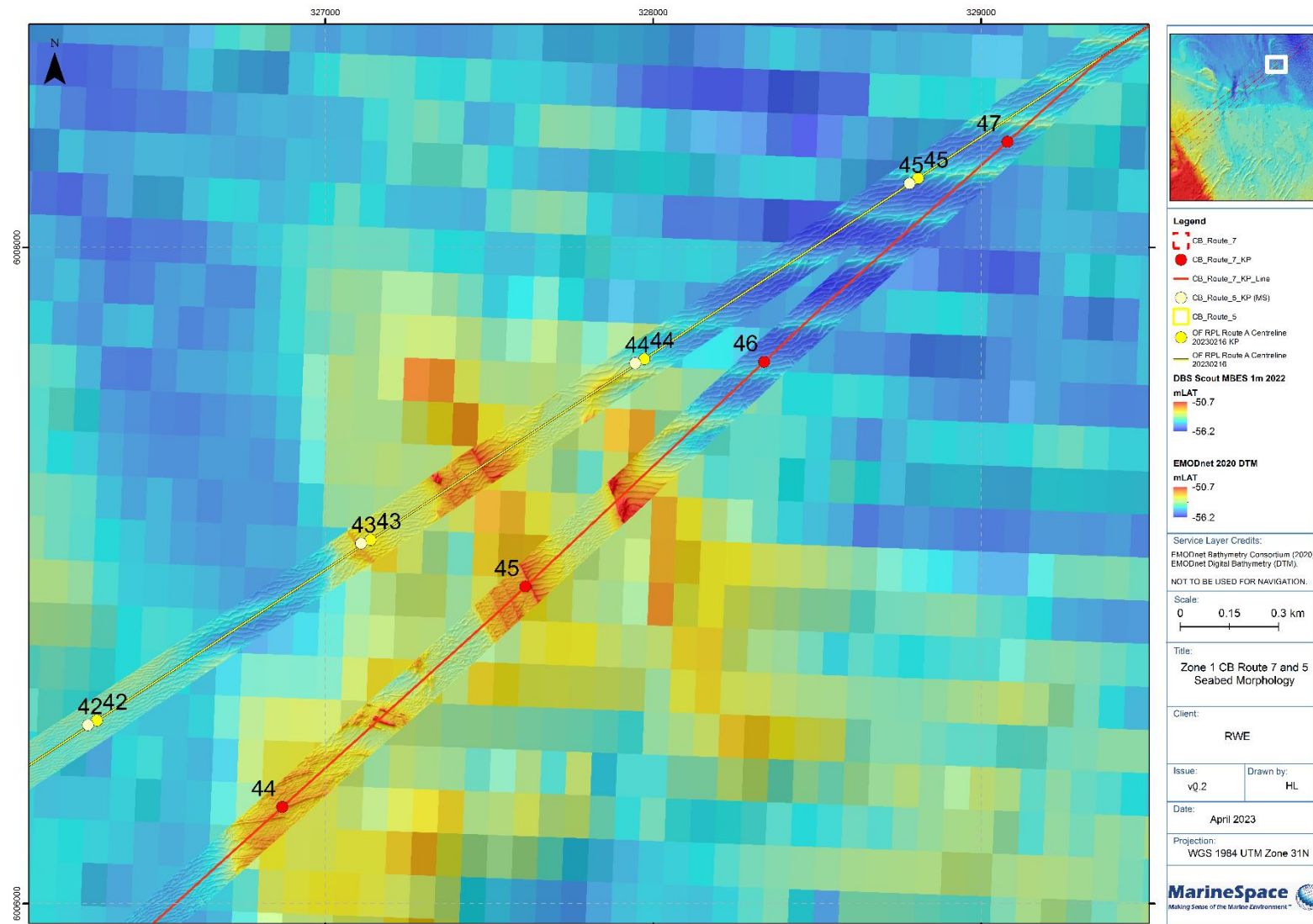


Figure 4-15: Outcropping West Sole Group, Oxford Clay and Corallian Group (with updated 2023 Route A Centreline and KPs visible)





From ~ KP 41.5 there is the increasing presence of small subaqueous dunes, oriented west-southwest to east-northeast continuing until ~KP 45. These bedforms have wavelengths of up to ~11m, heights of up to ~0.1 and a symmetrical cross-sectional profile. From ~KP 45.5 these bedforms become parasitic in nature being superimposed on longer wavelength (~200 m) higher amplitudes (up to ~2 m) west to east oriented bedforms that also have a symmetrical form. Such symmetry is commonly interpreted as being produced by wave induced currents or perfect symmetry of the tidal flows, however at these depths (~ -55 mLAT) it is unlikely to be actively wave induced except under very extreme events. It is therefore possible that these bedforms are moribund and the bed is stable under all conditions. Supporting this interpretation is the presence, at ~ KP 52.5, of the Langede Gas Pipeline from the Sliepner riser to Easington which was installed between 2005 and 2006 and which can provide a proxy indicator of seabed movement (Figure 4-16). At this location the pipeline shows no evidence of any backfill over a 16-year period whereas at other locations where the pipeline crosses more active bedform fields it has become buried. Again, this would suggest a currently stable bed along this section of the route.

Figure 4-17 displays the initial seismic interpretation of Zone 1 CB Route 7, showing that H05\_b and H10\_b (Table 2-1) tend to occur in tandem in areas where the bathymetry shoals, over large sand banks or where there are large to very large subaqueous dunes present. This is evident in the nearshore: ~KP 6.7 (where the seismic interpretation provided starts) to KP 8.0 (the eastern margin of the South Smithic Bank complex), the elongate topographic high at ~KP 21, intermittent thin (< ~ 1 m) surface veneers between ~KP 31.9 – 48.3, and then consistently from ~KP 45 to the end of Route 7 at ~KP 60. These 2 horizons define the base of the Upper Sand and Lower Laminated Sand Units respectively, which are Holocene, post-transgressive marine sands (Table 2-1).

H30b, “Bolders Bank Till 1” (Table 2-1) is the principal seismic unit underlying H05\_b and H10\_b and has been identified by Fugro along almost the entire route, generally 5m or greater below the seabed surface. This interpretation supports the bathymetric interpretation described above suggesting that Bolders Bank Formation tills are effectively exposed at the surface from ~KP 8.0 to 38.5 except for sporadic thin veneers of overlying marine sands just described. From ~KP 46 to 60 this same seismic unit is present at depth between the marine sands. Horizons H26\_i and H28\_i which are also interpreted as being reflectors within the “Bolders Bank Till 1” and “Channel Bolders Bank Till 1” (Table 2-1) respectively are present intermittently along the route but with limited extent and with no information on how they may sedimentologically differ. Similarly, H35\_b which is interpreted as being “Bolders Bank Till 2” (Table 2-1) and underlies “Bolders Bank Till 1” is potentially exposed at the surface between ~KP 22.6 and 24.4 but there is no information on the inferred sedimentological difference given between these 2 seismic units.

The seabed outcrops of potentially Corallian Group limestones between KP 38.5 and 39.5 and at ~KP 45.4 and the sandstones and mudstones associated with the underlying Oxford Clay (~KP 44.8 – 45) and West Sole Group (~ KP 43.8 – 44.5) all coincide with no near surface seismic horizons associated either with the post-transgressive marine sands nor the Bolders Bank Formation tills in the Fugro interpretation further supporting this bedrock interpretation.

Figure 4-16: Exposure of Langed Gas Pipeline with total lack of sedimentary infill (with updated 2023 Route A Centreline and KPs visible)

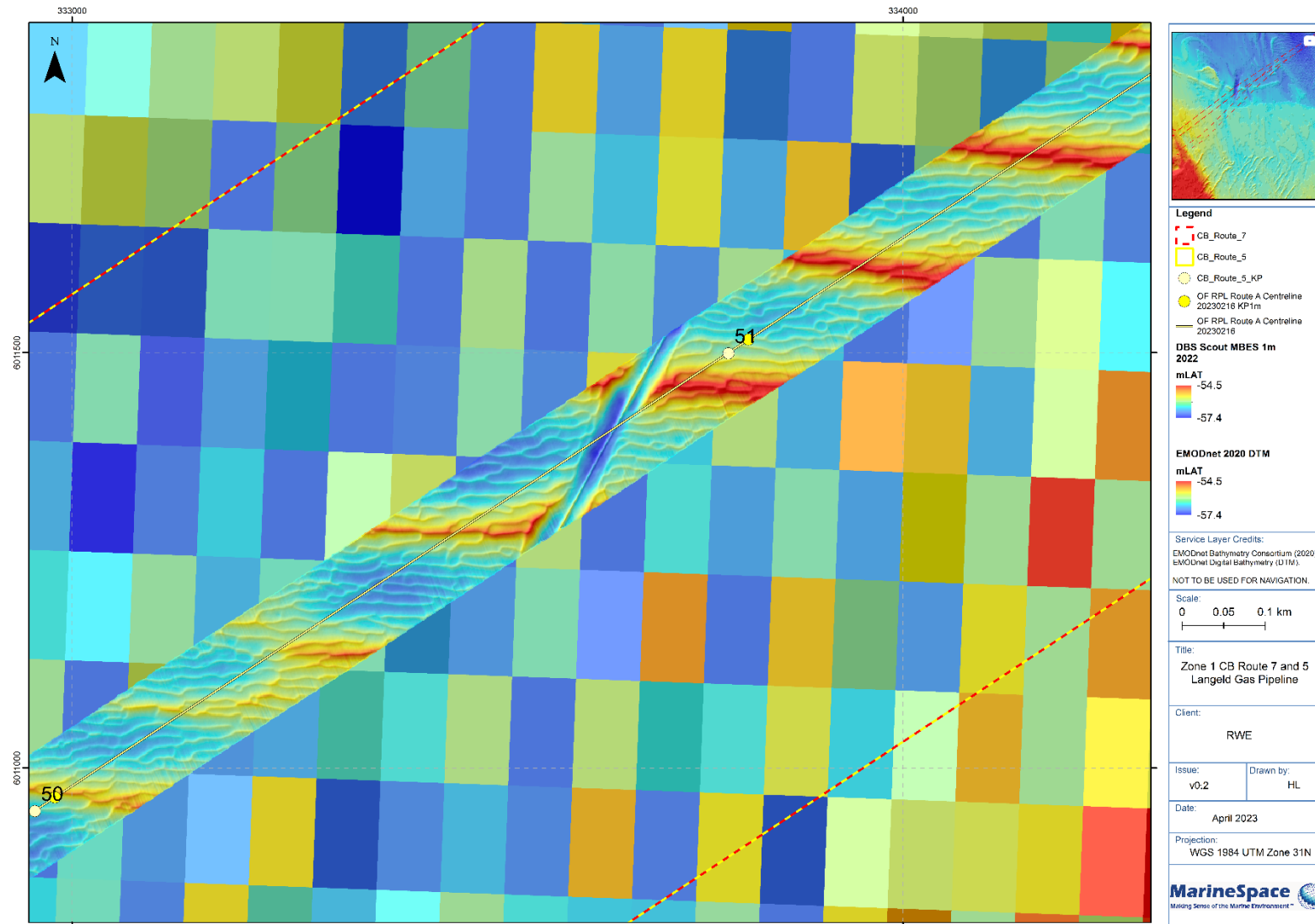
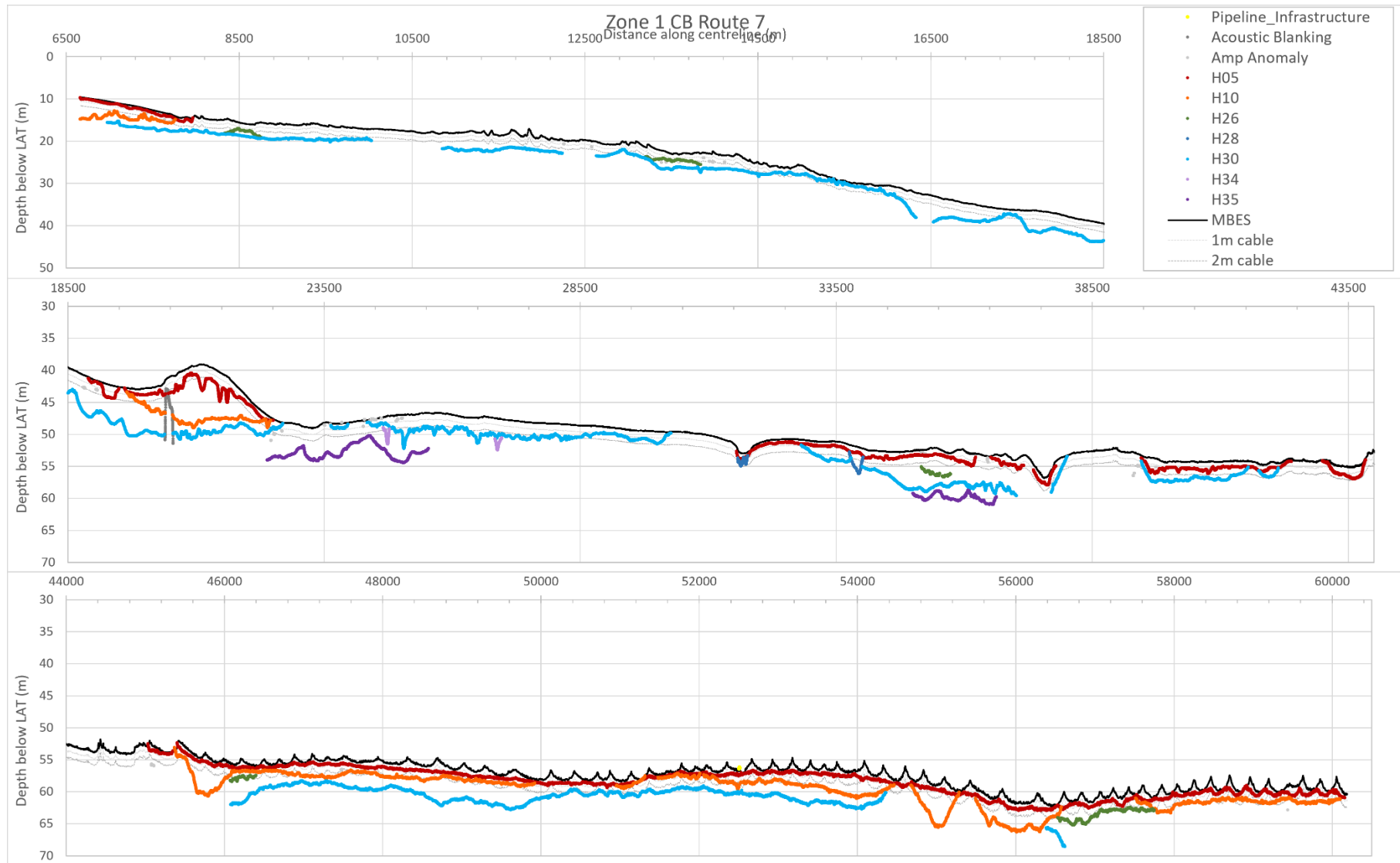


Figure 4-17: Cross-sections along Zone 1 CB Route 7, showing the horizons encountered by a cable at 1m or 2m depth below seabed



#### **4.1.2.3. Zone 1 - CB Route 5 (Route A)**

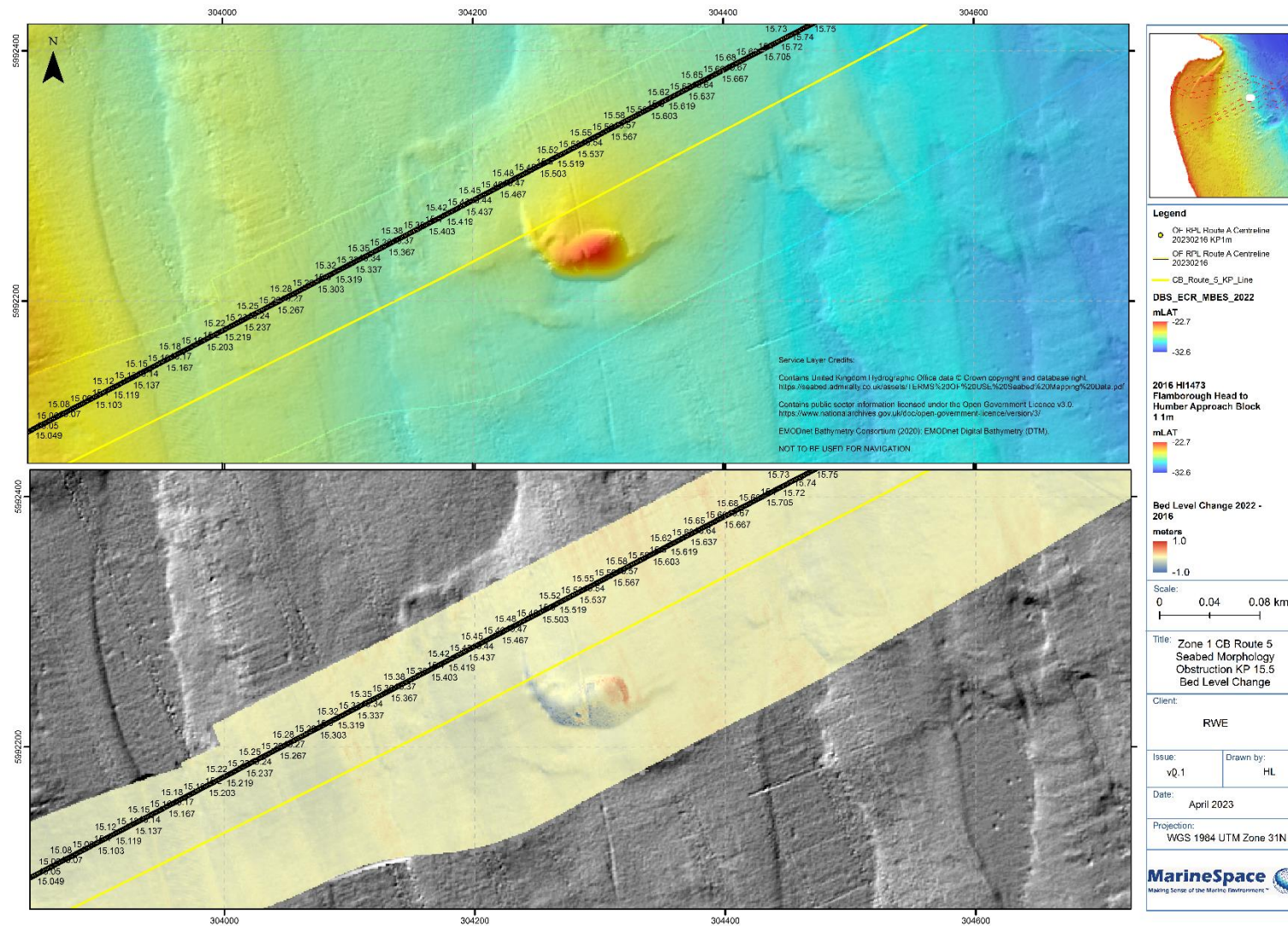
KP 0 – 6.75 is the same for CB Route 5 as for CB Route 7. From this point the routes diverge before re-joining at ~KP 45. As such, morphological description from KP 0 – 6.75 and KP 45 – 58.5 for CB Route 5 can be taken from KP 0 – 8.5 and KP 45 – KP 60 for CB Route 7 (Section 1.1.1.1) and will not be repeated.

CB Route 5 crosses the southern margin of the South Smithic Bank complex between ~ KP 7.5 and 8.25 and exhibits linear, bank perpendicular, erosion features with up to  $\pm 0.4$  m bed level change. The north to south oriented recessional moraine ridges interspersed with the shallow relief, north-northwest to south-southeast trending linear depressions are present to ~ KP 15.5, with the linear depressions extending a further ~ 3.5 km to ~ KP 19. Examples of similar features can be seen in Figure 4-12. Again minor (+ 0.3 m) sediment accumulations on the western margin of the ridges have occurred between 2020 and 2022, with no corresponding evidence of change associated with the depressions. An obstruction measuring 5 m high and ~ 100 m x 40 m in dimension protrudes from the seabed at ~ KP 15.5. Its position does not change between 2016 and 2022, although as with the ridges in the area there is some minor bed level increase of  $\leq 0.5$  m over this period, with some bed level decrease on its southern and western side to a maximum of -1 m (Figure 4-18). It is probable that this upstanding static glacial feature provides a sufficient obstacle to the combined tidal and wave driven flows to generate localised, small-scale, scour and accumulation.

To ~ KP 31 the seabed is relatively featureless and deepens only slightly across a large extent, encountering some gently undulating shallow plateaus and with minor channelisation. A small ridge (~ 0.7 m relief) is encountered along CB Route 5 at ~ KP 21.4. This feature is oriented north to south and is associated with two similar ridges on the southern margin of the ECC at this location. These are probably minor, isolated, moribund bedforms for which there is no evidence of mobility in a 6-year period between 2016 and 2022. CHP survey HI1473 (2016) covers the Zone 1 - CB Route 5 between KP 15 to KP 33.25, so bed level change across this area can be calculated for this six-year period, and is shown to be effectively zero being within a survey uncertainty of  $\pm 0.2$  m.



Figure 4-18: MBES anomaly and North-South oriented linear depressions along Zone 1 CB Route 5 at ~ KP 15.5 (with updated 2023 Route A Centreline and KPs visible)





Between ~ KP 29 and 30 the seabed drops by 2 m over a distance of ~ 600 m. This gentle break in slope extends from Flamborough Head due east and broadly corresponds to the boundary between Chalk Group and underlying Cromer Knoll Group (Section 3.1). From ~ KP 31 to 35.5 the route crosses a series of north to south oriented channels the most prominent of which is between ~ KP 34 and ~ KP 35. This V-shaped valley, approximately ~5m high and ~800m in width is delimited on each margin (at KP 33.7 and KP 35.2 respectively) by discrete, ~1 m high ridge features. These valleys feed into those that cross Zone 1 CB Route 7 further south. The V-shaped valley is cutting through an east west oriented prominent ridge (identifiable even in the coarse resolution EMODNET data) which correlates with the boundary between the Kimmeridge Clay Formation and the Corallian Group deposits (Figure 4-14). No clear bedrock outcrops are identifiable from the Fugro 2022 swath bathymetry data at this location. Between ~ KP 43 and 43.9 north-northwest to south-southeast striking beds, within the Oxford Clay and Corallian Group Formations, can be traced between the swath data from Zone 1 CB Route 7 and Route 5 (Figure 4-15).

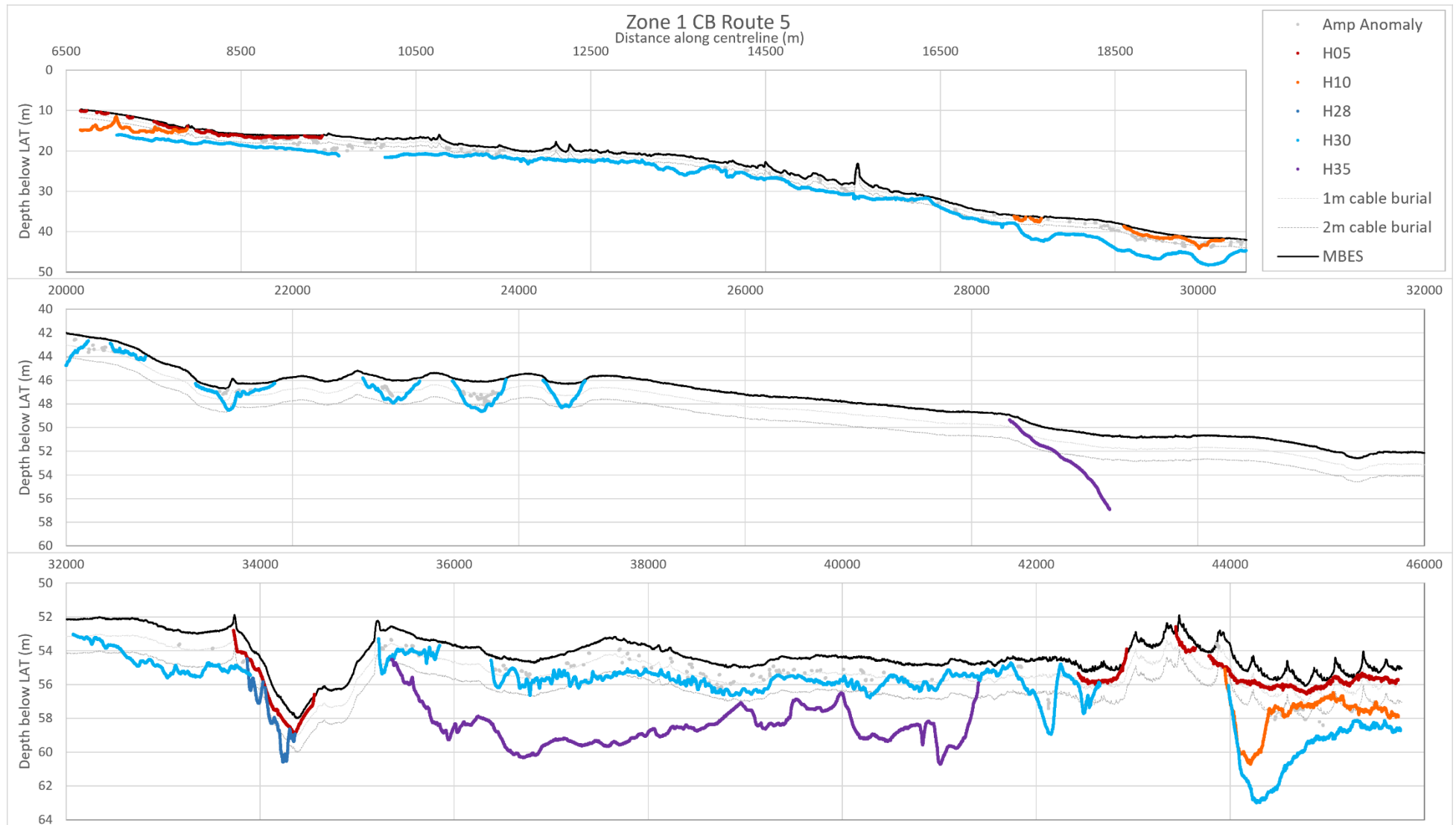
Finally, from KP 40 there is the increasing presence of small subaqueous dunes, oriented west-southwest to east-northeast which then transition (~ KP 44) into parasitic forms on larger west to east oriented bedforms. These bedforms have identical dimensions to those described at a similar location in Zone 1 CB Route 7 (Figure 4-15).

Figure 4-19 displays the initial seismic interpretation of Zone 1 CB Route 5. This route merges with Zone 1 CB Route 7 at ~KP 45 and as such, SBP data analysis from this point to KP 58.5 can be taken from the equivalent KP's (KP 47.5 – KP 60) for CB Route 7 (Section 1.1.1.1) and so will not be repeated here. As with Zone 1 CB Route 7 the Holocene, post-transgressive marine sands, H05\_b and H10\_b (Table 2-1) are present in the nearshore starting at ~KP 6.7 (where the seismic interpretation provided starts) and continuing to ~KP 9.4 beyond the eastern margin of the South Smithic Bank complex in contrast to Zone 1 CB Route 5 where the sand terminated at the Bank complex margin. This demonstrates the locally spatially variable nature of these recent sands deposits. These recent deposits then are locally identified between ~KP 17 and 20, 33.7 and 34.5 and then from ~KP 42.4 to the end of the route.

From ~KP 9.4 to ~KP20.2, the “Bolders Bank Till 1”, defined by H30\_b, is interpreted by Fugro to outcrop extensively within this part of the route with the exception of the Lower Laminated Sand Unit as described above. This is broadly mirrored in the bathymetry albeit the relative smoothness of the bed and the presence of linear depressions to ~KP19 would suggest a thin veneer of marine sands is presented but potentially lost in the seabed return.

From ~KP 20 to ~KP 32 it is unclear what deposits are at the surface as no clear horizons have been identified. Again the seabed from the bathymetry is relatively smooth which would suggest at least a very thin veneer of marine sands is present but it is likely that this will rapidly pass into some part of the Bolders Bank Formation deposits. Such a stratigraphy is seen in the region between ~KP 32 to ~KP 43.5. There is little evidence in this region of bedrock outcrops at the surface until the exposures at ~ KP 43 and 43.9 of Corallian Group deposits, can be traced between the swath data from Zone 1 CB Route 7 and Route 5 (Figure 4-15).

Figure 4-19: Cross-section along Zone 1 CB Route 5, showing the horizons encountered by a cable at 1m or 2m depth below seabed



#### **4.1.2.4. Zone 1 - CB Route 2 (Deselected)**

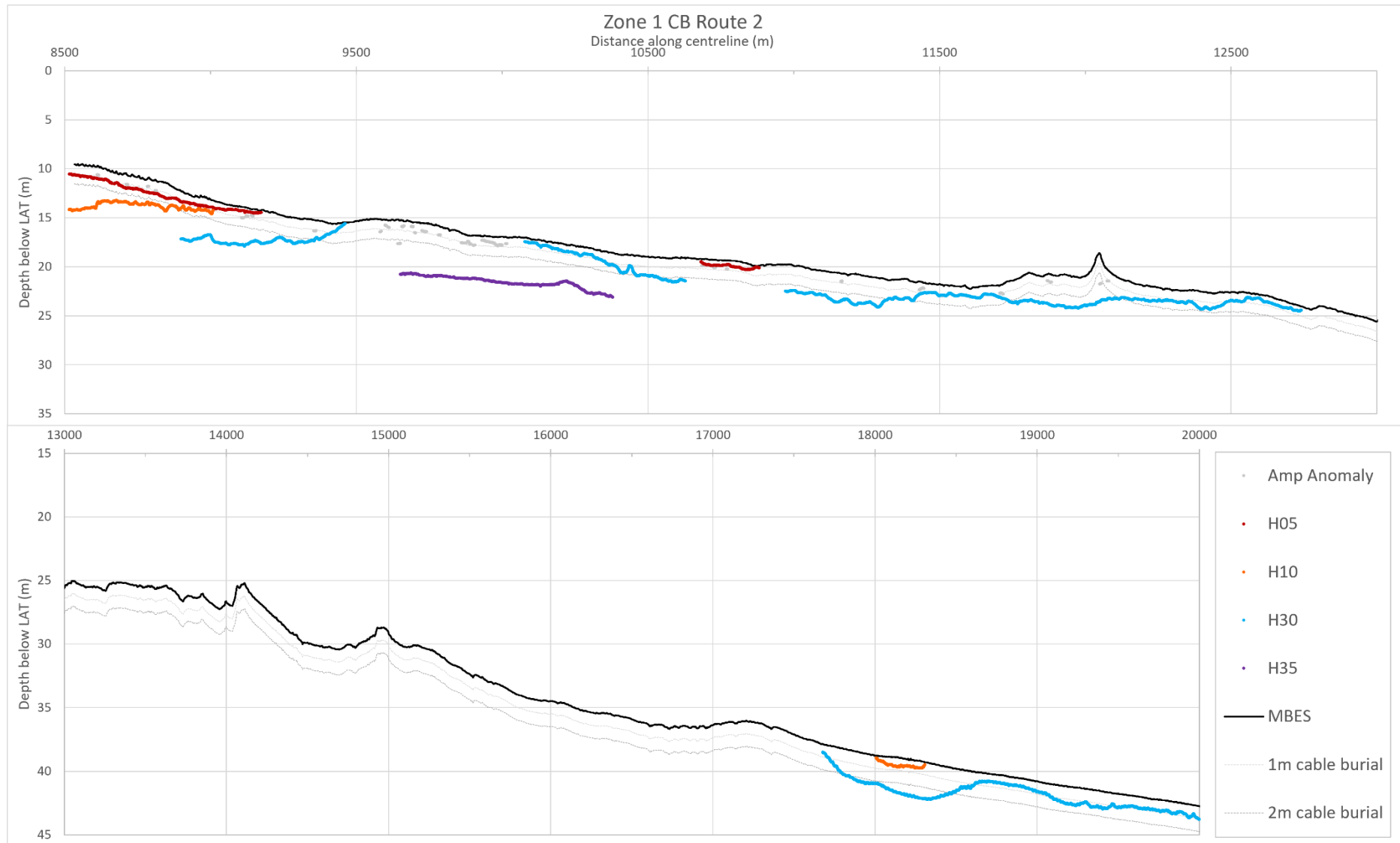
Zone 1 CB Route 2 extends from the northern landfall site, converging with CB Route 5. Therefore, CB Route 2, from KP 20 onwards, is the same as CB Route 5 and so descriptions will not be repeated.

From KP 0 at the back beach cliff line to KP 1.1 the “sandy” beach slopes to a depth of -6 mLAT and then flattens out (there is an ~ 250 m strip between the offshore end of the terrestrial datasets [Aerial Photography and LiDAR] and the start of the first swath dataset). Between KP 1 and 1.5 the underlying till is periodically exposed at the surface and it and fragmented exposures are found all the way to ~ KP 3.8 as the route starts to cross South Smithic Bank. Along the centreline of the route the bank reaches a minimum depth of -5.5 mLAT with the seabed morphology being relatively smooth and featureless. Between ~KP 7.8 and 9, moving off the eastern margin of the sandbank, a bedform field of small to medium subaqueous dunes up to ~0.4m high and with wavelengths up to 10m occur, oriented WNW-ESE (perpendicular to the dominant flow). They have a symmetrical cross-sectional profile and bed level change over a 2-year period, suggests up to a 0.4 m increase, and loss of up to 0.8 m.

From ~ KP 9 to 14.3 the seabed is dominated by the previously described glacial influenced surface. However, the inferred recessional moraine ridges are restricted to a zone between ~KP 11.5 to 15, with ~ KP 9 – 11.5 and ~ KP 15 to 18.5 having a seabed dominated by the north to south oriented, intercalated, linear depressions. These do not show bed level change over a two-year time scale. The recessional moraine features, as along CB Routes 5 and 7, show bed level accumulation on their western side, with a maximum bed level increase of up to 0.3 m in a two-year period. At ~KP 11.5, 60 m north of the CB Route 2 corridor, the wreck of the BIEBOSCH (UKHO ID: 5808) has only localised dishpan scour with depths of < ~0.5 m. From KP 18.5 to 20 the seabed surface is featureless, merging with CB Route 5 at this point.

For Zone 1 CB Route 2 the Fugro seismic interpretation starts at ~KP 8.5 as the route crosses the eastern margin of the South Smithic Bank. From this point to the edge of the bank at ~KP 9.2 the sub-surface is characterised by the marine Holocene sands defined by seismic boundaries H05\_b and H10\_b (Figure 4-20). These two seismic units are underlain by the “Bolders Bank Till 1” (defined by H30\_b) which becomes exposed at the surface from ~KP 9.2 eastwards. From ~KP 9.5 the seismic interpretation suggests that this unit pinches out and is replaced for ~ 900 m, to ~KP 10.1, by “Bolders Bank Till 2” as defined by H35\_b. From ~KP 10.1 to ~KP12.7 “Bolders Bank Till 1” is again exposed at the surface except for localised patches of the Holocene “Upper Sand Unit” defined by H05\_b. The sub bottom profile data identifies no horizons at depth from ~KP 12.7 to ~KP 17.7. Finally, from ~KP 17.7 to KP 20 (where the route joins CB Route 5) H30\_b is picked up again reaching a maximum of ~3 m below the seabed surface such that “Bolders Bank Till 1” dominates the surface. Correlating against the bathymetry there is no doubt that these till deposits are at or near the surface’ albeit from ~KP15 to KP20 there is probably a near surface very thin veneer of marine sands which results in the smooth seabed identified along this section of the route.

Figure 4-20: Cross-section along Zone 1 CB Route 2, showing the Horizons encountered by a cable at 1m or 2m depth below seabed.



#### **4.1.2.5. Zone 1 - CB Route 1 (Deselected)**

Cable Route 1 is as CB Route 2 from KP 16 offshore, and so this section will not be repeated.

From KP 0 at the back beach cliff line to KP 1.1 the “sandy” beach slopes to a depth of -6 mLAT and then flattens out (there is a ~ 400 m strip between the offshore end of the terrestrial datasets [Aerial Photography and LiDAR] and the start of the first swath dataset). KP 0.7 to 3.7 is largely featureless, although the exposure of till deposits ~ 600 m to the north and south would suggest that the glacial sequences are still in the near sub-surface. From KP 3.7 to KP 5.5 the seabed morphology is dominated by west-northwest to east-southeast oriented ridge and runnel features (Figure 4-21). The origin of these features is discussed in detail in Section 4.1.3, but their gross position is liable to be stable but with minor bed level fluctuations at their margins. In the vicinity of ~ KP 5, small (amplitudes ~ 0.2 m, wavelengths ~ 20 m) subaqueous dunes with an asymmetry to the north-east confirms the sediment transport directions described in Section 3.3.

From ~ KP 5.5 the bathymetry shoals as the corridor moves over South Smithic Bank and reaching a minimum depth of -3.3 mLAT. The route across South Smithic, to ~ KP 8, is featureless and smooth, at resolution of 4 m. On the southerly margin of the corridor, between KP 6 and 7, a field of isolated depressions and highs appears to be present but is difficult to resolve at the 4 m bin size of the data (Figure 4-21).

Higher resolution (2 m) Admiralty bathymetry cover starts from ~ KP 8. Moving off the bank from KP 8 to 10 results in a consistent drop in bathymetry, totalling ~14 m across 2 km. From KP 7.9 to KP 9.3 the bed, as on CB Route 2, is characterised by small to medium subaqueous dunes. These are up to 0.4m high, with wavelengths of 10-20 m, and generally have a slight asymmetry to the SE indicating south-eastward dominant flow direction. Over a two-year period, these bedforms show bed level increase up to 0.5 m and loss of up to 0.6 m (Figure 4-22).

From KP 9.3 to KP 12.1 the seabed surface is void of bedforms but is relatively flat. From ~KP 12.1 to 16 the bed is characterised by the northeast-southwest oriented shallow ridges, which become more north-south oriented the further offshore they are. Again north-south oriented shallow linear depressions are interspersed between the ridges. Within the 2016-2022 bathymetry data intersection areas, over a 6-year period, there is no clear pattern of bed level change on these ridges.

For Zone 1 CB Route 1 the Fugro seismic interpretation starts at ~KP 8.75 as the route crosses the eastern margin of the South Smithic Bank. From this point to the edge of the bank at ~KP 9.4 the sub-surface is characterised by the marine Holocene sands defined by seismic boundaries H05\_b and H10\_b (Figure 4-23). These two seismic units are underlain by the “Bolders Bank Till 1” (defined by H30\_b) which becomes exposed at the surface from ~KP 9.4 eastwards until ~KP 9.5. From this point eastwards to where the route merges with CB Route 2 at KP16 few seismic reflectors are identified. A small exposure of the Holocene “Upper Sand Unit”, defined by H05\_b, is identified between ~KP 10.4 to 10.8 and a small (50 m wide) “channel” feature, defined by H34\_i within the “Bolders Bank Till 2”, is centred on ~KP 11.55, otherwise no reflectors have been interpreted. The latter feature coincides with one of the shallow linear depressions that cross the area whilst the seabed morphology again would suggest the Bolders Bank Formation is at or near the surface throughout.



Figure 4-21: Seabed morphology along Zone 1 CB Route 1 nearshore of Dogger Bank South export cable corridor

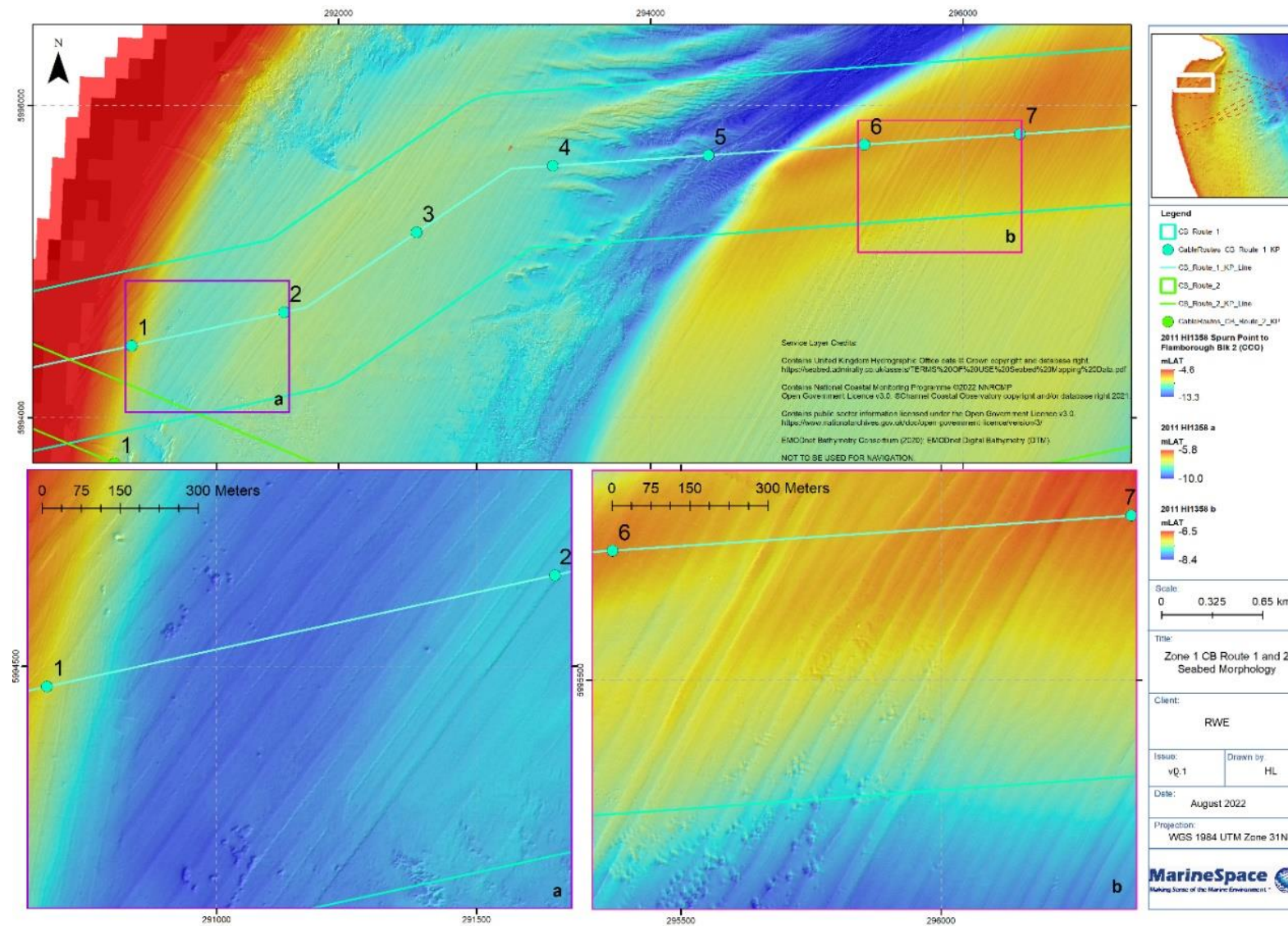


Figure 4-22: Seabed morphology of subaqueous dunes along Zone 1 CB Route 1 nearshore of Dogger Bank South export cable corridor, between KP 8 and 9, including bed level change

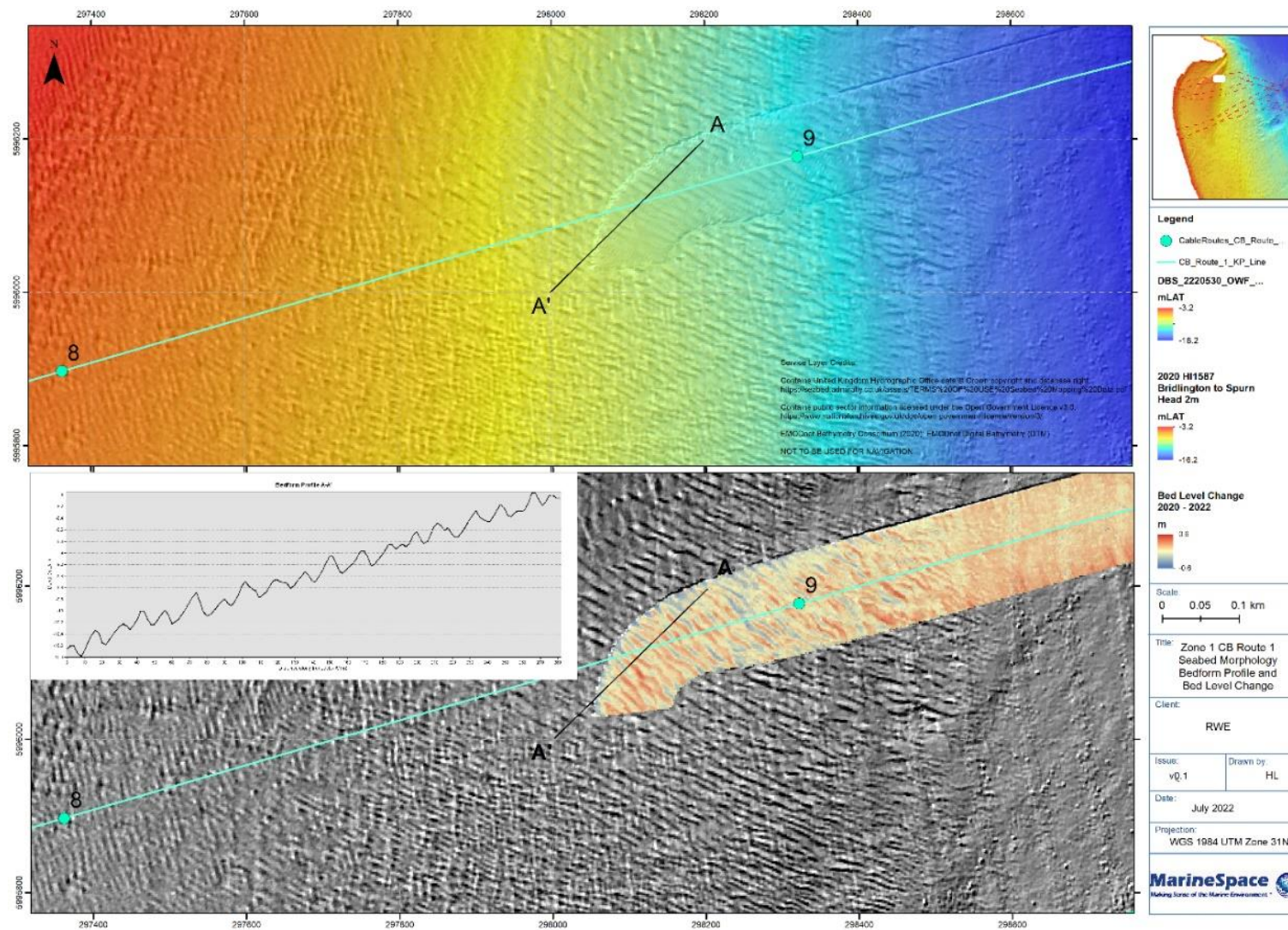
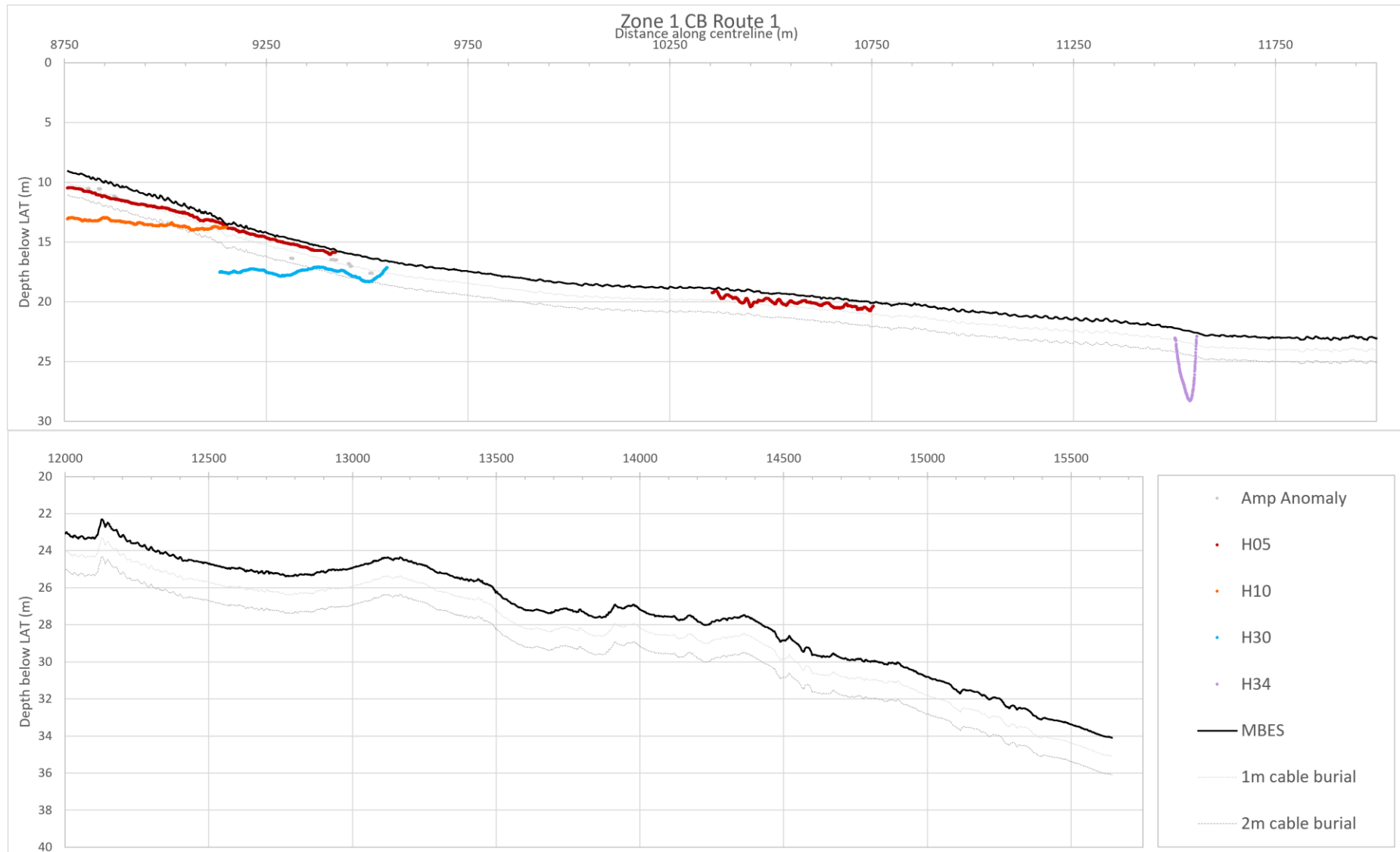




Figure 4-23: Cross-section along Zone 1 CB Route 1, showing the Horizons encountered by a cable at 1m or 2m depth below seabed



#### **4.1.2.6. Export Cable Corridor Zone 2 Introduction**

Zone 2 consists of CB Routes Options DBS-CB-1(A) through to DBS-CB-1(H) from ~ KP 60 to the OWF areas. For analysis purposes these have been split into 6 corridors (Figure 4-23), starting at ~KP 60 where Zone 1 CB Route 7 finished. The 3 main corridors are oriented approximately SW-NE and include: the northernmost (Zone 2 Corridor 1), central (Zone 2 Corridor 2) and southernmost routes (Zone 2 Corridor 3). The remaining 3 corridors are oriented approximately WNW-ESE, except one corridor oriented WSW-ENE: Zone 2 Corridor 4 parallels the southwestern margin of the DBS OWF sites; Zone 2 Corridor 5 extends from Zone 2 Corridor 2 at approximately KP 95 and runs subparallel to The Hills and the Outer Bank, to converge with Zone 2 Corridor 4 at the DBS OWF margin; finally Zone 2 Corridor 6 extends from KP 129 of Zone 2 Corridor 5 and converges with Zone 2 Corridor 3 at its KP 136.5.

Across the Zone 2 cable routes, the bathymetry shoals towards the Dogger Bank, and whilst relatively constant across much of the northernmost route ( $-60 \pm 5$  mLAT), all other corridor options cross The Hills and the Outer Bank – a group of large sandbanks oriented ENE – WSW, reaching a height of ~ - 27.3 mLAT along the cable corridors. The deepest point of ~ - 69.9 mLAT occurs in a valley feature between the Outer Bank and Dogger Bank SW margin (Figure 1-4). The seabed is largely characterised by regular, flow-transverse bedforms. The underlying bedrock geology in this zone is highly variable ranging from Cretaceous Chalk, Cromer Knoll Group, to Kimmeridge Clay, with some bands of Lias Group, West Sole Group, Oxford Clay Formation, and Corallian Group bedrock. Moving onto the Dogger Bank this changes to undifferentiated Palaeocene mudstones, sandstones and lignite, and undifferentiated Eocene Mudstone, Sandstone and Tuff at depth in the OWF (Figure 4-24– Section 3.1). The western margin of the Dogger Bank on which the OWF is being built consists of a thin veneer of post-transgressive marine sediments, overlying Dogger Bank Formation (Section 3.2).





#### **4.1.2.7. Zone 2 - Corridor 1 (Route A)**

Continuing from KP 60.12 of CB Routes 1, 2, 5 and 7, ~KP 60 – 74 of Zone 2 Corridor 1 is characterised by large to very large subaqueous dunes generally ~2m high but up to 4m, with a wavelength of 100 - 200m, oriented approximately east to west (according to the narrow 150-200m corridor visible in high resolution bathymetry data). From ~KP 74 amplitudes drop to < 1 m but wavelengths are at the same scale. All of these bedforms have an asymmetry indicating dominant flow in a northward direction (steeper lee slope of the bedform to the north). These very large bedforms have parasitic, small to large, subaqueous dunes oriented northeast to southwest with an apparent asymmetry to the northwest. From ~KP 78 the principal subaqueous dunes transition to medium to large sized, with wavelengths up to 20 m and varying heights to a maximum of ~0.6 m, oriented east to west to west-southwest to east-southeast. These also have their steeper lee slope facing to the north-northwest. Up to ~ KP 90.25 this proposed route crosses the bedforms at an acute angle but from KP 90.25 to ~KP 96 the route is almost parallel to the crest axes. At KP 96, these smaller bedforms are once again superimposed onto large to very large subaqueous dunes with heights less than 2m and wavelengths of ~350m, oriented east to west. These large to very large dunes dissipate between KP 101 to 105, becoming further spaced, whilst the superimposed dunes remain clearly present. From ~KP 104.8 a further change in the route orientation results in it once more crossing the bedforms at a more acute angle.

From ~KP 106 to KP 124.4 at the end of Zone 2 Corridor 2 the route crosses 2 sandbanks and associated inter-bank depressions at the northern most extension of the “Outer Bank” complex and where it transitions into the shallowing western margins of Dogger Bank known as the “North West Riff”. These banks have a broadly north-northwest to east-southeast orientation, albeit ultimately curving to the north as they follow the main contours of the western margin of Dogger Bank. A bank parallel linear depression between ~KP 106 to KP 111 reaches depths of -69.9 mLAT, with a relief of ~ 12 m, and within which there are large scale bedforms present, visible both in the Fugro and EMODnet data (Figure 1-4). These features are flow perpendicular with heights up to 3.5 m and wavelengths up to 700 m. The asymmetry of these larger features is difficult to determine from the 5 m resolution EMODnet data, however, cross-sectional profiles of the narrow corridor Fugro data suggests they have lee slopes oriented to the northwest with smaller parasitic forms, with amplitudes of < 0.3 m and wavelengths of 20 – 30 m with a similar orientation.

A similar inter-bank depression between ~ KP 112 and KP 114 contains similarly oriented large and parasitic bedforms. The intervening, symmetrical, sandbank between KP 111 – 112 reaches a minimum depth of approximately -48.0 mLAT with subaqueous dunes on its eastern flanks, with amplitudes < 0.5 m and wavelengths of ~ 20 m and an asymmetry to the northwest. A second sandbank intersects with the route between KP 114.6 and 117, with a very similar morphology to the previous one but reaching a minimum depth of -36.7 mLAT. It also hosts similar small subaqueous dunes, with the same overall dimensions and asymmetry.

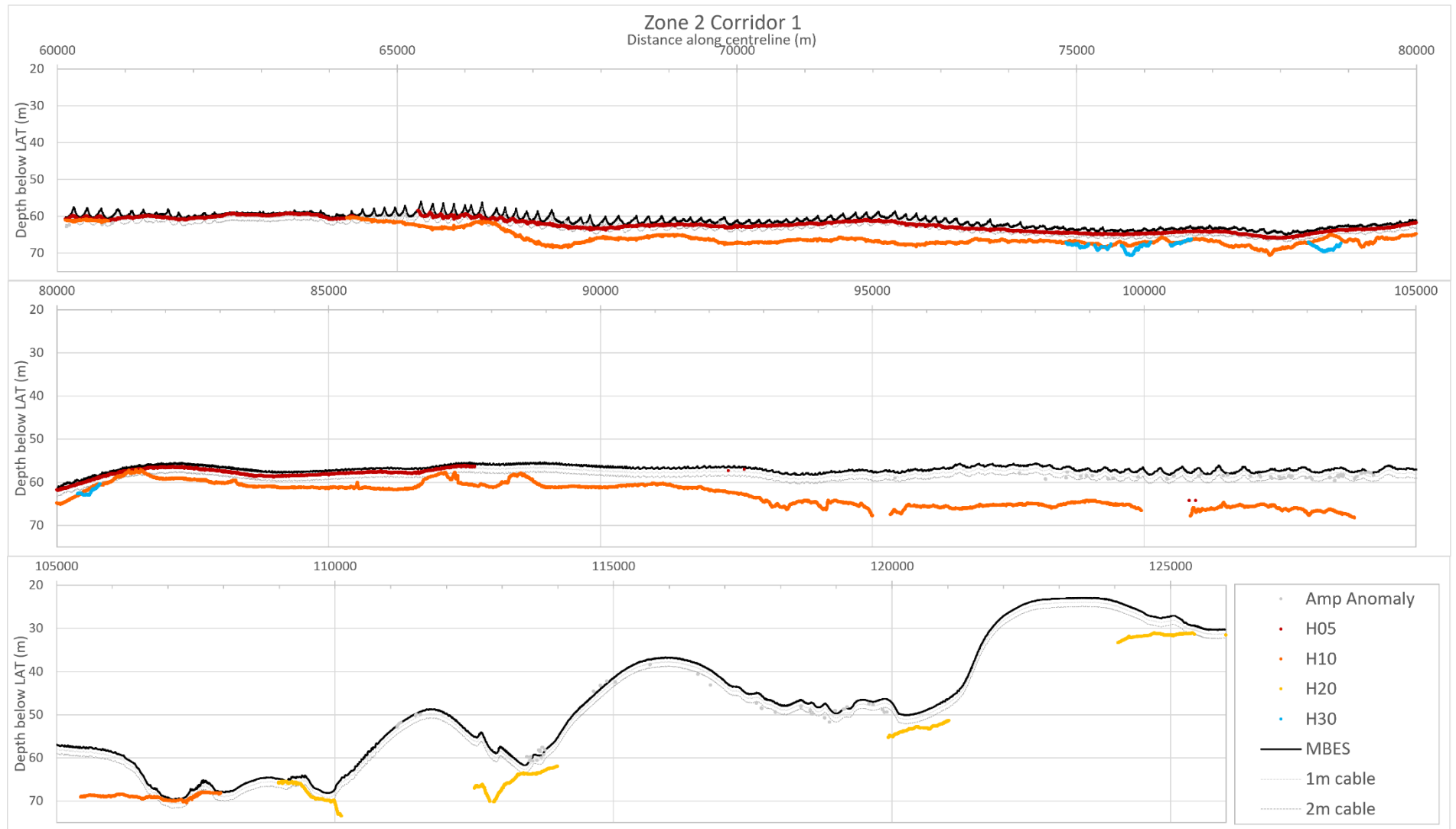
The final inter-bank depression, between ~KP 117 and 121 reaches -50 mLAT and again features large scale bedforms of the same character and dimensions. From KP 121 to 124.4 the route shelves to a depth of ~ -23 mLAT of the “North West Riff”. The bed becomes featureless except for a zone of small depressions between ~KP 123.5 and 123.8 which could be the expression of a small field of sorted bedforms discussed in detail in Section 4.1.3. Finally, at ~KP 124.5 the route transects a

crenulated ridge, oriented north-northwest to south-southeast, with a relief of 0.8 m and slope angles of up to 7.5°.

The entire sub-bottom profile of the initial section of Zone 2 Corridor 1 (from ~KP 60 to ~KP 107) is dominated by H10\_b which defines the post-transgressive marine Holocene Lower Laminated Sand seismic unit, with only a thin veneer (< 1 m) of the Upper Sand unit defined by H05\_b. H10\_b reaches a maximum of > 10m below the seabed thickening offshore until the horizon comes to the surface as the route crosses the valley north of the Outer Bank, around KP 107 (Figure 4-25). H30\_b occurs infrequently between KP 74.5 and 81, directly below H10\_b.

Between ~KP106 and the end of the line at ~KP 125 the route crosses the sandbanks and associated inter-bank depressions at the northern most extension of the “Outer Bank” complex. There has been limited seismic interpretation across this area except the identification of H20\_b associated with the base of each interbank depression. This “Lower Cross-bedded Sand Unit” (Table 2-1) suggests this whole area is founded on post-transgressive sands with no glacial deposits being identified at or near the surface in this preliminary interpretation.

Figure 4-25: Cross-section along Zone 2 Corridor 1, showing the horizons encountered by a cable at 1m or 2m depth below seabed



#### **4.1.2.8. Zone 2 Corridor 2 (Route B)**

Zone 2 Corridor 2 picks up from KP 60.12 of Zone 1 CB Route 7 and passes along the northern edge of “The Hills” sandbanks and the “Outer Bank” between KP 66 to 116.

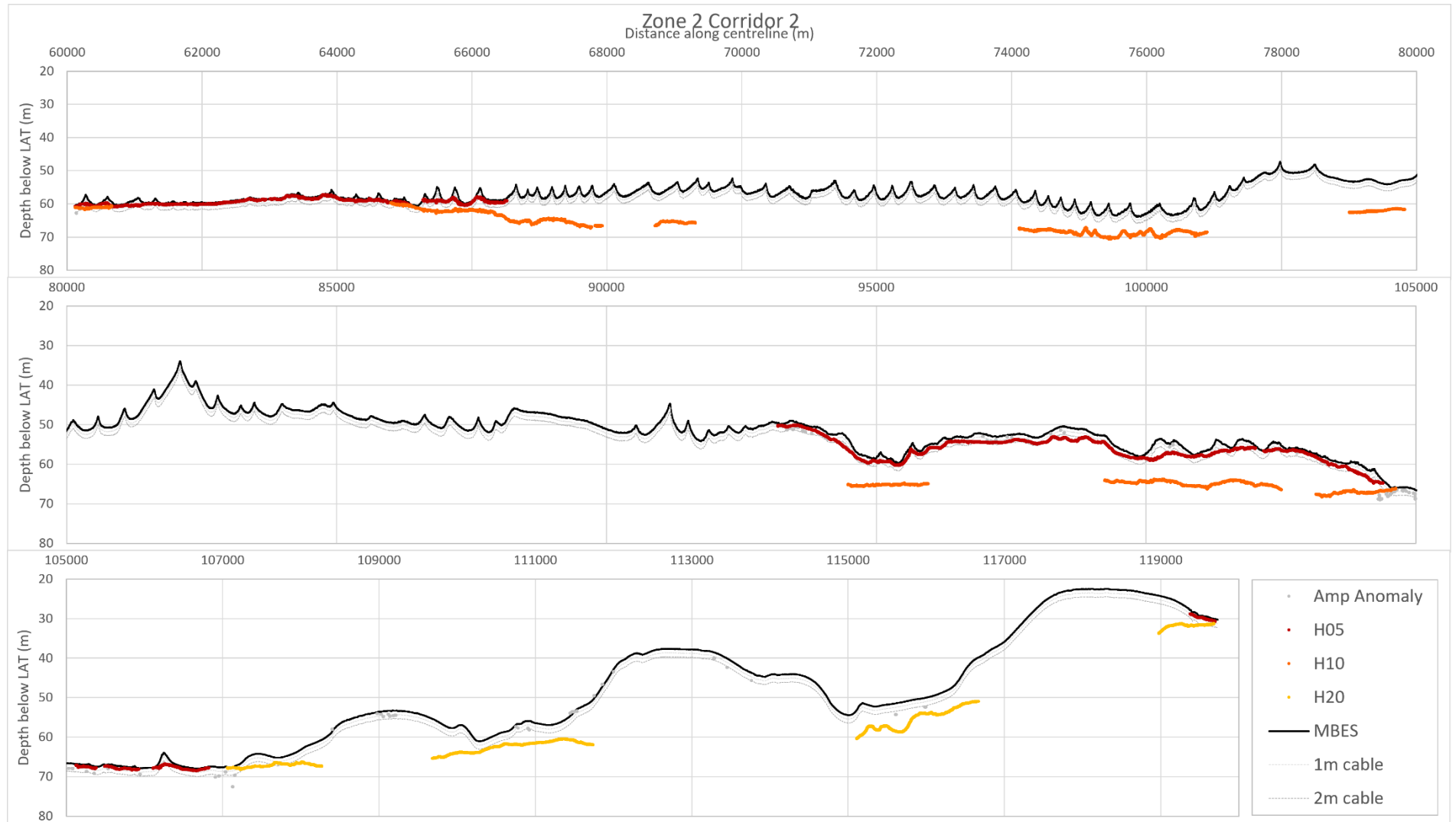
From KP 60.12 to ~KP 78 the seabed is made up of large to very large subaqueous dunes superimposed with small to large subaqueous dunes such as those between ~KP 60 – 74 of Zone 2 Corridor 1. These have similar dimensions to their Zone 2 Corridor 1 equivalents (Section 1.1.1.1), however the wavelengths increase up to ~500 m, with heights up to ~5.5 m but still with an asymmetry to the north. Again smaller parasitic bedforms, with a northwesterly asymmetry, wavelengths of up to 20 m and varying heights but all < 0.6 m are also present. Where wavelengths increase several hundred metres of this route are just formed of these smaller bedforms. Where the route skirts the very northern margin of the “Hills Sandbanks” the largest amplitude bedforms are crossed with slope angles up to 12.5°.

From ~KP 78 to 103 the route crosses the northerly tips of 4 of the “Outer Bank” with the greatest relief occurring at KP 82 where the top of the bank has a relief of 20 m above the ambient bed condition. On the flanks and in the interbank depressions very large subaqueous dunes are present with amplitudes up to 2.5 m. The orientation of these bedforms has rotated anticlockwise to have asymmetries to the northwest and north-northwest and so are effectively parallel to the smaller parasitic bedforms that are still present. Although not fully imaged within the narrow corridor of the Fugro route specific data they do relate to large scale isolate barchan type dunes with a north-westerly asymmetry.

From KP 103, the same valley and sandbank structures of the “Outer Bank” complex crossed by Corridor 1, and described in Section 1.1.1.1, are encountered until the routes meet at Corridor 2 at ~KP 119.7. Along Corridor 2, the deepest point is -68 mLAT in the valley between KP 104 and 108. The banks increase in height along the route, with the final bank along the route between KP 117 and 119.7, reaching a depth of -22 mLAT. The same scale of large and parasitic bedforms are present again with asymmetry to the northwest. From ~KP 116 to 118 the route shelves, to a depth of -24 mLAT, on to the “North West Riff”. The bed here is also featureless except for a zone of small depressions between ~KP 117.5 and 118.8 which could be the expression of a small field of sorted bedforms discussed in detail in Section 4.1.3. Finally, at ~KP 119.25 the route transects the same crenulated ridge as seen in Corridor 1, oriented north-northwest to south-southeast, with a relief of 0.8 m and slope angles of up to 8.5°.

As with Zone 2 Corridor 1, the entire sub-bottom profile of the initial section of Zone 2 Corridor 2 (from ~KP 60 to ~KP 107) is dominated by H10\_b which defines the post-transgressive marine Holocene Lower Laminated Sand seismic unit, with only a thin veneer (< 1 m) of the Upper Sand unit defined by H05\_b. Again H10\_b reaches a maximum of > 10m below the seabed thickening offshore until the horizon comes to the surface as the route crosses the valley north of the Outer Bank, around KP 107 (Figure 4-26). Again the route crosses sandbanks and associated inter-bank depressions of the “Outer Bank” complex, within which of H20\_b associated with the base of each interbank depression. This “Lower Cross-bedded Sand Unit” (Table 2-1) suggests this whole area is founded on post-transgressive sands with no glacial deposits being identified at or near the surface in this preliminary interpretation.

Figure 4-26: Cross-section along Zone 2 Corridor 2, showing the horizons encountered by a cable at 1m or 2m depth below seabed





#### **4.1.2.9. Zone 2 Corridor 3 (Deselected)**

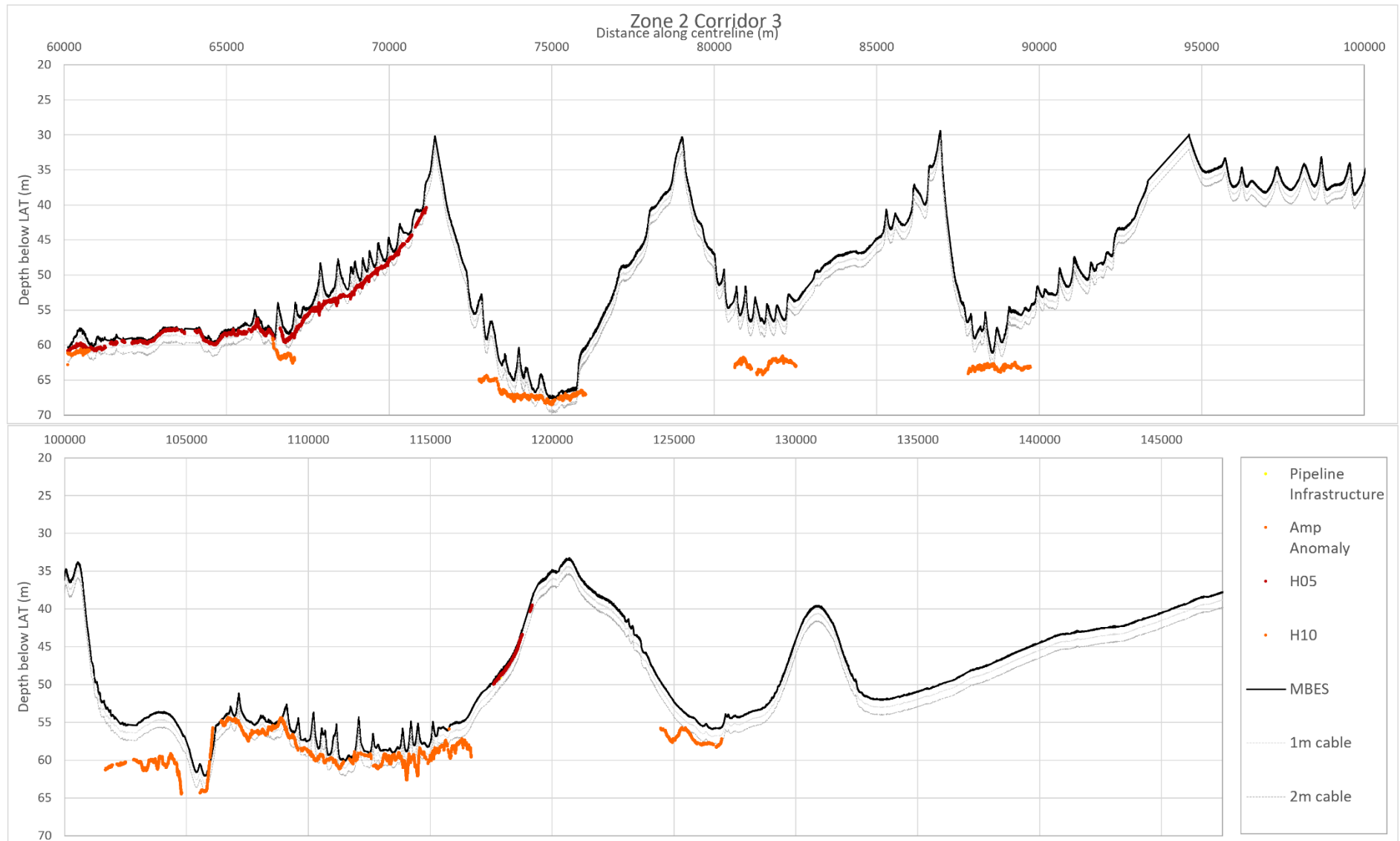
The southernmost route, Corridor 3, is oriented west-southwest to the east-northeast through “The Hills” sandbanks, south of the “Outer Bank” complex, and coming onto the southern margin of the Dogger Bank through the “Bolders Bank” sandbanks. The route passes north of the Kilmer and Trent Gas Fields. Bathymetric variation across the route is great, with a range of ~ -67.7 mLAT to -27.2 mLAT, with both the minimum and maximum value occurring across The Hills (Figure 1-4). The KP numbers again extend from Zone 1 CB Route 7’s KP 60.12.

KP 60.12 to ~KP 64 is characterised by the same bedform field as seen in the first few kilometres of Corridor 1 and 2 i.e. a combination of larger subaqueous dunes with smaller parasitic forms all with an asymmetry to the north / north-northwest / northwest. Between ~KP 64 and ~KP 133 the route crosses the apices of 8 individual banks, with shallowest points as follows: KP 71.35, minimum depth -27.7 mLAT, relief of 35 m; KP 79, minimum depth -30.9 mLAT, relief of 35 m; KP 86.9, minimum depth -29.9 mLAT, relief of 25 m; KP 94.2, minimum depth -27.8 mLAT, relief of 22 m; KP 100.5, minimum depth -34 mLAT, relief of 20 m – asymmetric to the east; KP 107, minimum depth -51.6 mLAT, relief of 10 m – asymmetric to the west; KP 120.5, minimum depth -33.3 mLAT, relief of 21 m; and KP 130.8, minimum depth -39.7 mLAT, relief of 12 m.

On the flanks of the individual sandbanks, and in their inter-bank depressions, are a series of large to very large subaqueous dunes with wavelengths ~500 m and heights up to 5m again with the smaller scale parasitic dunes seen throughout this area. The largest bedforms tend to have northwesterly asymmetry, with this angle rotating to the north for as the bedforms reduce in size. The exception to this is an area of relatively featureless seabed between ~KP 102 and KP 106.5, KP 115.2 and KP 116.8 and KP 124 and 127. From KP117 to KP 124 and KP 128.5 to KP132.6, further small to medium dunes are present, decreasing in size over the bank and dissipating into the next inter-bank depression. From KP 132.6 to the end of the route at KP147.4 the bed is featureless. This part of the route is purportedly crossed by the Shearwater to Bacton, Esmond to Bacton and the Cavendish export pipeline but none of them are evident in the bathymetry.

Horizons H05\_b and H10\_b are identified infrequently along Zone 2 Corridor 3 (Figure 4-27). H05\_b occurs on the western side of 2 of The Hills sandbanks at or very near to the seabed surface (~KP 60 - ~KP 71.1). H10\_b is identified in the bathymetric lows along the route, sometimes detected very near the surface and in others extending up to over 8 m below the seabed surface. These lows are frequently occupied by large to very large subaqueous dunes. From KP 128.5 the presence of subaqueous dunes lessens to the end of the route. No horizons are identified in the latter stages of the route, where the bathymetry shoals and the seabed is featureless. Neither bedrock nor till are identified at the seabed surface along this route.

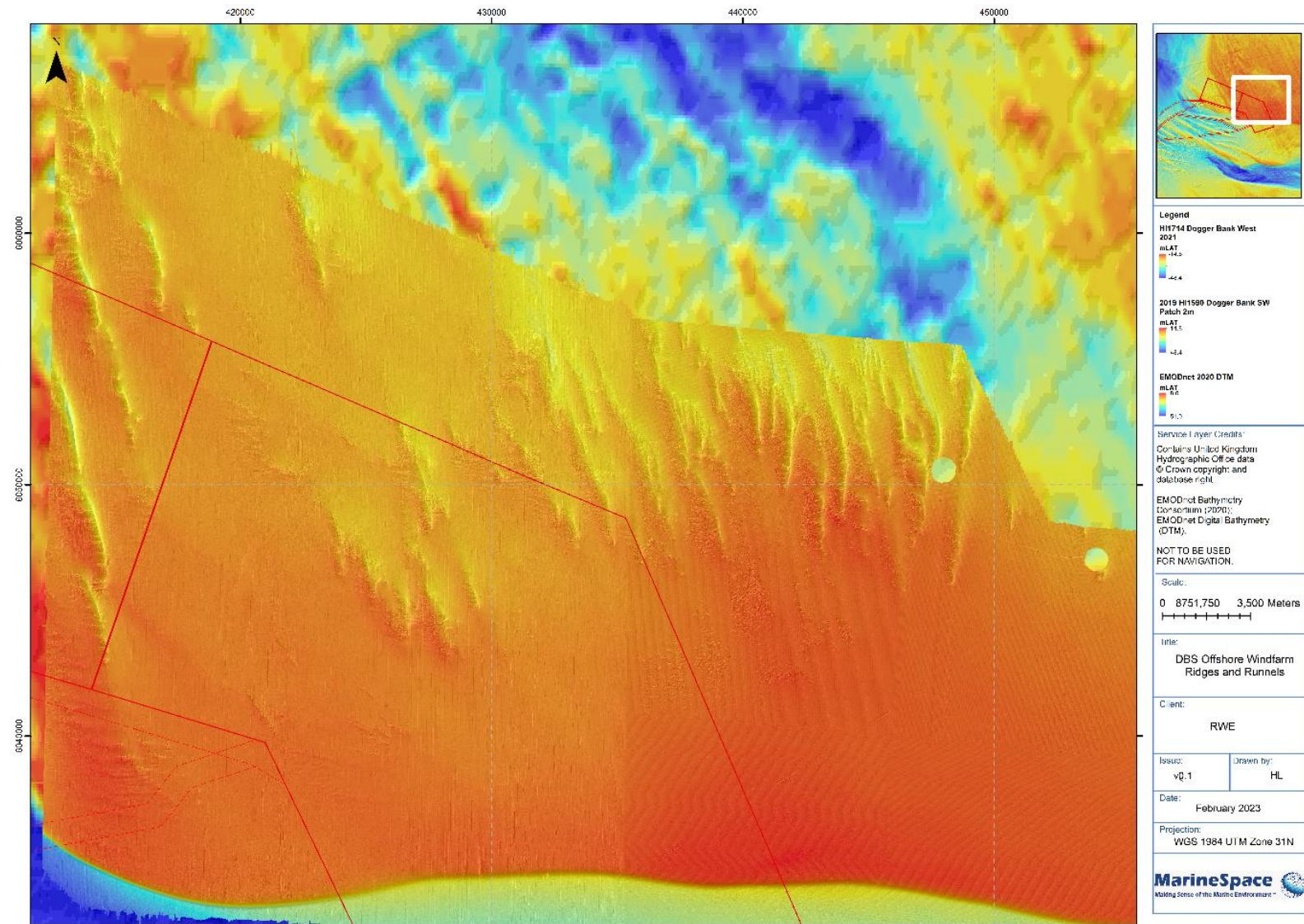
Figure 4-27: Cross-section along Zone 2 Corridor 3, showing the horizons encountered by a cable at 1m or 2m depth below seabed



#### **4.1.2.10. Zone 2 Corridor 4 (Route A1)**

Corridor 4 parallels the southwestern margin of the DBS OWF sites. The KP markers continue from the end of Zone 2 Corridor 1 (from KP 124.9). The route runs at an oblique angle across a number of north-northwest to south-southeast oriented ridges and runnels features to ~KP 153.5, along with evidence of rippled scour depressions in a number of locations e.g. ~KP 133, KP 134.5, KP 137 - 138 and KP 142.5. The scale of these features can be broadly ascertained by tracing the features in the grid of the OWF corridor data but more effectively in the HI1714 and HI1590 datasets which cover a significant component of the Eastern part of the OWF (Figure 4-28). Individual ridges can vary from a few hundred metres to 2.5 km in width with the associated runnels being significantly narrower at < 1 km. Their overall length can be difficult to define but is typically several kilometres, with the largest identified in this area being > 12 km in length. Overall relief is < ~4 m with individual runnels locally reaching a further 3 m beneath ambient bed level. On some of the larger ridges there are parasitic, west to east oriented, transverse bedforms, with amplitudes of ~1 m and wavelengths of ~600 m and a northly asymmetry. These ridge and runnel features are common along the southern margin of the Dogger Bank and will be discussed in more detail in Section 4.1.3.

Figure 4-28: Ridge and Runnel features on the southern margin of the Dogger Bank



The rippled scour depressions found associated with these ridge and runnel features at ~KP 133, KP 134.5, KP 137 – 138 and KP 142.5 have forms with both negative and positive relief (Figure 4-29). Calculating the exact dimensions due to the current partial coverage, but features are at a typical scale of ~80 – 100 m, with reliefs of < 1 m. Between ~KP 138.5 and KP142 the seabed has a distinctly roughened surface topography and is associated with outcropping to subcropping deposits defined by H25 which may relate to exposure of Upper Dogger Bank deposits. From ~KP 143.4 the seabed is featureless to KP 147.5, where expressions of fields of the ripple scour depressions and sections of the ridge and runnel features are crossed. Between ~KP 150 and KP153.5 the route crosses a major ridge and runnel feature with both transverse bedforms, with a northerly asymmetry, and rippled scour depressions being present. Bed level change across this feature in the vicinity of this cable corridor is limited to variability in the location of small scale rippled scour depressions resulting in change of <  $\pm 0.6$  m over a 1-year period. There is no evident movement of either the transverse bedforms nor the margin of the ridge and runnel feature on this timescale.

From KP 153 to the end of the corridor at KP160 the seabed is largely featureless, except for a localised field of elongated (long axis orientation north-northwest to south-southeast) rippled scour depressions between ~ KP 154 and 156. Individual scour depressions have long axis lengths of up to 150 m and widths up to 80 m, with maximum depths ~ 0.6 - 0.7 m below the ambient seabed level of ~ -18 mLAT. At the southern margin of these depressions are a series of raised ridges with a relief typically between 0.4 – 0.5 m above the ambient seabed level. Within the extent of the data crossover area, they show bed level change from 2021 to 2022 of  $\pm 0.7$  m, with some features becoming less pronounced, or becoming infilled during this time period (Figure 4-30).

From ~KP 125 to KP 142.4 Zone 2 Corridor 4 the top 2 metres of the seabed is dominated by the Holocene “Upper Marine Sands” defined by H05\_b. Between ~KP 137.5 and KP 140.5 and at two discrete locations, ~KP128.1 and ~KP135.6 H25\_b is identified beneath this layer (Figure 4-31). Fugro has described this as a “Buried Channel Sequence” (Table 2-1). This section of the route is associated with the ridge and runnel topography and this unit could represent near surface expressions of either the Botney Cut Formation deposits or the underlying Bolders Bank Formation (Section 3.2). Either way this unit may represent stiffer deposits that limit the bed level change at the margins of these sorted bedform features (see more detailed discussion in Section 4.1.3).

From ~KP 142.8 to ~KP 153 the surface deposits are dominated by the “Lower Cross Bedded Sand Unit” defined by H20\_b, with an intermediate reflector, H15\_i, being present between ~KP 144.5 and ~KP 150. From this point to the end of this section of the route, at ~KP 160, the “Upper Marine Sands” again dominate the top metre of the seabed.



Figure 4-29: Rippled Scour Depressions along Zone 2 Corridor 4, subparallel to the Doggerbank southwest margin (with updated 2023 Route A1 Centreline and KPs visible)

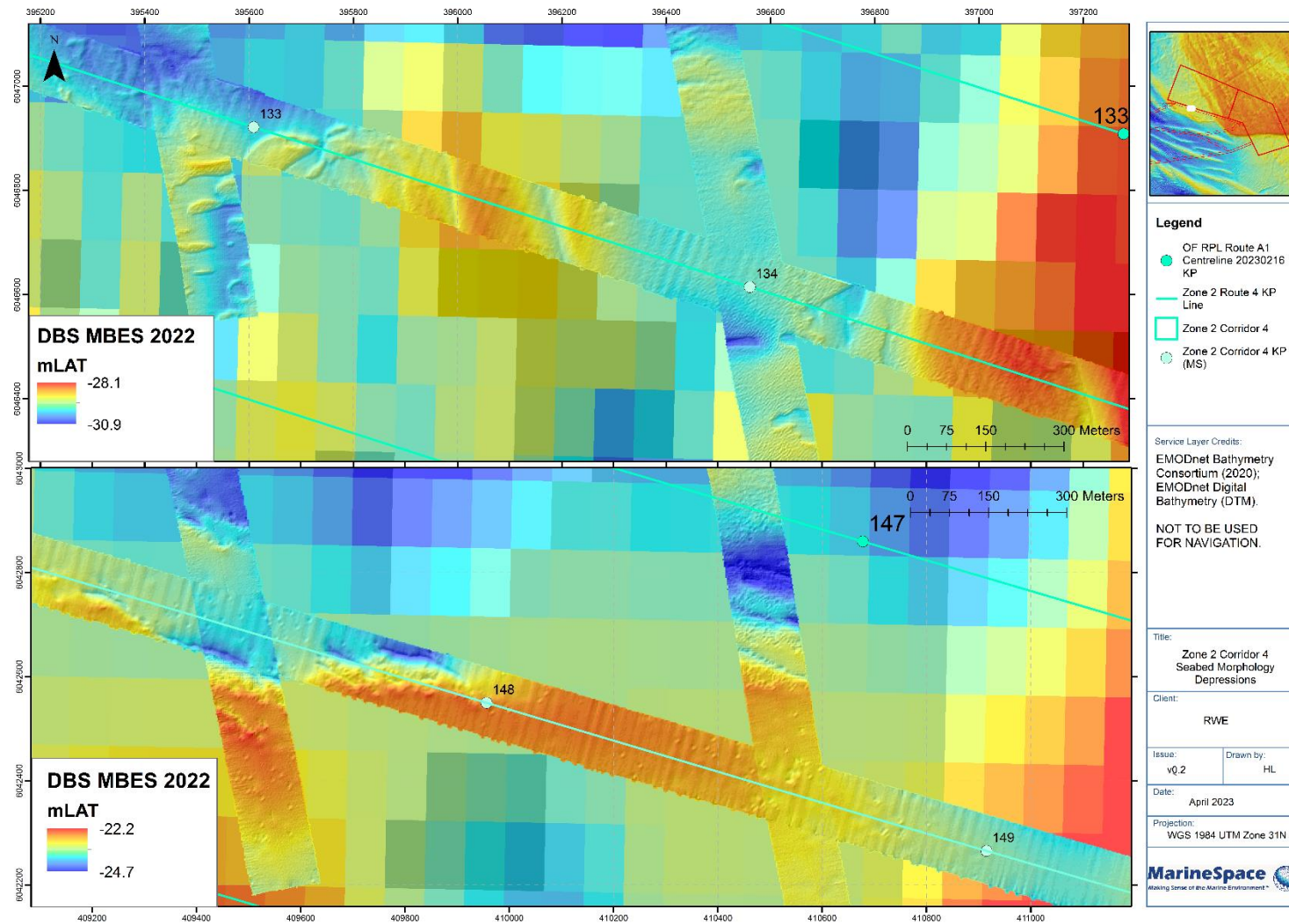
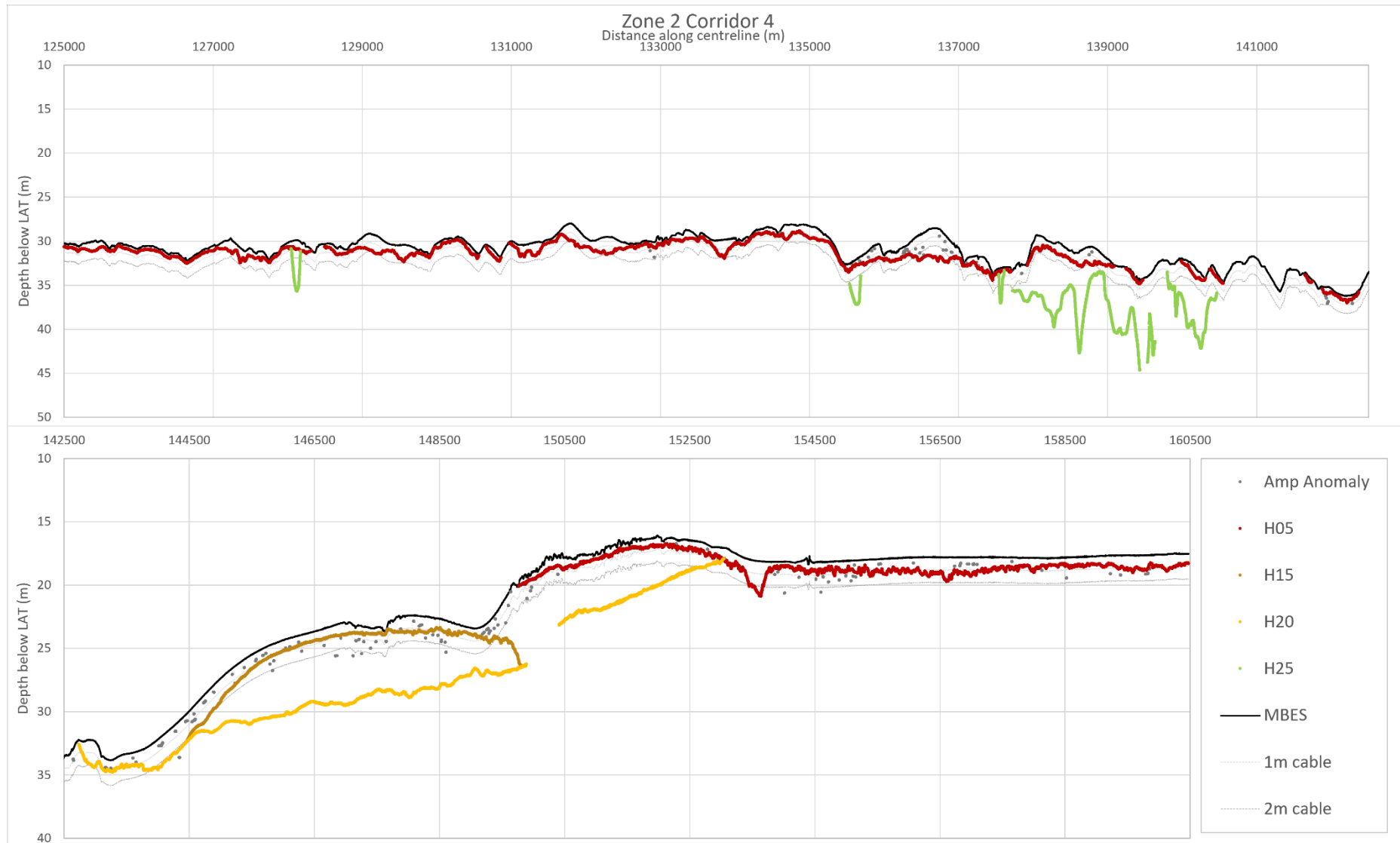






Figure 4-31: Cross-section along Zone 2 Corridor 4, showing the horizons encountered by a cable at 1m or 2m depth below seabed



#### **4.1.2.11. Zone 2 Corridor 5 (Route C)**

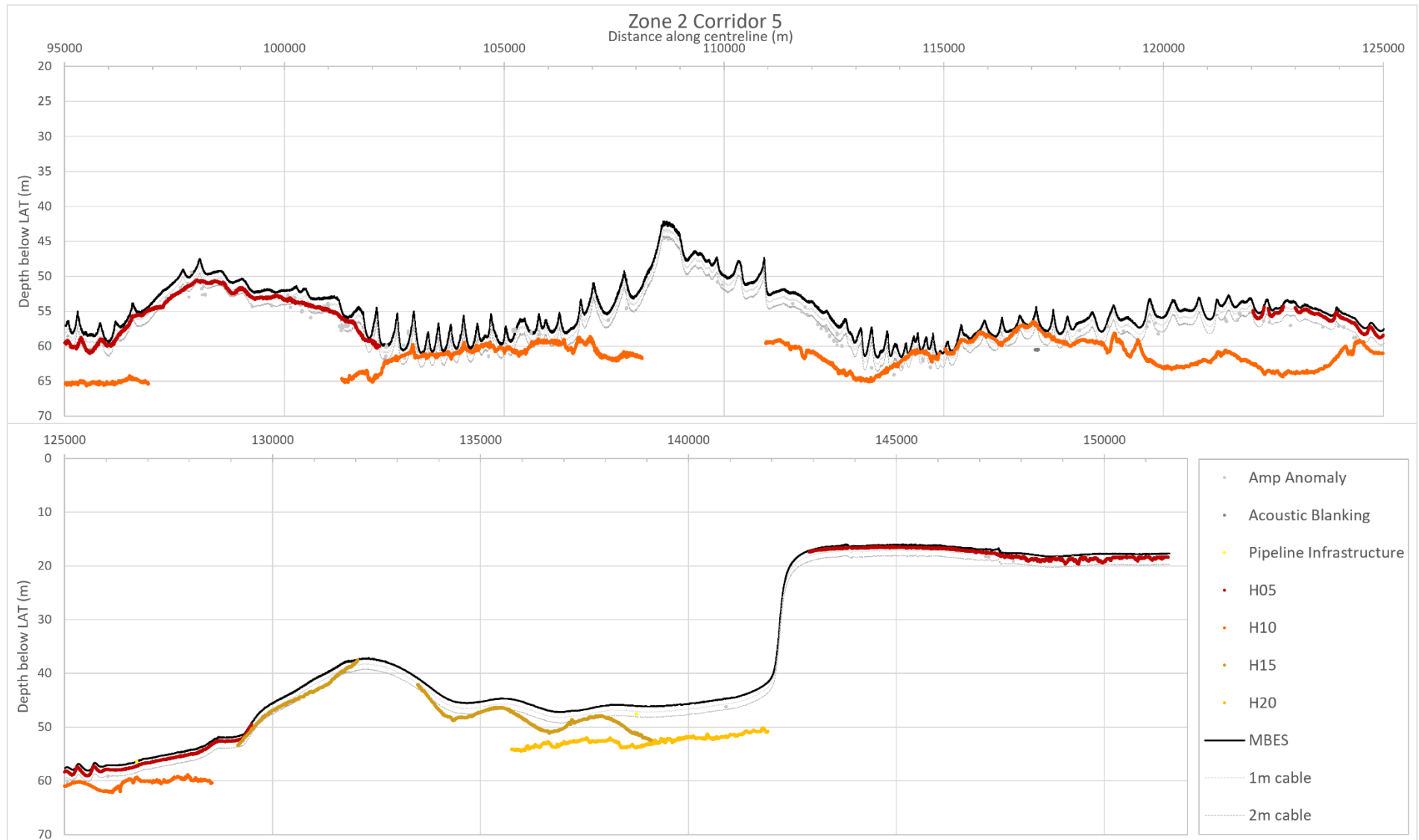
This route extends from Zone 2 Corridor 2 at ~KP 95, subparallel to The Hills and the Outer Bank, to converge with Zone 2 Corridor 4 at the DBS OWF margin. As such, the route morphology is as Zone 2 Corridors 2 and 3, crossing several flow oriented, large-scale sandbanks and interbank linear depressions, which contain flow perpendicular large to very large subaqueous dunes, superimposed with small to medium subaqueous dunes. The route crosses the apices of 2 individual banks, with shallowest points as follows: KP 108.7, minimum depth -41.7 mLAT, relief of 14 m and KP 132, minimum depth -37.2 mLAT, relief of 14 m.

From KP 133 towards the DBS margin the seabed becomes featureless in terms of bedforms. The route crosses the Esmond to Bacton pipeline at ~KP 138.9 but there is no evidence of its presence in the bathymetry. At KP 142 the route passes on to the western margin of the Dogger Bank which is defined by a relatively sharp break in slope with angles up to 7° over a 250 m distance. From here to the end of Corridor 5 at ~KP 151.4 the route crosses the very southerly margin of the major ridge and runnel feature described in Section 4.1.2.10 but the overall relief only fluctuates by < 2.5 m over a distance of ~ 9 km.

From KP 142 rippled scour depressions are present, with a well defined field between here and ~KP 146. These features are not present in the 2021 HI1714 data and so may have appeared in this short period. However, as these are relatively small compared to those described previously, being generally ~60 m wide and 16 m long, with depths up to ~0.4 m below ambient seabed level (-16.1 mLAT), and the 2021 dataset only being available as a 2 m bin sized raster this may partially (but not wholly) represent an issue of resolution. One individual depression at KP 148.3 exhibits bed level change of up to 1 m with an associated maximum accumulation on the southern margin of the feature being up to 0.4 m above the ambient bed level. From KP 148.3 to KP 151.4 at the route end no further features are identified.

As can be seen in (Figure 4-32) the flow-oriented, large-scale sandbanks and interbank linear depressions are formed in the Holocene marine sand units defined by H05\_b and H10\_b. These units dominated the near surface seabed sediments from ~KP 95 to ~KP 129.2. From this point to ~KP 142, where the route passes on to the Dogger Bank, the surface deposits are dominated by the “Lower Cross Bedded Sand Unit” defined by H20\_b and the intermediate reflector, H15\_i. This final section of the route on the Bank, ~KP 151.4, the “Upper Marine Sands” again dominate the top metre of the seabed.

Figure 4-32: Cross-section along Zone 2 Corridor 5, showing the horizons encountered by a cable at 1m or 2m depth below seabed





#### **4.1.2.12. Zone 2 Corridor 6 (Deselected)**

Corridor 6 extends from KP 129 of Zone 2 Corridor 5 and converges with Zone 2 Corridor 3 at its KP 136.5. It has no high-resolution bathymetric data coverage and so information has been inferred from EMODnet data and the other routes. It runs along one of the interbank liner depressions southwest of the Dogger Bank, and likely has a morphology devoid of the very larger bedforms, which are still visible in the EMODnet data (which has a cell size of ~ 80 x 130 m) elsewhere, although small to large subaqueous dunes with an asymmetry to the northwest are potentially present.

#### **4.1.3. Offshore Windfarm**

As described in Section 3.2 the Dogger Bank superficial near surface sediments are made up of Holocene marine dark olive-grey to very dark grey, fine-to medium-grained sands with variable gravel fractions. Thicknesses vary from up to 25 m where they infill irregularities in the underlying, glacio-tectonised, Dogger Bank Formation deposits, to thin veneers of < 1 m.

##### **4.1.3.1. Ridges and Runnels**

The dominant morphological features across both the West and East sections of the DBS OWF are a combination of large-scale ridge and runnel depressions<sup>1</sup>, oriented north-northwest to south-southeast, with co-located, spatially variable in density, small-scale discrete rippled scour depressions<sup>1</sup> (Figure 4-28). As the ridge and runnel structures terminate towards the southern margin of the Dogger Bank in the south of DBS East, spatially variable fields of rippled scour depressions (RSDs) continue to be present.

As described in Section 4.1.2.10 individual ridges can vary from a few hundred metres to 2.5 km in width with the associated runnels being significantly narrower at < 1 km. Their overall length can be difficult to define but is typically several kilometres, with the largest identified in this area being > 12 km in length. Overall relief is < ~4 m with individual runnels locally reaching a further 3 m beneath ambient bed level.

Features similar to the ridge and runnel features described here have been reported, in the academic literature, from both the US Continental Shelf (e.g. Murray & Thielert, 2004; Goff et al., 2005), the west coast of Jutland in the German Bight (Diesing et al., 2006), and the Aquitaine coast of France (Mazieres et al., 2015). These all occur in shoreface to inner shelf environments, in water depths up to 90 m, oriented perpendicular to the shore, and with dimensions 100's metres wide, kilometres in length and with a relief of 1 – 2 m. These features represent the inter-play of fine sands

---

<sup>1</sup> The nomenclature around these features is complicated. The original were described as either "Rippled Scour Depressions" (Cacchione et al, 1984) or "sorted bedforms" (Murray & Thielert, 2004) covered both scales of features. Ferrini & Flood (2005) and Coco et al (2007) generated simple classification schemes (RSD 1, II and III vs Linear, patchy and offshore widening [V-shaped] sorted bedforms respectively). Whilst Mazieres et al (2015) utilised the Coco et al. (2007) scheme but added the phrase "morphological ridges" to describe the very large scale linear forms. For clarity this report uses the terms "sorted bedforms" to describe the whole group of bedforms but "ridge and runnel" to describe the large scale linear ridges and associated depressions and "rippled scour depressions" to describe the smaller scale individual features found in clustered fields or on the margin of the "ridge and runnel" features.

and coarse gravels, with the coarse gravels tending, but not exclusively, representing the liner depressions (runnels) whilst the sands create the low relief ridges, typically with sharp boundaries between the two. Frequently, the coarser grained material in the depressions supports smaller scale bedforms. With no sidescan sonar data available for analysis, the sediment reflectivity can not be assessed to confirm whether or not there is a difference between the sediment within and surrounding these features within the DBS OWF. It is also not possible within the resolution of the 1m data to distinguish ripples of wavelength <1m.

These features have also been identified and described at 2 other RWE assets, SOFIA windfarm, to the northwest of DBS and Thor windfarm on the Jutland coast. Although only corridor swath bathymetry data is available between the SOFIA and DBS OWF (from the Gardline survey of Zone 3, Tranche B, of Dogger Bank – Section 2.1.1) it does suggest that the same ridge runnel field is being encountered. Such an interpretation is also broadly supported by the coarse gridded EMODnet Data.

Goff et al (2005) demonstrated, through the analysis of time-lapse geophysical survey, that the gross position of such features was stable over almost 4 decades, whilst decametre, oscillatory movement of the margins could occur over time periods of months. Diesing et al (2006) also observed no significant change in their distribution on annual to decadal timescales, whilst surveys over a 29-year period from the Aquitaine coast also showed large scale mobility with tens of meters of movement at their margins (Mazieres et al., 2015).

When considering these “ridge and runnel” features in the DBS OWF footprint, across coarse grid data taken in 2011 and 2022, the general large-scale structure remains relatively stable. Over this 11-year period the gross structure of the ridges and runnels remains relatively constant ( $< \pm 0.3$  m of change within the depression, which is  $\sim 0.03$  m yr<sup>-1</sup> at a linear rate between 2011 and 2022) whilst bed level change is limited to the banks and margins of the depressions (Figure 4-33). The depression running through the centre of the OWF area shows bed level change on its margins of between -1.4 and 1.2 m over this time scale (2011 – 2022) and - 1.3 m to 1.0 m between 2021 and 2022. This pattern is also demonstrated when comparing bed level change between 2019 and 2022 on a similar feature, located in the north of DBS East OWF area. The runnel structure remains stable, whilst the features on the margins of the runnel show total bed level change, over a 3-year period, of between – 0.9 and 0.7 m over that timescale (Figure 4-34).

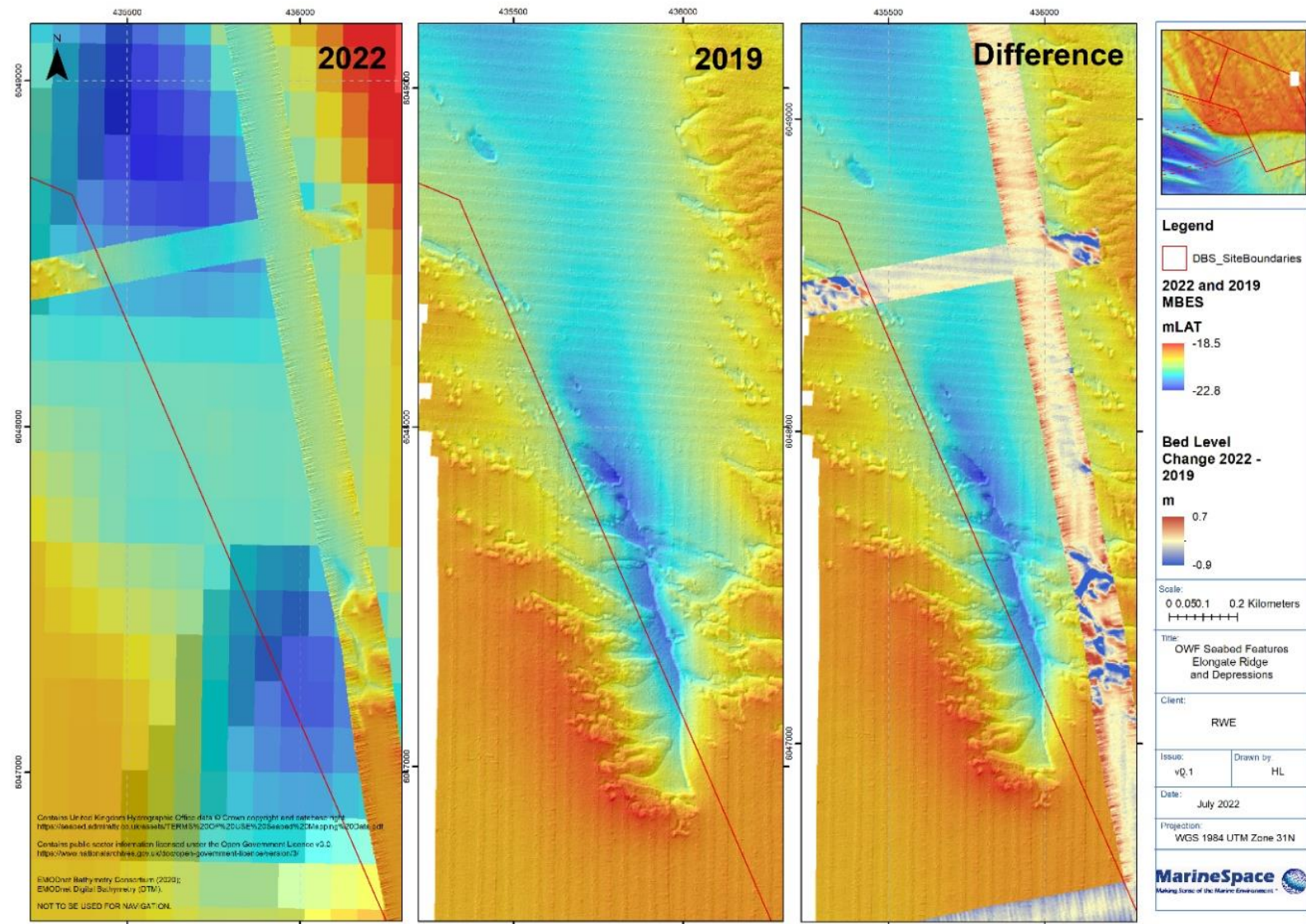
As with all forms of sorted bedforms the origin of these “ridge and runnel” features is the subject of significant debate. Diesing et al (2006) suggests extreme storm events play a major role in the initiation of these features, with the ridges forming perpendicular to the dominant storm wave direction, with “tidal” currents then moderating and maintain their final shape. Although the tidal flows in this area are approximately parallel / at an obtuse angle to these features (Section 3.3) the dominant wave directions are actually from the north suggesting they may not play the same role in the initiation of these features compared to their coastal analogues.



On some of the larger ridges there are parasitic, west to east oriented, transverse bedforms, with amplitudes of ~1 m and wavelengths of ~600 m and a northly asymmetry. These transverse bedforms appear to be stable in their location with no crest axis movement being identified over both an 11 and 1-year period (Figure 4-33), albeit the trough sections do appear to deepen over these same periods. Again, similar features have previously been described by Anthony & Leth (2002) from the west coast of Denmark. These examples have similar wavelengths of ~500 m and amplitudes of 1-3 m. Anthony & Leth (2002) interpreted these as being generated and maintained by a combination of the tide and the Jutland Coastal Current. Similar features have also been identified across the Thor windfarm and these do show migration rates of ~ 10 m/yr although the potential residual flow velocities are liable to be greater along the west coast of Denmark than on the southwestern margin of the Dogger Bank. This obviously needs to be tested with in situ and modelled hydrodynamic data.



Figure 4-34: Ridge and runnel features along the Dogger Bank South offshore wind farm margin, showing bed level change between 2019 and 2022



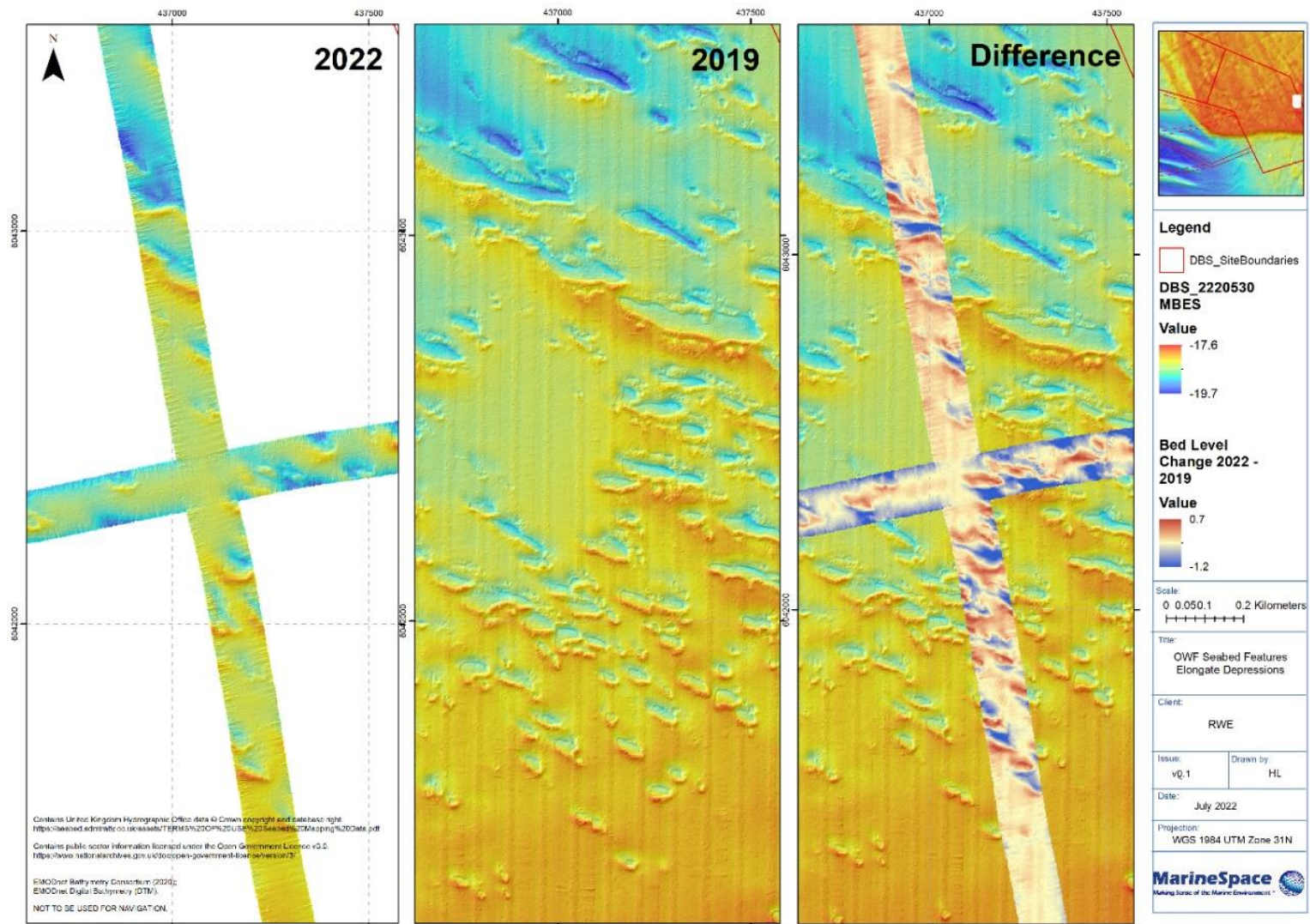


#### **4.1.3.2. Rippled Scour Depressions**

RSDs appear across the DBS OWF occur either in association with the, typically eastern, margins of the ridge features, often extending into the associated runnels (Figure 4-33), or in discrete fields in areas of no other relief (Figure 4-35). The RSD's are found as either linear, elongate or amorphous forms with a tendency for both individual forms and whole fields to have a northwest to southeast orientation (Figure 4-35). The RSDs are variable in size and shape: some are approximately spherical (up to 50 m in diameter) whilst others are thinner, more elongate features (approximately 50 m x > 150 m in length), the latter forms being the most common. Depths up to ~1.2 m below ambient bed level are recorded but most forms have a relief of < 0.6 m. RSDs commonly have a raised margin typically on the south or south-westerly edge of the depression (Figure 4-35).

Determining the exact dimensions of the RSD fields is difficult due to the grid resolution and is subjective as they do not have clearly defined boundaries. Within the HI1590 (2019) dataset which covers the eastern part of DBS East, one such field measures 3.1 km long and 2.1 km wide. Another, adjacent to but outside the OWF boundary, measures 4.1 km long and 1.5 km wide. Within the HI1714 (2021) dataset, which covers most of the northern and central part of DBS east, a field of these irregular features is ~4.5 km<sup>2</sup> in area, in the centre of DBS East, and is ~3 km long and 2.7 km wide. The Fugro survey corridor that covers DBS west partially images multiple RSDs but the coverage is insufficient to be able to define either individual fields or their relationship to ridge and runnel features.

Figure 4-35: A field of Rippled Scour Depressions along the northwestern margin of the Dogger Bank South offshore wind farm, with bed level change between 2019 and 2022



These fields of RSDs do exhibit movement. Bed level change analysis suggests that the RSDs seem to randomly appear and disappear, albeit within their general field. Bed level change across 1, 10 or 11-year periods remains within  $\pm 0.9$  m on the features shown in Figure 4-33. Over a 1-year period, between 2021 and 2022, bed level changes are in the range of - 0.8 m to 0.6 m. In the 10-years between 2011 and 2021, this range is between - 0.8 m and 0.9 m whilst across 11-years the range of bed level change measured across these features is - 0.8 m to 0.4 m. Bed level change of similar features (RSDs) in a different area of the OWF over a three-year period shows bed loss of up to -1.2 m and accumulation of up to 0.7 m (Figure 4-35). Note that over most time periods the maximum (rate of) loss is higher than that of accumulation. The majority of the RSD's show no persistent migration pattern more typically being created or infilled between surveys. It is therefore difficult to predict how they will develop in the future due to their seemingly random nature, compared to conventional flow perpendicular bedforms, albeit they do appear to be maintained within the individual fields.

In terms of their origin, Liu et al (2018) suggest “..there is a general consensus on how these sorted bedforms maintain the coarse-sand and fine-sand segregation: ripples that form in the coarse sand areas associated with large shear stress during orbital (wave) motion, preventing the settling of fine sand grains until they are transported to unrippled/ fine-grained areas; the result is a sediment sorting feedback process.” Their long-term evolution is still subject to debate but most applicable to the Dogger Bank site is the role of episodic storms or storm waves, plus or minus combined flows with the general tidal regimes. The random nature of their change would support the idea that these features do not develop under tides alone and extreme events play some role in their evolution.

#### **4.1.3.3. Pre-Holocene Surficial Expression**

Due to the potentially thin nature of the Holocene marine cover it is important to determine whether underlying deposits of the Dogger Bank Formation could outcrop/subcrop across the DBS OWF footprint. On the basis of the corridor surveys which dominate DBS West, a smaller number of locations in the southwest segment of DBS West, within the area described, as the “North West Riff” have irregular, low relief, morphologies that are not indicative of either the ridge and runnel features or the rippled scour depressions that are generally ubiquitous across the site and may represent localised exposures of pre-Holocene material.

The eastern section of DBS West and over two-thirds of DBS East have full swath bathymetry coverage from surveys HI1587 and HI1714 surveys and here the seabed shows no evidence of underlying glacial deposits. In the most southerly part of DBS East, where only corridor Fugro swath data was available, the bathymetry also indicates potential sub-cropping pre-Holocene transgression deposits as the windfarm extends beyond the Dogger Bank and into the deeper water Dogger Bight. The generation of the full ground model will elucidate if these pre-Holocene glacial deposits will occur within cable depth.

Finally, other features have been assessed to determine the potential magnitude of bed level change across the site. As has been described above bed level change is associated with both the margins of the ridge and runnel features and the RSD fields. However wider comparison of the available bathymetric datasets shows that, within the data crossover extent, over an:

- 11-year period (2011 to 2022) 77.8% of bed level change is  $< \pm 0.2$  m, and 42.3% is  $< \pm 0.1$  m;
- 10-year period (2011 to 2021) 87.5% of bed level change is  $< \pm 0.2$  m, and 46.9% is  $< \pm 0.1$  m;
- 3-year period (2019 to 2022) 88.1% of bed level change is  $< \pm 0.2$  m, and 69.8% is  $< \pm 0.1$  m;
- 1-year period (2021 to 2022) 87.1% of bed level change is  $< \pm 0.2$  m, and 58.0% is  $< \pm 0.1$  m.

The offset of  $\pm 0.1$  m would be within the survey budgets and even at  $\pm 0.2$  m most of this change will probably be related to survey inconsistencies related to different generations of data and survey quality. As the time periods are large, it should be mentioned that the changes may not have occurred steadily over that interval but could have occurred suddenly within a shorter time frame. Considering the spatial distribution of these corridors across almost the entire site a significantly large random sample suggests bed level change is actually quite restricted to the 2 types of sorted bedform features described above.

#### **4.1.3.4. Anthropogenic Features**

This assertion of limited sediment transport across the wider site is supported by the analysis of individual human structures found across the site namely, shipwrecks and oil and gas infrastructure. 4 shipwrecks and 2 obstructions are found within the HI1590 and HI1714 surveys which cover DBS East and the area immediately east. Of these the “Annemarie palm” (UKHO ID: 6772) and the UKHO ID: 6870 have scour pits that extend up to 50 m to the southwest with maximum depths of 1 m; 2, UKHO ID: 6900 and UKHO ID: 91528 show circular, dishpan scour, with depths to  $\sim 1.5$  m deep and with radii of 10-50 m; and 2 obstructions, seafloor structures probably associated with the Cygnus gasfields (UKHO ID: 92453 and 92454) show no scour at all. These are all relatively small scour features and would suggest limited large scale sediment transport is occurring.

Finally, seabed exposures of the Cygnus to ETS Gas Pipeline and the Cygnus A to Cygnus B gas pipeline (Installation 2014), the Cavendish export pipeline (Installation 2007) and the Hawksley EM to Murdoch DM gas line (Installation 2003) are found in the south of DBS East and across the HI1590 survey. The variability in the original installation depths achieved by these pieces of infrastructure makes it difficult to establish the exact sediment transport history, however, where they are clearly exposed on the seabed or within a cut trench there has been no evidence of post-installation back fill (Figure 4-36). Probably of greatest significance is the interaction of a number of RSDs with the Cygnus A to Cygnus B gas pipeline (Figure 4-37). Although there has been small scale ( $< 0.4$  m) erosion on the southerly margin of this feature in response to the natural scour processes operating across the object, in a number of places RSD's have developed on the southerly margin of the cable, achieving depths of up to 1.2 m below the ambient bed level along distances of up to 140 m. The 2 m grid of this data prevents spanning from being identified.



Figure 4-36: Cable and pipeline infrastructure present within the DBS East offshore wind farm area

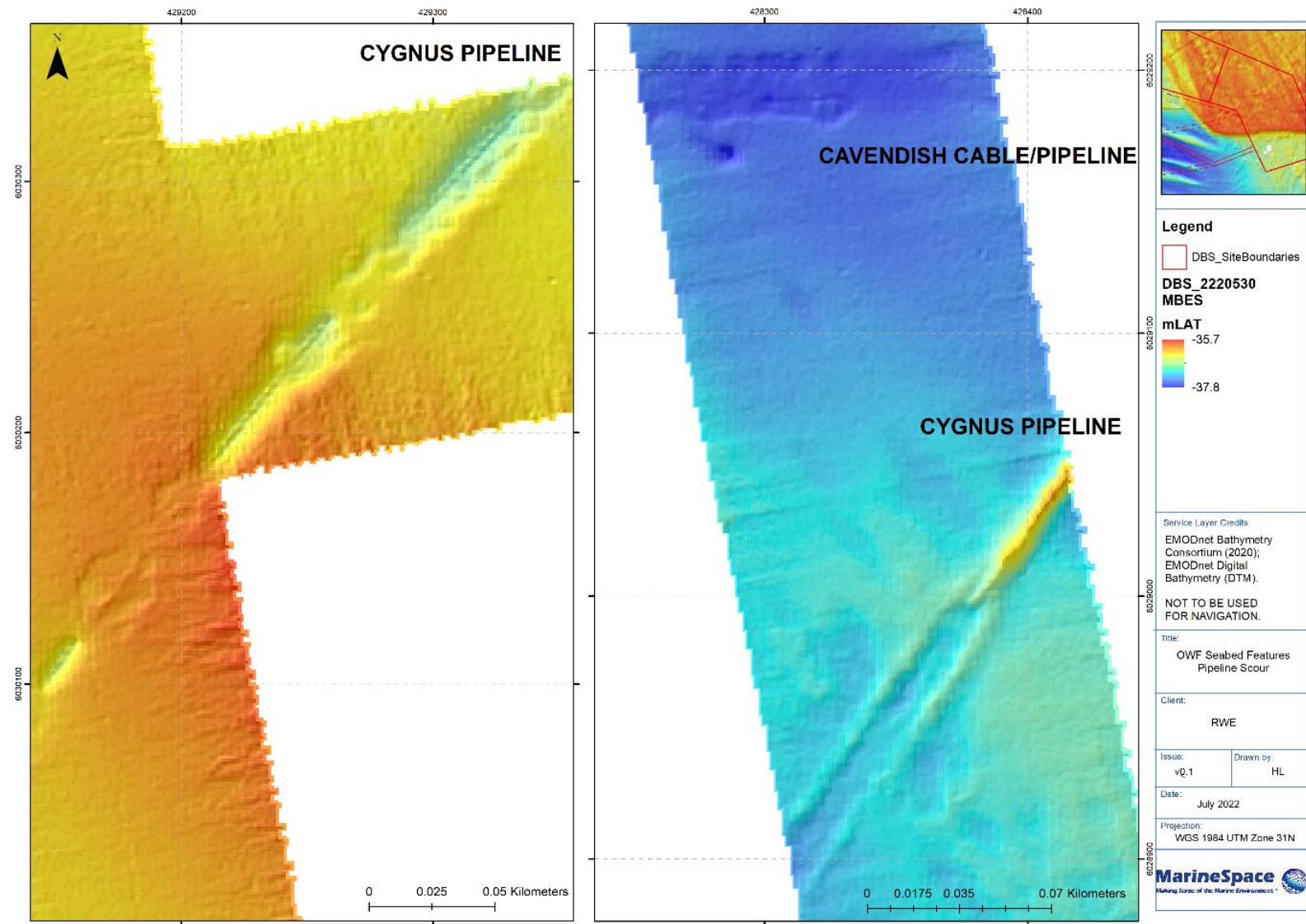
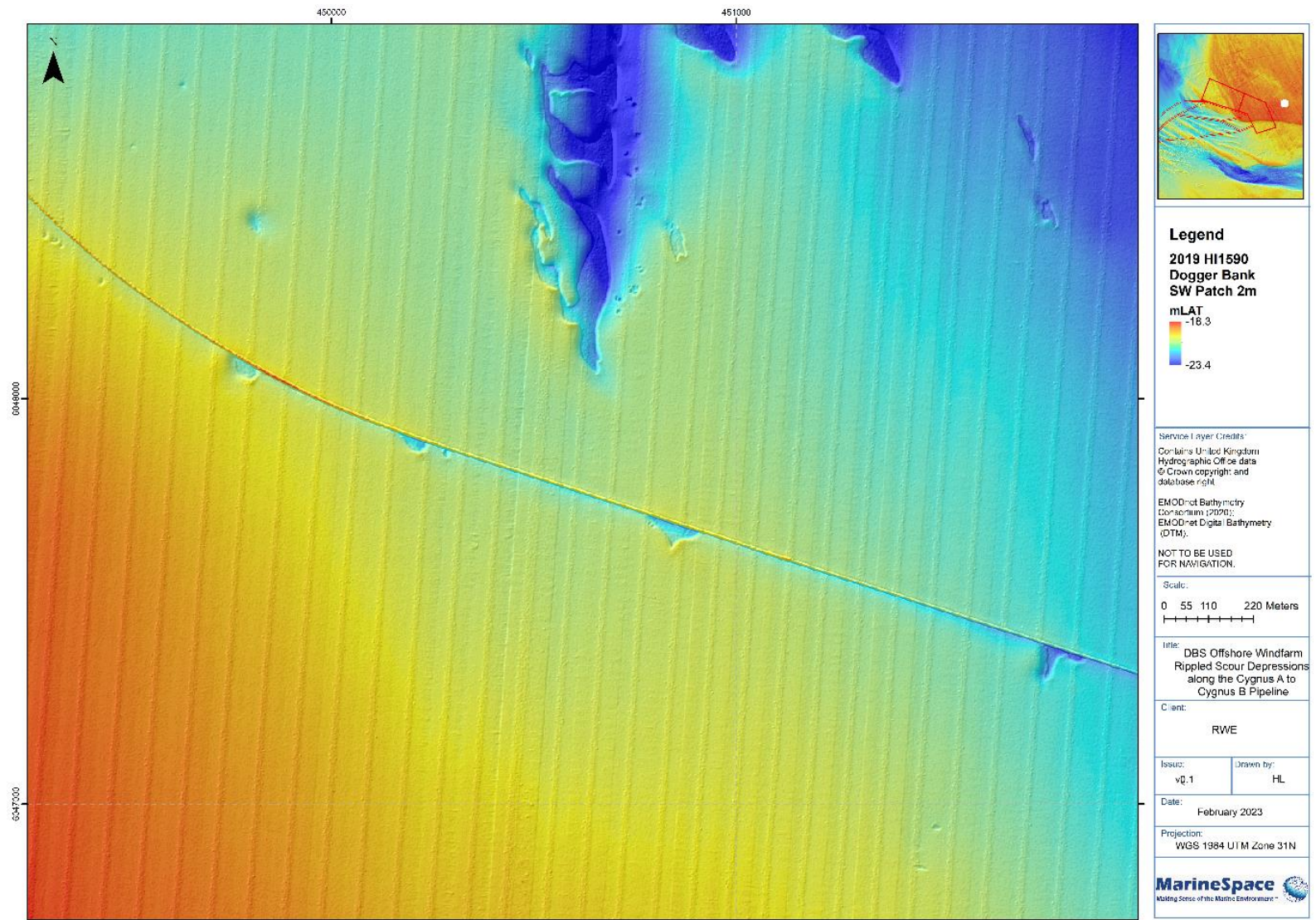




Figure 4-37: Rippled Scour Depressions interacting with the Cygnus A to Cygnus B gas pipeline



## 4.2. Gross Scale Morphology and Mobility

To supplement the annual to multi-annual bed level change presented for different sections of the potential Export Cable Corridors (Sections 4.1.2) and the Dogger Bank South OWF (Sections 4.1.3) footprint, decadal to centennial changes of the Dogger Bank margin has also been considered. Interpretation of Admiralty Charts, dating back to 1812, from a previous exercise undertaken on the western margin of the Dogger Bank were referred to (Dix, 2021). These charts were georectified following the approach of van der Waal & Pye (2003) and Burningham and French (2008, 2009 and 2017). This approach has a spatial accuracy of  $\pm 1$  km, which, when considering a bank 100 x 215 km in size, represents a  $< \pm 1$  % spatial error (Dix, 2021). In addition, the different vertical datums (Lowest Astronomical Tide (LAT), Mean Low Water Springs and datums 1' and 8' below MLWS) utilised by Charts of different eras had to be accounted for with all datums being converted back to mLAT. The depth conversion results in depth comparison being accurate to within 1 m, a vertical uncertainty of 3 - 4 % in the water depths being analysed (Dix, 2021).

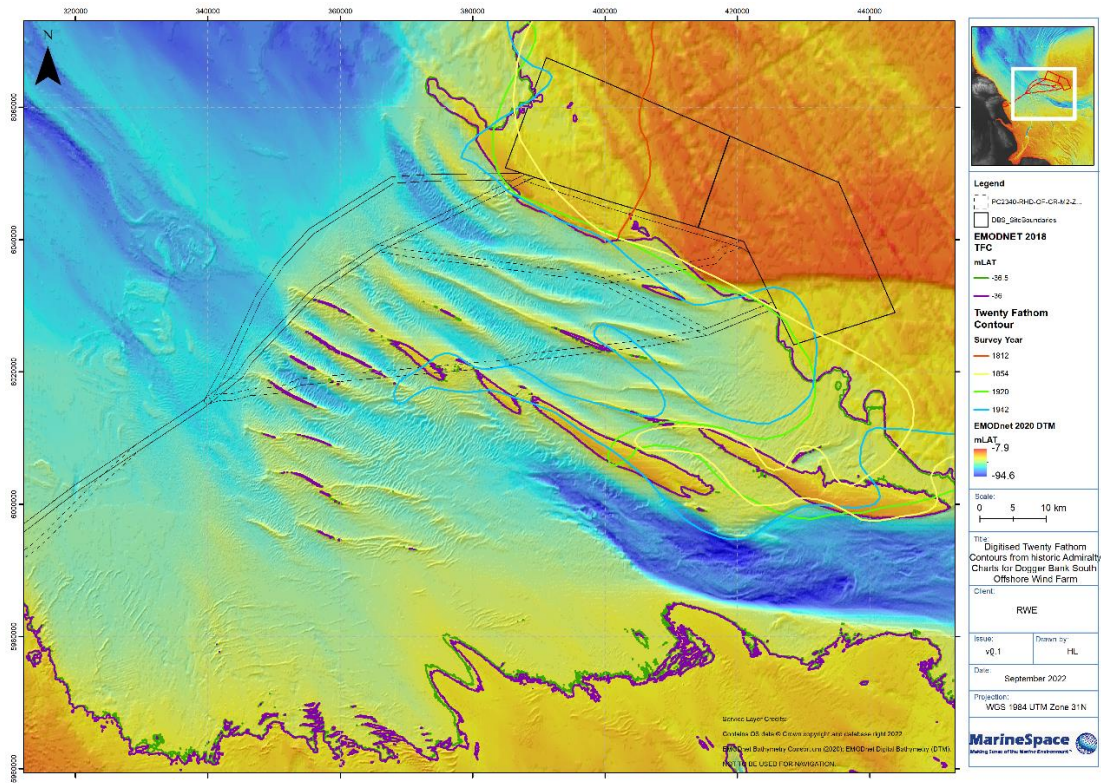
A historic 20 Fathom (approximately -36.5 mLAT) contours from 1812, 1854, 1916 and 1942 are compared against an EMODnet 2018, -36.5 and -36 mLAT, contours across the southwestern margin of the Dogger Bank (Figure 4-38). The 1916, 1942 and modern contours along the southern margin of the DBS West are all clustered within  $< 1$  km (the resolution of the chart rectification) and would suggest on the gross scale the margin is stable over a centennial period. Towards the boundary between the west and east sections of the OWF footprint the Dogger Bank margin has a northerly indent which is not so well captured by the previous surveys. The 1942 survey actually extending further offshore at this point to cross the inner most sandbank of the Bolders Bank Complex (which appears to be an interpolation effect in the production of the 1942 map towards the shallow at the top of this sandbank). East of this and towards the southern margin of DBS east the contours coalesce once more to be within  $\sim 1$  km. Beyond the margin of the Dogger Bank in the area of the Hills, Outer Bank and Bolders Bank the historic contours fail to capture the northwest to southeast trending sandbanks, but this appears to be in response to the minimal number of soundings available.

Figure 4-39 shows the digitised -20 and -30 mLAT contours from the geo-rectified 1973 data plotted against the EMODNET equivalent bathymetric contours, showing a close correspondence on a whole bank scale albeit with the inevitable detail smoothing of the earlier Chart contours (Dix, 2021). This gross relative stability, within the kilometric resolution of the historic chart comparisons, of the southwestern margin of the Dogger Bank is supported by the gross geological structure. As discussed in Section 3.2 the bank is dominated by glaciotectionised and almost certainly over-consolidated glacial deposits with a relatively thin veneer of potential mobile Holocene marine sands, a stratigraphy supported by the initial Fugro interpretation and analysis of the seabed morphology as described in the previous sections. Consequently, it is considered there is very limited potential for large scale bank movement across this margin.

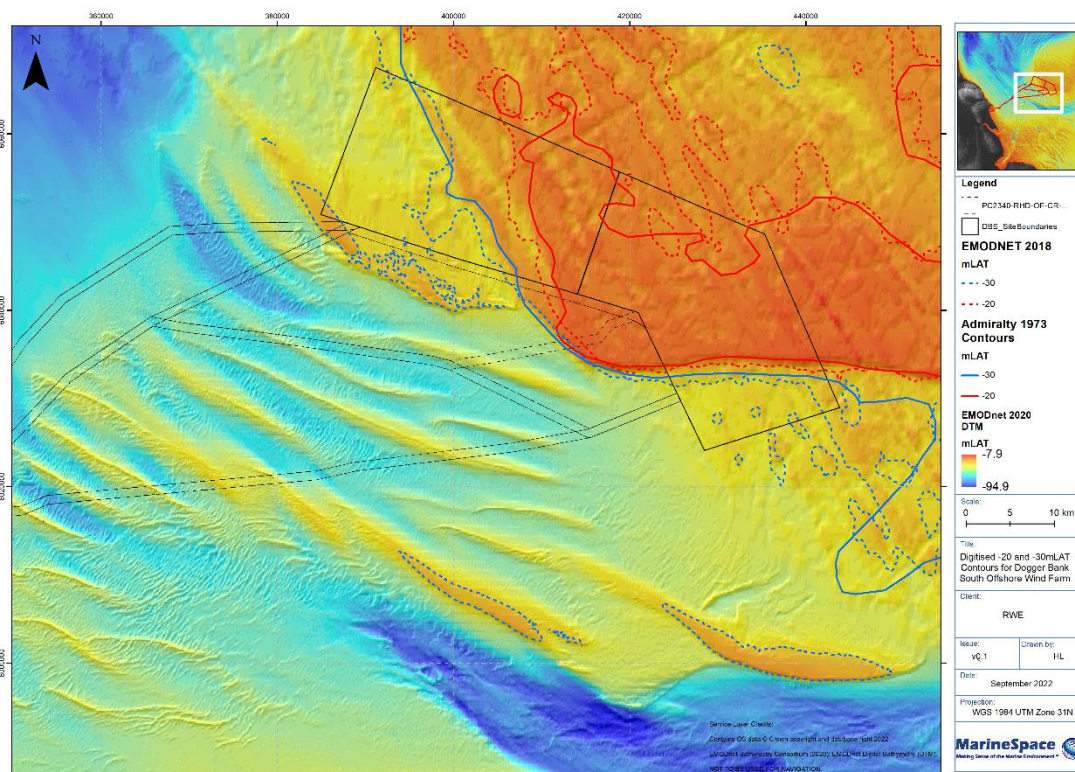
Kenyon et al (1981) consider the "Sand Hills" group (which clusters the 3 sandbank groups defined here) as being moribund (i.e. not actively moving) but with the presence of parasitic bedforms suggesting the possibility of minor bed level change by the present hydrodynamic conditions. The inference was that they were formed at lower sea-levels, likely between  $\sim 8$ -6 ka (Section 3.3) where the tidal currents would have been stronger and capable of building these features.



**Figure 4-38: Digitised Twenty Fathom Contours from the 1812, 1854, 1916 and 1942 Admiralty Charts. EMODNET -36.5 and -36 mLAT (equivalents of Twenty Fathom Contour) contours have been added for comparison against an extensive “modern” dataset**



**Figure 4-39: Digitised -20 and -30 mLAT contours from the 1973 Admiralty Charts. EMODNET contours are also plotted**



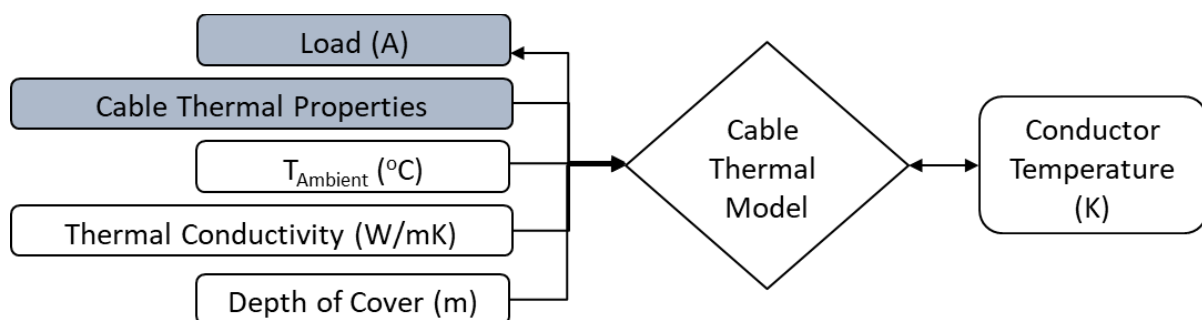
## 5. Thermal Analysis of Export Cable Route, Offshore Windfarm and Landfall Site

Crucial to the design, operation, maintenance, longevity, and actual power transfer capability of all marine high voltage (HV) export and inter-array cables, is their maximum operating temperature (which can be approaching 90°C for alternating current (AC) cables). In addition, the rate and mode of heat dissipation from operational cables needs to be understood for ensuring compliance with the “2K criterion”, where applicable, and for the interpretation of Distributed Temperature Sensor data for conditional monitoring including real-time thermal rating, fault detection and burial-depth estimation.

The operational current rating of any cable is primarily controlled by a combination of the thermal properties of the cable and the medium into which it is buried. For terrestrial cables, at least, the thermal environment of the burial medium accounts for 70% of the temperature rise of the conductor, and so significant research has gone into reducing the thermal resistance of backfilling material in on-land cable trenches. By comparison, there has been very limited work on the thermal environment encountered by buried HV cables in the marine environment. The key criteria for understanding heat dissipation from HV cables are (Figure 5-1):

1. Ambient temperature of the environment at cable depth. This is controlled by temporally and spatially varying ocean bottom temperatures and groundwater temperatures propagating to depth, the rate of which is controlled by the thermal diffusivity of the seabed soils;
2. Thermal conductivity/resistivity of the sediment and in certain circumstances the permeability of the soils (this, in turn, is controlled by grain size and porosity);
3. Temporally and spatially varying depth of cover over the cable.

**Figure 5-1: Simple model of controls on conductor temperature and hence cable rating. Boxes shaded in blue are non-environmental input parameters**



Ultimately, these three parameters are encapsulated in the  $T_4$  term of the steady state (IEC-60287) and dynamic (IEC-60853) ratings calculations. The following sections will provide an assessment of the three key environmental parameters as well as a specific assessment of the thermal environment of the landfall site.

## 5.1. Ambient Ocean Temperature Analysis

Hernandez-Colin et al. (2021) have recently demonstrated the importance of ambient temperature fluctuation on the overall HV cable temperatures even when buried in the sub-surface and operating under load. The temperature at cable depth is driven by a combination of Ocean Bottom Temperatures (OBT), the thermal conductivity of the seabed sediments and the cable depth. However, OBTs have conventionally been dealt with in the most cursory manner when considering cable ratings. The most recent CIGRE Working Group B1.35 review (2015) showed c. 75% of the industry just used standard minimum and maximum values of 10° and 15°C respectively. There has, therefore, been very limited consideration of temporal and spatial variation in this key parameter.

Ironically, OBTs are one of the most poorly studied oceanographic parameters and there is a relative paucity of data, with a sporadic spatial spread of point measurements (a few 100k over the entire northwest European Shelf taken over the last century), a limited number of time series data (most of which are short term – 10s of deployments) and an even smaller number of constantly monitoring *in situ* stations (<10). There are, however, publicly available numerical models, the most recent and best calibrated being developed by the UK Met Office: FOAM Shelf Seas Atlantic Margin Models – AMM7v5 and AMM15v2. These models have been calibrated against available *in situ* oceanographic datasets and so quantitative estimates of the accuracy of the models can be demonstrated:

- **AMM7v5** – this is the original FOAM, Atlantic Margin Model, with a 7 km resolution (Renshaw et al., 2021). This model has undergone a 27-year reanalysis simulation running from 1993-2019, the results from which provide a range of oceanographic parameters, including OBT, either as a daily or monthly average (Renshaw et al., 2021). These have been calibrated against *in situ* observations distributed across the shelf. Generally, AMM7v5 underestimates the temperature relative to the ensemble, most of the time, for depth between 30 m and 750 m. Without the outliers, the bias near the surface (0-5 m) varies between +0.23°C and -0.49°C; and for depths 30-75 m between +0.11°C and -0.51°C. The model has an overall cold bias of c. < 0.1°C. The Root-Mean-Square (RMS) values and mean bias for the full model domain are given in Table 5-1.

**Table 5-1: Estimated daily accuracy for AMM7 V5 (Renshaw et al., 2021).**

Variable	RMS Difference (°C)	Mean Bias (°C)
Temperature 0 - 5 m	0.45	-0.06
Temperature 5 - 30 m	0.61	-0.09
Temperature 30 - 80 m	0.64	-0.1
Temperature 80 - 300 m	0.49	-0.12

- **AMM15v2** – is the very latest MetOffice FOAM AMM model with a 1.5 km resolution (Tonani et al., 2021). This is a daily average modelled ocean bottom temperature time series



from 31 December 2016 to present (for this exercise, data downloaded 12 January 2022). It provides a daily, 6 Day forecast output. Model validation has been undertaken on time series data from the German Bight (Tonani et al., 2021) and a glider campaign from northern Scotland. Full domain daily RMS differences for these temperature profiles are 0.43°C, with a bias of -0.02°C (a warm bias – Tonani et al., 2021). From this data set we have generated monthly average values a time-step that is more appropriate for predicting ambient temperatures at cable depth.

Although both models provide daily values, propagation of ocean bottom temperature to cable depth will filter out short term temperature variations and generate a smoother temperature variation with a temporal lag depending on the time constant of the sediment. This time constant can be estimated from:

$$Time\ constant \propto \frac{Depth\ of\ Lowering^2}{Thermal\ Diffusivity}$$

With typical marine sediments having thermal diffusivities of between 3 and 7E-7 ms<sup>-1</sup> this equates to temperatures having to persist in the water column for typically 2-5 weeks to start to generate significant temperature changes at actual cable depth. Consequently, short term (hours to days) temperature spikes will invariably not propagate to depth. Consequently, monthly averaged time series provide the most useful input oceanographic data for cable design.

An independent validation exercise of the monthly averaged temperatures against 181,976 *in situ* data measurements from the World Ocean Database was undertaken by the University of Southampton. These give mean absolute errors of 1.27°C and 1.25°C for AMM15v2 and AMM7v5, with a warm bias of 1.05°C, suggesting values extracted from these models are a conservative estimate of the recorded monthly values. There is, however, a seasonal variation in these uncertainty statistics with Oct–Apr Mean Absolute Error (MAE) values of ≤1.2°C and May-Sep values of between 1.2-1.65°C.

Figure 5-2 shows a plan view of the spatial ocean bottom temperature (OBT) variation from the AMM15v2 model for the Dogger Bank South site. Data for March and September are shown to give an indication of the maximum temporal variation between winter and summer with a seasonal variation of up to 10.4°C. To capture the spatial variation across the area covered by the export cable corridor options and the windfarms, data extraction from these models and more detailed analysis of the northernmost and southernmost routes has been undertaken.

Figure 5-2: The spatial and temporal (March [Upper Panel] vs September [Lower Panel]) variation in ocean bottom temperature from the AMM15v2 model for the Dogger Bank South cable routes and OWF – please note the different legend scales

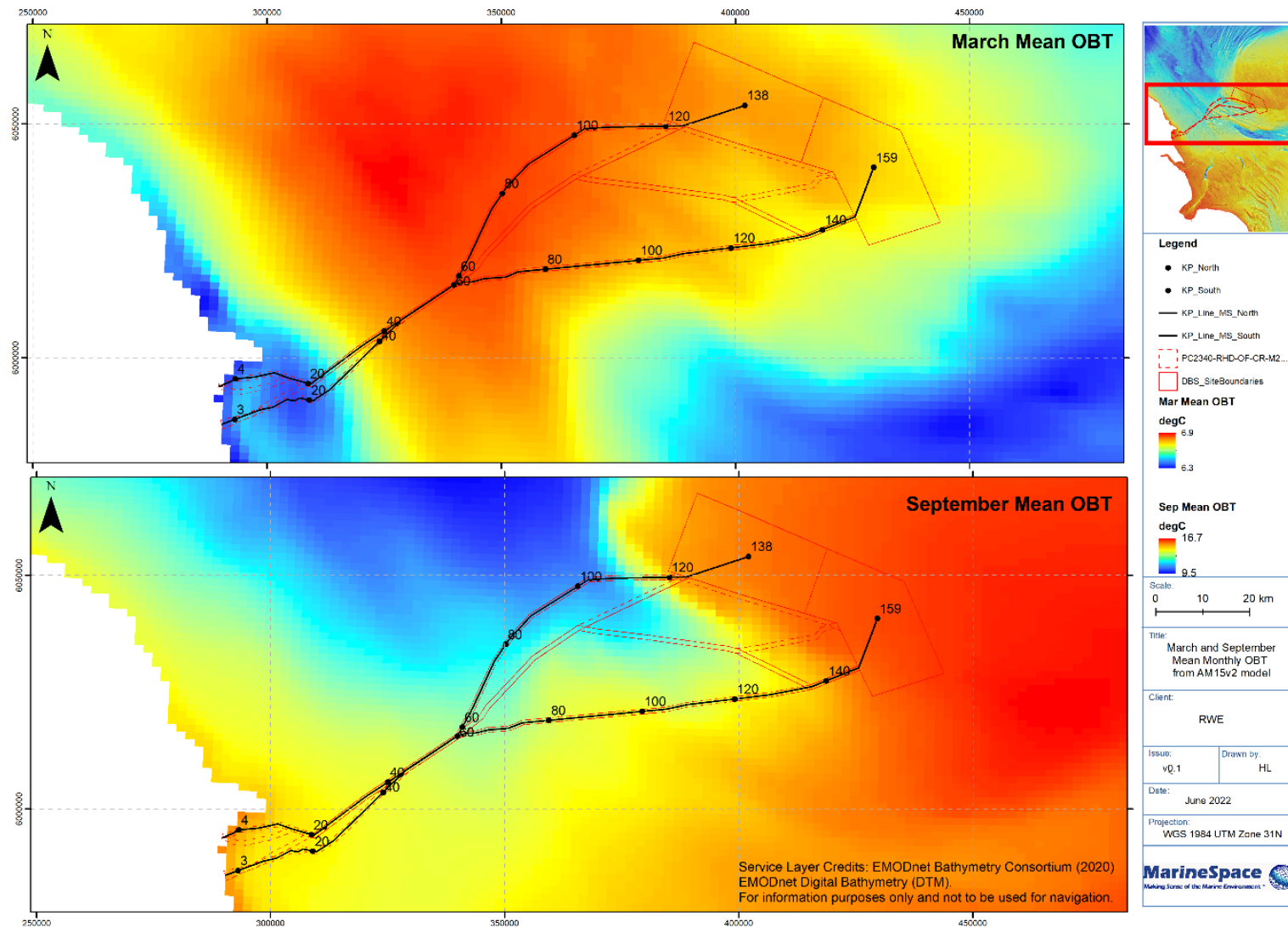


Figure 5-3 through to Figure 5-6 provide monthly OBT profiles along the northernmost and southernmost ECC routes to the centre of the OWF, from the AMM15v2 and AMM7v5 models respectively. These profiles demonstrate that the maximum temperatures are obtained in August in the coastal strip. The maximum monthly mean temperature of  $16.7 \pm 0.6^{\circ}\text{C}$  (@ 2STDEV) and  $15.8 \pm 0.6^{\circ}\text{C}$  (@ 2STDEV) for the respective models of the northernmost route. For the southernmost route the maximum monthly mean temperatures are  $17.1 \pm 0.5^{\circ}\text{C}$  (@ 2STDEV) and  $16.9 \pm 0.4^{\circ}\text{C}$  (@ 2STDEV) for the respective models. Minimum temperatures occur in February in the nearshore, and March offshore. OBT only goes below  $6^{\circ}\text{C}$  at the nearshore, in February, for both north ( $5.4 \pm 0.7^{\circ}\text{C}$  (@ 2STDEV)) and south ( $5.7 \pm 0.8^{\circ}\text{C}$  (@ 2STDEV)) routes. In both models the monthly mean OBT remains under  $17.1 \pm 0.5^{\circ}\text{C}$  (@ 2STDEV) across the cable route options to the nominal 'offshore substation' in the centre of each array. The seasonal signal is such that between November and May monthly mean temperatures are  $< 10.9^{\circ}\text{C}$  along the entire route in both models.

The warmest modelled OBTs occur in August at the nominal 'offshore sub-station' of DBS East and West OWF areas – at the site centres (Figure 5-3 to Figure 5-6). A time series for the daily mean OBT at these centres has been produced, with standard deviations of the monthly mean OBTs for the same location (Figure 5-7). Across almost 3 years, the maximum AMM15v2 modelled OBT is  $17.3 \pm 1.0^{\circ}\text{C}$  in late July 2021 for DBS West, whilst the minimum was  $4.7 \pm 0.7^{\circ}\text{C}$  in February 2021. The maximum AMM15v2 modelled OBT is  $18.2 \pm 1.1^{\circ}\text{C}$  in late July 2021 for DBS East, whilst the minimum was  $5.1 \pm 0.7^{\circ}\text{C}$  in early February (Figure 5-7).

Across the OWFs, AMM15v2 modelled August mean OBT is  $17.3^{\circ}\text{C}$  at maximum, and  $14.9^{\circ}\text{C}$  at minimum with a standard deviation of  $\pm 0.5^{\circ}\text{C}$  and  $\pm 0.4^{\circ}\text{C}$  respectively (Figure 5-8), a total range of  $2.4^{\circ}\text{C}$ . The AMM7v5 model gives a minimum August OBT of  $14.7^{\circ}\text{C}$  in a more southwest location in the DBS West array whilst the maximum value is at the same location but  $0.1^{\circ}\text{C}$  cooler, hence a range of  $2.5^{\circ}\text{C}$  (Figure 5-9).

For comparison the maximum recorded in situ ocean bottom temperature, from a 1,000 World Ocean Database catalogued measurements, from within the Dogger Bank South cable corridor and offshore wind farm site over the last 120 years, is  $18.2^{\circ}\text{C}$  (August, 2018) in a CTD cast in the offshore windfarm. This appears to be an anomalously high value, with the next greatest temperature recorded being  $17.5^{\circ}\text{C}$  taken in 1959. The maximum three values were all recorded in the DBS East area, towards the eastern boundary of the site. These values, and their easterly asymmetry fits with the daily mean modelled values of OBT (Figure 5-7).

**Figure 5-3: Monthly ocean bottom temperature variation, from the AMM15v2 model at 20 km intervals along the Dogger Bank South northernmost cable route to DBS West centre. Smaller 1km intervals are shown between 110 and 120 to better demonstrate the variation along the Dogger Bank margin**

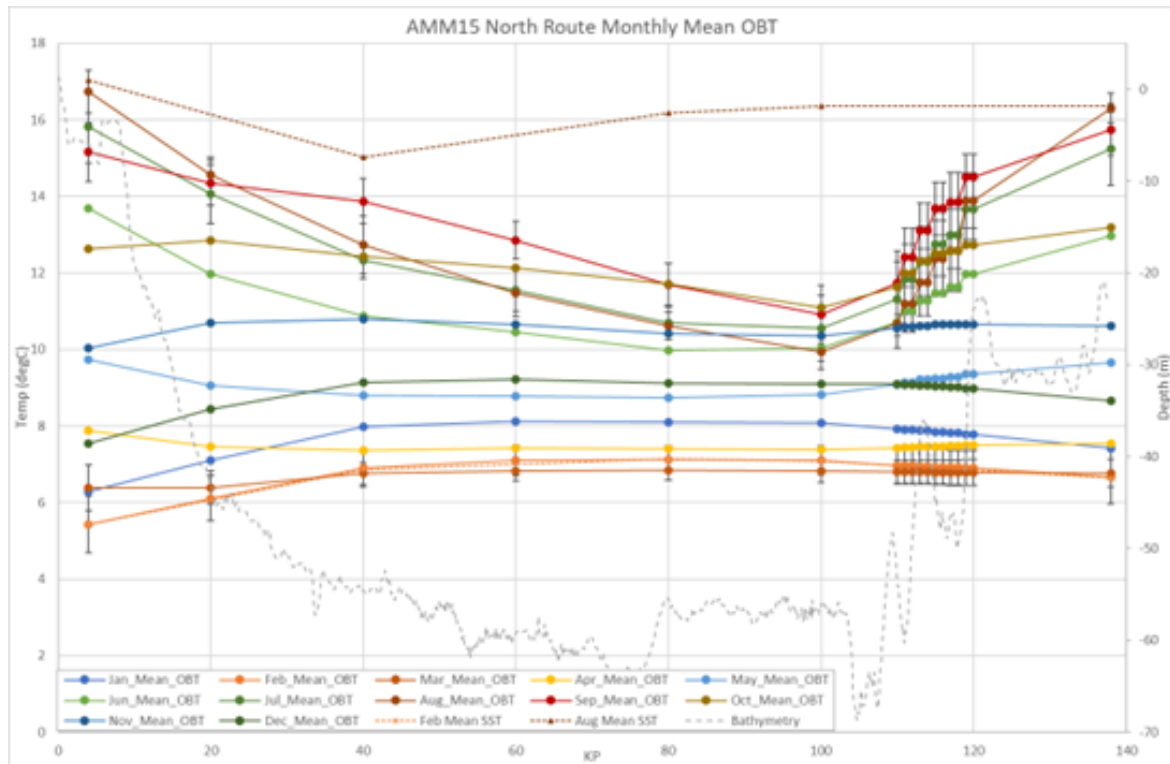


**Figure 5-4: Monthly ocean bottom temperature variation, from the AMM15v2 model at 20 km intervals along the Dogger Bank South northernmost cable route to DBS East centre**

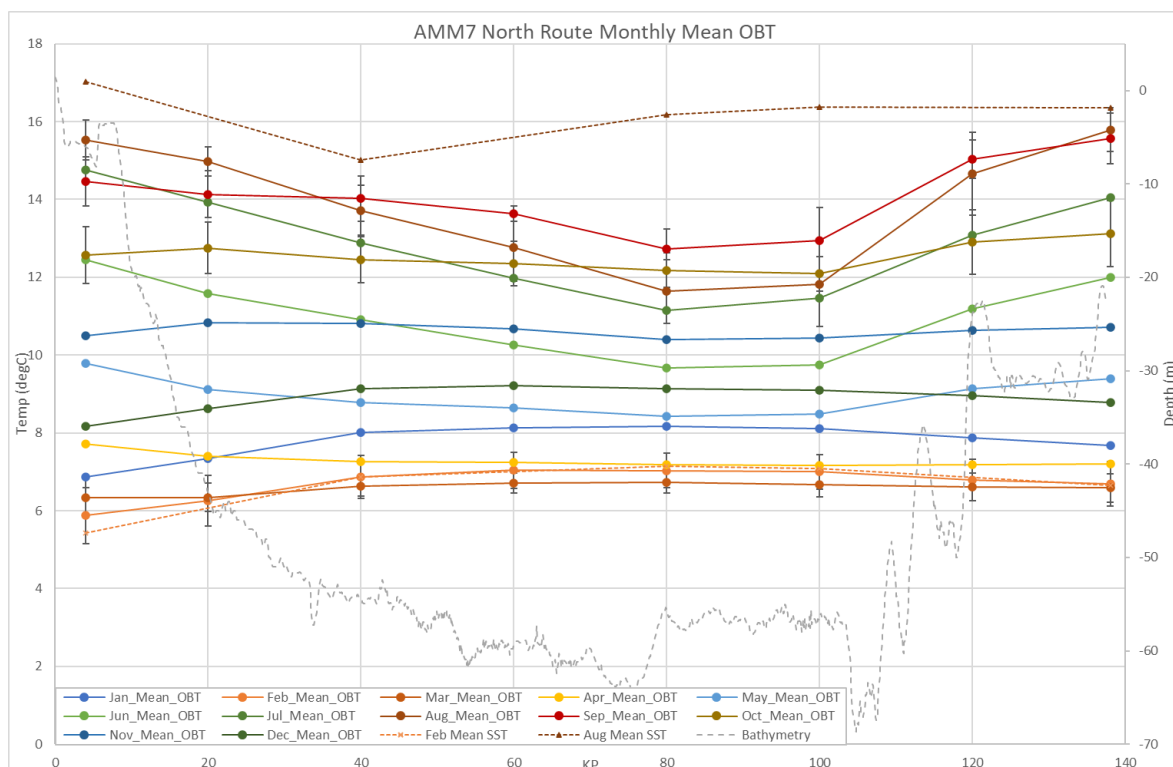




**Figure 5-5: Monthly ocean bottom temperature variation, from the AMM15v2 model at 20 km intervals along the Dogger Bank South southernmost cable route to DBS East centre**

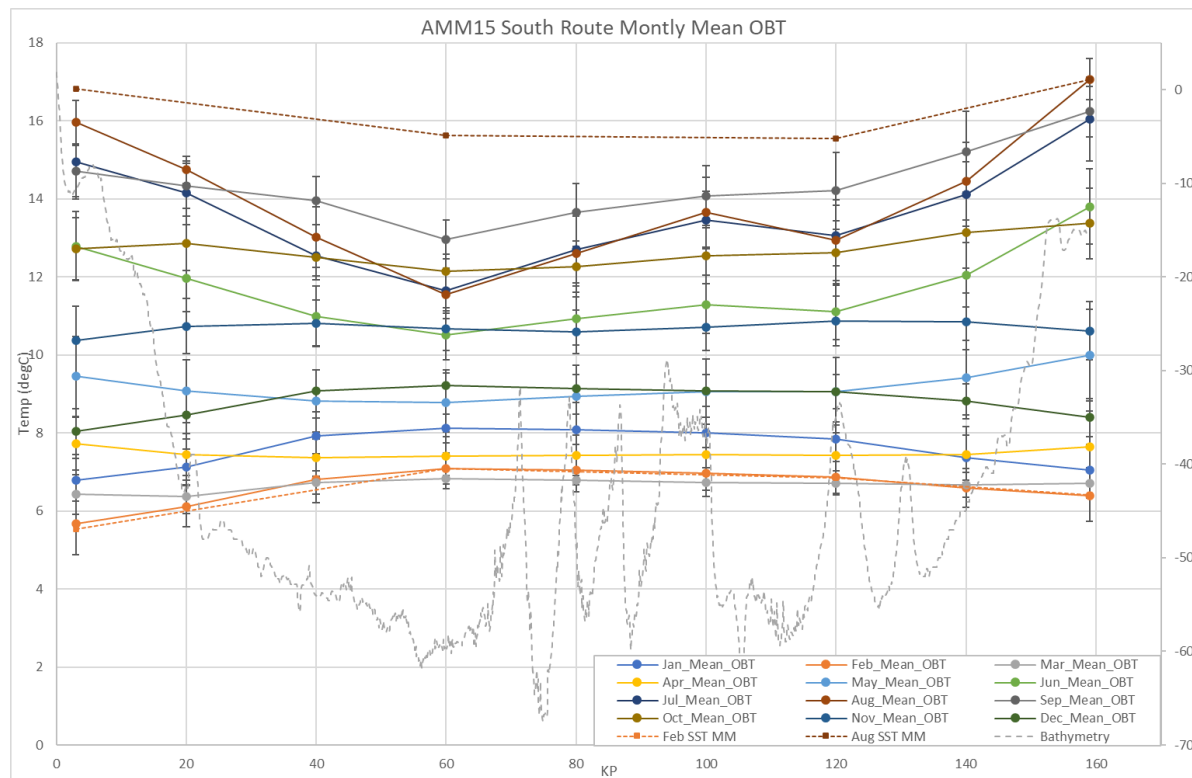


**Figure 5-6: Monthly ocean bottom temperature variation, from the AMM7v5 model at 20 km intervals along the Dogger Bank South southernmost cable route to DBS East centre**

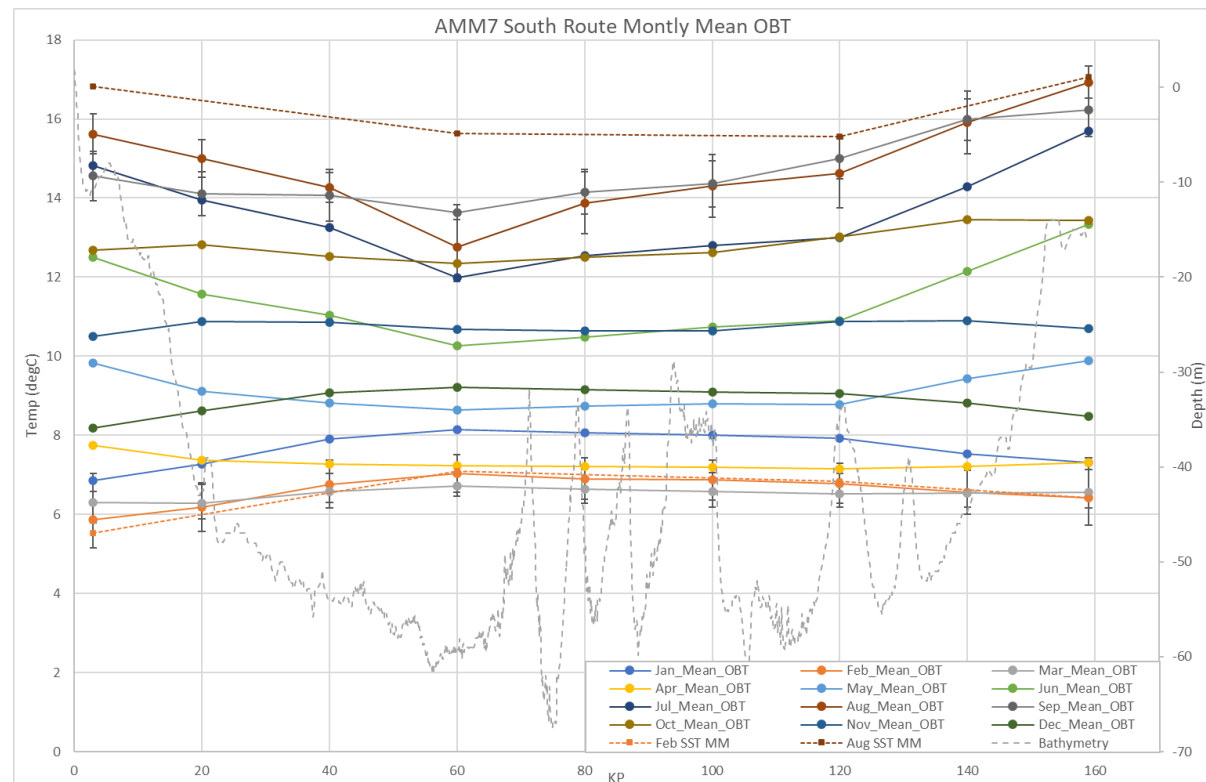
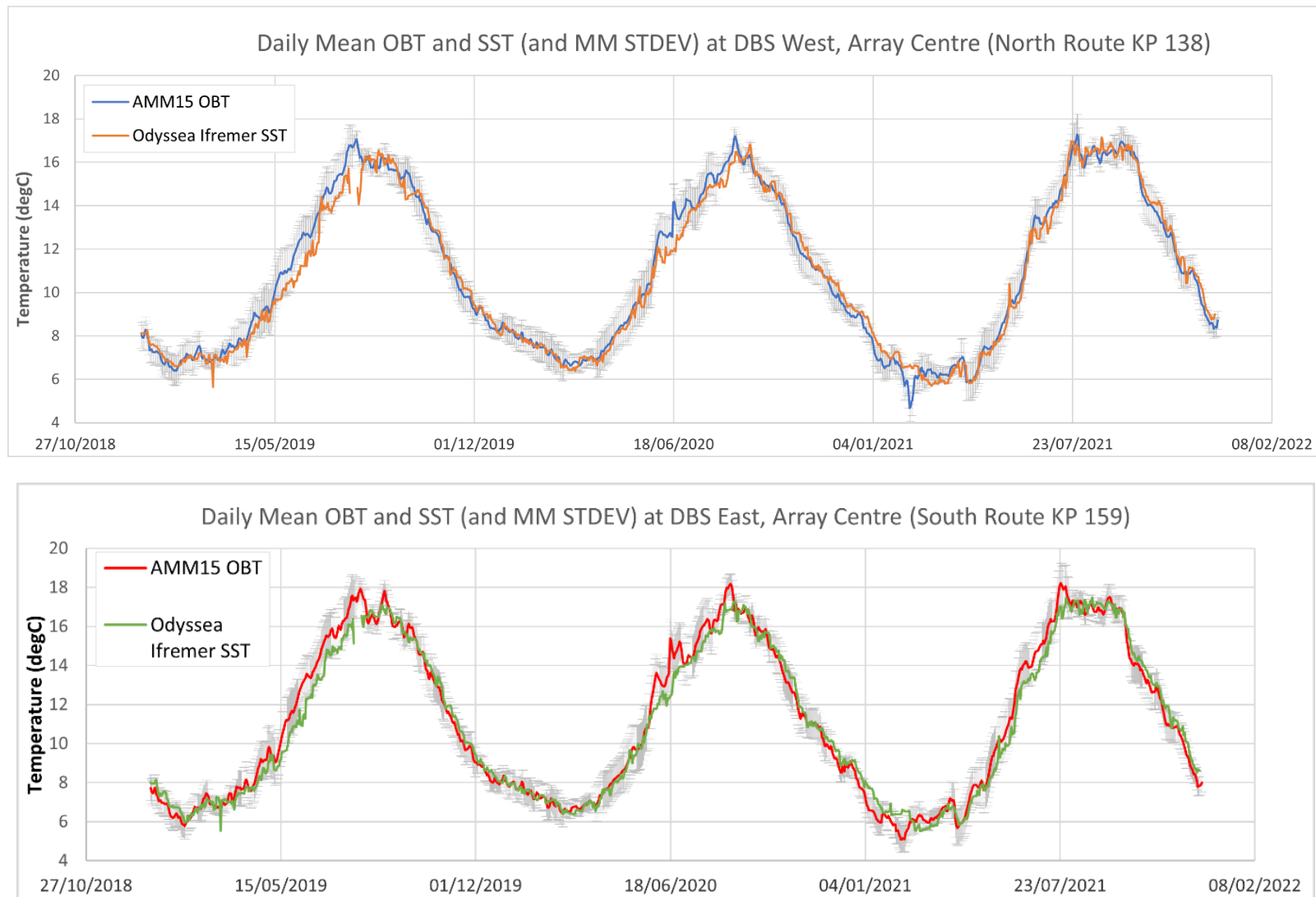
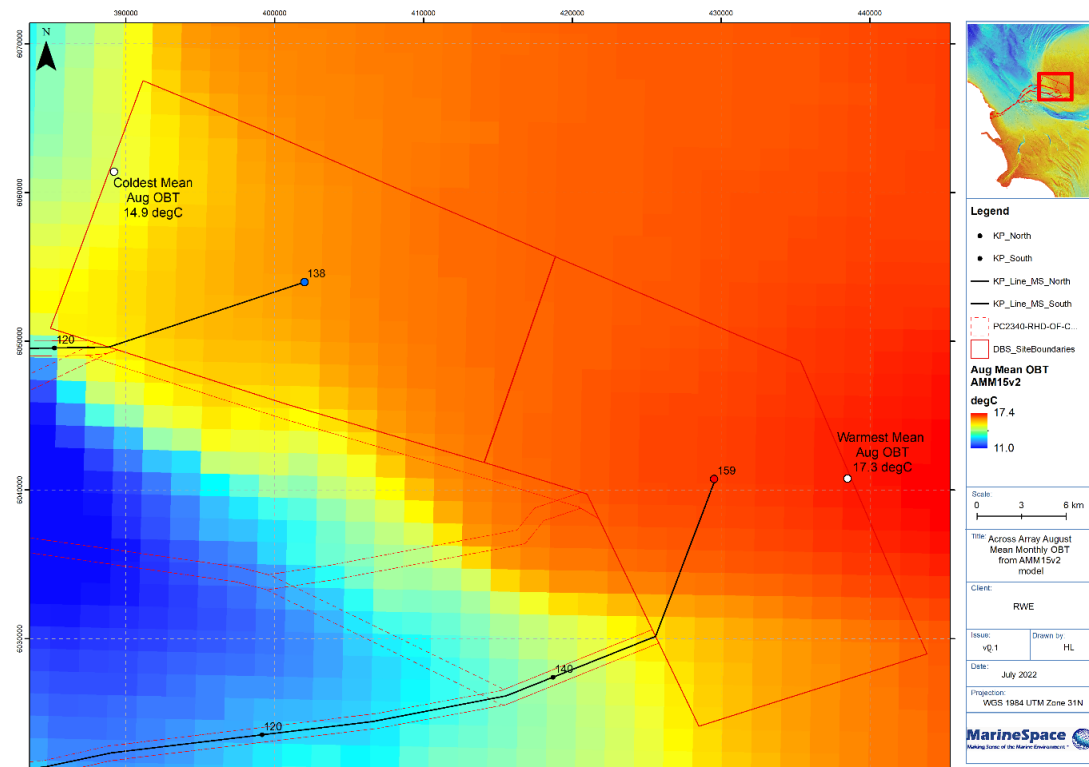


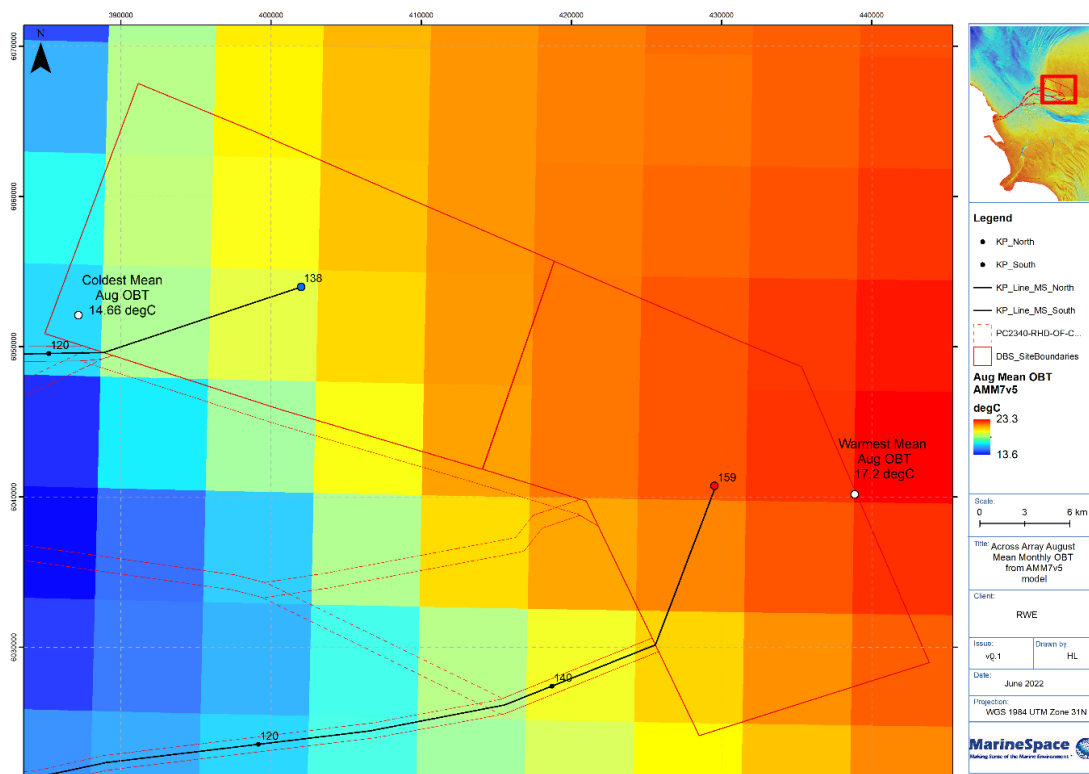
Figure 5-7: Daily mean ocean bottom temperature time series from the AMM15v2 model and the ODYSSEA satellite derived SST at each Dogger Bank South array centre



**Figure 5-8: Location of the minimum and Maximum in August mean monthly ocean bottom temperature from the AMM15v2 model across the Dogger Bank South OWF areas**



**Figure 5-9: Location of the minimum and Maximum in August mean monthly ocean bottom temperature from the AMM7v5 model across the Dogger Bank South OWF areas**



The difference between SST and OBT is minimal in the shallower waters of the coast (~KP0 – KP20) and over the Dogger Bank (~KP 120 on the northern route and KP 150 on the southern route to the OWF footprint) in response to greater tidal mixing. This observation means satellite derived Sea Surface Temperature (SST) measurements can also be used as an actual observed proxy time series of water temperature at the seabed. Data has therefore been extracted from the CMEMS ‘SST\_ATL\_SST\_L4\_NRT\_OBSERVATIONS\_010\_025’ data product (known as ODYSSEA), which is a multi-sensor level 4 analysis, covering the European northwest shelf/Iberia Biscay Irish Seas, at 0.02° horizontal resolution (Autret et al., 2021). It is produced from the merging of various satellite SST level 2 data, which have passed a significant number of quality controls, and which have been inter-calibrated through an inter-sensor bias correction procedure, using a median field generated from a set of ‘best quality’ sensors, to provide an estimate of the night-time SST based on original SST observations. These data have a MAE of 0.1 °C. These data have also been plotted in Figure 5-7 along with the modelled OBT. There is clear correspondence between the two datasets with a Mean Absolute Error of 0.4 and 0.5°C and a Mean Bias Error of -0.09 and -0.13 °C (DBS West and East respectively). This means that the model is predicting slightly warmer OBTs than is actually being recorded at the surface.

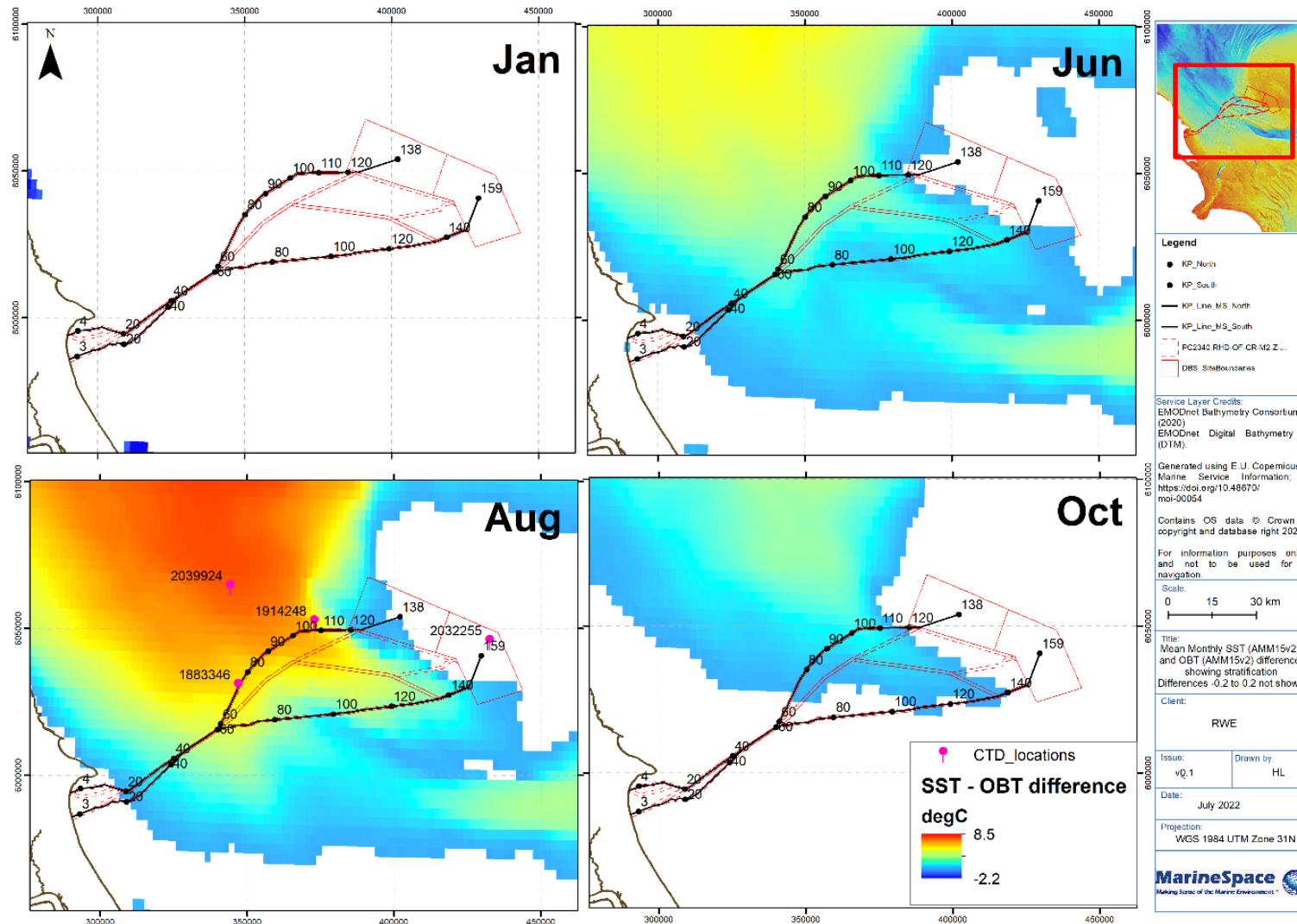
From ~KP 20 to the edge of the Dogger Bank the water column for large sections of the routes has the potential to become thermally stratified. A proxy value of  $> \pm 0.2$  °C temperature differential between SST and OBT has been used for defining thermal stratification (de Boyer Montégut et al., 2004). Figure 5-10 shows the extent of thermal stratification across the area. In January the whole area is well mixed, the onset of thermal stratification starts in late Spring / early Summer and reaches a peak in August, then reducing again during the Autumn becoming fully mixed across the entire area by Autumn.

The strongest seasonal stratification occurs in August for both the northernmost and southernmost cable corridor options. The difference between SST and OBT does not exceed 3°C from landfall to KP 40 for both routes. Up to ~KP 60, the end of nominal Zone 1, where the cable route options diverge, mean SST to OBT difference was  $\leq 4.3$  °C.

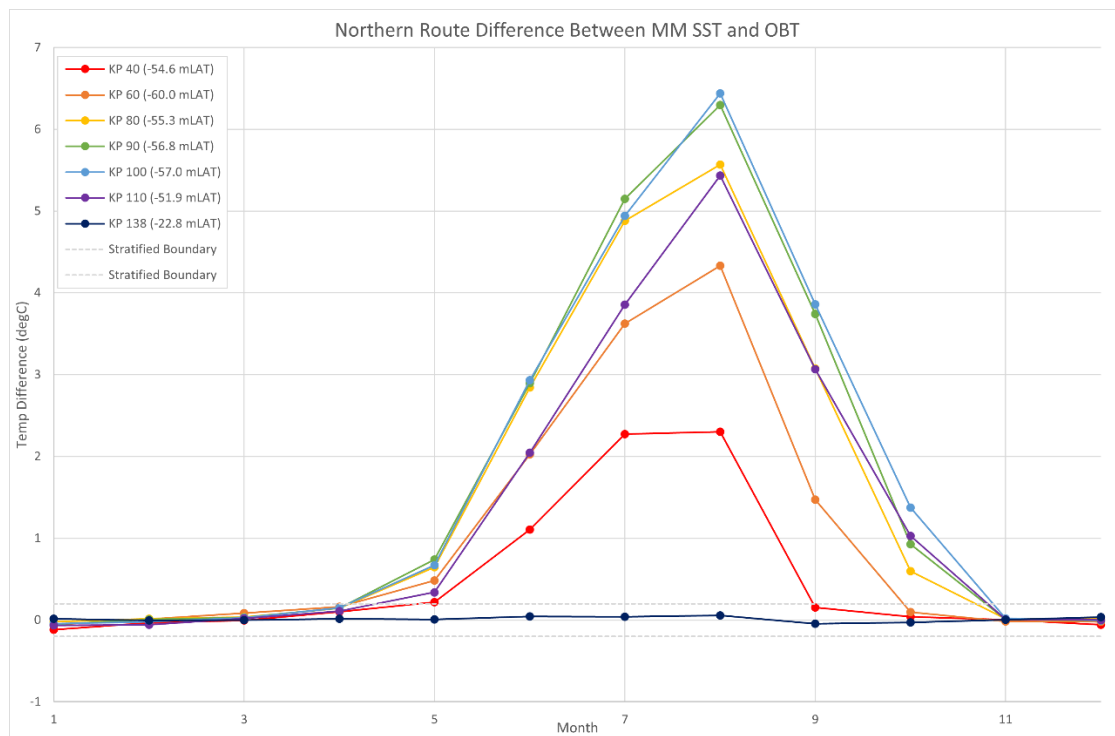
The northernmost route passes through the most stratified parts of the area, with the route between KP 60 and 80 showing a differential of up to 5.5 °C. From KP 80 to KP 110, seasonal stratification is strongest with a maximum difference of up to 6.5 °C from monthly mean AMM15v2 SST and OBT values. The difference in SST and OBT decreases heading over the Dogger Bank southwest margin into shallower water at the DBS West centre (Figure 5-11). The southernmost route is subject to less temperature variability. For this route, strongest seasonal stratification occurs at ~KP 70, with a AMM15v2 modelled difference between SST and OBT of 4.5 °C (Figure 5-12).



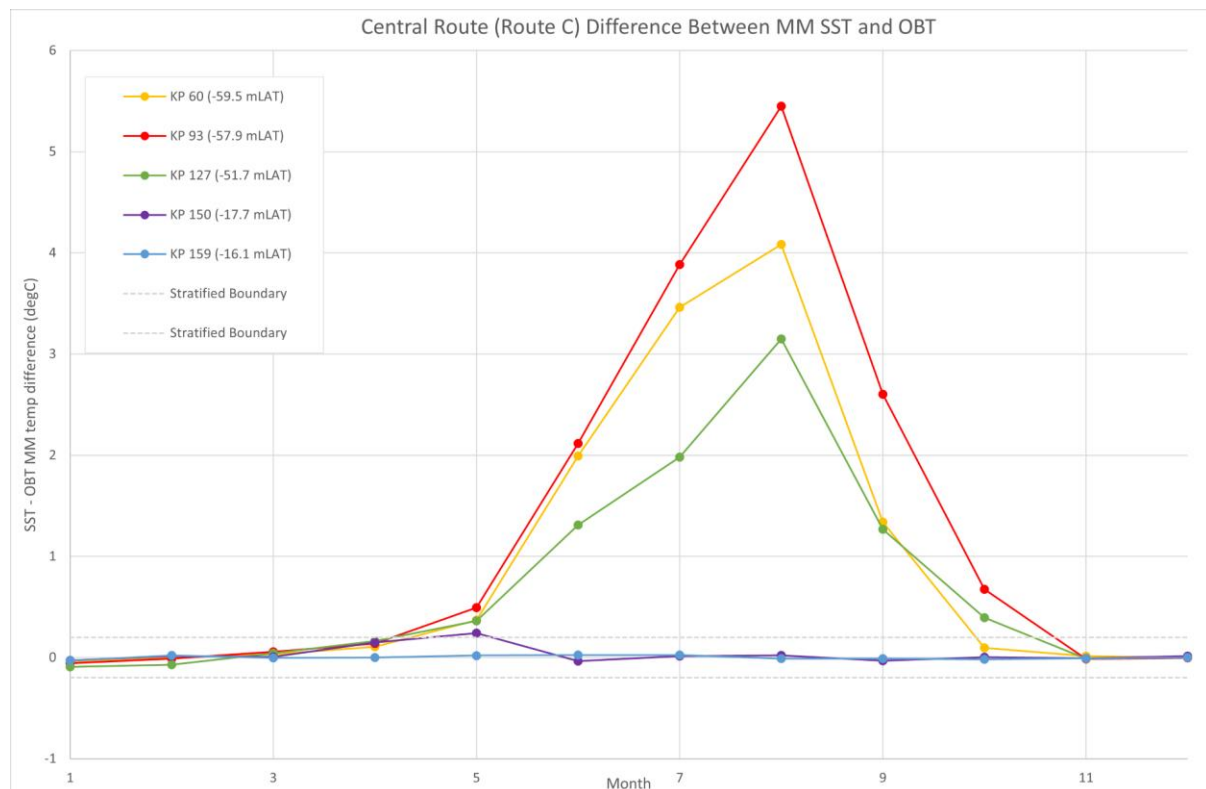
Figure 5-10: The spatial and temporal variation in difference between sea surface temperature and ocean bottom temperature from the AMM15v2 model for the Dogger Bank South cable routes and OWF, with values < 0.2 °C blanked out, showing onset of thermal stratification



**Figure 5-11: Difference between monthly mean sea surface temperature and sea surface temperature from the AMM15v2 model, at key intervals along the northernmost Dogger Bank South cable route (equivalent to Route A)**

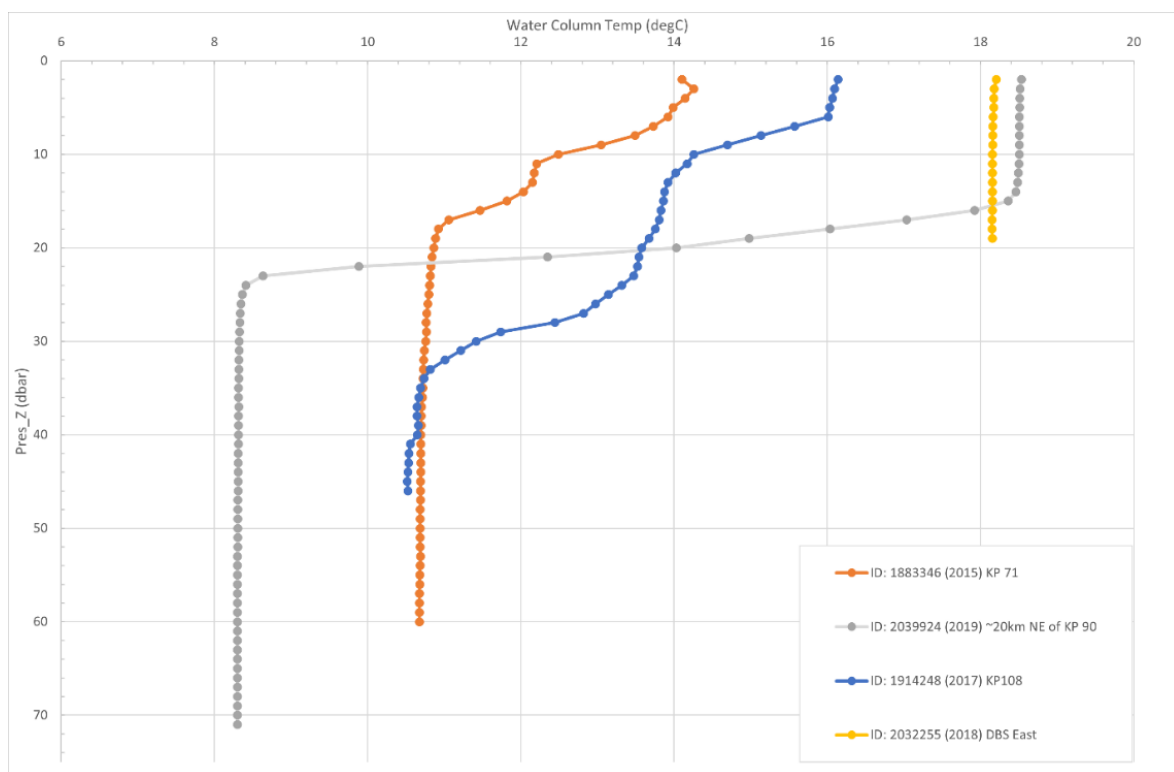


**Figure 5-12: Difference between monthly mean sea surface temperature and sea surface temperature from the AMM15v2 model, at key intervals along Route C**



By considering the water column temperature profile from recent (2015-2019) CTD casts across the area in August (the month with strongest stratification), we can better understand the stratification strength across the area (Figure 5-10 and Figure 5-13). At ~KP 71, along the northernmost ECR option, the CTD profile (1883346) shows a temperature difference from sea surface to bottom of 3.6°C. Further along the ECR at ~KP 108 (CTD 1914248), stratification is stronger still with a difference of 5.9°C within the zone previously identified as being the most strongly stratified (KP 90-110). This zone of stratification extends and strengthens to the northwest, visible in the profile of CTD 2039924 which lies ~20 km northwest of KP 90, with a strong thermocline and an SST-OBT difference of 10.2°C. In contrast, the CTD in the DBS East array area shows shallow, well-mixed water column at 18.2°C throughout, indicating no stratification. This CTD over Dogger Bank, is the highest recorded temperature value from the World Ocean Database within the survey area.

**Figure 5-13: CTD profiles taken across the general Dogger Bank South site in August (when stratification is strongest). The locations of the CTD profiles are marked in Figure 5-10**

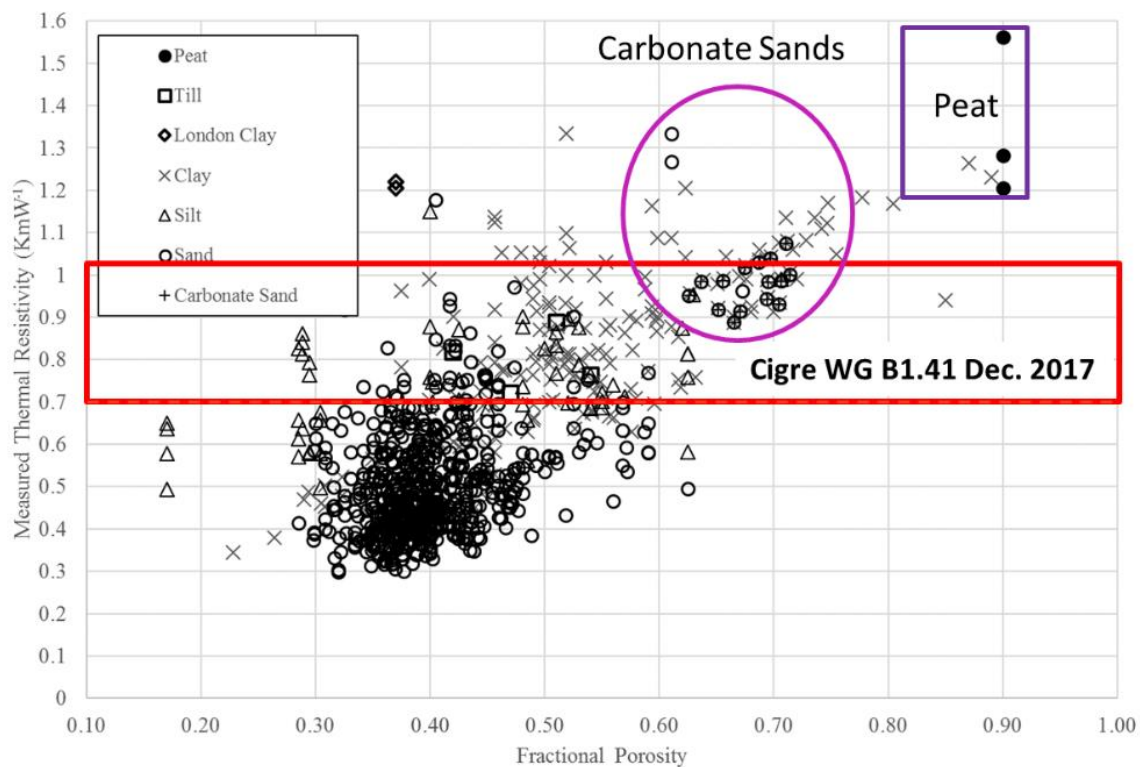


It is important to understand the effects of cable design as it facilitates a proper understanding of ambient temperature along the route for both cable design and post-installation operation. For instance over 50 km of the northernmost route will have a temperature differential of > 5.5 °C than the surface waters during the summer months. Further for those areas which are well mixed during the year, publicly available (within 24 hours of acquisition) satellite SST can provide actual measured inputs to conditional monitoring software for Real-time Thermal Rating or Burial Depth prediction. It must be remembered that these are seabed temperatures a propagation to cable depth using Fourier's Law will result in the temperatures at cable depth being ameliorated (cooler in the summer warmer in the winter) and with ~ a months lag in timing. Once the thermal properties of the sediment have been acquired across the site these can be calculated.

## 5.2. Thermal Conductivity and Thermal Resistivity Overview

The most recent, 2017, CIGRE WGB1.41 technical review (CIGRE, 2017) that dealt with the thermal resistivity of marine sediments, quoted typical values of 0.7 and 1 Km/W, in line with the IEC 60287-3-1 standards, but showing no understanding of the actual range encountered on the continental shelf. Dix *et al.* (2017) have undertaken a review of publicly and industrial thermal conductivity/resistivity (one is simply a reciprocal of the other but the site investigation community measures conductivity, whilst electrical engineers use resistivity in their designs) datasets and demonstrated that thermal resistivities (TRs) can vary from ~ 0.3 Km/W to > 1.5 Km/W, with typical quartz marine sands having TRs between 0.3 and 0.6 Km/W, carbonate sands (typically with carbonate concentrations > 50%) have TR values between 0.9 and 1.1 Km/W, marine clays varying from 0.7 – 1.2 Km/W, while the really thermally limiting materials are organic rich sediments and peats with TR values up to 1.6 Km/W (Figure 5-14).

**Figure 5-14: 1015 thermal resistivity and porosity measurements taken on marine sediments from across the globe**



Although there is a significantly greater range of thermal resistivities of typical seabed soils than generally appreciated, the thermal resistivities of landfall sites have an even higher range. This is primarily driven by the sediments not being fully saturated, either permanently or temporarily (i.e. during a tidal-cycle), this can result in thermal resistivities of >2.5 Km/W and, sometimes, significantly higher than this, making landfall sites a common thermal pinch point. Frequently, coastal landfall sites are installed in horizontal directional drilling (HDD) ducts, but often such installations do not maximise the natural thermal properties of the geology at these locations.



Thermal conductivity measurements are typically taken on retrieved samples from the seabed using a needle probe, following standards such as the ASTM D5334-14. However, care needs to be taken on sample preparation, with particularly careful consideration of saturation states (must be >80%) and sample densities, as they both can have a major effect on the thermal conductivity values recorded. Further, there is a growing move towards acquiring *in situ* measurements using either passive or active probes, but the accuracy and precision of such systems need to be well constrained. Combining *in situ* and laboratory-based measurements must be undertaken carefully, whilst the choice of statistical parameters of the analysed thermal measurements (maximum,  $P_{99}$ ,  $P_{90}$ ,  $P_{75}$ , or mean) that are actually used in the cable design needs to be carefully considered. For the same set of measurements, the use of different statistical parameters can result in up to two cable size difference in design for the same material, which equates to a significant cost differential.

Ultimately, these measurements are only of the ambient soil condition and how these may be altered during installation is an area of active research. The theoretical implications of trenching on cable properties, and hence cable rating, has been the focus of a recent Carbon Trust the outcomes of which are soon to be released.

Finally, in coarse grained seabed sediments (medium to coarse sands and coarser) the permeability of the soil (how interconnected the spaces between sediment grains are) can enhance heat dissipation by allowing convection to occur, and so more rapidly move heat away from the cables. In sediments with permeabilities  $> 1E-11 \text{ m}^2$ , this can start to become quite significant and is a useful parameter to check during any cable design process (Hughes *et al.*, 2015).

No landfall nor offshore site investigation campaign has been completed for Dogger Bank South OWF or ECCs, and no actual soil thermal data for the route and OWF is available. Therefore estimated ranges of potential thermal conductivity values for the materials likely to be encountered from the route are provided. These are sourced from a combination of an extant geodatabase, values acquired from the SOFIA site investigation works undertaken by RWE ~ 30 km to the north of the DBS area and measurements reported in the academic literature.

### 5.2.1. Thermal Data preparation

Simple, normal distribution, statistical analysis has been undertaken for on thermal conductivity measurements from both the geodatabase and the SOFIA data separately, with the calculation of a series of standard parameters for each broad sediment group. The statistics calculated are defined in Table 5-2, and visually presented as a combined box and whisker and “beeswarm” scatter plots (Figure 5-15). The beeswarm component has jitter in the X-axis added so individual data points can be clearly seen (Figure 5-15).

Outlier detection of the normally distributed data have been calculated using a classic approach to calculate “Outlier Fences” as a function of the Lower and Upper Quartiles, plus/minus the Inter-Quartile range with a multiplication factor of 1.5 (to generate “inner” or “mild” outliers) or 3 (to generate “outer” or “extreme” outliers) applied (Table 5-2). Standardly, a multiplication factor of 1.5 is used and a factor only applied if a significant number of data points exceed the “inner” outlier classification criteria. These criteria are not used to automatically exclude data but to identify data points that require further investigation and only then are data potentially excluded. For non-normal distribution data (e.g. a log-normal distribution), the outlier criteria can be determined on the

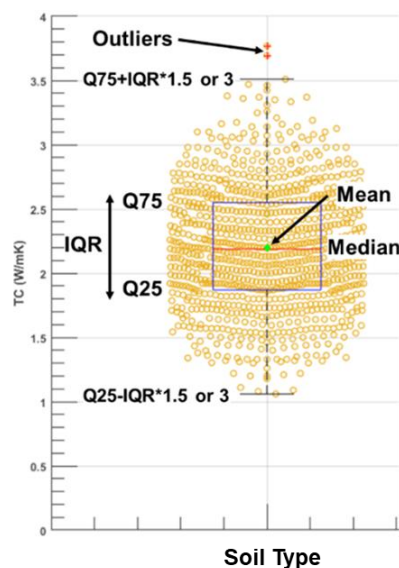
transformed (e.g. logarithms of the data) datasets and quality control undertaken on identified outliers.

As described in Section 5.2 cable design will rely on either the Maximum value or more typically P90 thermal resistivity values for more spatially restricted areas of a specific site investigation dataset. For this exercise the mean thermal conductivity values  $\pm 1$  Standard Deviations and the range of thermal conductivity values are regarded as providing a general overview of the potential thermal environment likely to be encountered along the route.

**Table 5-2: Normal Distribution Statistical Parameters used in WP2**

Statistical Definition	Definition
MAX TC (W/mK)	Maximum value
MIN TC (W/mK)	Minimum value
MEDIAN [P50] TC (W/mK)	Median, 50 <sup>th</sup> Percentile, middle value
MEAN TC (W/mK)	Mean Value
STDEV (W/mK)	Standard Deviation
P10 (W/mK)	10 <sup>th</sup> Percentile
P90 (W/mK)	90 <sup>th</sup> Percentile
Upper Quartile (UQ) (W/mK)	75 <sup>th</sup> Percentile
Lower Quartile (LQ) (W/mK)	25 <sup>th</sup> Percentile
Inter Quartile Range (IQR) (W/mK)	UQ-LQ
IQR*1.5 (W/mK)	Mild whisker magnitude
IQR*3 (W/mK)	Extreme whisker magnitude
UQ+IQR*3 (W/mK)	Extreme upper whisker threshold – outlier identification
UQ+IQR*1.5 (W/mK)	Mild upper whisker threshold – outlier identification
LQ-IQR*1.5 (W/mK)	Mild lower whisker threshold – outlier identification
LQ-IQR*3 (W/mK)	Extreme lower whisker threshold – outlier identification
N	Number of data points

**Figure 5-15: Generic combined box, whisker & beeswarm scatter plot to define statistical parameters. In cases where the Maximum or Minimum values are within the  $IQR \times 1.5$  or 3 limits the whiskers automatically snap to those real values. In this representation the whiskers represent.**



As described in Sections 3 and 4 the DBS Export Cable Corridor is likely to encounter the following deposits in the near surface (top 2 – 5 m): Holocene, post-transgressive marine Quartz Sands; Bolders Bank Formation and potentially Dogger Bank Formation glacial tills; minor exposures of Botney Cut Formation; outcropping and subcropping exposures of Lias Group Mudstones & Limestones, West Sole Group sandstones, siltstones and mudstones, Oxford Clay mudstones Corallian Group limestones, marls, sandstones, siltstones and mudstones, Kimmeridge Clay Formation mudstones, Cromer Knoll Group calcareous claystones, siltstones and marlstones and the Chalk Group. Figure 5-16 and Figure 5-17 provide combined box and whisker and beeswarm scatter plots for the thermal geodatabase and SOFIA datasets respectively, whilst Table 5-3 and Table 5-4 provided the statistics for both of these datasets split into unconsolidated materials and bedrock respectively. The thermal properties of each of these groups will be considered in turn with a box:

- Holocene, post-transgressive marine Quartz SANDS:** these deposits are found across the route either dominating the near surface sediments between ~KP 60 – the OWF footprints; thick accumulations of the nearshore and offshore sandbank systems (e.g. South Smithic Bank Complex, “The Hills”, the “Outer Bank Complex” and the “Bolders Bank Complex”) or thin < 1 m veneers over the underlying glacial deposits and/or bedrock. These quartz SANDS are the most thermally conductive materials across the site with geodatabase mean value of  $2.2 \pm 0.47$  W/mK (@ 1 STDEV) and a more constrained and higher SOFIA value of  $2.58 \pm 0.27$  W/mK (@ 1 STDEV) with a minimum and maximum of 1.92 and 3.46 W/mK respectively. The range of values is significantly higher for the marine geodatabase. Such values if actually indicative of the DBS area would suggest these deposits should represent the preferential burial medium for any offshore cable system. The equivalent mean and maximum thermal resistivity values for the SOFIA dataset are  $0.39 \pm 0.04$  Km/W (@ 1 STDEV) and 0.52 Km/W respectively which are significantly lower than the 0.7 Km/W frequently used in cable design.

Figure 5-16: Combined box, whisker & beeswarm scatter plot of a thermal conductivity geodatabase. *Whiskers are based on  $UQ+1.5*IQR$  and  $LQ-1.5*IQR$  and snapped to highest/lowest values within these.*

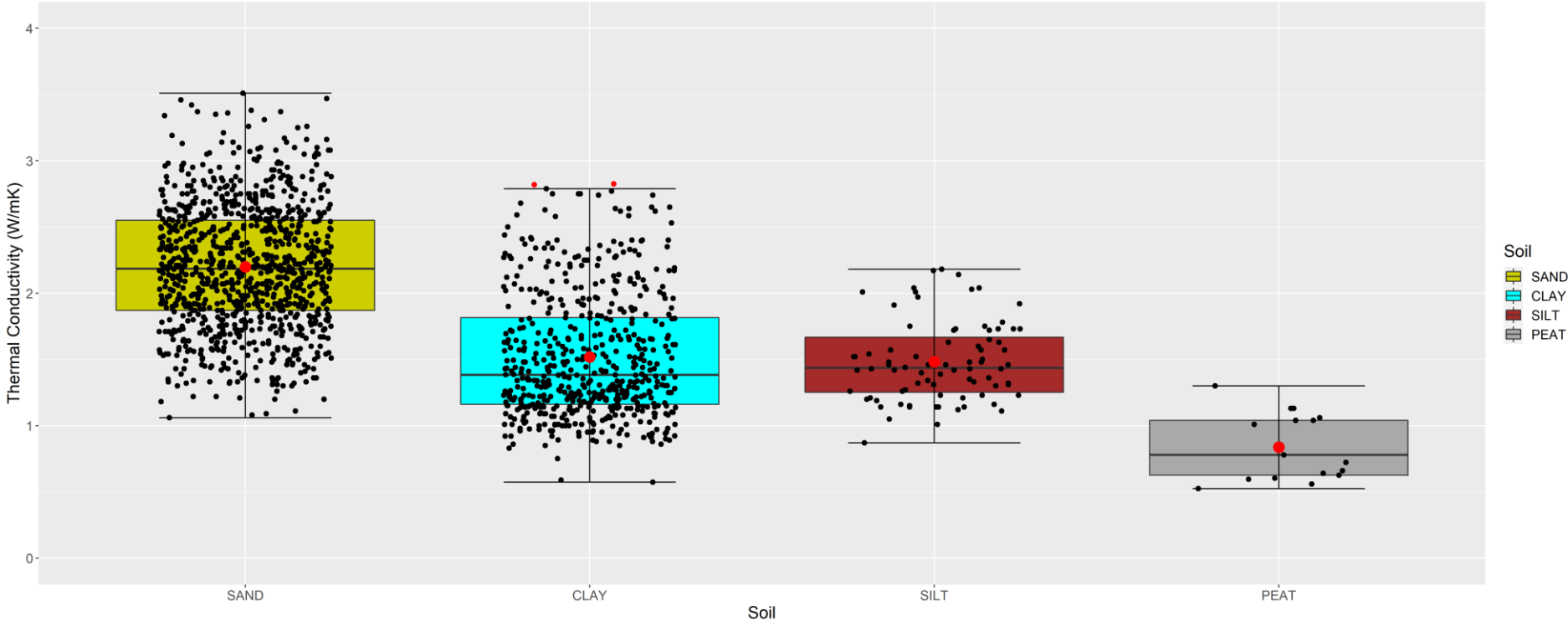
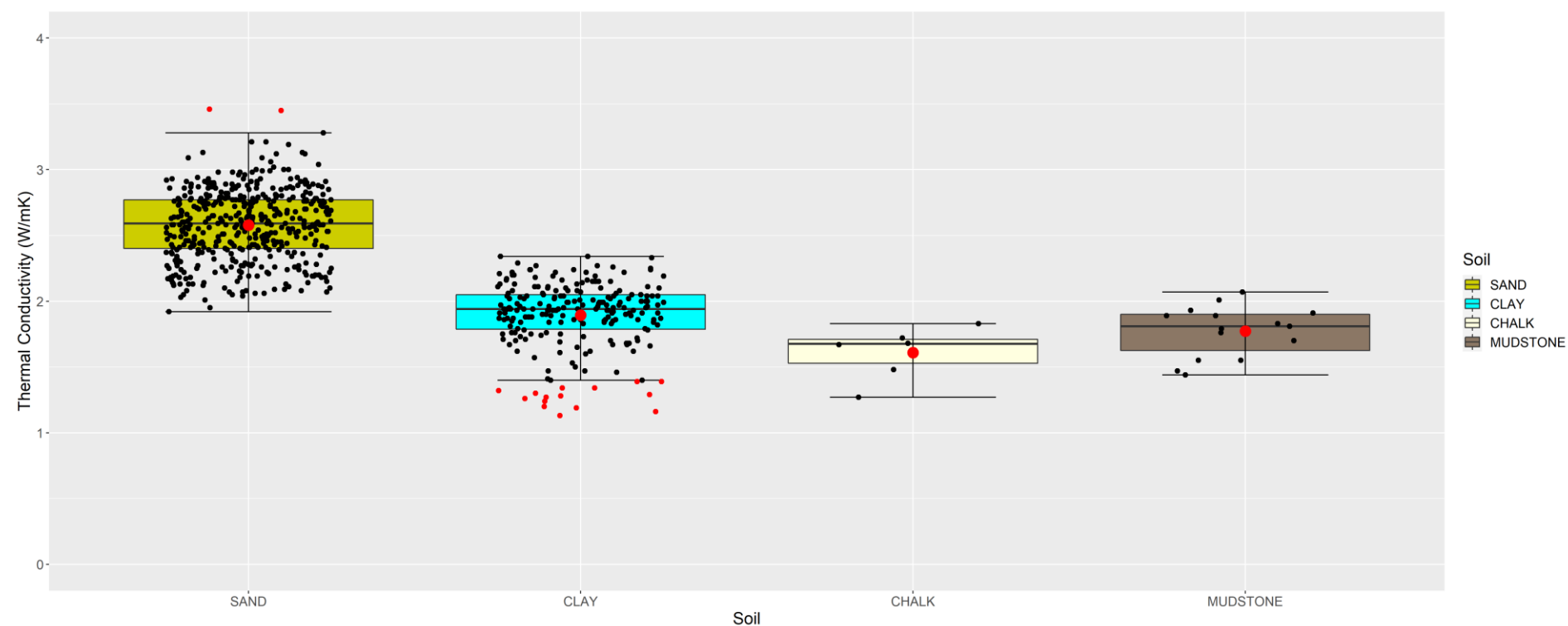


Figure 5-17: Combined box, whisker & beeswarm scatter plot of the SOFIA thermal conductivity. *Whiskers are based on  $UQ+1.5*IQR$  and  $LQ-1.5*IQR$  and snapped to highest/lowest values within these.*





**Table 5-3: Thermal Conductivity (W/mK) Geodatabase values and equivalents from the SOFIA site investigation campaign of potential sediments encountered in the Dogger Bank South area**

Statistical Definition	Database Quartz SAND	SOFIA SAND	Database CLAY	SOFIA CLAY	Database SILT	Database PEAT
MAX TC (W/mK)	3.51	3.46	2.83	2.34	2.18	1.30
MIN TC (W/mK)	1.06	1.92	0.57	1.13	0.87	0.53
MEDIAN TC (W/mK)	2.18	2.59	1.38	1.94	1.44	0.78
MEAN TC (W/mK)	2.20	2.58	1.52	1.90	1.48	0.84
STDEV (W/mK)	0.47	0.27	0.47	0.25	0.30	0.25
P10 (W/mK)	1.58	2.19	1.01	1.52	1.14	0.58
P90 (W/mK)	2.81	2.90	2.26	2.19	1.97	1.13
Upper Quartile (UQ) (W/mK)	2.55	2.40	1.81	1.79	1.67	1.04
Lower Quartile (LQ) (W/mK)	1.88	2.77	1.17	2.05	1.26	0.63
Inter Quartile Range (IQR) (W/mK)	0.67	0.37	0.65	0.26	0.41	0.42
IQR*1.5 (W/mK)	1.01	0.56	0.97	0.39	0.62	0.63
IQR*3 (W/mK)	2.02	1.11	1.95	0.79	1.24	1.25
UQ+IQR*3 (W/mK)	4.57	3.88	3.76	2.84	2.92	2.29
UQ+IQR*1.5 (W/mK)	3.56	3.33	2.79	2.44	2.29	1.67
LQ-IQR*1.5 (W/mK)	0.87	1.85	0.19	1.39	0.63	0
LQ-IQR*3 (W/mK)	0	1.29	0	1.00	0.01	0
N	980	451	562	216	80	17

- **CLAY rich glacial tills of the Bolders Bank Formation and potentially the Dogger Bank Formation:** deposits of the Bolders Bank formation dominate the near surface seabed deposits across most of the route until ~KP 60, excluding where they are overlain by the South Smithic Bank complex SANDS and where they pinch out associated with bedrock coming to the surface between ~KP 33 – ~KP 45. Beyond this they are still identified at depth but under a varying thickness of the Quartz marine sands and would need only to be considered if a deeper depth of lowering  $\sim > 2$  m would be required. These deposits probably pinch out at the bank margin being replaced by similar deposits, of the Dogger Bank Formation, which are probably encountered in the ridge and runnel systems that cross the OWF area.

Both of these deposits are characterised as CLAY-rich glacial tills with laterally discontinuous SAND horizons with the primary difference being the presence of clasts in the Bolders Bank Formation and which are absent in the Dogger Bank Formation Deposits. From the marine geodatabase CLAYS have a mean thermal conductivity of  $1.52 \pm 0.47$  W/mK (@ 1 STDEV) and a more constrained and again higher SOFIA mean value of  $1.90 \pm 0.25$  W/mK (@ 1 STDEV) the latter with a minimum and maximum value of 1.13 and 2.34 W/mK respectively. As can be seen from Figure 5-16 and Figure 5-17 these values are consistently lower than the stratigraphically younger Quartz SANDS in both sets of data. There is overlap between the SAND and CLAY thermal conductivities in both cases and this is almost certainly in response to misidentification of the lithologies by the original measurement laboratories. However, the offset is real. In case of the SOFIA measurements which are also derived from similar deposits further north it may well reflect sampling of mixed bimodal deposits associated with the tills.

The equivalent mean and maximum thermal resistivity values for the SOFIA dataset are  $0.54 \pm 0.09$  Km/W (@ 1 STDEV) and 0.88 Km/W respectively. For such CLAY rich deposits these are regarded as being quite low and again are significantly lower than the 0.7 Km/W frequently used in cable design. It would therefore be important to ensure that these deposits are sufficiently sampled during the subsequent site investigation campaign to ensure confidence in designing to these values.

- **Botney Cut Formation:** these essentially channel fill deposits of clays, silts and interbedded sands but frequently with high organic concentrations. Buried channel sequences have been identified within the Fugro seismic interpretation, occurring along Zone 2 Corridor 4 parallel to the southern margin of the DBS West OWF. These are the only deposits that have the potential to have high organic contents, and potentially the development of PEAT, which in turn has very low thermal conductivities. No similar deposits were identified along the SOFIA route but values from the geodatabase provide mean PEAT thermal conductivities of  $0.84 \pm 0.25$  W/mK (@ 1 STDEV) significantly lower than the other sediments described so far. The equivalent mean and maximum thermal resistivity values for the SOFIA dataset are  $1.29 \pm 0.37$  Km/W (@ 1 STDEV) and 1.9 Km/W respectively. These are therefore clear thermal limiters and it is important to establish from both the full ground model and the in situ / laboratory sampling their presence and if appropriate distribution as mitigation may be necessary.

- Jurassic Mudstones, siltstones, limestones and sandstones:** there are no measurements within the extant marine geodatabase for bedrock materials, however 15 measurements were taken on mudstones along the SOFIA export cable corridor and these do represent potential lateral correlatives of the mudstone rocks identified along the DBS export cable corridor. Table 5-4 provides the statistics for these samples with a mean thermal conductivity of  $1.77 \pm 0.19$  W/mK (@ 1 STDEV). Values from the UK literature are: Lias Mudstones  $1.80 \pm 1.1$  (n = 37: Bloomer, 1981a) and  $1.27 \pm 0.03$  W/mK (n = 11: Bloomer, 1981b); Oxford Clay Mudstones:  $1.57 \pm 0.03$  (n = 11: Bloomer, 1981a) and  $1.56 \pm 0.09$  W/mK (n = 27: Bloomer, 1981b); Kimmeridge Clay Mudstones:  $1.51 \pm 0.09$  (n = 58: Bloomer, 1981a) and  $1.28 \pm 0.04$  W/mK (n = 27: Bloomer, 1981b). Finally, in situ thermal response tests (which frequently give slightly higher effective thermal conductivities than needle probe measurements on retrieved samples gave a range for Upper Jurassic to Lower Cretaceous mudrocks of 1.43-2.21 (n=5: Banks et al., 2013). These measurements tend to be higher as they may capture advection through groundwater flow which will increase the measured thermal conductivity. These data give a range of values from 1.28 – 1.80 W/mK with the mudstones of SOFIA fitting towards the top end of this. A single measurement of a limestone bed was made from the SOFIA site and this had a thermal conductivity of 1.53 W/mK so within the range of mudstone rocks. This represents a thermal resistivity range of 0.56 - 0.78 Km/W so comparable with the CLAY rich glacial deposits but with some end member components of potentially higher thermal values. If it is decided to actually trench in to these mudrocks these thermal properties will need to be determined, however, installation in cut bedrock can frequently result in a very different thermal environments (e.g. mixed backfill with higher thermal conductivity SANDS; increased permeability and hence heat dissipation due to cutting process) that would need to be considered.
- Cretaceous Chalk:** there are no measurements in the marine geodatabase but 6 measurements were taken on Chalk samples from the SOFIA export cable. Table 5-4 provides the statistics for these samples with a mean thermal conductivity of  $1.61 \pm 0.20$  W/mK (@ 1 STDEV). Values from the UK literature are  $1.79 \pm 0.54$  (n = 41: Rollins, 1987) with Banks et al (2013) quoting a range from ~1.7 – 2 W/mK from thermal response tests. With thermal resistivities of 0.5 – 0.62 W/mK these do not represent thermal limiters to cable design. As with the mudstone rocks post-installation conductivity and permeability changes do need to be taken into consideration once actual route specific measurements have been taken.

### 5.2.1.1. Conclusions

These database and literature derived estimates provide a set of framing thermal values for the very initial stages of cable design, however, these would not be sufficient for a full cable design. A site investigation sampling campaign should still be undertaken taking targeted measurements from the 5 broad lithological groups described here. Sampling strategies would be different for each group. The Holocene marine SANDS would best be sampled by in situ thermal measurements by either a passive or active thermal conductivity probe in tandem with a number of co-located samples (from vibrocores or boreholes) to assess the accuracy and precision of the 2 techniques. The CLAY rich tills of the glacial till sequences will be challenging to measure in situ, particularly with a passive system,

due to the difficulties in being able to generate a sufficient temperature differential for thermal conductivity calculations, these therefore would be best sampled and measured in the laboratory but with careful consideration of the stratigraphy to ensure fine scale layering and/or bimodal deposits are properly sampled. As the potential of the Botney Cut Formation being a thermal limiter is high (due to the potential presence of high organic concentration soils and PEATS) full reference to the ground model needs to be taken and any potential high amplitude anomalies or clearly channel fill deposits need to be accurately sampled. Depending on the installation strategy for those areas with bedrock outcrop representative sites need to be sampled and measured in the laboratory.

As discussed in Section 4.1.1 the landfall site is always considered a thermal limiter. The stratigraphy of both potential landfall sites is dominated by Skipsea Tills with overlying beach sands and Chalk at depth (typically > 15 m). The Chalk has the potential to support higher effective thermal conductivities due to fast groundwater flows but speeds are spatially variable (Section 1.1.1.1) and so the potential for using this effect would require in situ measurement. However, if higher flow rates are present they could significantly contribute to mitigating against the increased temperatures typically anticipated at depth.

If HDD drilling is considered through the Skipsea till sequences, in situ sampling of the thermal properties of the cliff deposits, as well as cores at depth, could rapidly establish the thermal conductivity values for the area and cheaply add to the database of measurements for the Bolders Bank Formation (its offshore correlative). There is no doubt, for the southern landfall route at least the presence of highly friable SAND lenses within the CLAY rich tills would have more thermally preferable properties but the spatial variation of the geometry of these deposits would make utilising them along an entire HDD section challenging if not impossible. Shallowing trenching within the beach deposits could be considered but at present there is no information available on the thickness of these deposits.

Table 5-4: Standard statistical parameters calculated for each soil classification

Statistical Definition	CHALK	MUDSTONE
MAX TC (W/mK)	1.83	2.07
MIN TC (W/mK)	1.27	1.44
MEDIAN TC (W/mK)	1.68	1.81
MEAN TC (W/mK)	1.61	1.77
STDEV (W/mK)	0.20	0.19
P10 (W/mK)	1.38	1.50
P90 (W/mK)	1.78	1.98
Upper Quartile (UQ) (W/mK)	1.53	1.63
Lower Quartile (LQ) (W/mK)	1.71	1.90
Inter Quartile Range (IQR) (W/mK)	0.18	0.28
IQR*1.5 (W/mK)	0.27	0.41
IQR*3 (W/mK)	0.55	0.83
UQ+IQR*3 (W/mK)	2.26	2.73
UQ+IQR*1.5 (W/mK)	1.98	2.31
LQ-IQR*1.5 (W/mK)	1.25	1.21
LQ-IQR*3 (W/mK)	0.98	0.80
N	6	15

### 5.3. Post-Installation Depth of Cover Changes

Only ~30% of the Export Cable Corridor Fugro swath bathymetry data crosses an extant swath bathymetry dataset from extant sources. However the distribution of these overlapping datasets is not evenly distributed. Zone 1 CB route sections 1, 2 and 5 have ~50-52% multiple survey coverage whilst CB route 7 has ~70.5% multiple coverage. By comparison Zone 2 Corridors 1-3 and 6 (which



also has no Fugro swath bathymetry data) have no independent data and so bed level change can only be inferred from the single time step data. Zone 2 Corridors 4 and 5 overlap with the HI1590 and HI1714 Admiralty surveys on the margin of the Dogger Bank providing ~28.5 and 17% multiple survey coverage respectively. Similarly, of the DBS OWF footprint 47.3% is covered by two extant Admiralty surveys (HI1590 and HI1714) however due to the nature of the coarse corridor grids of the Fugro data over the site only ~9.8% has had the potential for bed level change assessment (note this also includes a small percentage of overlap between the Fugro OWF coarse grids and the Gardline Geosurvey, Zone 3, Tranche B, reconnaissance surveys).

The detail of these bed level change analyses is provided in Sections 4.1.2 and 4.1.3 however it can be summarised as follows:

- For the export cable corridors there is very limited evidence of bed level change over the last decade and more confidently over the last 2 years. There is minor evidence of bed level change associated with the eastern margin of the South Smithic Bank complex with change up to  $\pm 0.6$  m related to bank margin perpendicular erosion features and minor bedforms;
- The seabed dominated by the Bolders Bank Formation deposits effectively shows no bed level change with the first ~34 km of the main north and south routes having bed level change over a 6 year period of within  $\pm 0.2$  m (effectively within survey error). The limited amount of movement is also supported by the presence of only very localised scour around shipwrecks. The one exception to this is a small amount ( $< 0.3$  m) of accumulation on the western margin of the shore parallel glacial ridges;
- From ~KP 34 on the northern and southern routes no time-lapse bathymetry exists. There is the abundant presence of a range of bedform features, from small to very large subaqueous dunes, and including parasitic forms. Evidently the bed has been in motion at some time in its history but it is not clear if some or all of these are currently moribund. The exposure of the Langede Gas Pipeline from the Sliepner riser to Easington (~KP 52.5 on Zone 1 CB Route 7) currently shows no evidence at all of backfilling and so suggesting this moribund interpretation is correct. With these offshore bedforms starting to appear in water depths of ~55 m they are likely to experience only weaker tidal currents and the impact from major storms. If active sediment transport is occurring the bedform asymmetry strongly infers there would be north to north-westerly movement. The small scale bedforms on the shallower sections of some of the sandbanks have the greater potential for mobility as at significantly shallower water depths although this needs to be proved;
- The major evidence of mobility is associated with the sorted bedforms, both larger scale ridge and runnel and smaller scale rippled scour depressions which are found extensively along the southern margin of the Dogger Bank. The ridge and runnel features over the 1 year period for which there is data do not show major change but measurements from elsewhere on the Dogger Bank and at other sites across the North-west European Shelf would suggest that although they are stable at the gross levels the margins can fluctuate their position at the decametre level resulting in vertical bed level change at the  $\sim < 1$  m level. The rippled scour depressions are seen to be active even over the 1-2 year time steps available for analysis with scouring of up to 1 m being identified along with localised decimetre accumulations. Again these RSDs occur within fields but individual features do not

necessarily migrate but appear and disappear within each field. The impact of existing structures can clearly be seen on the Cygnus A to Cygnus B gas pipeline (Figure 4-37).

### **5.3.1. Conclusions**

In summary, large sections of the route show limited evidence of bed level change based on the available evidence and the current understanding of the sediment transport regime. Certainly, for the first ~ 60 kilometres of the export cable corridors sediment movement appears to be limited and where it does occur very localised. The large section of the route with only one swath bathymetry dataset is covered does have abundant evidence of bedforms at all scales but whether these are currently active is not easily demonstrated. Indeed, the limited evidence available to date suggests they could be moribund. This hypothesis needs to be confirmed through both sediment transport modelling (the currently available models only extend along the first ~50 Km of the cable. Finally, mobility associated with the sorted bedforms prevalent on the Dogger Bank and covering large sections of the DBS OWF footprint are the primary sources of bed level change and this will need to be considered fully in the design of the inter-array cables and the latter sections of the export cable.

## 6. References

Anthony, D. and Leth, J.O., 2002. Large-scale bedforms, sediment distribution and sand mobility in the eastern North Sea off the Danish west coast. *Marine Geology*, 182(3-4), pp.247-263.

Ashley, G. M. et al., 1990. Classification of large-scale subaqueous bedforms - A new look at an old problem. *Journal Of Sedimentary Research*, Volume 60, pp. 160-172. 16 pp.

Autret, E., Prevost, C. and Piolle, J-F, 2021. QUID for High Resolution SST analysis over the European North West shelf/Iberia Biscay Irish Seas. SST\_ATL\_SST\_L4\_NRT\_OBSERVATIONS\_010\_025

Bateman, M., Evans, D., Buckland, P., Connell, E., Friend, R., Hartmann, D., Moxon, H., Fairburn, W., Panagiotakopulu, E. and Ashurst, R., 2015. Last glacial dynamics of the Vale of York and North Sea lobes of the British and Irish Ice Sheet. *Proceedings of the Geologists' Association*, 126(6), pp.712-730.

Bateman, M., Evans, D., Roberts, D., Medialdea, A., Ely, J. and Clark, C., 2018. The timing and consequences of the blockage of the Humber Gap by the last British–Irish Ice Sheet. *Boreas*, 47(1), pp.41-61.

Banks, D., Withers, J.G., Cashmore, G. and Dimelow, C., 2013, August. An overview of the results of 61 in situ thermal response tests in the UK. *Quarterly Journal of Engineering Geology and Hydrogeology*, 46, 281-291.

Barron, A.J.M., Lott, G.K. and Riding, J.B., 2012. Stratigraphical framework for the Middle Jurassic strata of Great Britain and the adjoining continental shelf. British Geological Survey.

Bloomer, J.R., 1981. Thermal conductivities of mudrocks in the United Kingdoms. *Quarterly Journal of Engineering Geology*, 14(4), pp.357-362.

Boston, C., Evans, D. and Cofaigh, C., 2010. Styles of till deposition at the margin of the Last Glacial Maximum North Sea lobe of the British–Irish Ice Sheet: an assessment based on geochemical properties of glacial deposits in eastern England. *Quaternary Science Reviews*, 29(23-24), pp.3184-3211.

Bradley, S.L., Milne, G.A., Shennan, I. and Edwards, R., 2011. An improved glacial isostatic adjustment model for the British Isles. *Journal of Quaternary Science*, 26(5), pp.541-552.

British Geological Survey, 2002a. *North Sea Geology*. Strategic Environmental Assessment – SEA2 & SEA3.

British Geological Survey, 2022b. *BGS GeoIndex Offshore WMS*, electronic dataset, viewed 17 June 2022.

British Geological Survey, 2022c. *BGS GeoIndex Onshore WMS*, electronic dataset, viewed 17 June 2022.

Burningham, H. and French, J., 2008. 'Historical changes in the seabed of the greater Thames estuary'. The Crown Estate, 54 pp., ISBN: 978-1-906410-04-9

Burningham, H. and French, J.R., 2009. Seabed mobility in the greater Thames estuary. The Crown Estate, 62 pp. ISBN: 978-1-906410-09-4

Burningham, H., French, J.R. (2017). Evaluating potential hazards to seafloor infrastructure associated with submarine morphodynamics. CERU Report No. 1711-1, The Crown Estate, 51pp.

Busfield, M., Lee, J., Riding, J., Zalasiewicz, J. and Lee, S., 2015. Pleistocene till provenance in east Yorkshire: reconstructing ice flow of the British North Sea Lobe. *Proceedings of the Geologists' Association*, 126(1), pp.86-99.

Cameron, T., Crosby, A., Balson, P., Jeffrey, D., Lott, G., Bulat, J. and Harrison, D., 1992. *The Geology of the southern North Sea*. London: Her Majesty's Stationery Office for the British Geological Survey.

Castedo, R., de la Vega-Panizo, R., Fernández-Hernández, M. and Paredes, C., 2015. Measurement of historical cliff-top changes and estimation of future trends using GIS data between Bridlington and Hornsea – Holderness Coast (UK). *Geomorphology*, 230, pp.146-160.

Chadha, D., n.d. *Saline intrusion in the chalk aquifer of North Humberside*. York: Yorkshire Water Authority.

CIGRE WGB1.35, 2015. *A guide for rating calculations of insulated cables*, s.l.: s.n.

Clark, C., Ely, J., Greenwood, S., Hughes, A., Meehan, R., Barr, I., Bateman, M., Bradwell, T., Doole, J., Evans, D., Jordan, C., Monteys, X., Pellicer, X. and Sheehy, M., 2018. BRITICE Glacial Map, version 2: a map and GIS database of glacial landforms of the last British-Irish Ice Sheet. *Boreas*, 47(1), pp.11-e8.

Clark, C.D., Ely, J.C., Hindmarsh, R.C., Bradley, S., Ignéczki, A., Fabel, D., Ó Cofaigh, C., Chiverrell, R.C., Scourse, J., Benetti, S. and Bradwell, T., 2022. Growth and retreat of the last British–Irish Ice Sheet, 31 000 to 15 000 years ago: the BRITICE-CHRONO reconstruction. *Boreas*, 51(4), pp.699-758.

Coco, G., Murray, A.B., Green, M.O., Thieler, E.R. and Hume, T.M., 2007. Sorted bed forms as self-organized patterns: 2. Complex forcing scenarios. *Journal of Geophysical Research: Earth Surface*, 112(F3).

Cotterill, C., Phillips, E., James, L., Forsberg, C., Tjelta, T., Carter, G. and Dove, D., 2017a. The evolution of the Dogger Bank, North Sea: A complex history of terrestrial, glacial and marine environmental change. *Quaternary Science Reviews*, 171, pp.136-153.

Cotterill, C., Phillips, E., James, L., Forsberg, C. and Tjelta, T., 2017b. How understanding past landscapes might inform present-day site investigations: a case study from Dogger Bank, southern central North Sea. *Near Surface Geophysics*, 15(4), pp.403-414.

De Boyer Montégut, C., Madec, G., Fischer, A.S., Lazar, A. and Iudicone, D., 2004. Mixed layer depth over the global ocean: An examination of profile data and a profile-based climatology. *Journal of Geophysical Research: Oceans*, 109(C12).

Deschamps, P., Durand, N., Bard, E., Hamelin, B., Camoin, G., Thomas, A.L., Henderson, G.M., Okuno, J.I. and Yokoyama, Y., 2012. Ice-sheet collapse and sea-level rise at the Bølling warming 14,600 years ago. *Nature*, 483(7391), pp.559-564.

Diesing, M., Kubicki, A., Winter, C. and Schwarzer, K., 2006. Decadal scale stability of sorted bedforms, German Bight, southeastern North Sea. *Continental Shelf Research*, 26(8), pp.902-916.

Dix, J.K., 2021. Reference Bed Level Review, SOFIA Offshore windfarm

Dix, J., Hughes, T., Emeana, C., Pilgrim, J., Henstock, T., Gernon, T., Thompson, C. and Vardy, M. Substrate controls on the life-time performance of marine HV cables. Offshore Site Investigation Geotechnics 8<sup>th</sup> International Conference Proceeding. 2017. Society for Underwater Technology, pp.88-107.

Dong, Y., McCartney, J. and Lu, N., 2015. Critical Review of Thermal Conductivity Models for Unsaturated Soils. *Geotechnical and Geological Engineering*, 33(2), pp.207-221.

Dove, D., Evans, D., Lee, J., Roberts, D., Tappin, D., Mellett, C., Long, D. and Callard, S., 2017. Phased occupation and retreat of the last British–Irish Ice Sheet in the southern North Sea; geomorphic and seismostratigraphic evidence of a dynamic ice lobe. *Quaternary Science Reviews*, 163, pp.114-134.

East Riding of Yorkshire Council, 2022. Beach profile drawings, electronic data, viewed 5 August 2022.

Elliot, T., Chadha, D.S. and Younger, P.L., 2001. Water quality impacts and palaeohydrogeology in the Yorkshire Chalk aquifer, UK. *Quarterly journal of engineering geology and hydrogeology*, 34(4), pp.385-398.

Emery, A., Hodgson, D., Barlow, N., Carrivick, J., Cotterill, C., Mellett, C. and Booth, A., 2019a. Topographic and hydrodynamic controls on barrier retreat and preservation: An example from Dogger Bank, North Sea. *Marine Geology*, 416, p.105981.

Emery, A., Hodgson, D., Barlow, N., Carrivick, J., Cotterill, C. and Phillips, E., 2019b. Left High and Dry: Deglaciation of Dogger Bank, North Sea, Recorded in Proglacial Lake Evolution. *Frontiers in Earth Science*, 7.

Environment Agency, 2017. *LIDAR Composite DTM 2017 – 1m*, electronic dataset, viewed 15 June 2022.

Environment Agency, 2020. *LIDAR Composite DTM 2020 – 1m*, electronic dataset, viewed 15 June 2022.

Evans, D. and Thomson, S., 2010. Glacial sediments and landforms of Holderness, eastern England: A glacial depositional model for the North Sea Lobe of the British–Irish Ice Sheet. *Earth-Science Reviews*, 101(3-4), pp.147-189.

Evans, D., Roberts, D., Bateman, M., Clark, C., Medialdea, A., Callard, L., Grimoldi, E., Chiverrell, R., Ely, J., Dove, D., Ó Cofaigh, C., Saher, M., Bradwell, T., Moreton, S., Fabel, D. and Bradley, S., 2021. Retreat dynamics of the eastern sector of the British–Irish Ice Sheet during the last glaciation. *Journal of Quaternary Science*, 36(5), pp.723-751.



Ferrini, V.L. and Flood, R.D., 2006. The effects of fine-scale surface roughness and grain size on 300 kHz multibeam backscatter intensity in sandy marine sedimentary environments. *Marine Geology*, 228(1-4), pp.153-172.

Gale, I. and Rutter, H., 2006. *The Chalk aquifer of Yorkshire*. British Geological Survey Research Report RR/06/04. Keyworth, Nottingham: British Geological Survey.

Goff, J. A., Mayer, L. A., Traykovski, P., Buynevich, I., Wilkens, R., Raymond, R., Glang, G., Evans, R. L., Olson, H. and Jenkins, C. 2005. Detailed investigation of sorted bedforms, or “rippled scour depressions,” within the Martha’s Vineyard Coastal Observatory, Massachusetts. *Continental Shelf Research*, 25: pp. 461-484.

Hernandez Colin, M. A., Dix, J. & Pilgrim, J., 2021. Export cable rating optimisation by wind power ramp and thermal risk estimation. *IET Renewable Power Generation*, 15(7).

Hogarth, P., Hughes, C.W., Williams, S.D.P. and Wilson, C., 2020. Improved and extended tide gauge records for the British Isles leading to more consistent estimates of sea level rise and acceleration since 1958. *Progress in Oceanography*, 184, p.102333.

HR Wallingford, The Centre for Environment, Fisheries and Aquaculture Science, University of East Anglia, Posford Haskoning and B. D’Olier, 2002. *Southern North Sea Sediment Transport Study, Phase 2*. Sediment Transport Report.

Hughes, T. J., Henstock, T. J., Pilgrim, J. A., Dix, J. K., Gernon, T. M. and Thompson, C. E. 2015. Effect of sediment properties on the thermal performance of submarine HV cables. *IEEE Transactions on Power Delivery*, 30: pp. 2443-2450.

Kenyon, N.H., Belderson, R.H., Stride, A.H. and Johnson, M.A., 1981. Offshore tidal sand-banks as indicators of net sand transport and as potential deposits. *Holocene Marine Sedimentation in the North Sea Basin*, pp.257-268.

Kuchar, J., Milne, G., Hubbard, A., Patton, H., Bradley, S., Shennan, I. and Edwards, R., 2012. Evaluation of a numerical model of the British–Irish ice sheet using relative sea-level data: implications for the interpretation of trimline observations. *Journal of Quaternary Science*, 27(6), pp.597-605.

Leatherman, S.P., 1990. Modelling shore response to sea-level rise on sedimentary coasts. *Progress in physical geography*, 14(4), pp.447-464.

Lee, E., 2011. Reflections on the decadal-scale response of coastal cliffs to sea-level rise. *Quarterly Journal of Engineering Geology and Hydrogeology*, 44(4), pp.481-489

Lee, J., Busschers, F. and Sejrup, H., 2012. Pre-Weichselian Quaternary glaciations of the British Isles, The Netherlands, Norway and adjacent marine areas south of 68°N: implications for long-term ice sheet development in northern Europe. *Quaternary Science Reviews*, 44, pp.213-228..

Lee, E.M. and Clark, A.R., 2002. *Investigation and management of soft rock cliffs*. Thomas Telford.

Liu, S., Goff, J. A., Flood, R. D., Christensen, B., Austin, J. A. and Walsh, J. P. 2018. Sorted bedforms off Western Long Island, New York, USA: Asymmetrical morphology and twelve-year migration record. *Sedimentology*, 65: pp. 2202-2222.

- MacDonald, A. and Allen, D., 2001. Aquifer properties of the Chalk of England. *Quarterly Journal of Engineering Geology and Hydrogeology*, 34(4), pp.371-384.
- Mathiesen, M. and Nygaard, E. 2010. Dogger Bank Wind Power Sites Metocean Design Basis. Statoil Report PTM MMG MGE RA 63, Rev no 1, June 2010, 129pp.
- Mathiesen, M., Nygaard, E. and Andersen, O.J. 2011. Dogger Bank Wind Power Sites Metocean Design Basis. Statoil Report PTM MMG MGE RA 63, Rev no 3, October, 2011, 129pp
- Mazières, A., Gillet, H., Idier, D., Mulder, T., Garlan, T., Mallet, C., Marieu, V. and Hanquiez, V., 2015. Dynamics of inner-shelf, multi-scale bedforms off the south Aquitaine coast over three decades (Southeast Bay of Biscay, France). *Continental Shelf Research*, 92, pp.23-36.
- Montreuil, A. and Bullard, J., 2012. A 150-year record of coastline dynamics within a sediment cell: Eastern England. *Geomorphology*, 179, pp.168-185.
- Murray, A. B. and Thieler, E. R. 2004. A new hypothesis and exploratory model for the formation of large-scale inner-shelf sediment sorting and “rippled scour depressions”. *Continental Shelf Research*, 24: pp. 295-315.
- National Network of Regional Coastal Monitoring Programmes, 2018. *National Coastal Monitoring – Storm Catalogue*. [online] Coastalmonitoring.org. Available at: <<https://coastalmonitoring.org/ccoresources/stormcatalogue/>> [Accessed 2 August 2022].
- Ordnance Survey, 2022. *OS Terrain 50*, electronic dataset, viewed 9 June 2022.
- Phillips, E., Cotterill, C., Johnson, K., Crombie, K., James, L., Carr, S. and Ruiter, A., 2018. Large-scale glacetectonic deformation in response to active ice sheet retreat across Dogger Bank (southern central North Sea) during the Last Glacial Maximum. *Quaternary Science Reviews*, 179, pp.24-47.
- Phillips, E., Johnson, K., Ellen, R., Plenderleith, G., Dove, D., Carter, G., Dakin, N. and Cotterill, C., 2022. Glacetectonic evidence of ice sheet interaction and retreat across the western part of Dogger Bank (North Sea) during the Last Glaciation. *Proceedings of the Geologists’ Association*, 133(1), pp.87-111.
- Pye, K. and Blott, S., 2015. Spatial and temporal variations in soft-cliff erosion along the Holderness coast, East Riding of Yorkshire, UK. *Journal of Coastal Conservation*, 19(6), pp.785-808.
- Quinn, J., Philip, L. and Murphy, W., 2009. Understanding the recession of the Holderness Coast, east Yorkshire, UK: a new presentation of temporal and spatial patterns. *Quarterly Journal of Engineering Geology and Hydrogeology*, 42(2), pp.165-178.
- Renshaw, R., Wakelin, S., Goldbeck, I. and O’Dea, E., 2021. QUID for NWS MFC Reanalysis (Physical). NWSHELF\_MULTIYEAR\_PHY\_004\_009, 74 pp.
- Roberts, D., Evans, D., Callard, S., Clark, C., Bateman, M., Medialdea, A., Dove, D., Cotterill, C., Saher, M., Cofaigh, C., Chiverrell, R., Moreton, S., Fabel, D. and Bradwell, T., 2018. Ice marginal dynamics of the last British-Irish Ice Sheet in the southern North Sea: Ice limits, timing and the influence of the Dogger Bank. *Quaternary Science Reviews*, 198, pp.181-207.

Rollin, K.E., 1987. Catalogue of geothermal data for the land area of the United Kingdom. Third revision: April 1987. Investigation of the Geothermal Potential of the UK.

Shennan, I., Bradley, S. and Edwards, R., 2018. Relative sea-level changes and crustal movements in Britain and Ireland since the Last Glacial Maximum. *Quaternary Science Reviews*, 188, pp.143-159.

Shennan, I., Bradley, S., Milne, G., Brooks, A., Bassett, S. and Hamilton, S., 2006. Relative sea-level changes, glacial isostatic modelling and ice-sheet reconstructions from the British Isles since the Last Glacial Maximum. *Journal of Quaternary Science: Published for the Quaternary Research Association*, 21(6), pp.585-599.

Soulsby, R., 1997. *Dynamics of Marine Sands*. S.I.:Thomas Telford Services Limited.

Sumbler, M.G., 1999. The stratigraphy of the Chalk Group in Yorkshire and Lincolnshire.

Tonani, M., Bruciaferri, D., Pequignet, C., King R., Sykes, P., McConnell, N. and Siddorn, J., 2021. QUID for NWS MFC Products. NORTHWESTSHELF\_ANALYSIS\_FORECAST\_PHY\_004\_013. 48 pp.

Törnqvist, T.E. and Hijma, M.P., 2012. Links between early Holocene ice-sheet decay, sea-level rise and abrupt climate change. *Nature Geoscience*, 5(9), pp.601-606.

Toucanne, S., Zaragosi, S., Bourillet, J., Cremer, M., Eynaud, F., Van Vliet-Lanoë, B., Penaud, A., Fontanier, C., Turon, J. and Cortijo, E., 2009. Timing of massive 'Fleuve Manche' discharges over the last 350kyr: insights into the European ice-sheet oscillations and the European drainage network from MIS 10 to 2. *Quaternary Science Reviews*, 28(13-14), pp.1238-1256.

United Kingdom Hydrographic Office, 2022. *Global Wrecks and Obstructions Shapefiles, electronic dataset, downloaded 14 April 2022*.

Van Der Wal, D. and Pye, K., 2003. The use of historical bathymetric charts in a GIS to assess morphological change in estuaries. *Geographical Journal*, 169(1), pp.21-31.

Younger, P.L. and McHugh, M., 1995. Peat development, sand cones and palaeohydrogeology of a spring-fed mire in East Yorkshire, UK. *The Holocene*, 5(1), pp.59-67.

## Appendix A. Data Sources

The following data sources were used in the development of this bed mobility and thermal assessment:

### 6.1. Client Provided Reports

**Table 6-1: Extant reports for the Dogger Bank South, Landfall Site, Export Cable Corridor and Offshore Windfarm**

Item	Title	Document Reference Number/URL	Author	Rev.	Date
1.	Validation of Metocean Data against Measurements at Dogger Bank	002681383-01	DHI Water Environments (UK) Ltd.	1	29/06/2018
2.	Sofia Offshore Wind Farm Metocean Hindcast Study, Marine Operations Technical Note	003581034-03	DHI Water Environments (UK) Ltd.	03	29/10/2020

### 6.2. Client Provided Data

**Table 6-2: Extant data for the Dogger Bank South, Landfall Site, Export cable Corridor and Offshore Windfarm**

Item	Title	Document Reference Number/URL	Author	Date
3.	Cable Route Option Shapefiles	PC2340-RHD-OF-CR-M2-Z-0121_CB_ShortList_1kmOptions_P02	RWE	2022
4.	MBES 1m coarse grid Cable Route	RWE_CableRoute_1pt0m_CUBE_Tide	RWE	30/05/2022
5.	MBES 1m coarse grid OWF	20220530_DBS_MPG_All_MBES_1m_LAT_FLT	RWE	30/05/2022
6.	MBES 1m coarse grid ECR	DBS_ECRScout_MBES_GRID_1pt0m_20220614	RWE	14/06/2022
7.	Seabed Interpretation Shapefiles (Features, Line Features and Outcrop)	DBS_ECRScout_MBES_Interp_Features_20220615 DBS_ECRScout_MBES_Interp_Line_Features_20220615 DBS_ECRScout_MBES_Interp_Outcrop_20220615	RWE	15/06/2022

Item	Title	Document Reference Number/URL	Author	Date
8.	.dat files of interpreted seismic surfaces and horizons, with interim allocations, in depth and time, below mLAT and below seafloor.	Eg: DBS_ECRScout_SBP_H05_b_Upper_S and_Unit_m_bLAT  DBS_ECRScout_SBP_H10_b_Lower_L aminated_Sand_Unit_m_bLAT  DBS_ECRScout_SBP_H15_i_Lower_Cr ossbedded_Sand_Unit_m_bLAT	RWE	17/06 /2022

### 6.3. Additional Information Sources

Table 6-3: Extant data from external sources for the Dogger Bank South, Landfall Site, Export cable Corridor and Offshore Windfarm

Item	Title	Document Reference Number/URL	Author	Rev.	Date
9.	EMODnet DTM Resolution: 1/16 * 1/16 arc minutes	<a href="https://doi.org/10.12770/bb6a87dd-e579-4036-abe1-e649cea9881a">https://doi.org/10.12770/bb6a87dd-e579-4036-abe1-e649cea9881a</a>	EMODnet		2020
10.	2011, Gardline Geosurvey, Zone 3 Dogger Bank Tranche B Southern Reconnaissance Export Cable Route, Geophysical Survey: Bathymetry	<a href="#">2011, Gardline Geosurvey, Zone 3 Dogger Bank Tranche B Southern Reconnaissance Export Cable Route, Geophysical Survey   Marine Data Exchange</a>	Marine Data Exchange (MDE) / Gardline Geosurvey		2011
11.	2011 HI1358 Spurn Point to Flamborough Head Blk2	<a href="#">National Coastal Monitoring - Hydrographic Survey</a>	Channel Coastal Observatory (CCO)		2011
12.	2016 HI1473 Flamborough Head to Humber Approach	2016_HI1473_Flamborough_Head_to_Humber_A	UKHO Admiralty		2016



## Dogger Bank South Background Review: Bed mobility & Thermal Environment

	Block 1 1m CUBE	pproach_Block_1_1m_CUBE	Portal		
13.	2019 HI1590 Dogger Bank SW Patch 2m SDTP	2019_HI1590_DoggerBank_SW_Patch_2m_SDTP	UKHO Admiralty Portal		2019
14.	2020 HI1587 Bridlington to Spurn Head 2m SDTP	2020_HI1587_Bridlington_to_Spurn_Head_2m_SDTP	UKHO Admiralty Portal		2020
15.	BRITICE v2 Filtered Data	<a href="https://doi.org/10.1111/bor.12273">https://doi.org/10.1111/bor.12273</a>	Clark, C. D., Ely, J. C., Greenwood, S. L., Hughes, A. L. C., Meehan, R., Barr, I. D., Bateman, M. D., Bradwell, T., Doole, J., Evans, D. J. A., Jordan, C. J., Monteys, X., Pellicer, X. M. and Sheehy, M.		2018
16.	1:50000-scale onshore geological maps. WMS 1.3.0.		BGS		2022
17.	1:250000-scale offshore geological products WMS 1.3.0.		BGS		2022
18.	LIDAR Composite 1m DTM 2017	<a href="#">LIDAR Composite DTM 2017 - 1m - data.gov.uk</a>	Environment Agency		2017
19.	LIDAR Composite 1m DTM 2020	<a href="#">LIDAR Composite DTM 2020 - 1m - data.gov.uk</a>	Environment Agency		2020
20.	SurfZone 2m DEM 2019	<a href="#">SurfZone Digital Elevation Model 2019 - data.gov.uk</a>	Environment Agency		2019
21.	North West European Shelf Production Centre, NWSHELF_MULTIYEAR_PH Y_004_009	CMEMS	Renshaw, R., Wakelin, S., Goldbeck, I. and O'Dea, E.		2021

22.	North West European Shelf Production Centre, NORTHWESTSHELF_ANALYSIS_FORECAST_PHY_004_013	CMEMS	Tonani, M., Bruciaferri, D., Pequignet, C., King, R., Sykes, P., McConnell, N., Siddorn, J.		2021
23.	High Resolution ODYSSEA L4 Sea Surface Temperature Analysis, SST_ATL_SST_L4_NRT_OBSERVATIONS_010_025	CMEMS	Autret, E., Prévost, C. and Piollé, J-F.		2021

## Appendix B.

Onshore Borehole records:

Location	BGS ID	Easting (BNG)	Northing (BNG)	Link	Surface level (if given)	Depth of top of chalk (from surface)	Water depth (if given)
Hamilton Hill / Fraisthorpe	TA16SE29	516700	460600	<a href="#">Page 1   Borehole TA16SE29   Borehole Logs (bgs.ac.uk)</a>	17' OD	23.8 m	
Barmston	TA15NE9	516600	459140	<a href="#">Page 2   Borehole TA15NE9   Borehole Logs (bgs.ac.uk)</a>	30' OD	84 ft (25.6 m)	
Skipsea Sands Caravan Park	TA15NE14	517350	456030	<a href="#">Page 1   Borehole TA15NE14   Borehole Logs (bgs.ac.uk)</a>		19.5m	

Village Pump Skipsea	TA15NE3	516775	455010	<a href="#">Page 1   Borehole TA15NE3   Borehole Logs (bgs.ac.uk)</a>	25' OD	73ft (22.3 m)	17'
Land at Skipsea	TA15NE11	515700	455300	<a href="#">Page 1   Borehole TA15NE11   Borehole Logs (bgs.ac.uk)</a>		36.5 m	
East Gate Farm Ulrome	TA15NE2	516957	457068	<a href="#">Page 1   Borehole TA15NE2   Borehole Logs (bgs.ac.uk)</a>	40' OD	85'	35'
Hornsea British Gas BH A3	TA15SE49	517860	451800	<a href="#">Page 2   Borehole TA15SE49   Borehole Logs (bgs.ac.uk)</a>		35m	
High Stone Hills Farm Barmston	TA16SW9	514530	460370	<a href="#">Page 1   Borehole TA16SW9   Borehole Logs (bgs.ac.uk)</a>	35' OD	70 ft (21.34 m)	
Lissett	TA15NE12	515300	457800	<a href="#">Page 1   Borehole TA15NE12   Borehole Logs (bgs.ac.uk)</a>		41 m	
Carnaby Trading Estate	TA16SW14	514400	464100	<a href="#">Page 1   Borehole TA16SW14   Borehole</a>		17 m	

## Dogger Bank South Background Review: Bed mobility & Thermal Environment

				<a href="#">Logs</a> (bgs.ac.uk)			
<b>Bessingby Estate</b>	TA16NE63	516900	466100	<a href="#">Page 1   Borehole TA16NE63   Borehole Logs</a> (bgs.ac.uk)		17 m	25 m and 42 m

Offshore core and drill records:

ACTIVITY_ID	SAMPLE_NAME	X_WGS84	Y_WGS84	SAMPLE_SOURCE	EQUIPMENT_TYPE
1962311	+54+000/544/VE/1	0.915336	54.649481	Cruise: 1981/8	Corer: Vibrocorer
2018876	+54+000/480/VE/1	0.818156	54.591808	Cruise: 1981/8	Corer: Vibrocorer
2018876	+54+000/480/VE/1	0.818156	54.591808	Cruise: 1981/8	Corer: Vibrocorer
2018876	+54+000/480/VE/1	0.818156	54.591808	Cruise: 1981/8	Corer: Vibrocorer
2018841	+54+000/543/VE/1	0.804875	54.592258	Cruise: 1981/8	Corer: Vibrocorer
2018841	+54+000/543/VE/1	0.804875	54.592258	Cruise: 1981/8	Corer: Vibrocorer
1962309	+54+000/542/VE/1	0.686026	54.490073	Cruise: 1981/8	Corer: Vibrocorer
1962309	+54+000/542/VE/1	0.686026	54.490073	Cruise: 1981/8	Corer: Vibrocorer
1962309	+54+000/542/VE/1	0.686026	54.490073	Cruise: 1981/8	Corer: Vibrocorer
2019109	+54+000/166/VE/1	0.668676	54.472182	Cruise: 1981/8	Corer: Vibrocorer
2019109	+54+000/166/VE/1	0.668676	54.472182	Cruise: 1981/8	Corer: Vibrocorer
2019096	+54+000/150/CS/1	0.57256	54.281705	Cruise: 1981/8	Corer: Sediment Gravity
2019096	+54+000/150/CS/1	0.57256	54.281705	Cruise: 1981/8	Corer: Sediment Gravity
2019096	+54+000/150/CS/1	0.57256	54.281705	Cruise: 1981/8	Corer: Sediment Gravity
2019096	+54+000/150/CS/1	0.57256	54.281705	Cruise: 1981/8	Corer: Sediment Gravity
2019096	+54+000/150/CS/1	0.57256	54.281705	Cruise: 1981/8	Corer: Sediment Gravity
2019096	+54+000/150/CS/1	0.57256	54.281705	Cruise: 1981/8	Corer: Sediment Gravity
2018988	+54+000/320/CS/1	0.57013	54.277725	Cruise: 1981/8	Corer: Sediment Gravity
2018986	+54+000/316/CS/1	0.411498	54.224651	Cruise: 1981/8	Corer: Sediment Gravity
1962449	+54+000/372/	0.3985	54.2422	Cruise: 1981/8	Corer: Sediment

**Dogger Bank South Background Review: Bed mobility & Thermal Environment**

	CS/1	97	21		Gravity
<b>1962492</b>	+54+000/315/ CR/1	0.3566 67	54.2353 11	Cruise: 1981/8	Corer: Rock Gravity
<b>1962510</b>	+54+000/338/ CS/1	0.2100 37	54.1155 95	Cruise: 1981/8	Corer: Sediment Gravity
<b>1962510</b>	+54+000/338/ CS/1	0.2100 37	54.1155 95	Cruise: 1981/8	Corer: Sediment Gravity
<b>1962236</b>	+54+000/627/ DR/1	0.2795 22	54.3277 33	Cruise: 1983/1	Drill
<b>1962236</b>	+54+000/627/ DR/1	0.2795 22	54.3277 33	Cruise: 1983/1	Drill
<b>1962236</b>	+54+000/627/ DR/1	0.2795 22	54.3277 33	Cruise: 1983/1	Drill
<b>1962236</b>	+54+000/627/ DR/1	0.2795 22	54.3277 33	Cruise: 1983/1	Drill
<b>1962236</b>	+54+000/627/ DR/1	0.2795 22	54.3277 33	Cruise: 1983/1	Drill
<b>1962236</b>	+54+000/627/ DR/1	0.2795 22	54.3277 33	Cruise: 1983/1	Drill



End page left blank